SORPTION AND DESORPTION OF SELECTED ORGANIC AND INORGANIC POLLUTANTS IN SOILS COLLECTED FROM DIFFERENT AGRO-ECOLOGICAL ZONES OF NIGERIA

PAUL NKEM DIAGBOYA

MATRIC NUMBER: 139802

JANUARY, 2015

SORPTION AND DESORPTION OF SELECTED ORGANIC AND INORGANIC POLLUTANTS IN SOILS COLLECTED FROM DIFFERENT AGRO-ECOLOGICAL ZONES OF NIGERIA

BY

PAUL NKEM DIAGBOYA

B.Sc. Biochemistry (Benin), M.Sc. Environmental Chemistry and Pollution Control (Ibadan)

A Thesis in the Department of Chemistry,
Submitted to the Faculty of Science,
in partial fulfillment of the requirements for the award of the Degree of

DOCTOR OF PHILOSOPHY

of the

UNIVERSITY OF IBADAN

JANUARY, 2015

ABSTRACT

Environmental pollution caused by persistent and bioaccumulative toxic chemicals is a global issue in view of its effects on biota. Researches abound on the sources and concentration of soil pollutants but there is paucity of information on their sorption/desorption in Nigerian soils. This is necessary for accurate prediction of toxicity and effective remediation strategy. Therefore, this study was aimed at assessing the sorption/desorption of selected organic and inorganic pollutants in soils from different Agro-Ecological Zones (AEZs) of Nigeria.

Representative composite soil samples (0-30 cm depth) were collected from the eight AEZs (15 each) and their physicochemical characteristics determined using standard methods. Soil treatments were carried out by removing Organic Matter (OM) and iron oxides to give Organic-Matter-Removed (OMR) and Iron-Oxides-Removed (IOR) samples, respectively. Batch sorptions/desorptions of pyrene and fluorene [Polycyclic Aromatic Hydrocarbons (PAHs)], Pentachlorophenol [PCP; Pesticide], and Pb(II), Cu(II), and Cd(II) [Heavy Metals (HM)] were investigated at varying times (0-4320 min.), solution pH (3-9), sorbate concentrations (20-100 μg/L PAHs; 10-40 mg/L PCP; 50-300 mg/L HM), and temperatures (25 and 40 °C) for untreated, OMR and IOR soil samples. Competitive sorptions/desorptions were investigated using batch method. Data were fitted to four kinetics models [Pseudo-First-Order (PFO), Pseudo-Second-Order (PSO), Elovich, and Intra-Particle-Diffusion (IPD)] and three adsorption isotherm models [Langmuir, Freundlich, and Distributed Reactivity Model (DRM)]. Thermodynamic parameters (Gibb's free energy-$\Delta G°$, entropy-$\Delta S°$, and enthalpy-$\Delta H°$) were determined and the regression analyses were carried out.

Soil pH values ranged from 6.2 to 7.4, while their Cation Exchange Capacity (CEC) ranged from 2.4 to 8.3 meq/100g. The OMR soils exhibited acidic pH (4.1-6.1) and reduced CEC (2.1-3.9 meq/100g), while IOR soils were alkaline (pH of 7.8-8.1) with increased CEC (17.9-37.9 meq/100g). Equilibrium sorptions were attained within 1440 minutes for all sorbates. Increasing pH decreased organics sorption (16.0-42.0%) but increased metals sorption (≥75.0%). Competition decreased the sorptions of organic pollutants while higher temperature increased sorptions. Metal distribution coefficients

(K_d) values were directly proportional to OM content, and single and competitive sorptions followed the same trend: Pb(II)>Cu(II)>Cd(II). Desorptions hystereses were related to OM content: the higher the OM, the higher the hysteresis. Sorptions data fitted PSO (R^2=0.99-1.00), Elovich (R^2=0.90-1.00) and IPD (R^2=0.71-0.96) models which suggested some degree of boundary-layer-control. Sorptions data were better described by DRM and Freundlich adsorption isotherms for PAHs and PCP, respectively; while both Langmuir and Freundlich isotherms described the metals confirming the heterogeneous nature of the soils. Sorptions of selected pollutants were spontaneous and feasible ($\Delta G° <$ –15.5kJmol^{-1}), accompanied by low $\Delta S°$ values (≤1.3 kJmol^{-1}K^{-1}). The $\Delta H°$ values (<45.0 kJmol^{-1}) were in the energy range associated with weak forces of interactions such as Van-der Waals, electrostatic, and π-π interactions.

The sorptions of selected organic and inorganic pollutants were partly surface adsorption and partly partitioning between phases in soils. Organic matter, iron oxides and temperature were major factors controlling sorptions/desorptions. Low levels of organic matter, iron oxides and high temperature may negatively impact biota and aquifer.

Keywords: Soil Sorption, Agro-Ecological Zones in Nigeria, Pyrene, Fluorene, Pentachlorophenol.

Word count: 480

CERTIFICATION

We certify that this work was carried out by Paul Nkem Diagboya in the Department of Chemistry, University of Ibadan Nigeria, National Center for Nanoscience and Technology (NCNST) Beijing China, and Institute of Geographic Sciences and Natural Resources Research, Chinese Academy of Sciences (CAS) Beijing China under our supervision.

……..

Supervisor

Bamidele I. Olu-Owolabi,

B.Sc., M.Sc., Ph.D. (Ibadan)

Professor, Department of Chemistry,

University of Ibadan, Nigeria

……..

Supervisor

K.O. Adebowale,

B.Sc., M.Sc., Ph.D. (Ibadan)

Professor, Department of Chemistry,

University of Ibadan, Nigeria

DEDICATION

This work is dedicated to the Almighty Father whose Holy Spirit helped me all through.

And to the memory my late grand Mum (Mrs. Rebecca A. Okoh) and my late Dad (Mr. John E. Diagboya) who gave me guidance in my early day.

ACKNOWLEDGEMENTS

I specially acknowledge all who helped actualize this dream of mine. Special thanks go to:

The Head of Department Chemistry, University of Ibadan. My amiable supervisors: Prof. Bamidele I. Olu-Owolabi and Prof. K.O. Adebowale – your professional, financial and moral supports were invaluable. Professors P.C. Onianwa, F. Bamiro, and O. Ekundayo, other Professors, Lecturers and other Staff of the Department of Chemistry, University of Ibadan, Nigeria.

The World Academy of Sciences (TWAS), Trieste, Italy; and the Chinese Academy of Sciences (CAS), China. Prof. Romain Murenzi of TWAS and Madam Fu of CAS, Delta State Scholarship Board (Nigeria), National Center for Nanoscience and Technology (NCNST), Beijing, China; Head (Prof. Han Bao-Hang) and members of the Laboratory of supra-molecular nanomaterials and devices, NCNST, Dr. Wenbin Liu, State Key Laboratory of Environmental Chemistry and Ecotoxicology Research, Center for Eco-Environmental Sciences, CAS, Beijing, China, Institute of Geographic Sciences and Natural Resources Research, Chinese Academy of Sciences, Beijing, China.

My dear and wonderful friends and colleagues: Peter C. Okoli, Ighoroje O. Precious, Ibor Richard, Bunmi Ayodele, friends in Tafawa Belewa Hall, my Facebook friends, members of the Wisdom of God Catholic Charismatic Renewal, Our Lady Seat of Wisdom, University of Ibadan, and others too numerous to mention who assisted me during the course of this research.

My uncle: Mr. Victor P.O. Okoh, your supports (both financial and otherwise) have been very instrumental to this journey. My lovely family members: Mum (Mrs. Caroline Diagboya), Ehima, and Theresa, Late Mrs. Rebecca Okoh, Ebere A. Dibie, and the Aghaulor family. Your prayers, moral and financial supports have been invaluable and are highly appreciated. I LOVE YOU ALL.

TABLE OF CONTENTS

LIST OF TABLES

LIST OF FIGURES

LIST OF APPENDICES

LIST OF SYMBOLS

SYMBOL	MEANING (UNIT)
AEZ	Agroecological zone
AG	Agbor
GSF	Gembu
IB	Ibadan
JB	Jos
LF	Lokoja
MA	Maiduguri
MG	Monguno
PH	Port Harcourt
IOR	Iron Oxides-Removed sample
OMR	Organic-Matter-Removed sample
CEC	Cation Exchange Capacity
DRM	Distributed Reactivity Model
IPD	Intra-Particle Diffusion model
PFO	Pseudo First-Order
PSO	Pseudo Second-Order
f_{OC_i}	Organic carbon mass fraction
k_i	Rate parameter of IPD
K_{OC_i}	Organic carbon-normalized partition coefficient for *i* sorption component
$q_{e,l}$	Linear contribution to sorption (μg/g or mg/g)
$q_{e,nl}$	Nonlinear contribution to sorption (μg/g or mg/g)
$\Delta G°$	Gibbs free energy change (kJ mol^{-1})
$\Delta H°$	Enthalpy change (kJ mol^{-1})
$\Delta S°$	Entropy change (kJ mol^{-1} K^{-1})
b	Langmuir Solute–surface interaction energy-related parameter
C	Surface concentration of sorbate in the IPD model (μg g^{-1})
C_{ads}	Equilibrium aqueous-phase solute concentration (μg L^{-1} or mg L^{-1})
C_e/C_{eq}	Equilibrium aqueous-phase solute concentration (μg L^{-1} or mg L^{-1})

C_o	Initial sorbate concentrations in solution (μg L^{-1} or mg L^{-1})
k_1	Rate constant of PFO (min^{-1})
k_2	Rate constant of PSO (g mg^{-1} min^{-1})
K_c	Equilibrium constant
K_d	Distribution or Partition coefficient
k_F	Freundlich isotherm model capacity factor ($\mu g^{1-1/n}$ $cm^{3/n}$ g^{-1})
M or m	Mass of sample or sorbent (g)
n	Freundlich isotherm model linearity parameter
q_e	Amount adsorbed or Equilibrium solid-phase concentration (μg/g or mg/g)
q_em	Total sorption capacity (μg/g or mg/g)
Q_o	Estimated maximum sorption capacity per unit weight (μg/g or mg/g)
q_t	Amount adsorbed at time t (mg/g)
R	Ideal gas constant (= 8.3145) (J mol^{-1} K^{-1})
r^2	Correlation coefficient
T	Temperature (K)
V	volume of the solution (mL)
α	Initial sorption rate of Elovich (mg^{-1} g^{-1} min^{-1})
β	Desorption constant of Elovich (g/mg)

CHAPTER ONE

INTRODUCTION

1.1 Background Information

Soils are increasingly becoming important in global development issues such as food security and global burden of disease. Their importance stems from pollution by persistent and bio–accumulative toxic chemicals (Site, 2001). Since soil is the final sink of most pollutants in the environment, these have aroused widespread concern by scientists and environmentalists because of the effects of these pollutants on biota and environment (Hamdi et al., 2007; Khadhar et al., 2010; Site, 2001). The contamination of food sources as well as the direct toxicity to man are major aspects of these concern. Hence, it is necessary to understand the chemical fate of pollutants in environmental media, especially in soils, if they are to be managed appropriately.

Pollutants in the environment include inorganic (metals and metalloids such as Pb, Hg, Cd, As, etc.) and organic chemicals (pesticides, polycyclic aromatic hydrocarbons (PAHs), and other persistent organic pollutants). In the 1950s, the inorganic pollutants were of major health concern because of the popular incidences of the Cd "*itai–itai*" disease and the Hg "*Minamata*" disease, both in Japan, and the *Love Canal* waste episodes (United States of America). It took the work of Carson (1962), titled '*Silent Spring*', to draw the world's attention to the havocs being caused by organic pollutants on the ecosystem. Since then several studies have been reported on the harmful effects of these chemicals in the environment and on biota (Hamdi et al., 2007; Khadhar et al., 2010, Liu et al., 2009; Gupta and Bhattacharyya, 2006; Hong et al., 2012; Shin and Han, 2012).

Several international organizations concerned with the health of the environment, such as the World Health Organization (WHO) and the United States Environmental Protection Agency (USEPA), have categorized some environmental chemicals as priority. This categorization is due to their resistance to biological and other natural degradation

processes; and hence, they bioaccumulate (and bio-magnify) in higher trophic organisms. Such pollutants include PAHs, some commonly used chlorinated pesticides, and heavy metals. The use of these pollutants are wide spread in several products and their environmental occurrence have been linked to several severe health disorders in biota including anemia, mutagenic effects and carcinogenesis, kidney malfunction, brain damage, impaired function of the peripheral nervous system, bone demineralization, high blood pressure, reproductive abnormalities, developmental defects, abnormal vitamin D metabolism, and in extreme cases death (Liu et al., 2009; Gupta and Bhattacharyya, 2006).

Some of these chemicals are produced naturally and are ubiquitous in the environment (Rao et al., 2007), but in minute quantities. Some are natural constituents of soils depending on the soil forming parent materials. However, in recent times, their levels in the environment, especially in soils and surface waters, have been enormously supplemented in excess of the natural background concentration by anthropogenic inputs from sectors such as industry and agriculture as well as inappropriate waste disposal practices. This has led to unprecedented environmental degradation such as shortage of land for agricultural use and clean water supply due to seepage of these pollutants to the aquifer; and thus, impacting negatively on the ecosystem. For instance, worldwide, over one billion people lack reliable access to clean water and 2.3 billion people of the global population live in water-stressed areas, a number that will increase 52 percent by 2025 (Hejazi et al., 2011).

The fate of these pollutants in soil is mainly controlled by sorption – a phase distribution process that accumulates solutes at surfaces and inter-phases (adsorption) or from one phase to another (partitioning). These processes are known to affect the transport and reduce chemical and biological reactivity of hydrophobic organic chemicals (HOCs) (Huang et al., 2003) and inorganic chemicals in surface aquatic and groundwater systems. The fate of these chemicals in soils is of particular environmental concern, and the understanding requires the knowledge of the sorption characteristics of the pollutants as well as the knowledge of the soil type/composition and its characteristics. Soil composition/characteristics (clay mineral type and percentage composition, organic matter, pH, cation exchange capacity (CEC), etc) are vital soil properties which affect

pollutants bioavailability and bioactivity, phytotoxicity, as well as the chemical or microbial transformations (Site, 2001).

Studies of pollutants sorptions on soils from various Agro-Ecological Zones (AEZs) of the world abound on metals (Agbenin and Olojo, 2004; Agbenin, 2010; Sha'ato, 1996; Serrano et al., 2005; Gomes et al., 2001; Gupta and Bhattacharyya, 2006; Carey et al., 1996; Olu-Owolabi et al., 2010), PAHs (Chilom et al., 2005; Guo et al., 2010; Javier Rivas et al., 2008; Kohl and Rice, 1999; Liu et al., 2009; Zeledon–Toruno et al., 2007; Oren et al., 2006; Cottin and Merlin, 2007; An et al., 2010; Ramirez et al., 2001; Teixeira et al., 2011), and Pesticides (Abdel Salam and Burk 2010; Bouras et al., 2010; Li et al., 2009; Pu and Cutright, 2006; Iglesias et al., 2010; He et al., 2006; Site, 2001; Shu et al., 2010; Viraraghavan and Slough, 1999; Wang et al., 2008). In all these studies, only a few used Nigerian soils (Olu-Owolabi et al., 2010; Agbenin and Olojo, 2004; Sha'ato, 1996; Agbenin, 2010). Most of them were on metals sorptions, with little or no comprehensive information on sorption of organic pollutants. Hence, it is necessary to have a comprehensive study of sorption of organic and inorganic pollutants on Nigerian soils using selected model inorganic and organic pollutants.

Ambient environmental conditions affect soil forming factors, and have direct influence on soil properties. Thus, soils from different AEZs may exhibit varying clay mineralogy, organic matrices composition and physicochemical properties. Since these soil properties determine to a large extent the sorption characteristics of the soils, the soils may exhibit different pollutants sorption properties, and this may determine the severity of harm available pollutants may cause in the environment (Arias et al., 2002). Nigeria is a large country (923,768 sq km) having eight distinct AEZs with heterogeneous climatic and vegetative conditions; hence, the need to study soil samples from all AEZs of Nigeria so as to determine the physicochemical and pollutants sorption properties.

For an effective soil management system in Nigeria, there is need for comprehensive information on the soil response in the presence of these pollutants, and the extent and nature of soil processes which control pollutants mobility. It is therefore on this basis that effective predictions of the behavior of these pollutants in soil can be made. This is imperative because without this knowledge, it will be difficult to propose a cost effective

and environmentally friendly remediation technique for these pollutants when in soil. Hence, the aim of this study was to establish a comprehensive pollutant–soil sorption relationship with regard to the soil properties in the representative soil samples from the AEZs of Nigeria. Two PAHs (pyrene and fluorene), one pesticide (pentachlorophenol), and three heavy metals (Pb(II), Cu(II), and Cd(II)) were used as model pollutants for this study. These pollutants were chosen because they are among the commonly encountered in the environment and have high potential to cause harm to biota as well as the ecosystem.

1.2 Research objectives

The objectives of this study are:

i. The physicochemical characterization of the selected representative soils as well as the heavy metals contamination levels of the soils,
ii. Determination through the batch equilibrium sorption studies of optimum parameters (pH, time and temperature) responsible for pollutants' sorption by the various soils,
iii. Competitive sorption of pollutants on the soils.
iv. Determination of the effect of organic matter and iron oxide removal on pollutants' sorption,
v. Interpretation of the data generated using kinetics models (pseudo first order, pseudo second order, Elovich, and intra–particle diffusion) and adsorption isotherms (Langmuir, Freundlich, and Distributed reactivity models), as well as generating and explaining the thermodynamics parameters.

CHAPTER TWO

LITERATURE REVIEW

2.1 Soil

Soil is a complex mixture of primary and secondary minerals, a variety of organic compounds, microorganisms and more, all being produced and transformed during the long process of its formation. These pores contain soil solution (liquid) and air (gas) (Taylor and Ashcroft, 1972). Accordingly, soils are often treated as a three state system (McCarty, 2002). Soil is also known as earth: it is the substance from which our planet takes its name. Colour is the first impression one has when viewing soil. Striking colors and contrasting patterns are especially memorable. Soil color results from chemical and biological weathering. As the primary minerals in parent material weather, the elements combine into new and colorful compounds. Iron forms secondary minerals with a yellow or red color; organic matter decomposes into brown compounds; and manganese, sulfur and nitrogen can form black mineral deposits (USDA, 1978).

Soil structure is the arrangement of soil particles into aggregates. These may have various shapes, sizes and degrees of development or expression. Soil texture refers to sand, silt and clay composition. Sand and silt are the products of physical weathering while clay is the product of chemical weathering. Clay content is particularly influential on soil behavior due to a high retention capacity for nutrients and water (Brown, 2003).

Soil is always changing and the pedogenesis (soil formation) is the combined effect of physical, chemical, biological, and anthropogenic processes on soil parent material resulting in the formation of soil horizons. The long periods over which change occurs and the multiple influences of change mean that simple soils are rare. While soil can achieve relative stability in properties for extended periods of time, the soil life cycle ultimately ends in soil conditions that leave it vulnerable to erosion (Buol et al., 1973). Despite the inevitability of soils retrogression and degradation, most soil cycles are long and

productive. How the soil life cycle proceeds is influenced by at least five classic soil forming factors: regional climate, biotic potential (vegetation), topography, parent material, and the passage of time. An example of soil development from bare rock occurs on recent lava flows in warm regions under heavy and very frequent rainfall. In such climates plants become established very quickly on basaltic lava, even though there is very little organic material. The plants are supported by the porous rock becoming filled with nutrient bearing water, for example carrying dissolved bird droppings. The developing plant roots themselves gradually breaks up the porous lava and organic matter soon accumulates but, even before it does, the predominantly porous broken lava in which the plant roots grow can be considered a soil.

2.2 Soil classification

The purpose of any classification is to organize soil properties on the basis of their commonalities (Cline, 1949; Smyth and Montgomery, 1962). Although many soil classification systems exist, there are three widely used systems: the United States Department of Agriculture (USDA) soil taxonomy, the Food and Agriculture Organization/United Nations Educational, Scientific and Cultural Organization (FAO/UNESCO) legend, and the French system – Office de la recherché scientifique et technique d'outre-mer (ORSTROM). Among soil scientists, classification is a controversial subject, and soil classes have imprecise information which can be misleading most times. Information from such general soil classifications will be too inaccurate to help understand the sorption behavior of pollutants at very low concentrations. Hence, to understand the investigated soils better in relation to specific soil properties, focus has been shifted to the soil physical and chemical characterization rather than general soil classification. However, quick view of popular soil classifications will be examined.

2.2.1 USDA soil taxonomy

This classification system was developed by the USDA Soil Conservation Service Soil Survey staff between 1951 and 1975 and published as *Soil Taxonomy* (Soil Survey Staff, 2006). The classification system focuses on soil properties that for the most part can be measured quantitatively rather than on soil–forming processes or factors. Some of these

properties are soil depth, moisture, temperature, texture, structure, cation exchange capacity, base saturation, clay mineralogy, organic matter content and salt content. Yet, the system certainly cannot exclude soil genesis since many soil properties quantified have considerable significance in soil genesis. In this soil classification, the item classified is the soil profile. Morphologically, soils are composed of a series of horizons. Soil horizons are layers of different appearance, thickness, and properties which have arisen by the action of various soil-forming processes. The horizons are normally parallel to the surface. Collectively, the horizons make up what is called the soil profile or "pedon". A hypothetical soil profile having all the principal horizons, with a brief description of the characteristics of each horizon is shown in Figure 2.1. Individual soils have one or more of these horizons. Younger soils might have few or none of these soil horizons because the horizonization process is time dependent.

The primary objective of soil taxonomy is to establish hierarchies of classes that permit us to understand, as fully as possible, the relationship among soils and between soils and the factors responsible for their character. A second objective is to provide a means of communication for the discipline of soil science (Soil Survey Staff, 2006). An overview of this classification system will be described in this thesis since the system is too extensive to relate here.

2.2.1.1 Hierarchy of categories in the Soil Taxonomy

Soil Taxonomy has six categories for classification of soils listed from top to bottom: order, suborder, great group, subgroup, family and series. The highest categories have the fewest classes and criteria separating classes, while the lowest categories have the most classes and criteria. The ‘‘soil type,’’ a soil series subdivision, commonly used in other classification systems is not a category in Soil Taxonomy.

There are ten orders, and the criteria used to differentiate them are highly generalized but based mainly on gross morphological features by the presence or absence of diagnostic horizons or features which show the dominant set of soil-forming processes that have taken place. These ten orders and their major characteristics are described in Table 2.1.

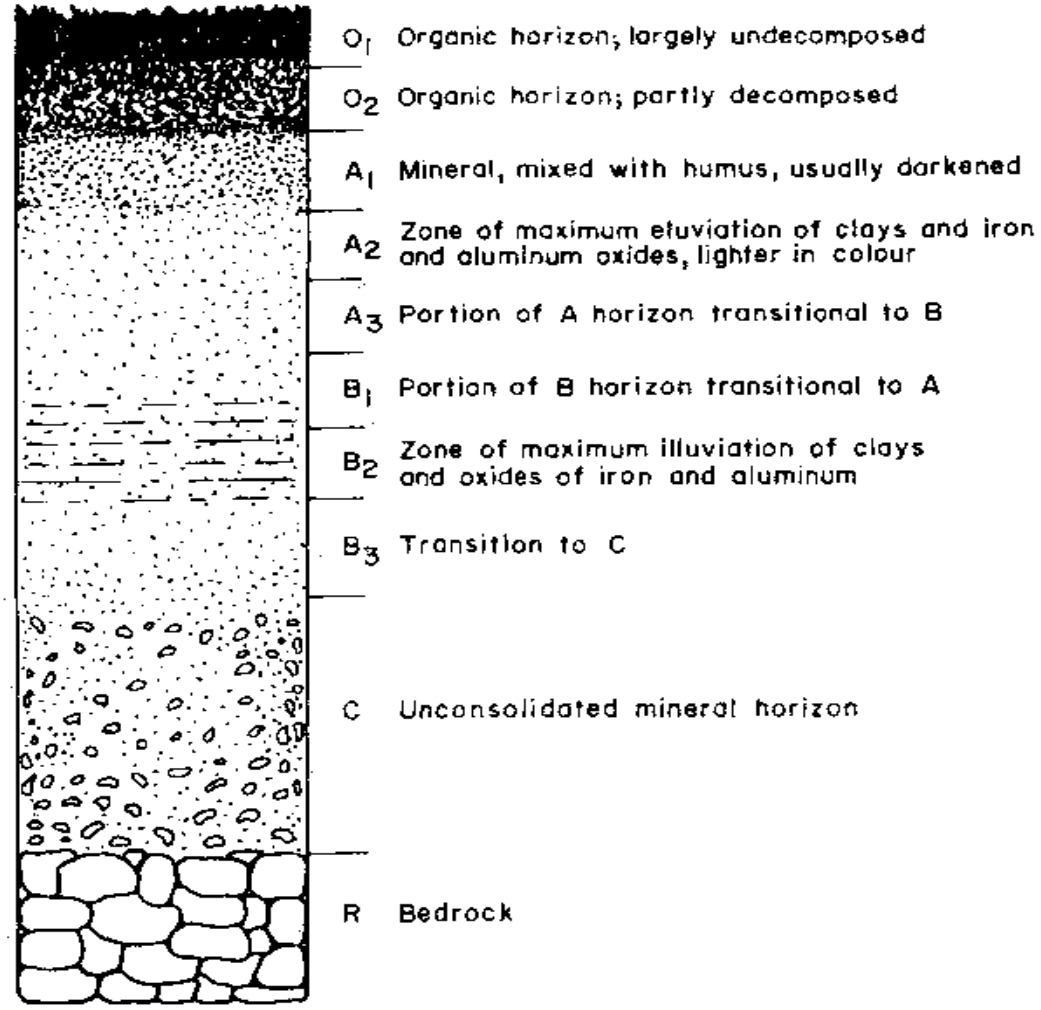

Figure 2.1. A typical soil profile (Soil Survey Staff, 2006)

Table 2.1. Brief descriptions of the ten soil orders according to Soil Taxonomy (Soil Survey Staff, 2006).

Soil orders	Description
Alfisols	Mineral soils relatively low in organic matter with relatively high base saturation (> 50%). Contains horizon of illuvial clay. Moisture is available to mature a crop. It occurs mainly in Savanna and drier forest zones
Ultisols	Mineral soils with an illuvial clay horizon. Has low base saturation (< 50%). Generally they are acidic, leached soils from humid areas of the tropics and subtropics. It occurs mainly in Rain forest zone and derived savanna
Oxisols	Mineral soils with no weatherable minerals. High in iron and aluminum oxides. Contain no illuvial horizons. They have very little variation in texture with depth. Some strongly weathered, red, deep, porous oxisols contain large amounts of clay-sized Fe and Al oxides. It occurs mainly in Rain forest and savanna.
Vertisols	Clayey soils with large amounts of swelling clay minerals (smectite). The soils crack widely during the dry season and become very sticky in the wet season. Moisture content varies. It occurs mainly in Alluvial plains in savanna
Mollisols	Mineral soils with thick, dark surface horizons relatively high in organic matter and with high base saturation. They are formed from colluvial materials.
Inceptisols	Mineral or young soils containing limited profile development in its horizons other than one of illuvial clay. They are mostly formed from colluvial and alluvial materials. Moisture is available to mature a crop. Soils derived from volcanic ash are considered a special group of Inceptisols, presently classified under the Andept suborder (also known as Andosols). They can be found in all regions of the world.
Entisols	Mineral soils lacking developed soil horizons in its profile. They are mostly derived from alluvial materials. Moisture content varies.
Aridisols	Mineral soils relatively low in organic matter. Contain developed soil horizons. Moisture is inadequate to mature a crop without irrigation in most years. Occurs in soils of arid region, such as desert soils. Some are saline.
Spodosols	Soils that contain an illuvial horizon of amorphous aluminum and organic matter, with or without amorphous iron. Usually moist or well leached. These soils are mostly formed under humid conditions and coniferous forest in the temperate region.
Histosols	Soils composed mostly of organic matter such as peat and muck. Moisture content varies.

A suborder category is a subdivision of an order within which genetic homogeneity is emphasized. Soil characteristics used to distinguish suborders within an order vary from order to order. For example, soil moisture and temperature are the important factors that differentiate the suborders in the order Alfisols. The presence or absence of an argillic horizon, on the other hand, distinguishes the two suborders of the order Aridisols. Forty-seven suborders are recognized in the United States Soil Taxonomy. The names in the suborders consist of two syllables. The first connotes the diagnostics properties; the second is the formative element from the soil order name. For example, an Ustalf is an Alfisol with an ustic moisture regime (associated with sub-humid climates). Typical soil order/sub–order names and formative elements are shown in Tables 2.2a and b (Soil Survey Staff, 2006).

The great group category is a subdivision of a suborder. They are distinguished one from another by kind and sequence of soil horizons. All soils belonging to one of the suborders of Aridisols have argillic horizons. They also may have additional diagnostic horizons such as a petrocalcic as well as several others. Soils having these additional horizons are placed in separate great groups. A total of 230 great groups are recognized in the United States Soil Taxonomy. The name of a great group consists of the name of the suborder and a prefix suggesting diagnostic properties. For example, a Plinthustalf is an ustalf that has developed plinthite in the profile. Plinthite development is selected as the important property and so forms the prefix for the great group name.

Great group categories are divided into three kinds of subgroups: typic, intergrade and extragrade. A typic subgroup represents the basic concept of the great group from which it derives. Intergrade subgroup contains soils of one great group, but has some properties characteristic of soils in another great group or class. These properties are not developed or expressed well enough to include the soils within the great group toward which they grade. Extragrade subgroup soils have aberrant properties that do not intergrade to any known soil. There are about 1,000 kinds of subgroups. A soil family category is a group of soils within a subgroup that has similar physical and chemical properties that affect response to management and manipulation.

Table 2.2a. Soil Order Names and Formative Elements (Soil Survey Staff, 2006)

Order	Formative Element	Derivation	Mnemonicon
Alfisols	Alf	(nonsense syllable)	Pedalfer
Aridisols	Id	L.--aridus, dry	arid
Entisols	Ent	(nonsense syllable)	recent
Histosols	Ist	Gr.--histos, tissue	histology
Inceptisols	Ept	L.--inceptum, beginning	inception
Mollisols	Oll	L.--mollis, soft	mollify
Oxisols	Ox	Fr.--oxide, oxide	oxide
Spodosols	Od	Gr.--spodos, wood ashes	Podzol; odd
Utisols	Ult	L.--ultimus, last	ultimate
Vertisols	Ert	L.--verto, turn	invert

*L.=Latin G.=Greek Fr.=French

Table 2.2b. Examples of Formative Elements of Suborder Names (Soil Survey Staff, 2006)

Formative Element	Meaning
Aqu	A soil that is very wet or that has been artificially drained.
Arg	A soil that has an illuvial horizon of clay.
Fluv	A soil that is composed of recent alluvium.
Orth	A soil that is the most representative.
Psamm	A soil that has sandy texture, sand or loamy sand.
Torr	A soil that is too dry to mature a crop without irrigation.
Ud	A soil that is moist but not wet.
Ust	A soil that is dry for long periods but moist in a growing season for 90 days or more.
Xer	A soil that is moist in winter and dry in summer.

The principal characteristics used to differentiate soil families are texture, mineralogy and temperature. Family textural classes, in general, distinguish between clayey, loamy and sandy soils. For some soils the criteria also specify the amount of silt, sand and coarse fragments such as gravel, cobbles and rocks. Typical family names are *clayey, kaolinitic, isohyperthermic*, etc

The soil series is the lowest category. It is a grouping of individual soil on the basis of narrowly defined properties, relating to kind and arrangement of horizons; colour, texture, structure, consistence and reaction of horizons; chemical and mineralogical properties of the horizons. The major difficulty in classifying soils is that soils are a continuum in which properties may change gradually with distance. Unlike the classification of biota, where an individual biota is readily recognized, defining the basic soil entity or entities that are to be grouped into classes is very challenging. Soil Taxonomy has defined the basic soil diagnostic entity as being the smallest volume within the landscape needed to sample and describe the soil (Soil Survey Staff, 2006). This description usually includes the nature and arrangement of soil horizons and the variability of other properties (physicochemical properties). The term ‘‘pedon’’ is applied to this small volume of soil or a unit of sampling. A soil individual, called a *polypedon*, is composed of a group of contiguous pedons that belong to the same soil series (Figure 2.2). The soil series are given local place names following the earlier practice in the old systems in naming soil series. There are tens of thousands of series.

2.2.2 FAO/UNESCO system

This is another major system of soil classification. It was devised more as a tool for the preparation of a small-scale soil map of the world rather than a comprehensive system of soil classification. The map shows only the presence of major soils, being associations of many soils combined in general units. The legend of the soil map of the world lists 106 units classified into 26 groupings. The soil units correspond roughly to great groups from the USDA Soil Taxonomy, while larger main grouping are similar to the USDA soil suborder (UNESCO, 1974). Table 2.3 shows the correlation between systems of soil classification: the Soil Taxonomy, FAO/UNESCO legend and the Institut National de la Recherche Agronomique (INRA) system.

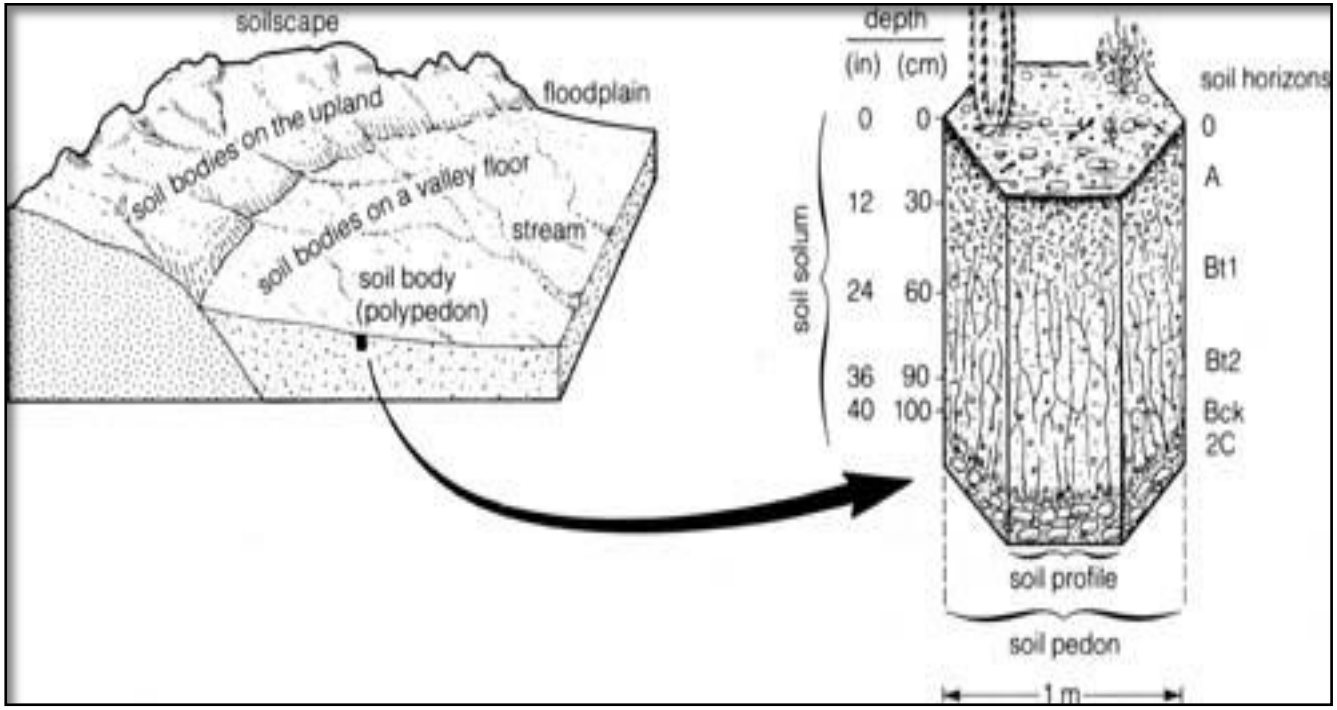

Figure 2.2. Soil profile showing soil pedon and polypedon (Soil Survey Staff, 2006)

Table 2.3. Comparison between systems of soil classification: the Soil Taxonomy, FAO/UNESCO legend and the INRA system (UNESCO, 1974)

FAO/UNESCO	Soil Taxonomy*	INRA System
Acrisols	Ultisols	Sols Lessive
Andosols	Andepts	Andosols
Arenosols	Psamments	Sols mineraux bruts
Cambisols	Tropepts	Sols bruns eutrophes tropicaux
Ferralsols	Oxisols (Latosols)	Sols Ferraltique
Fluvisols	Fluvents (Alluvial soils)	Sols mineraux bruts
Gleysols	Aquepts and Aquents (Aquic great groups of Entisols, Inceptisols)	Sols a gley peu profond peu humiferes
Histosols	Histosols	Sols hydromorphes organiques
Lithosols	Lithic subgroups	Lithosols
Luvisols	Alfisols	Sols lessives modaux
Nitosols	Tropics, Rhodic great groups of Alfisols and Ultisols	
Podzols	Spodosols	Podsols
Regosols	Orthents, Psamments	Sols mineraux bruts d'apport; eolien ou volcanique; sols peu evolves regosolique d'erosion etc.
Vertisols	Vertisols	Vertisols

* = Name in old USDA system.

2.2.3 French system (ORSTROM/INRA)

The French System of classifying soils is based on principles of soil evolution and degree of evolution of soil profiles. It also takes into account humus type, structure, and the degree of hydromorphism. The system was developed by the ORSTROM (now Institut français de recherche scientifique pour le développement en coopération).

2.3 Environmental soil chemistry

Soil chemistry is the branch of soil science that deals with the chemical composition, chemical properties, and chemical reactions of soils (Sparks, 2003). Soil is a complex mixture of primary and secondary minerals, a variety of organic compounds, microorganisms and more, all being produced and transformed during the long process of its formation. Soil chemistry is concerned with the chemical reactions involving these phases. For example, carbon dioxide in the air combined with water acts to weather the inorganic solid phase. This complexity is the source of the large variation of soil types worldwide (Du et al., 2008). Many too often regard the soil as an entity in itself, rather than as a part of ecosystems that provide services to mankind, such as the water cycle and nutrient cycle, not to mention the vegetation. This is especially true when considering natural or semi-natural systems used for grazing or areas covered with forests. Thus, the ambient environmental conditions such as the ecosystem and the climate determine the state of the soil; and these make up the agro–ecological zones (AEZs).

Chemical reactions between the soil solids and the soil solution influence both plant growth and water quality. Soil chemistry has traditionally focused on the chemical reactions in soils that affect plant growth and plant nutrition. However, beginning from the 1970s as concerns increased about inorganic and organic contaminants in water and soil and their impact on plant, animal, and human health, the emphasis of soil chemistry is now on environmental soil chemistry (Sparks, 2003).

Environmental soil chemistry is the study of chemical reactions between soils and environmentally important plant nutrients, radionuclides, metals, metalloids, and organic chemicals. Knowledge of environmental soil chemistry is fundamental in predicting the fate of contaminants in the surface and subsurface environments. An understanding of the

chemistry and mineralogy of inorganic and organic soil components is necessary to comprehend the array of chemical reactions that contaminants may undergo in the soil environment. These reactions, which may include equilibrium and kinetic processes such as dissolution, precipitation, polymerization, adsorption/desorption, and oxidation–reduction, affect the solubility, mobility, speciation (form), toxicity, and bioavailability of contaminants in soils and in surface waters and ground waters. These information will help in making sound and cost effective decisions about remediation of contaminated soils (Sparks, 2003).

2.4 Soil pollution and origin of soil chemistry

Until the 1850s soils were generally regarded as inert material that did not interact chemically. However, in 1848, H. S. Thompson added a solution of ammonium sulfate to a column of soil and to his surprise found calcium sulfate in the solution leaching out of the column (Thompson and Goyne, 2012). Soil chemistry evolved with the work of Way who refined this study in 1850 (Sparks, 2003). He is considered the father of soil chemistry and carried out a series of experiments on the ability of soils to exchange ions. He found that soils could adsorb both cations and anions, and that these ions could be exchanged with other ions. He noted that ion exchange was rapid, that clay was an important soil component in the adsorption of cations, and that heating soils or treating them with strong acid decreased the ability of the soils to adsorb ions. His observations launched a century of studies on nutrient retention and release by soil and the identification of minerals and organic matter as key components affecting chemical mobility (Thompson and Goyne, 2012). These earlier researches were directed primarily at improving agricultural crop production, but today it forms the foundation for global efforts to characterize the fate of environmental contaminants and the retention of organic matter in soils and sediments; and it has also impacted immensely other disciplines including chemical engineering and chemistry

Recent incidences have emphasized the threat of soil pollution (poisoning from persistent and bio-accumulative toxic chemicals), and these have led to soils becoming increasingly important in global development issues such as food security and global burden of disease (Site, 2001). Japan’s Minamata bay Hg incidence, the Love canal episodes (United States

of America) and the Zamfara Pb poisoning (Nigeria) are popular cases. Several recent researches have reported the presence of toxic chemicals originating from soil and water in foods and human specimen (Hong et al., 2012; Shin and Han, 2012). Pollutants in soils include organic and inorganic chemicals which could be both naturally-occurring in soil and man-made. For toxic chemicals which occur naturally in soils, pollution will occur when the levels of these chemicals in soil exceed the levels that are naturally present as has been observed in the Zamfara Pb poisoning. Although pollutant accumulation in soils due to natural processes is possible (Rao et al., 2007), recent anthropogenic activities such as accidental leaks and spills, agricultural chemicals, dumping and discharge from manufacturing processes have contributed immensely to both organic or inorganic soil pollutions. Pollutants of priority concern include those that are resistant to natural and biological degradation (non-biodegradable) and hence bioaccumulate (or bio-magnify) in higher trophic organisms. These include the polycyclic aromatic hydrocarbons (PAHs) and heavy metals.

Depending on the degree, symptoms of exposure to toxic chemicals varies and include damage to the nervous system, which causes fatigue, weakness, headaches, poor concentration, and emotional disturbance. Serious cases involve cognitive and sensory disorders, peripheral neuropathy, tremor, gait disturbance, visual, auditory, hormonal and metabolic disorders, or even cancer (Gupta and Bhattacharyya, 2006; Liu et al., 2009; Hong et al., 2012; Shin and Han, 2012).

Some notable sources of soil pollution (Sparks, 2003) include:

i. Discharge of industrial waste into the soil;
ii. Percolation of contaminated water into the soil;
iii. Rupture of underground storage tanks;
iv. Seepage from landfills;
v. Irrigation of agricultural lands with polluted water;
vi. Condensation of pollutants from areas with polluted air;
vii. Use of agricultural treatments such as pesticides, insecticides, and/or herbicides;
viii. Agricultural application of pollutant containing sewage sludge and/or fertilizers.

Soil characteristics, interacting with the complex soil environment involving the presence of the pollutant as well as other chemicals and natural conditions, have been known to influence the release of anthropogenic toxic chemicals in soils by either decreasing or increasing the level of bioavailable pollutants in the soil and by implication its toxicity to biota and the environment.

2.5 Pollutants in soil and water

Soil or water pollution is the presence of toxic chemicals or disease causing agents in soil and water in high enough concentrations to be of risk to biota and/or the environment. Pollutants in soils include organic and inorganic chemicals which could be both naturally-occurring in soil and man-made. There are several inorganic and organic pollutants that are important in water and soil, and these include plant nutrients such as nitrate and phosphate; heavy metals such as cadmium, chromium, and lead; oxyanions such as arsenite, arsenate, and selenite; organic chemicals such as polycyclic aromatic hydrocarbons, polychlorinated biphenyls, and several chlorinated organic compounds; inorganic acids; and radionuclides. The sources of these pollutants include fertilizers, pesticides, acidic deposition, agricultural and industrial waste materials, and radioactive fallout. These pollutants can be grouped into two basic types depending on their sources – point and nonpoint sources.

Point source pollution is contamination that can be traced to a particular source such as an industrial site, septic tank, or wastewater treatment plant. Nonpoint source pollution results from large areas and not from any single source and includes both natural and human activities. Sources of nonpoint pollution include agricultural, human, forestry, urban, construction, and mining activities and atmospheric deposition. There are also naturally occurring nonpoint source pollutants that are important. These include geologic erosion, saline seeps, and breakdown of minerals and soils that may contain large quantities of nutrients.

Pollutant chemicals may be grouped into three categories depending on their charged state:

i. anionic pollutants are negatively charged because they have more electrons than protons (e.g., the nutrient orthophosphate, PO_4^{3-});

ii. cationic pollutants are positively charged because they have fewer electrons than protons (e.g., the divalent cations Zn^{2+}, Cd^{2+}, Cu^{2+}, and Pb^{2+}); and

iii. uncharged organic pollutants that may exhibit a range of polarities (non-polar to polar) based on the distribution of electrons across the molecule as well as the pH condition of the aqueous medium (e.g., pentachlorophenol (PCP) which is affected by pH and the polycyclic aromatic hydrocarbons (PAHs) which usually have uniform electron distribution and hence are non-polar).

In this study, pollutants from categories ii and iii origins will be studied.

2.5.1 Polycyclic aromatic hydrocarbons (PAHs)

Polycyclic aromatic hydrocarbons (PAHs) represent a subgroup of the class of polycyclic aromatic compounds (PACs) which contain two or more aromatic benzo rings fused together in a linear or angular configuration. While PAHs consist of carbon and hydrogen only, PACs may contain hetero–atoms such as N, S, or O as part of their molecular structure. On the other side, PAHs may contain non–aromatic molecule substructures such as alkyl side chains (e.g. 5-methylchrysene), ethylene bridges (e.g. 3-methylcholanthrene), or pentacyclic rings (e.g. fluorene). Due to their aromaticity and lack of polar substituents, PAHs are lipophilic and chemically inert compounds.

PAHs are divided into two groups, low molecular weight PAHs (LPAHs) and the high molecular weight PAHs (HPAHs). LPAHs contain two or three aromatic rings and HPAHs are those with four or more rings. The distinction of low and high molecular weight is subtle because the actual difference in molecular weight between 2- and 6-ring compounds is not dramatic. Even though these designations seem unimportant, they are relatively important for toxicity considerations because the LPAHs and HPAHs generally exhibit very different physicochemical properties, bioavailability, bioaccumulation, and toxic potential.

PAHs occur naturally in the environment and are especially associated with petroleum products, such as the residual products derived from carbonization of bituminous coal at 1000–1200 °C. PAHs can be formed via thermal decomposition of virtually any organic material. PAH formation is due to incomplete combustion (pyrolysis), intermolecular

condensation, and cyclization reactions and was found to be most productive in the temperature range of 660–740 °C under low oxygen pressure. At this temperature, a wide range of unsubstituted PAHs and modified congeners (containing methyl side chains or non–aromatic substructures) are formed. Although local fires and volcanic activities might cause significant increases in local PAH concentrations, natural sources count for only a small percentage of the overall release into the environment. PAHs present in the human environment usually originate from anthropogenic sources. More important in total quantities, PAHs are released into the environment during combustion for residential heating, power generation, incineration, open fires, and traffic (ATSDR, 1995). As a result of input from these sources, PAHs are ubiquitous in the environment.

PAHs from coal tar derived from the coking of bituminous coal are among the most important sources in the occupational environment. Some of the most important industries with decreasing but still considerable PAH exposures are the coke production and aluminum smelting, iron and steel sintering, and asphalt production. PAHs in the environment have found its way to food sources. Depending on the kind of processing and preparation (grilling, frying, or smoking), food samples such as barbecued meat or charbroiled food may contain extremely high levels of PAHs including carcinogenic representatives such as benzo[a]pyrene (ATSDR, 1995). Airborne PAHs in the form of aerosols can be inhaled and penetrate the lower respiratory tract toward gas-exchanging alveoli. Tobacco smoke has been linked to about 90% of all lung cancer cases, other smoking-related cancer types, and approximately 1.2 million worldwide deaths annually (Hecht, 2003), and may be one of the most important sources of PAHs in indoor air. More than 500 different unsubstituted and methylated PAHs, many of them known as strong carcinogens, could be identified in tobacco smoke condensate and about 10 ng of benzo[a]pyrene has been estimated to be inhaled into the lungs from each cigarette (Swauger et al., 2002). No matter the source, humans are always exposed to complex mixtures of PAHs with different degrees of biological activity. In the biological systems, PAHs are known to distort physico-chemical and biological characteristics. Sixteen different PAHs have been categorized as priority by the United States Environmental Protection Agency (US EPA) (ATSDR 1995). Their names and structures are shown in Figure 2.3.

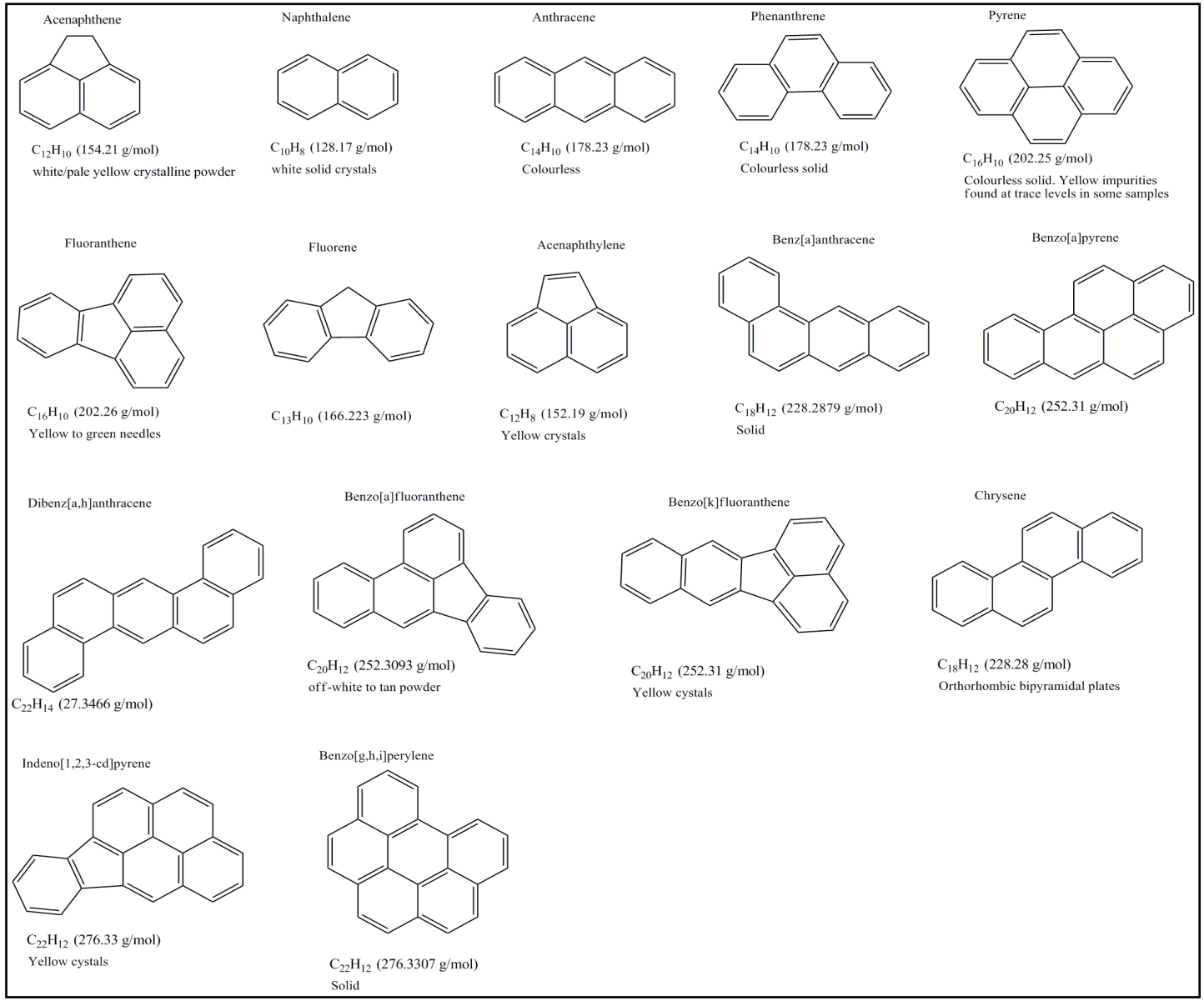

Figure 2.3. The structures and molecular weights of the sixteen priority PAHs (ATSDR, 1995)

2.5.1.2 Determination of PAHs: Synchronous Scan Fluorescence Spectroscopy (SSFS)

Several methods have been applied to detect PAHs in the solution, such as Gas Chromatography and Liquid Chromatography (Giessing et al., 2003; Kang et al., 2010). However, apart from being costly and time–consuming, these methods require the separation of individual components in a mixture before detection can be carried. Synchronous Scan Fluorescence Spectroscopy (SSFS) is an alternative method for PAHs detection and quantification. It can detect the different components in a mixture. SSFS functions by scanning of excitation and emission spectra simultaneously with the difference between the emission and excitation wavelengths ($\Delta\lambda$) – wavelength diffeerence. Components of a mixture can be identified and quantified by a single synchronous scans at optimized $\Delta\lambda$. Its major benefits are that mixtures of PAHs can be detected without using any separation; faster than other methods; economical; and a convenient method.

For each compound, the emission and excitation peaks and their corresponding parameters are determined and recorded. The difference between the maximum emission and excitation wavelengths for a compound gives the $\Delta\lambda$ value which is used for synchronous scanning. In some cases, scanning around this $\Delta\lambda$ gives more practical value of the $\Delta\lambda$. The scanning speed, scanning wavelength range, excitation and emission slits are optimized before further reading. These optimized values are used for further readings – preparation of calibration curve and determination of the actual analytes in solution. Before using the SSFS method for detection and quantification of analytes in solution, a standard curve should be generated using nearly the same solution as the solution containing the analyte of interest (to cancel out matrix effect). The lowest concentration is tested first and the testing is continued in increasing order of concentration to avoid contamination between samples.

2.5.2 Pesticides

Any substance or mixture of substances intended for preventing, destroying, repelling, or mitigating any pest or weed is a pesticide (Arias–Estévez et al., 2008). Some examples include diazinon, carbaryl, chlorpyrifos, malathion, atrazine, metolachlor, simazine, prometon, 2,4-D, diuron, and tebuthiuron. Pesticides are usually classified based on their target organisms. These classifications include herbicides, insecticides, fungicides, nematicides and rodenticides (details are shown in Table 2.4). Pesticides were first used in agricultural production in the second half of the 19th century. Examples include lead, arsenic, copper, and zinc salts, and naturally produced plant compounds such as nicotine. These were used for insect and disease control on crops. In the 1930s and 1940s 2,4-D, a herbicide, and DDT, an insecticide, were introduced; subsequently, increasing amounts of pesticides were used in agricultural production worldwide (Arias–Estévez et al., 2008).

More than 500 different pesticide formulations are being used in the environment mostly in the agricultural sector (Arias–Estévez et al., 2008). The benefits that these pesticides have played in increasing crop production at a reasonable cost are unquestioned. However, with increasing amounts used, concern about their adverse effects on non–target organisms, including human beings, has also grown. Non-target pesticide poisoning has been identified as the cause of fish kills, reproductive failure in birds and illness in humans. In fact, it has been estimated that less than 0.1% of the pesticide applied to crops actually reach the target pest; the rest enters the environment gratuitously, contaminating soil, water and air, where it can poison or otherwise adversely affect non–target organisms. Furthermore, many pesticides can persist for long periods in an ecosystem—organochlorine insecticides, for instance, were still detectable in surface waters 20 years after their use had been banned; and once a persistent pesticide has entered the food chain, it can undergo ‘‘biomagnification’’, that is, accumulation in the body tissues of organisms, where it may reach concentrations many times higher than in the surrounding environment. It is presumably because of the similarity of the threats they pose to health and the environment that in U.S. law the term ‘‘pesticide’’ is defined to cover not exclusively pesticides, but also defoliants, desiccants and plant growth regulators used for different purposes than pest control (Arias–Estévez et al., 2008).

Table 2.4. Classifications of pesticides (Arias–Estévez et al., 2008)

by target		by mode or time of action	
Type	Target	Type	Action
Bactericide (sanitizers/ disinfectants)	Bacteria	Contact	Kills by contact with pest
Defoliant	Crop foliage	Eradicant	Effective after infection by pathogen
Desiccant	Crop foliage	Fumigants	Enters pest as a gas
Fungicide	Fungi	Nonselective	Toxic to both crop and weed
Herbicide	Weeds	Post-emergence	Effective when applied after crop or weed emergence
Insecticide	Insects	Pre-emergence	Effective when applied after planting and before crop or weed emergence
Miticide (acaricide)	Mites and ticks	Preplant	Effective when applied prior to planting
Molluscicide	Slugs and snails	Protectants	Effective when applied before pathogen infects plant
Nematicide	Nematodes	Selective	Toxic only to weed
Plant growth regulator	Crop growth processes	Soil sterilant	Toxic to all vegetation
Rodenticide	Rodents	Stomach poison	Kills animal pests after ingestion
Wood preservative	Wood-destroying organisms	Systemic	Transported through crop or pest following absorption

2.5.2.1 Environmental residues

Information on the actual input of pesticides into the environment is crucial for proper risk assessment and the rational design of risk reduction measures. Total pesticide use in the United States, for instance, has stayed constant at about 409 million kg per year after increasing significantly through the mid-1970s due to greater herbicide use. Agriculture accounts for 70–80% of total pesticide use. About 60% of the agricultural use of pesticides involves herbicide applications (Sparks, 2003). The greatest concern regarding human exposure to pesticides is their presence in water. In 1999, the U.S. Geological Survey found widespread contamination of U.S. water resources; in particular, more than 95% of samples collected from streams and almost 50% of samples collected from wells, contained at least one pesticide. The U.S. Environmental Protection Agency (EPA, 1980) had previously reported that normal agricultural use had led to the presence of at least 46 pesticides in groundwater and 76 in surface waterbodies (Arias–Estévez et al., 2008).

All pesticides in ground-water, and most residues present in surface water enter via the soil. There are two main routes by which pesticides enter the soil: spray drift to soil during foliage treatment plus wash-off from treated foliage and release from granulates applied directly to the soil. It is of paramount importance to study the dynamics of pesticides in soil: sorption–desorption, transport, and the dependence of transport on entry dynamics and transformation processes (Arias–Estévez et al., 2008). Hence, the reason for pentachlorophenol (PCP) sorption studies on these Nigerian soils.

2.5.2.2 Pentachlorophenol (PCP)

Pentachlorophenol (PCP) is a synthetic substance, made from other chemicals, and does not occur naturally in the environment. PCP and its water soluble salt, sodium pentachlorophenate, are commercially produced organochlorine compounds used primarily as preservatives of wood and wood products, and secondarily as herbicides, insecticides, fungicides, molluscicides, and bactericides. Before 1984, it was one of the most widely used biocides. PCP compounds are sold under a variety of trade names such as Chem-Penta, Chemtrol, Chlorophen, Dow Pentachlorophenol, Dowicide 7, Dowicide EC-7, Dowicide G, Durotox, PCP, Penchlorol, Penta, Penta General Weed Killer, Pentacon, Pentanol, Pentasol, Penwar, Permacide, Permaguard, Permasem, Permatox,

Priltox, Santobrite, Santophen, Sinituho, Term-l-trol, Weed-Beads, Weedone, etc. (Eisler, 1989).

Pentachlorophenol is readily soluble in most organic solvents, oils, and highly aromatic and olefinic petroleum hydrocarbons – a property that makes it compatible for inclusion in many pesticide formulations. Pure PCP is practically insoluble in water; hence, the readily water – soluble sodium pentachlorophenate salt is substituted in many industrial applications. The solubility of its sodium and potassium compounds in water is pH-dependent; it increases from 79 mg/L at pH 5.0 to >4000 mg/L at pH 8.0 (Eisler, 1989). But differential toxicity of PCP in solution is primarily attributable to variations in uptake as a function of pH and not to water solubility. For instance, at pH 4.0, PCP is fully protonated and highly lipophilic, and has its greatest accumulation potential. Conversely, PCP is completely ionized at pH 9.0 and its lipophilicity is markedly reduced.

In soils, PCP can persist for 15 to more than 60 days, depending on soil conditions and application rate. Because of its widespread use and persistence, animals and humans are exposed to significant amounts of PCP. The primary sources of PCP in man include direct intake by way of diet, air, or water and through contact with PCP-contaminated materials. Detectable PCP levels are found in most people living in industrialized societies, probably as a result of food chain exposure to PCP in the environment. Pentachlorophenol tends to accumulate in mammalian tissues unless it is efficiently conjugated into a readily excretable form. In man, however, the observed elimination half-life indicates that steady-state body burdens are 10 to 20 times higher than values extrapolated from animal pharmacokinetic data (Eisler, 1989; Fisher, 1991).

PCP is not a carcinogen, and the evidence for mutagenicity is not conclusive. Cases of PCP poisoning, including fatalities, were characterized by high fever, renal insufficiency, profuse perspiration, rapid heartbeat and breathing, abdominal pain, dizziness, nausea, spasms, and death 3 to 25 hours after onset of symptoms (EPA, 1980). Postmortem examination showed kidney degeneration, inflamed gastric mucosa, edematous lungs, and centrilobular degeneration of liver. Symptoms of nonfatal PCP intoxication in man include conjunctivitis, chronic sinusitus, nasal irritation, upper respiratory complaints, sneezing, coughing, recurring headache, neurological complaints, weakness, and several types of

skin lesions (EPA, 1980). At the cellular level, PCP– like other halogenated phenols – uncouples oxidative phosphorylation. A possible antidote to PCP poisoning is the administration of cholestyramine, a compound that interferes with the enterohepatic cycle of PCP, and also increases its elimination directly across the intestinal wall (Fisher, 1991; Eisler, 1989).

2.5.3 Heavy metals

Heavy metals are metals with specific gravities greater than 4.0. They include elements between copper and lead in the periodic table of the elements; having atomic weights between 63.546 and 200.590. Copper, zinc, cadmium, mercury and lead are all within the confines of this classification. Some of these metals are outrightly harmful to living organisms while others are harmful at high concentrations. Living organisms require trace amounts of some micro–nutrients/heavy metals (Copper, vanadium, chromium, manganese, iron and nickel) but excessive levels can be detrimental to the organism. Excessive levels of these micro–nutrients can have the same detrimental effect as the heavy metals, and thus these micro–nutrients have been interchangeably regarded as heavy metals. In this work, these metals will be regarded as heavy metals.

Heavy metals enter the environment via atmospheric deposition and fertilization as well as by the application of sewage sludge, wastewater, or compost. Transport of sorbed solutes is strongly influenced by sorption properties of the soil such as pH and organic carbon content. Besides solute transport, plant uptake is another important process in the environmental fate of heavy metals. Some metals can be transferred to other oxidation states in soil, thus affecting their mobility, bioavailability, and toxicity (Mclean and Bledsoe, 1992).

The mobilization of metals by mechanism of adsorption and precipitation will prevent movement of metals to ground water. Metals-soil interaction is such that when metals are introduced at the soil surface, downward transportation does not occur to any great extent unless the metal retention capacity of the soil is overloaded, or metal interaction with the soil matrix enhances mobility. It has been reported that changes such as degradation of organic matter, changes in pH, redox potential, or soil solution composition due to various

anthropogenic or natural weathering processes may or may not enhance metal mobility (Mclean and Bledsoe, 1992). Thus, vertical contamination is ultimately related to the soil solution and surface chemistry of the soil.

Also, in the soil, metals are found in one or more forms (Shuman, 1991) as shown below.

i. Dissolved in the soil solution
ii. Occupying exchange sites on the inorganic soil constituents
iii. Specifically adsorbed on inorganic soil constituents
iv. Associated with insoluble soil organic matter
v. Precipitated as pure or mixed solids
vi. Present in the structure of secondary or primary minerals

Most often, these metals are associated with the first five forms depending on the geological history of the area and the anthropogenic activities taking place. The aqueous fractions and those fractions in equilibrium with this fraction, i.e. the exchangeable fractions, are of primary importance when considering the migration potentials of metals associated with soils. As earlier mentioned, metals in soil solution are subject to mass transfer out of the system by leaching to ground water, plant uptake and volatilization. At the same time, metals participate in chemical reaction with the soil solid phase. Hence the concentration of metals in the soil solution at any given time is governed by the number of interrelated processes which include: inorganic and organic complexation, oxidation–reduction reactions, precipitation/dissolution, and adsorption/desorption. In trying to explain the behaviour of metals in soil, most studies have been carried out under equilibrium conditions. These equilibrium thermodynamic data can then be applied not only to predict which precipitation/dissolution, adsorption/dissolution and/or oxidation/reduction reactions are likely to occur, but also to estimate the solution composition i.e. metal concentration in solution at equilibrium. This approach, however, has been found to rely heavily on the accuracy of the thermodynamic data generated (Mclaren and Crawford, 1973).

Metals have the potential to be toxic to living organisms if present at above a threshold level. This threshold varies between taxa and metal speciation. Most urban and industrial runoff contains a component of trace and heavy metals in the dissolved or particulate form

(Defew et al. 2005). Contamination caused by trace metals affects the ocean waters, the continental shelf and the coastal zone, where besides having a longer residence time; metal concentrations are higher due to the input and transport by river runoff and the proximity of industrial and urban zones. The impact of anthropogenic perturbation is most strongly felt by estuarine and coastal environments adjacent to urban areas. Heavy metals from incoming tidal water and fresh water sources are rapidly removed from the water body and are deposited onto the sediments (Guzman and Garcia, 2002). Since heavy metals cannot be degraded biologically, they are transferred and concentrated into plant tissues from soils and pose long-term damaging effects on plants. Nevertheless, different plants react differently to wastewater irrigation; some are more resistant to heavy metals. Heavy metals that accumulate in soils not only exert deleterious effects on plant growth, but also affect the soil microbial communities and soil fertility. Yim and Tam (1999) found that microbial biomass and enzyme activities decreased with increasing heavy metal pollution, but the decrease vary depending on the types of enzymes.

The potential hazard to the marine environment of pollutants depends mostly on their concentration and persistence. Persistence pollutants, such as heavy metals, can remain in the environment unchanged for years and thus may pose a threat to man and other organisms. Inadequate or no sewage treatment, increasing waste from industrial and particularly agricultural activities, oil spill and soil erosion (Thapa and Weber, 1991) are just a few of the chronic problems that developing countries have faced over the last two decades.

All the problems associated with heavy metal pollution will increase considerably in the years to come if measures for control and management are not created. Metal accumulation in agricultural soils together with associated natural metal erosion will remain a chronic pollution problem in the future (Guzman and Jimenez 1992).

2.5.3.1 Functional groups in soil

Surface complexation theory describes adsorption in terms of complex formation reactions between the dissolved solutes and surface functional groups. The existence of surface functional groups is vital for adsorption. A surface functional group is a chemically

reactive molecular unit bound into the structure of a solid phase at its periphery such that the reactive components of this unit are in contact with the solution phase. Its nature controls the stoichiometry of pollutants removal from solution (i.e., whether binding is monodentate or bidentate) as well as influences the electrical properties of the interface. Thus, adsorption capacity is a function of soil functional group density (Bradl, 2004).

Soils are very heterogeneous with a variety of organic matter and hydrous oxide minerals. These soil components possess hydroxyl groups whose protons can be donated to the surrounding solution in exchange for charged molecules. Usually, retention of charged molecules in this manner is a function of pH.

The clay minerals are important sorbents in soils. They include the alumosilicates, micas, zeolites, Fe and Mn oxides, which are known for their well defined structures and surface charge. These minerals possess sites with exchangeable ion in addition to surface protons. The hydroxyl groups found on the soil surfaces have varying reactivities. For instance, alumina surface possess terminal –OH groups which are more likely to accept an additional proton in acidic medium compared to a bridging –OH group. The terminal –OH group (being a weaker acid) will form a positively charged $\equiv Al–OH_2^+$ site as it resists dissociation to the anionic $\equiv Al–H^-$ form. Upon deprotonation, the terminal –OH group binds more strongly to metals than the bridging –OH group. Alumosilicates display both aluminol (≡Al–OH) and silanol (≡Si–OH) edge-surface groups. The deprotonated aluminol group (i.e.,≡Al–O−) binds metals in the form of more stable surface complexes (Bradl, 2004). Another soil mineral, goethite (α–FeOOH) possesses four types of surface hydroxyls, whose reactivities depend on the coordination environment of the oxygen atom in the ≡Fe– OH group. In general, soil colloidal particles provide large specific surface areas and interfaces, which play important roles in regulating the concentrations of several pollutants in natural soils.

Soil organic matter possesses the carboxyl (–COOH), carbonyl and phenolic groups as the major surface functional groups. At the common pH observed for most natural soils (pH 4–7), sorption by carboxylic groups is more important than the sorption by phenolic groups due to the wide difference between their acidity constants. Some of these heavy metals and their effect on environmental media will be discussed below.

2.5.3.2 Lead (Pb)

Lead occurs naturally in the environment. However, most lead concentrations that are found in the environment are a result of anthropogenic activities. Only a few comes from natural sources. Lead is among the most recycled non-ferrous metals and its secondary production has therefore grown steadily in spite of declining lead prices. Its physical and chemical properties are applied in the manufacturing, construction and chemical industries. Lead is most commonly used in batteries and as petrol additives.

Exposure to lead can result in a wide array of biological effects depending on the level and duration of exposure. Various effects occur over a broad range of doses, with the developing young and infants being more sensitive than adults. Lead poisoning, which is so severe as to cause evident illness, is now very rare, though a recent case was reported in Nigeria's Zamfara State. Lead fulfils no essential function in the human body, it can merely do harm after uptake from food, air or water. Lead is a particularly dangerous chemical, as it can accumulate in individual organisms and along food chains (Greaney, 2005).

Soluble Pb(II) added to soils react with clays, phosphates, sulphates and carbonates, etc. At pH values >6, Pb is strongly adsorbed onto clay surfaces. Most works on Pb(II) adsorption studies discovered that amongst the trace metals investigated, Pb(II) was the most retained by the soils under most study conditions (Olu-Owolabi et al., 2010). However, Puls *et al.* (1991) demonstrated decreased adsorption of Pb(II) in the presence of complexing ligands and the competing cations. Generally, Pb(II) has a strong affinity for soluble organic ligands and the formation of such complexes may equally increase the mobility of Pb(II) in soil.

2.5.3.3 Copper (Cu)

Copper is an essential micro–nutrient required in the growth of both plants and animals. In humans, it helps in the production of blood haemoglobin. In plants, Cu(II) is especially important in seed production, disease resistance and regulation of water. Cu(II) is indeed essential, but in high doses it can cause anaemia, liver and kidney damage, and stomach and intestinal irritation. Cu(II) normally occurs in drinking water from copper pipes, as

well as from additives designed to control algal growth. While copper's interaction with the environment is complex, research shows that most copper introduced into the environment is, or rapidly becomes, stable and results in a form which does not pose a risk to the environment. In fact, unlike some man–made materials, Cu(II) does not biomagnify in the body or bioaccumulate in the food chain (Greaney, 2005).

Cu(II) is retained in soils through exchange and specific adsorption mechanism. At concentrations typically found in natural soils, Cu(II) precipitates are unstable. As reported by McBride and Bouldin (1984), Cu(II) is adsorbed to a great extent by soils and soil constituents than other metals with the exception of Pb(II). Cu(II) also has a high affinity for soluble organic ligands and the formation of these complexes may greatly increase Cu(II) mobility in soils.

2.5.3.4 Nickel (Ni)

Nickel is a compound that occurs in the environment only at very low levels and is essential in small doses but it can be dangerous when the maximum tolerable amounts are exceeded. This can cause various kinds of cancer on different sites/parts within the bodies of animals, mainly of those that live near refineries. The most common application of nickel is as ingredient of steel and other metal products. Nickel is released into the air by power plants and trash incinerators and will settle to the ground upon precipitation reactions. It usually takes a long time for nickel to be removed from air. Nickel can also end up in surface water when it is a part of wastewater. The larger part of all nickel compounds that are released to the environment will be adsorbed to sediment or soil particles and become immobile as a result. In acidic ground however, nickel becomes more mobile and will often leach out to the groundwater (McBride and Bouldin, 1984).

Microorganisms can also suffer from growth decline due to the presence of nickel, but they usually develop resistance to nickel after a while. Nickel is not known to accumulate in plants or animals and as a result nickel has not been found to biomagnify up the food chain. For animals, nickel is an essential foodstuff in small amounts (Greaney, 2005).

Nickel does not form soluble precipitate in soils. Hence, the retention of Nickel is exclusively through the adsorption mechanism. Nickel will adsorb to clays, iron and

manganese oxides and organic matter and is hence removed from the soil solution. The formation of complexes of Ni(II) with soluble inorganic and organic ligands will also increase nickel mobility in soils (Greaney, 2005).

2.5.3.5 Mercury (Hg)

Mercury is a toxic substance which has no known function in human biochemistry or physiology and does not occur naturally in living organisms. It rarely occurs free in nature and is found mainly in cinnabar ore (HgS). Mono–methyl–mercury (CH_3Hg) is probably the most common toxic form of mercury found in the marine environment. It has been known to travel through marine food chains and causes damage to human consumers (Diagboya et al., 2015).

Mercury is a metal that occurs naturally in the environment. It enters the environment as a result of normal breakdown of minerals in rocks and soil through exposure to wind and water. The release of Hg(II) from natural sources has remained fairly the same over the years, yet Hg(II) concentrations in the environment are increasing; this is ascribed to anthropogenic activities. Most of the mercury released from anthropogenic activities are released into air through fossil fuel combustion, mining, smelting and solid waste combustion. Some forms of anthropogenic activities release mercury directly into soil or water, for instance the application of agricultural fertilizers and industrial wastewater disposal. All forms of mercury released into the environment will eventually end up in soils or surface waters (Diagboya et al., 2015).

2.5.3.6 Cadmium (Cd)

Cadmium is produced as an inevitable by-product of zinc and occasionally lead refining. Cadmium has a chemical similarity to that of zinc, an essential micronutrient for plants, animals and humans. Cadmium is very biopersistent but has toxicological properties and once absorbed by an organism, remains resident for many years. In fact it has been implicated as the culprit in the "*itai–itai*" case in Japan where Cd poisoning caused severe body pains and disrupted several body functions. The most significant use of cadmium is in nickel/ cadmium batteries, as rechargeable or secondary power sources exhibiting high output, long life, low maintenance and high tolerance to physical and electrical stress. Cadmium provides good corrosion resistance coating to vessels and vehicles, particularly

in high stress environments such as marine and aerospace. Other uses of cadmium are as pigments, stabilizers for PVC (Polyvinyl chloride), in alloys and electronic compounds. Cadmium is also present as an impurity in several products, including phosphate fertilizers, detergents and refined petroleum products (Unuabonah et al., 2008).

Like other trace metals, Cd(II) is adsorbed onto clay minerals. However, this property is to a great extent affected by pH. Under acidic conditions, Cd(II) solubility increases and very little adsorption takes place on soil colloids. At pH >6, Cd(II) is adsorbed by the solid phase and the solution concentration of Cd(II) is greatly reduced. Cd(II) also forms soluble complexes with inorganic and organic ligands; in particular Cl^-. The formation of these complexes with Cd(II) equally increases its mobility in the soil.

2.5.3.7 Vanadium (V)

Vanadium is an element associated with crude oils refining and it is considered a toxic element in the environment. It has inhibitory effect on some organisms and has been used as a proxy tracer of oil pollution. Vanadium can be found in the environment in algae, plants, invertebrates, fishes and many other species. In mussels and crabs, vanadium strongly bioaccumulates which can lead to concentrations of about 10^5 to 10^6 times greater than the concentrations that are found in seawater (Guzman and Jarvis 1996).

Vanadium causes the inhibition of certain enzymes in animals leading to severe neurological effects. Apart from these neurological effects vanadium has been implicated in breathing disorders, paralyses and severe damage to the liver and kidneys. Laboratory tests with laboratory animals have shown that vanadium can cause harm to the reproductive system of male animals, and that it accumulates in the female placenta. Vanadium can cause DNA alteration in some cases, but it cannot cause cancer in animals (Guzman and Jarvis 1996).

2.5.3.8 Zinc (Zn)

Zinc occurs naturally in air, water and soil, but environmental zinc concentrations are becoming alarming due to anthropogenic additions. These high environmental concentrations have been adduced to inputs from industrial activities such as mining, coal and waste combustion and steel processing. Zinc is a very common substance that occurs

naturally. Many foodstuffs contain certain concentrations of zinc. Drinking water also contains certain amounts of zinc which may be higher when it is stored in metal tanks. Industrial sources or toxic waste sites may cause the zinc amounts in drinking water to reach levels that can cause health problems. Zinc is a trace element that is essential for human health. Zinc-shortages can cause birth defects. The world's zinc production is still rising which implies that more zinc will likely end up in the environment (Greaney, 2005).

2.6 Bioavailability and remediation strategies of pollutants in the environment

Bioavailability is a measure of accessibility of chemicals to, or their absorbability by, living organisms (Huang et al., 2003). In the case of microbial degradation of organic pollutants associated with soils and sediments, it is widely assumed that microorganisms can utilize substrates dissolved in the bulk solution phase as well as those bound to external surfaces of aggregate particles but those bound internally in pores have to be transferred out before they can be degraded or accessed. Reports also show that: mass transfer rates constrain the overall rates of degradation of pollutants in soils/sediments, the rates and extents of pollutant mineralization appear to be a function of the pollutant–soil contact time or 'aging', and the soil organic matter (SOM) properties affecting the rates and equilibria of sorption and desorption also influence the degradation and mineralization of organic pollutants (Lueking et al., 2000; Lamoureux and Brownawell, 1999). Lueking et al. (2000) also reported that the rates of mineralization, rates of pollutant desorption, sorption and desorption hysteresis, and the physicochemical properties of SOM are apparently correlated.

Once these chemicals are released into the environment, they stay around for years. They bioaccumulate in the food chain and can be biomagnified in higher tropic biota where they buildup up in fatty tissues.

Concern about soil contamination and remediation relates directly to the extent to which natural background levels are exceeded as well as contaminants mobility or bioavailability to biota and seepage to aquifer. Soil contamination can have dire consequences as mentioned earlier. Hence, attention has been focused on remedying polluted soils. Remediation can either be insitu or ex-situ. Major techniques include soil excavation and

dumping, containment methods (vitrification, stabilization), extraction (either in-situ or ex-situ) and immobilization (Huang et al., 2003).

Techniques such as excavation, extraction and soil containment are generally expensive and harmful to soil properties. Ex-situ extraction is a highly risk laden process that uses hazardous extractants, expensive and has coupled extra cost of treating secondary effluents. Phyto-extraction and electrokinetic are in-situ extraction processes (Huang et al., 2003). Phyto-extraction bio-accumulates the pollutants using specific pollutant hyper-accumulator plants, while electro-kinetics promotes the migration of pollutant ions toward the cathode through application of electrical gradients between two electrodes inserted into the ground. Both methods, however, require very long periods of time to accomplish reasonable remediation.

Immobilization is an inexpensive in-situ remediation technique that uses inexpensive chemicals added to contaminated soil to reduce the solubility or immobilize the contaminants. Unlike other processes, it is nondestructive of the natural landscape, hydrology, as well as the ecosystem. Several immobilizing agents, including bentonite (Mockovciakova et al., 2010), resins (Huang et al., 2011; Sun et al., 2011), hydroxyapatite (Bouyarmane et al., 2010), and zeolites (Ali et al., 2012), have been investigated for remediation. Their mechanism of action is to bond strongly with the contaminants or create sparingly soluble chemical associations leading to the immobilization of the contaminants or their chemical transformation into less mobile forms by pH changes. Hence, the success of chemical immobilization is evaluated by its ability to reduce contaminant bioavailability and human exposure to contaminants in treated contaminated soil.

This method is best applied to medium or low contaminated areas and often used in emergency cases to prevent the contaminated area from spreading. In addition to the aforementioned, it has the following advantages:

i. Simple and fast
ii. Relatively inexpensive
iii. Wide spectrum of pollutants

This method is used for the immobilization of inorganic contaminants such as heavy metals but has rarely being applied to organic contaminants.

2.7 Factors influencing the persistence of organic pollutants in soil

2.7.1 Degradation and sorption

The behaviour of organic pollutants in soils is governed by a variety of complex dynamic physical, chemical and biological processes, including sorption–desorption, volatilization, chemical and biological degradation, uptake by plants, run-off, and leaching. These processes directly control the transport of organic pollutants within the soil and their transfer from the soil to water, air or food. The relative importance of these processes varies with the chemical nature of the organic pollutants and the properties of the soil, but two processes stand out: degradation and sorption (Arias–Estévez et al., 2008).

Degradation is fundamental for attenuating organic pollutants residue levels in soil. It is governed by both abiotic and biotic factors (the latter including enzymatic catalysis by microorganisms) and can follow complex pathways involving a variety of interactions among microorganisms, soil constituents and the organic pollutants. Thus, degradation rates depend on many microbiological, physical and chemical properties of the soil, as well as the properties of the organic pollutants (Arias–Estévez et al., 2008).

Sorption plays a fundamental role in the advective–dispersive transport dynamics, persistence, transformation and bioaccumulation of organic pollutants. The sorption of neutral compounds has been extensively investigated and appears to depend on soil organic matter content. The molecular nature of soil organic matter has been proved to be the key in determining sorption of nonionic organic pollutants. The organic pollutants which are most likely to bind covalently to soil humic matter have functionalities similar to the components of humus. Oxidative coupling reactions contribute to link humus together during humification and are mediated not only by abiotic catalysts (inorganic chemicals, clay, etc.) but also by biotic catalysts, including plant and microbial enzymes. Therefore, microorganisms have been reported to mediate in both soil–bound organic pollutants formation and organic pollutants degradation (Arias–Estévez et al., 2008).

The sorption of weak organic acids in soils has also attracted considerable research; kinetic studies have shown that bentazone and 2,4-D are weakly sorbed by a variety of soils just after their application but the sorption of these and other weak organic acids depends on soil pH (Boivin et al., 2004). This is partly because of their acid–base equilibria but also partly because of the effects of pH on other soil properties such as electric charge and ionic strength. Other soil constituents than organic matter, including clays and Fe-oxides, are important sorbents for the sorption of ionic organic pollutants. Lots of studies have determined sorption isotherms in order to investigate the influence of soil parameters (organic matter content, clay content, pH, etc.) on the sorption of weakly acidic, weakly basic and neutral organic pollutants by a wide array of soils.

2.7.2 Pollutants aging in soil and their bioavailability

Kinetically, the sorption of most organic chemicals is a two-step process: an initial fast step that accounts for the greater part of total sorption is followed by a much slower step tending towards final equilibrium. Increased sorption as organic pollutants ‘‘ages’’ in soil has been observed for a variety of pesticide classes using a variety of methods (Barriuso et al., 1997; Koskinen et al., 2003). Furthermore, with longer contact times between soil and chemical, the fraction of strongly bound residues increases at the expense of extractable residues (Boivin et al., 2004). In some instances, the sorbed fraction of the organic pollutants becomes totally resistant to microbial metabolism, although in others, sorption does not totally preclude biodegradation.

The mechanisms of aging are poorly understood: slow diffusion within small pores of soil aggregates, hydrophobic partitioning into solid humic materials (Kristensen et al., 2001), entrapment in nanopores in hydrophobic surfaces (Brusseau et al., 1991) and sorption at irreversible sorption sites of soil organic matter have all been proposed as possible mechanisms involved in the aging process. With longer residence times in the soil, bound organic pollutants’ residues tend to lose their biological activity and become even more resistant to degradation and extraction (Nam and Alexander, 1998). The bioavailabilities of organic pollutants depend not only on the amount sorbed, but also on its distribution among sorption sites of different strengths (Sharer et al., 2003). Organic pollutants distribution variation during successive wetting–drying cycles is due to the fact that

sorption–desorption processes in soil characteristically exhibit hysteresis**.** As in the case of aging, the exact mechanisms responsible for this remain largely unknown.

2.8 Sorption

As the retention mechanisms of environmental pollutants on soil are often unknown, the term "sorption" is preferred. Sorption general involves the loss of a pollutant from an aqueous to a contiguous solid phase and consists of three important processes: adsorption, surface precipitation, and fixation. Sorption can be defined simply as any removal of a compound from solution to a solid phase constituent**,** whereas desorption is the inverse process — the release of ions or molecules from soil solids into solution (Sposito, 2008). When discussing sorption processes, solid phase is called the sorbent, solute in the liquid phase that could potentially be sorbed is known as sorptive, and solute that accumulate on or within a solid are termed sorbate. The term sorption is useful when the removal mechanism(s) occurring on the solid phase is not established. Sorption phenomenon is complex and comprises the following processes below:

i. adsorption – the accumulation of molecules at the solid-liquid interface;
ii. partitioning or fixation – the accumulation of molecules within existing voids in the solids; and
iii. precipitation – the incorporation of substances within an expanding three-dimensional solid.

It is generally believed among adsorption experts that the removal of a compound from solution to a homogeneous solid phase, such as activated carbon, is mainly adsorption, while for a heterogeneous solid phase, for example soil, such removal is mainly termed sorption.

The major solid phase materials in soils are layer silicate clays, metal–(oxyhydr)oxides, and soil organic matter (SOM). Layer silicate clays are primarily negatively charged because their stacks of aluminum-oxygen and silicon-oxygen sheets are often chemically substituted by ions of lower valence. In many soils, they represent the largest source of negative charge. Metal–(oxyhydr)oxides are variably charged because their surfaces become hydroxylated when exposed to water (Thompson and Goyne, 2012) and assume anionic, neutral, or cationic forms based on the degree of protonation ($\equiv M–O^-$, $\equiv MOH$ or

$\equiv MOH_2^+$, where ≡M represents a metal bound at the edge of a crystal structure), which varies as a function of solution pH. Thus, these variably charged minerals adopt a net positive surface charge at low pH and a net negative surface charge at high pH.

SOM includes living and partially decayed (non-living) materials as well as assemblages of biomolecules and transformation products of organic residue decay known as *humic substances*. SOM contains a multitude of reactive sites ranging from potentially anionic hydroxyls (R-OH) and carboxylic groups (R-COOH) to cationic sulfhydryl (R-SH) and amino groups ($R\text{-}NH_2$), as well as aromatic (-Ar-) and aliphatic ($[\text{-}CH_2\text{-}]_n$) moieties which are the main uncharged and nonpolar regions of the soil solid phase. Variations in the abundance, surface area and chemical composition of these functional groups significantly influence the sorption characteristics of a given soil (Thompson and Goyne, 2012).

2.9 Soil and pollutant characteristics that affect sorption of pollutants

The sorption of a chemical pollutant on a natural solid is a very complicated process involving many sorbent properties besides the physicochemical properties of the chemical itself. These properties are especially the pH, relative amount of the mineral and organic material in soil. The affinity of inorganic pollutants/hydrophobic organic compounds for natural sorbents phases is an important determinant of both the rate of the natural sorbent's detoxification and its response time to changing loadings. The pollutant distribution between sorbent and solvent phases results from its relative affinity for each phase, which in turn relates to the nature of forces which exist between molecules of the solute and those of the solvent and sorbent phases. The type of interaction depends on the nature of the sorbent as well as the physicochemical features of the sorbate (degree of how hydrophobic or polar the sorbate is). Possible interactions between solute and sorbent can be loosely categorized as physical, chemical, and/or electrostatic sorption processes: where the physical involve interactions between dipole (permanent or induced) moments of the sorbate and sorbent, which is amplified in a hydrophobic media by substantial thermodynamic gradients for repulsion from the solution in which they are dissolved; the chemical interactions involve covalent and hydrogen bonds; while electrostatic interactions involve ion–ion and ion–dipole forces (Site, 2001). Sorption sometimes can be explained with the simultaneous contribution of two or more of these mechanisms,

especially when the nonpolar or polar character of the compounds is not well defined. Some sorbate-sorbent physicochemical properties and the way they affect sorption are discussed below.

2.9.1 Clay mineralogy

Fundamentals to the existence of soil are the inorganic mineral fraction. Indeed, of all soil constituents only this one is required. Without the inorganic mineral fraction, soil ceases to be soil. Organic matter, bacteria, and fertilizer chemicals greatly enhance various properties of the soil, but without the inorganic minerals, it is reduced to soilless medium incapable of the diverse range of functions that are often taken for granted. Thus, a complete understanding of soil requires an understanding of soil mineralogy (Stucki, 2012).

Soil minerals are not inert, unchanging, or nonlabile. They provide the backbone for active chemical surfaces where many reactions are catalyzed and basic behaviors of the soil are born and changed. These active surfaces of soil minerals react with organic matter, invoking mutual alterations in the behaviour of both the minerals and organic matter. Liquids are held at their surfaces as well as within the interstitial pores. Oxidation–reduction reactions alter the chemical and physical properties of the constituent Fe – and Mn – bearing minerals, thus creating real time transformations that are critical to many soil processes. Soil minerals come in various particle sizes and morphologies, which add texture and body to the soil, and vary in their degree of crystallinity. Their colours also vary, ranging from intense reddish brown to very light gray, green, yellow, or blue. They are also dynamic in their properties, constantly changing with climate, time, and other environmental conditions. Some changes are rapid; while others are slow. These attributes bring the soil to life, as it were, creating the framework within which biota spring forth and are sustained through every season and in every clime or agroecological zones (Stucki, 2012).

Minerals, the heart of the soil, are dynamic and essential resources, classified according to their properties. They include the phyllosilicates, the plate–shaped minerals; iron, aluminum, and other (oxyhydr)oxides, which represent the more highly weathered constituents; and amorphous minerals, which display active chemical properties but lack

high order in their crystals. These minerals occur in association with the reactive organic materials in soils, and it is inferred that knowledge of the properties of these reactive materials should enable close predictions of useful soil properties, whether for agriculture, immobilizing contaminants, or other purposes. Soil is a heterogeneous milieu that is a dynamic part of the biosphere continually changing in response to climatic variations over all scales of time and space. It is not all surprising that the minerals in the soil can be quite different in their chemical and physical characteristics from those of the same minerals formed in environments with which they share the same name and ideal crystalline structure (Stucki, 2012). Major minerals found in the studied soils and their characteristics are shown in Table 2.5.

Soil mineralogy (the types and relative amounts of the minerals present in soil) is determined routinely because of its strong influence on soil behavior, its use in soil classification, and its relevance to soil genetic processes. X-ray diffraction (XRD) is the most powerful technique used for analysis of minerals and offers mineral phase identification and quantification, providing detailed information about the atomic structure of crystalline substances. It takes two types of approaches namely

(i) Clay fraction approach where the clay fractions are physically separated from the rest of the sample and made into an orientated layer of clay supported by a substrate; and

(ii) Whole soil approach where the sample is prepared into a random powder which helps in analysis of total amounts and identification of non-clay minerals present.

This latter approach has been employed in this study.

XRD has a wide range of applications in environmental sciences such as in Agriculture where it is used in qualitative and quantitative analysis of actual minerals in soils (Meeker et al., 2006). Basically, *X*-ray diffraction uses a beam of x-rays to determine the crystal structure of minerals. Minerals are uniquely identified by the wavelength distribution and relative intensities of *X*-ray reflections produced during the analysis.

Table 2.5. Some common soil minerals (Stucki, 2012)

Mineral group	Mineral	Chemical Formula	Characteristics	Occurrence
Carbonate	Aragonite	$CaCO_3$	Highly soluble compared to the alumino-silicates	prevalent in arid and semi arid regions
Carbonate	Calcite	$CaCO_3$		
Carbonate	Dolomite	$CaMg(CO_3)_2$		
Carbonate	Siderite	Fe_2CO_3		not very common
(oxyhydr)oxides	Gibbsite	$Al(OH)_3$	Hexagonal crystals	Where Si low, especially in strongly leached soils
(oxyhydr)oxides	Goethite	αFeOOH	Yellow to yellow brown colour	Widespread – most common iron oxide
(oxyhydr)oxides	Hematite	αFe_2O_3	Bright red colour	Soils of warmer climates
	Illite	$K_{0.6}(Ca,Na)_{0.1}S_{3.4}Al_2$ $Fe^{111}Mg_{0.2}O_{10}(OH)_2$	2:1 expansible clay mineral	Widespread, high in weakly weathered soils
Kaolin	Kaolinite	$Al_2S_2O_5(OH)_4$	Very small euhedral particles associated with much Fe. 1:1 clay mineral, very little expansion in water, except when complexed with other expansive clays	Widespread, high in well weathered soils
Kaolin	Montmo-rillonite	$M_{0.25}Si_4Al_{1.5}Mg_{0.5}O_{10}(OH)_2$	2:1 expansible clay mineral	Most common expansible clay mineral
Oxides/hydroxides	Quartz	SiO_2	It's a continuous framework of SiO_4 (silicon–oxygen tetrahedral with each oxygen being shared by two tetrahedra)	Second most abundant mineral after feldspar

Clay minerals can be considered good sorbents for non-ionic compounds. Methylene containing organic compounds has been assumed to form hydrogen bonding with Ca-montmorillonite of the type C–H···O–Si.

The structural compositions of clay mineral determine the degree of adsorption of these non-ionic compounds onto its surface. For instance, sorption of acetoaceticethylester and β, β-oxydipropionitrile on clay gibbsite, kaolinite, Ca-and Na-montmorillonite have shown sorption trend in the order: gibbsite > Kaolinite > montmorillonite (Brindley et al. 1963). It was assumed that the hydroxyl surfaces, which comprise the basal area of gibbsite and half the basal area of Kaolinite, sorb more effectively than the oxygen surfaces which occur in montmorillonite and comprise half the basal area of kaolinite. The hydroxyl surfaces aid sorption via hydrogen bonding while the oxygen surfaces of montmorillonite are less effective in sorbing organic molecules by hydrogen bonding, due to the competition of water molecules as well as the presence of exchangeable cations on montmorillonite, Ca and Na, which readily form hydration complexes thus screening a large portion of the surface area. In comparison, Kaolinite has fewer exchangeable cations in the extended basal surfaces while gibbsite is thought to have none (Brindley et al. 1963). If the same set of clays were to be used for sorption of heavy metal cations, the same sorption trend is expected to be observed due to similar charges present on the sorbates.

2.9.2 Organic matter

Soil organic matter (SOM) is defined as the summation of plant and animal residues at various stages of decomposition, cells and tissues of soil organisms, and well-decomposed substances (Brady and Weil, 2008). SOM is found in all soils, though amount and type may vary considerably. Colloidal soil organic matter has a major influence on the chemical properties of soils and can be divided into non-humic and humic substances. The non-humic substances comprises unaltered biochemicals such as amino acids, carbohydrates, organic acid, fats and waxes that have not changed from the form in which it were synthesized by living organisms. Humic substances are a series of moderately high molecular weight compounds such as polycyclic aromatic hydrocarbons, peptides and proteins that were formed by secondary synthetic reactions involving microorganisms and

thus have characteristics which are dissimilar to any compound in living organisms. They have a variety of functional groups such as carboxyl, hydroxyl, and esters which provide sites for metal adsorption as well as interactions for organics. Binding of metals to SOM involves reactions ranging from weak forces of attraction to strong chemical bonds. Soils organic matter can be the main source of cation exchange capacity, contributing >200mg/100g of organic matter in surface mineral soils (Stevenson, 1991).

SOM is more important than any other soil component in the sorption of non-polar compounds. The K_d values of a particular non-polar organics have been found to be different for different sorbents and are directly proportional to the SOM content. Hydrophobic organic chemicals (HOCs) sorption by soils and sediments is driven by hydrophobic interactions (Site, 2001; Huang et al., 2003) including the

(i) entropic effects of the aqueous phase,
(ii) non-specific interactions of the HOCs with soil/sediment organic matter (SOM),
(iii) sorptions on the external surfaces as well as the
(iv) internal voids of a molecular sieve-type structural arrangement of SOM materials.

The removal of SOM using a series of SOM removal agents (ether, ethanol, hot water, 2% HCl, and hydrogen peroxide) have demonstrated the role of SOM on sorption of non-polar organic pollutants because results showed that these procedures affected the sorption of the pollutants. Though other soil properties are also responsible for adsorption, their role could be masked by the presence of SOM as has been reported for parathion (Site, 2001).

2.9.3 Ion exchange capacity; non-ionizable and ionizable compounds

Sorption of polar and ionizable compounds depends to varying degrees on moisture content in the adsorbing system, the presence of exchangeable cations, electrolyte concentration and pH. Water solubility may also affect sorption. When soils are fully hydrated, adsorption of the non-polar organic solutes by soil minerals becomes relatively insignificant compared to the uptake by partitioning into soil organic matter, presumably because water is preferentially adsorbed by minerals. However, for polar organic solutes

like parathion, it is suggested that the sorption on dry soils occurs by cation–dipole interaction, a much stronger interaction than hydrogen bonding in wet soils (Site, 2001).

The effects of pH and exchangeable cation on the sorption of organic pollutants vary depending on the polarity of the organic pollutant. Sorption of two substituted urea and five triazines on large surface area ($8\ X\ 10^6\ m^2\ kg^{-1}$) 2:1 expandable lattice clay (montmorillonite) showed that both factors did not affect the ureas, whereas triazines sorptions were influenced by both (Site, 2001). It was postulated that the less polar ureas were sorbed by physical forces and possibly the formation of coordination complexes with exchangeable cations, while the basic triazines were sorbed by a combination of these two mechanisms as well as protonation and consequent ion exchange reactions, the relative importance of each process being determined by pH, exchangeable cation and the characteristics of the sorbate molecule (Hance, 1969). Lowering pH increased the extent of sorption until a sorption maximum is reached. Further reduction in pH resulted in the releasing of a portion of each of the compounds into solution. The maximum sorption of each compound by the montmorillonite clay occurs in the vicinity of the pK_a value (Weber, 1970). At pH values higher than pK_a the compound is present primarily in the molecular form and is sorbed by hydrogen bonding or through polar sorption forces. A decrease in pH results in increasing the protonation; the sorption of the resulting monovalent cation occurs by displacing a Na^+ ion from the clay surface. At pH values lower than the pKa the increased concentration of H^+ ions may compete with the cation for sites on the clay. The presence of other ions like Na^+ or Ba^{2+} has the effect of decreasing the amount of protonated compound adsorbed because of some competition effect at the sorption sites (e.g. carboxyl groups) of the organic colloids.

Several mechanisms have been suggested for adsorption of polar organic compounds by clay alumino-silicates: physical sorption, hydrogen bonding, coordination complexes, association or bridging complexes and chemical sorption. Some of them may occur simultaneously, depending on the nature of the functional groups of the molecules, the type of clay mineral, and the pH of the system (Bailey et al., 1968). It is also known that regardless of chemical character of the polar organic compound sorption occurred to the greatest extent on the highly acid H–montmorillonite compared to the near neutral Na–

montmorillonite. The magnitude of sorption of organic compounds with widely different chemical character is governed by their degree of water solubility, the dissociation constant of the adsorbate, and the pH of the clay system (Site, 2001).

Soil sorption of low polarity organics depends little on soil pH and the presence of exchangeable ions. SOM content is of primary importance because of the high correlations between sorption on soils/sediments and SOM content (Yuen and Hilton, 1962; Liu et al., 1970).

A study of the effect of pH on sediment and aquifer materials sorption of nine chlorinated phenols in the pH range of 6.5 and 8.5 has shown that both the non-dissociated phenols as well as their conjugate bases (phenolates) were sorbed. However, there was a marked increase of the overall distribution coefficients with decreased pH, suggesting that the contribution of the sorption of the deprotonated species is generally small except for those cases where the difference between pH and pK_a is large. This was true for 2,3,4,6-tetra-chloro-phenol (2,3,4,6-TeCP) and pentachlorophenol (PCP). Thus, as a first approximation, the experimental data were analyzed by using a simple partitioning model neglecting phenolate sorption as well as a possible dissociation of the phenol in the organic phase (Schellenberg et al., 1984).

2.9.4 Dissolved organic matter

Several dissolved substances are found in natural waters. Notable among these are the high molecular weight organic substances – humin, humic and fulvic acids, etc. These are particularly referred to as dissolved organic matter (DOM) and they can bind organic chemicals through interactions such as hydrogen bonding, van der Waals forces or hydrophobic association (Wijayaratne and Means, 1984). For neutral PAH molecules it is believed that binding is dominated by van der Waals type interactions (Gauthier et al., 1987). For instance, the binding of benzo(a)pyrene (BaP) to DOM has been shown to be completely reversible and the extent of reversibility is unrelated to the sorption time (McCarthy and Jimenez, 1985). The binding rate of BaP was also found to be very rapid and reached equilibrium within 10 min.

Site (2001) has observed that a significant fraction of organic chemicals found in natural waters may be bound to DOM and that the extent of binding depends on the source of the humic material, the pH, the ionic strength, and the concentration of humic materials. When increase of the hydrogen and metals ions concentrations change the structure of the humic polymer, which becomes less hydrophilic as its charge is neutralized, this less hydrophilic form of the polymer would then bind the hydrophobic organic contaminant more effectively.

Ding and Wu (1995) have shown that when DOM released from the soil/sediment bulk organic matter is similar to that of the soil/sediment bulk organic matter, the ratio of the association constants of the DOM to that of the SOM is approximately unity, but if the DOM is more hydrophilic than the soil/sediment bulk organic matter, this ratio will be less than unity. However, for SOM and DOM from different sources with varying nature, this ratio will have a wide variation.

Generally, binding of hydrophobic organic contaminants to dissolved humic substances reduces their bioavailability and toxicity. The nature of the DOM especially in the prevailing solution pH determines to a large extent the effectiveness of this binding. A hydrophilic DOM will be less effective for this binding for some organic contaminants like PCP whose ionic form is prevalent at around neutral pH. This ionic form does not bind effectively with DOM (Site, 2001).

2.9.5 Sorptive Concentration

Irrespective of the heterogeneity in the chemical composition of the solid phase, sorptive concentration is perhaps the most influential factor on the accumulation of a sorbate on or within a sorbent. At low solution concentration, Le Chatelier's Principle of chemical equilibrium predicts that increasing (or decreasing) sorptive concentration will result in an increase (or decrease) in sorbate concentration. For instance, adding fertilizer to a soil will increase the solution potassium (K^+) concentration and subsequently increase the amount of K sorbed by the solid phase. Conversely, as growing plants uptake K^+ from the soil solution, this will drive desorption of the sorbate K^+ from the soil. In this way, the soil serves as a nutrient reserve for plants and soil organisms (Thompson and Goyne, 2012).

A common method for assessing sorption characteristics of a soil is to measure the relationship (or distribution) between the equilibrium concentration of the sorptive (C_{eq}) and the sorbate (C_{eds}) across a range of sorptive concentrations while holding temperature and other parameters constant. The resulting dataset is termed the sorption isotherm and is often used in a predictive fashion to describe sorption behavior. For many organic compounds and ions in solution at low concentration (Thompson and Goyne, 2012), this relationship is linear and summarized by a distribution coefficient (K_d) (equation 2.1):

$$K_d = \frac{C_{ads}}{C_{eq}} \qquad 2.1$$

However, at higher ion concentrations the relationship between (C_{eq}) and (C_{eds}) can exhibit significant nonlinearity (Thompson and Goyne, 2012), often approaching a maximum sorption plateau after which subsequent increases in sorptive concentration do not result in additional sorption.

2.9.6 Sorptive and Sorbent Charge

For ionic sorptives, the sign and magnitude of electrical charge on the sorptive and sorbent are important determinants of sorptive fate. Anions will be attracted to positively charged sorbents and cations will be attracted to negatively charged sorbents.

Ionic sorptives are attracted to oppositely charged sorbents by long-range electrostatic forces. For example, on negatively charged sorbents, these forces result in a preferential accumulation of cations relative to anions near the sorbent surface. However, diffusive and dispersive forces act to homogenize this ion distribution such that the ratio of cations to anions decreases exponentially with distance from the sorbent until the bulk solution ion balance is obtained. A precise description of the resulting ion distribution is complex and remains incomplete, but is commonly approximated by concepts involving an inner layer of cations immediately adjacent the sorbent surface — often termed the Stern layer — and a diffuse collection of cations and anions — termed the diffuse layer — which undergo diffusive exchange with the bulk solution (Thompson and Goyne, 2012). Figure 2.4 describes this scheme.

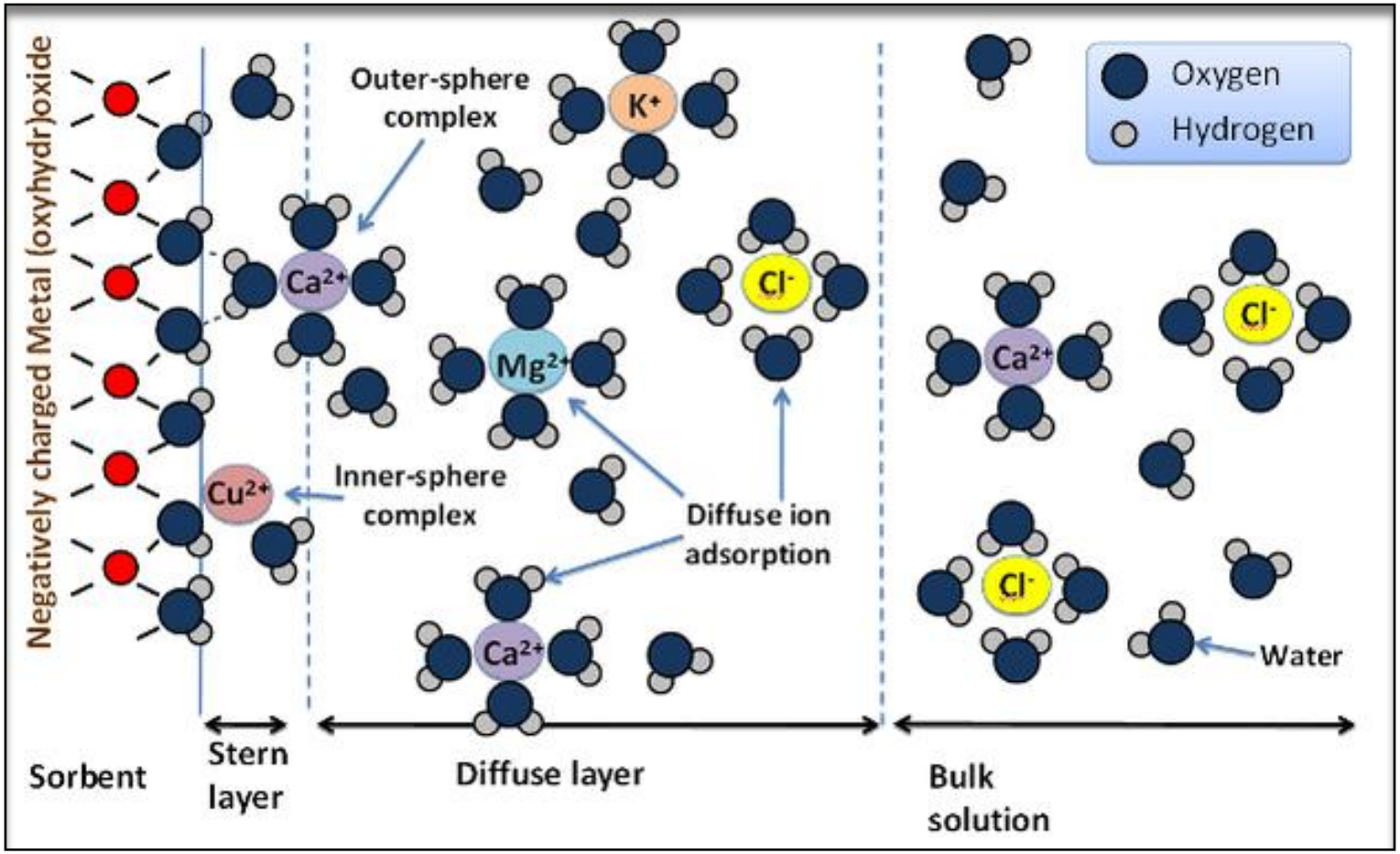

Figure 2.4. Schematic arrangement of sorbates at a charged sorbent interface**.** To accommodate a negatively charged sorbent, cations accumulate closer to the surface than anions. Inner-sphere and outer-sphere complexes occupy the first layer of sorbates, with the remainder of the sorbent charge balanced by preferential cation accumulation in the diffuse layer (Thompson and Goyne, 2012)

Sorbates within the Stern layer that shed one or more of their surrounding water molecules (i.e., waters of hydration) and form direct ionic and/or covalent (electron sharing) bonds with the sorbent are considered inner-sphere adsorption complexes, while those ions retaining their hydration spheres and maintaining proximity to the surface solely through electrostatic interactions are considered outer-sphere adsorption complexes (Sposito 2004).

2.9.7 Solution pH

The pH of the sorptive solution has pronounced effect on sorption because it influences both the magnitude and sign of sorptive and sorbent charge. As the solution pH increases, sorbent hydroxyl and carboxyl functional groups of metal-(oxyhydr)oxides and SOM deprontonates. In turn, this increases negative charge density on the sorbent thus facilitating cation adsorption, while decreasing anion adsorption. Consequently, the ability of a soil to retain cations (e.g., Ca^{2+}, Mg^{2+}, K^{+}, Pb^{2+}, Cd^{2+}, Zn^{2+}, Cu^{2+}, etc) generally improves when soil pH is increased. Sorptives that can undergo acid dissociation or hydrolysis reactions also exhibit strong pH-dependent sorption trends (Thompson and Goyne, 2012). For pentachlorophenol, a pesticide, at pH value of 7.0 approximately 95 % of PCP in solution exist in the anionic form while most soil components are in their charged forms. The reverse is obtainable at pH value of 2.0 when the soil surface sorption sites are uncharged (low polarity) as well as the PCP molecules due to stiff competition for these sites by protons in solution (Li et al., 2009; Wang et al., 2008). Thus, depending on the soil components responsible for sorption of PCP in a particular soil and the prevailing pH condition, sorption of PCP is expected to vary.

Soil pH is the most important parameter influencing metal–solution and soil–surface chemistry. The number of negatively charged surface sites increases with pH. In general, heavy metal adsorption is small at low pH values. Adsorption then increases at intermediate pH from near zero to near complete adsorption over a relatively small pH range; this pH range is referred to as the pH–adsorption edge. At high pH values, the metal ions are completely removed.

In general, adsorption of heavy metals onto oxide and humic constituents of soil follows the basic trend of metal-like adsorption, which is characterized by increased adsorption

with pH. The pH is a primary variable, which determines cation and anion adsorption onto oxide minerals (Bradl, 2004).

2.9.8 Sorptive Size

For inorganic sorptive of equivalent charge and concentration, the ion size becomes an important determinant of their comparative sorption behaviour. This is conveniently encapsulated within the concept of ionic potential (IP), defined as the ratio of ion charge to ion radius (Site, 2001). It is generally observed that affinity for a sorbent increases with decreasing ionic potential for a given valence (e.g., IP_{Ca}^{2+} = 20 and IP_{Mg}^{2+} =48). This derives from two general principles:

i. it requires less energy to remove a water molecule from a hydration sphere of a large ion than it does for an equivalently charged ion of smaller size. This provides larger ions with an energetic advantage in forming inner-sphere bonds with the sorbent.

ii. as ionic radius increases the electron cloud extends further away from the nucleus and can more easily distort and engage in covalent bonds with the sorbent.

As a consequence, sorptive ion affinity for many sorbents follows common trends based on ionic radius within a single group of the periodic table, and such ionic radius based selectivity is most readily observed for Group IA, IIA, and IIB elements. For example, Group IA element affinity decreases as a function of ionic radii: Cs^+ (0.167 nm)> Rb^+ (0.148 nm) > K^+ (0.138 nm)> Na^+ (0.102 nm) > Li^+ (0.059 nm) (Sparks, 2003). Such relationships can be useful for predicting cation behavior in soil, as constituents bound in inner-sphere surface complexes are inherently more difficult to desorb, hence they are less mobile than ions sorbed via outer-sphere complexes.

2.9.9 Sorbent Mass

Sorption of environmental pollutants on soil/sediment is generally seen as a distribution or partition between two different homogeneous phases. This implies that the distribution coefficients should not be dependent on the mass of sorbent. However, several laboratory studies show an inverse relationship between partition coefficient and mass of adsorbing solids (Olu-Owolabi et al., 2012). This is ‘‘solids effect’’ and it’s very pronounced for

constituents characterized by large partitioning. For constituents that are represented by intermediate partitioning, the effect is less, while it approaches a constant value for substances of low partitioning. This effect has been found with a variety of elements and organic compounds adsorbed on various sorbents. This effect may have very serious consequences in assessing the fate of hydrophobic pollutants in natural water systems since the pollutant sorbed on suspended solids and accumulated in sediments can be released to the interstitial water (Site, 2001).

A soil sorption study of two pollutants (linuron and atrazine) as a function of the soil to water ratio (Grover and Hance, 1970) showed a fivefold increase in the sorption of linuron in a 1:10 rather than a 4:1 ratio. The sorption in a 1:1 soil:water mixture was intermediate. For atrazine the difference between slurry conditions and the 4:1 ratio was approximately threefold.

Solids effect has been demonstrated by batch adsorption tests for phenol adsorption on Kaolinite, heavy metal sorption to quartz and montmorillonite, and PCB sorption to lake sediments (Celorie et al., 1989).

Solids effect is less pronounced on column studies than batches. However, soil column studies require a long time to be completed, thus, a centrifugation procedure of the soil column was suggested to alleviate these disadvantages, by imposing a confining stress on the soil and by producing a greater pore water velocity (Site, 2001).

2.10 Hysteresis in sorption–desorption process

A sorption process is sometimes reversible, however often a ‘‘hysteresis’’ effect is observed. It’s more pronounced in soils with high SOM. Hysteretic desorption phenomenon is practically important because the increased K_D for desorption corresponds to a lowered chemical activity of the sorbed chemical at a fixed q_d condition, suggesting a reduced biological reactivity and decreased toxicity of the chemical (Huang et al., 2003).

Studies have shown that entrapment of sorbates within inorganic matrices and SOM causing the slower rate of desorption than the sorption are most likely the major mechanisms for the observed hysteresis for sorbates (Huang et al., 2003). Entrapment of

sorbed molecules within the meso/micro-porous structures of the inorganic aggregates may be important for soils and sediments having high contents of minerals (clays) with high internal surface areas and very low SOM. Irreversible chemical binding to humic acids is also predicted to be an important cause of hysteresis for ionizable and polar organic pollutants (Huang et al., 2003).

Rates of hysteresis varies with different sorbent as well as sorbate. For instance, no hystereses were observed for the desorptions of pyrene and methoxychlor from sediment coarse silt fraction (Karickhoff et al., 1979). Karickhoff (1980) also noted that sorption of PAHs on sediments was achieved within a few hours, but drastic changes in the ease of desorptions using hexane of sorbed PAHs were frequently observed with increased incubation time. Fairbanks and O'Connor (1984) showed that desorption of PCBs from soil was minimal, between 2% and 9.5% per cycle depending on the equilibrium solution concentration. The addition of sewage sludge to the soil increased PCB adsorption as well as hysteresis in proportion to incubation time suggesting that the transport of PCBs by soil water in the presence of sewage sludge is minimal.

Hance (1967) reported that the desorption of four herbicides, monuron, linuron, atrazine, and chlorpropham, from two soils, a soil organic matter fraction and bentonite appeared to be some-what slower than adsorption. A period of 24 h or less was taken for equilibria to be established in sorption processes. However, for most of the cases desorption equilibrium was attained after 72h.

Miles et al. (1981) showed that urea herbicides were easily desorbed from a sandy loam soil (1.77% SOM) and a heavy clay soil (4.15% SOM), but not from a high organic loam soil (10.5% SOM). The same trend of decreasing desorption rate with increasing SOM content in four soils was found for fensulfothion and its sulfide and sulfone derivatives.

Fluometuron sorbed on a loam soil showed hysteresis effect. The same effect was found with fluometuron when a soil was subjected to seven consecutive desorption equilibrations (Site, 2001). It was suggested that the shift in the sorption equilibrium with repeated equilibration was most likely due to a physical change in the sorptive character of the soil complex. This change may be associated with increased dispersion or weathering of the

clay–organic matter micro-aggregates with repeated wetting and shaking, resulting in an increased number of sites available for sorption.

The observed slow rates of desorption may be attributed to retarded sorbate diffusion within both inorganic minerals and SOM matrices due to the fact that resistance to molecular diffusion within the pores having sizes slightly larger than that of sorbates is much greater than within the pores of sizes several times larger than sorbing molecules (Huang et al., 2003).

2.11 Understanding solids effect and hysteresis in sorption–desorption processes

Solids effect and hysteresis in the adsorption of organic and inorganic sorbates by different sorbents might be due to the same factors which are connected to the experimental methods in most experimental setups. Site (2001) has identified some major factors in solids effect and the sorption–desorption hysteresis processes.

The experimental method involved has been suggested to play a role. For instance, the batch equilibrium method involves repeated centrifugation and re-suspension of the soil followed by prolonged agitation, which may breakdown the soil particles, thus increasing the number of sorption sites during the desorption phase leading to hysteresis.

The microbiological transformations of the compound may sometimes be important to explain hysteresis in sorption–desorption isotherms, but cannot be a significant factor for most persistent organics because of the practice of using antibiotics to sterilize the soil and hence minimize microbial activity during the sorption experiments.

Another explanation of the solids effect and the sorption–desorption hysteresis might be due to the presence of DOM released from the soil. UV spectra have revealed the presence of more than 50% of paraquat in the water phase sorbed on particulates not removed by centrifugation leading to apparent significant interferences in measurements in an adsorption experiment of paraquat using a hectorite suspension.

2.12 Effect of temperature on sorption

Temperature is an important parameter that influences the sorption equilibrium as well as the state of the pollutant in solution. Most laboratory experiments dealing with sorption

processes are done at room temperature, which is either lower or higher than the mean temperatures of surface soils depending on whether the soil is temperate or tropic. Thus, in order to understand the sorption process and make meaningful predictions from data obtained, it is pertinent to understand the effects of temperature on the sorption of pollutants in the environment.

Generally sorption coefficients decrease with increasing temperature (Podoll et al., 1989; Kipling 1965; He et al., 1995). An inverse relationship exists for organic compounds between sorption coefficients (K_d) and solubilities (Chiou et al., 1979). Lower K_d values have been found at higher temperatures for most organic compounds for which solubility increases with temperature, while increased sorption at higher temperatures can be expected for compounds for which solubility decreases with temperature (Podoll et al., 1989; Chiou et al., 1979). Therefore, due to the dependence of both sorption coefficients and solubility on temperature, the measured effect of temperature on sorption isotherms is the result of combined sorption and solubility contributions (Site, 2001). However, some examples of increasing equilibrium sorption with increasing temperature and of no effect of temperature on sorption equilibrium have also been reported (Hulscher and Cornelissen, 1996).

The effect of temperature on the partitioning behavior (aqueous activity coefficients or solubilities) of PAHs and other pollutants can be explained in terms of the thermodynamics. The free energy driving the (linear) partitioning process for large non–polar compounds like PAHs is largely determined by the excess free energy of dissolution with a larger contribution of enthalpy than of entropy, in contrast to the dominance of entropy governing the hydrophobicity of small organic compounds like benzene. In general, the effect of temperature on the enthalpy of sorption can be directly compared to the (negative) excess free enthalpy of dissolution, which is a measure for the deviation from ideal behavior in the aqueous phase. This is based on the assumption that for PAHs, as opposed to more polar compounds, the contribution of dissolved organic matter enthalpy to the enthalpy of sorption is much smaller than the general enthalpy of sorption. The interactions between PAHs dissolved organic matter are therefore more nearly ideal than the interactions between PAHs and water (Haftka et al., 2010).

Thus, sorption of a chemical on a solid sorbent occurs when the free energy (ΔG) of the sorptive exchange is negative (equation 2.2)

$$\Delta G = \Delta H - T\Delta S \qquad 2.2$$

where ΔG is the change of the Gibbs free energy (kJ mol^{-1}); ΔH is the change in enthalpy (kJ mol^{-1}), and ΔS is the change in entropy (kJ mol^{-1} K^{-1}). ΔH represents the difference in binding energies between the sorbent and the sorbate and between the solvent and the solute. Thus, sorption may occur as the result of two types of forces: enthalpy-related and entropy-related forces. Hydrophobic bonding is an example of an entropy-driven process; it is due to a combination of London dispersion forces (instantaneous dipole-induced dipole) associated with large entropy changes resulting from the removal of the sorptive from the solution. For polar chemicals, the enthalpy-related forces are greater, due to the additional contribution of electrostatic interactions (Olu-Owolabi et al., 2012).

The equation 2.2 above can be obtained by calculating the equilibrium constant (K_C) from equation 2.3, where C_{ads} and C_e are the amount of sorbate sorbed and the amount remaining in solution after equilibrium.

$$K_C = \frac{C_{ads}}{C_e} \qquad 2.3$$

The values of the enthalpy (ΔH^o) and entropy (ΔS^o) can be calculated from the slope and intercept of the plot of $\log K_C$ vs. $1/T$ by using the equation 2.4, where R is the ideal gas constant (equal to 8.3145 J mol^{-1} K^{-1}) and T (K) is the temperature.

$$\log K_C = -\frac{\Delta H^o}{2.303RT} + \frac{\Delta S^o}{2.303R} \qquad 2.4$$

The Gibbs free energy, ΔG^o, and the entropy, ΔS^o, values of a specific sorption can be calculated from the (K_C) value using equations 2.5 and 2.6, respectively.

$$\Delta G^\circ = -RT \ln K_c \qquad 2.5$$

$$\Delta S^\circ = \frac{(\Delta H^\circ - \Delta G^\circ)}{T} \qquad 2.6$$

Table 2.6. Comparison between Physisorption and Chemisorption

Physisorption	Chemisorption
1. Low heat of adsorption usually in the range of 20-40 kJ mol^{-1}	High heat of adsorption in the range of 40-400 kJ mol^{-1}
2. Force of attraction are van der Waal's forces	Forces of attraction are similar to or of the same magnitude as chemical bond forces
3. It usually takes place at low temperature and decreases with increasing temperature	It takes place at higher temperature
4. It is reversible	It is irreversible
5. It is related to the ease of liquefaction of the gas	The extent of adsorption is generally not related to liquefaction of the gas
6. It is not very specific	It is highly specific
7. It forms multi-molecular layers	It forms monomolecular layers
8. It does not require any activation energy	It requires activation energy

2.13 Types of adsorption

Depending upon the nature of forces existing between adsorbate molecules and adsorbent, the adsorption can be classified into two types – physical adsorption and chemical adsorption. A comparison of both adsorption types is shown in Table 2.6.

2.13.1 Physical adsorption (physisorption)

If the force of attraction existing between adsorbate and adsorbent are van der Waal's forces, the adsorption is called physical adsorption. It is also known as van der Waal's adsorption. In physical adsorption, the force of attraction between the adsorbate and adsorbent is very weak, therefore this type of adsorption can be easily reversed by heating or by decreasing the pressure.

Physisorption is always exothermic, but the energy involved is generally not much larger than the energy of condensation of the adsorbate. However, it is appreciably enhanced when physorption takes place in very narrow pores. Physisoption systems generally attain equilibrium fairly rapidly, but equilibrium may be slow if the solution to surface diffusion process is rate-determining.

2.13.2 Chemical adsorption (chemisorption)

If the force of attraction existing between adsorbate and adsorbent is almost same strength as chemical bonds, the adsorption is called chemical adsorption. In chemisorption the force of attraction is very strong, therefore adsorption cannot be easily reversed. Activation energy is often involved in chemisorption and at low temperature the system may not have sufficient thermal energy to attain thermodynamic equilibrium.

2.14 Sorption isotherms

Sorption isotherms describe the relationship between sorbate and equilibrium analyte concentration at a constant temperature. The nature of this relationship depends on the interaction between the sorbate and equilibrium analyte concentration. The amount of sorbate that can be absorbed by a sorbent depends on its chemical and physico-chemical compositions. Consequently, the isotherm shape is unique to each sorbate type due to differences in capillary, surface, and colligative effects (Figure 2.5a). Simply put, the equilibrium between the fluid phase and the adsorbent phase is expressed by adsorption isotherms. The first classification of physical adsorption isotherms was by Brunauer et al.

(1940), that is, the Brunauer, Deming, Deming, and Teller (BDDT) system. The BDDT system describes five different types of adsorption isotherms as discussed below.
However, in 1985 the International Union of Pure and Applied Chemists (IUPAC) Commission on Colliod and Surface Chemistry proposed modification of this classification by addition to the original BDDT classification a sixth type, the stepped isotherm.

2.14.1 BDDT Basic Adsorption Isotherms

Type I (the Langmuir isotherm) is typical of microporous adsorbents (activated carbon and zeolites) or very hygroscopic materials. A typical type I adsorption isotherm is depicted in Figure 2.5a. The y-axis represents the amount adsorbed (q_e) while the x-axis represents the amount unadsorbed or concentration in solution (P).

i. Type I adsorption isotherms depicts monolayer adsorptions.
ii. The isotherm can be explained by the Langmuir adsorption isotherm.

Type II is sigmoidal and typical of nonporous (macroporous) materials with strong fluid-surface forces. A typical type II adsorption isotherm is depicted in Figure 2.5b.

i. Type II adsorption isotherms show large deviation from the Langmuir adsorption model.
ii. The intermediate flat region in the isotherm corresponds to monolayer formation.

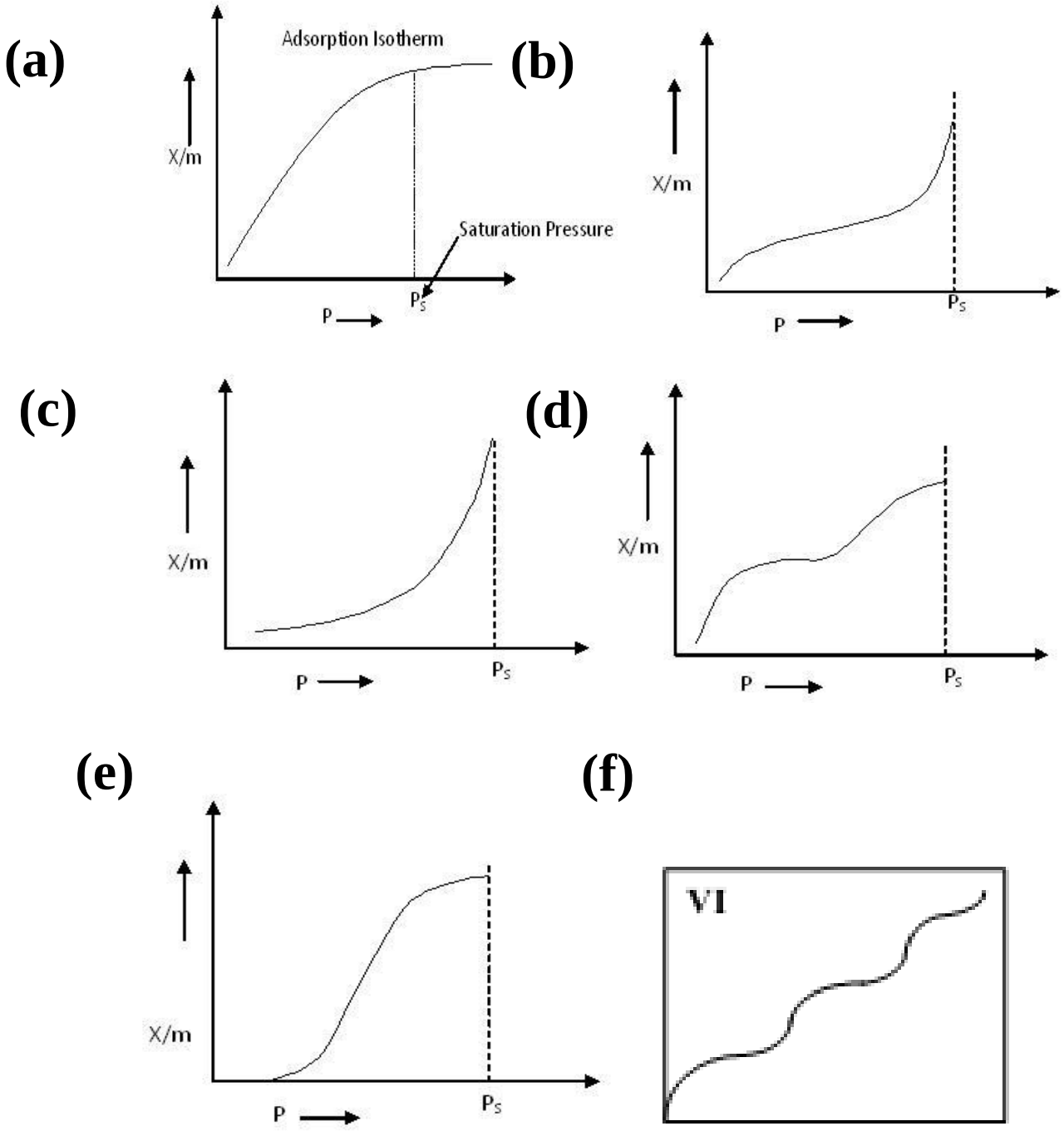

Figure 2.5. (a) Type I (b) Type II, (c) Type III, (d) Type IV, (e) Type V (Brunauer et al., 1940) and (f) Type VI adsorption isotherms

Type III is J-shaped and typical of nonporous (crystalline and coated) materials with strong weak-surface forces. A typical type III adsorption isotherm is depicted in Figure 2.5c.

i. Type III adsorption isotherms depicts multilayer adsorptions.
ii. The isotherm does not contain flat portions indicating the absence of monolayer adsorptions.

Type IV and V are typical of mesoporous materials when capillary condensation occurs, and these types exhibit hysteresis loop. Typical type IV and V adsorption isotherms are depicted in Figures 2.5d and 2.5e.

Type IV Adsorption Isotherm

i. Type IV adsorption isotherms have intermediate flat regions corresponding to monolayer formation.
ii. Type IV adsorption isotherms are similar to Type II at low pressure/concentration regions of the isotherm. This explains formation of monolayer followed by multilayer.

Type V Adsorption Isotherm

i. Type V adsorption isotherm is similar to the Type IV in most respect.

Type VI (Figure 2.5f) occurs for materials with relatively strong fluid-surface forces, usually when the temperature is near the melting point for the adsorbed molecules.

2.14.2 Solution sorption isotherm classification by Giles et al. (1960)

The above isotherm type classifications best describe adsorption of gases. Giles et al. (1960) proposed another set of isotherm classifications similar to the BDDT but suits solution adsorption isotherms better.

This classification divides isotherms for adsorption of organic solutes into four main classes, according to the nature of slope of the initial portion of the curve, and thereafter into sub-groups (Figure 2.6). The main classes are:

(i) *S* Curves, indicative of vertical orientation of adsorbed molecules at the surface.

(ii) *L* Curves, the normal or "Langmuir" isotherms, usually indicative of molecules adsorbed flat on the surface, or, sometimes, of vertically oriented adsorbed ions with particularly strong intermolecular attraction.

(iii) *H* Curves ("high affinity") (commencing at a positive value on the "concentration in solid" axis), often given by solutes adsorbed as ionic micelles, and by high-affinity ions exchanging with low-affinity ions.

(iv) *C* Curves ("constant partition"), linear curves, given by solutes which penetrate into the solid more readily than does the solvent.

The variations in each class are divided into sub-groups. The sub-groups are arranged according to the shape of the parts of the curves farther from the origin. For instance, if the adsorbed solute molecules in the monolayer are so oriented that the new surface they present to the solution has low attraction for more solute molecules, the curve has a long plateau; if they are oriented so that the new surface has high attraction for more solute; the curve rises steadily and has no plateau.

The *L* isotherms are the best known; indeed the L2 shape (Figure 2.6) occurs in probably the majority of cases of adsorption from dilute solutions.

Initial Slope – This depends on the rate of change of site availability with increase in solute adsorbed. As more solute is taken up, there is usually progressively less chance that a bombarding solute molecule will find a suitable site on which it can be adsorbed; i.e., to cause adsorption of a given additional amount of solute, the external solution concentration must be raised by ever-increasing amounts. This applies to the normal *L* curves and to the later stages of the *S* and *H* curves. In the initial part of the *S* curves, however, the opposite condition applies, and the more solute there is already adsorbed, the easier it is for additional amounts to become fixed. This implies a side-by-side association between adsorbed molecules, helping to hold them to the surface. This has been called "co-operative adsorption". In the *C* curves the availability of sites remains constant at all concentrations up to saturation. The probable causes of these effects will be described briefly.

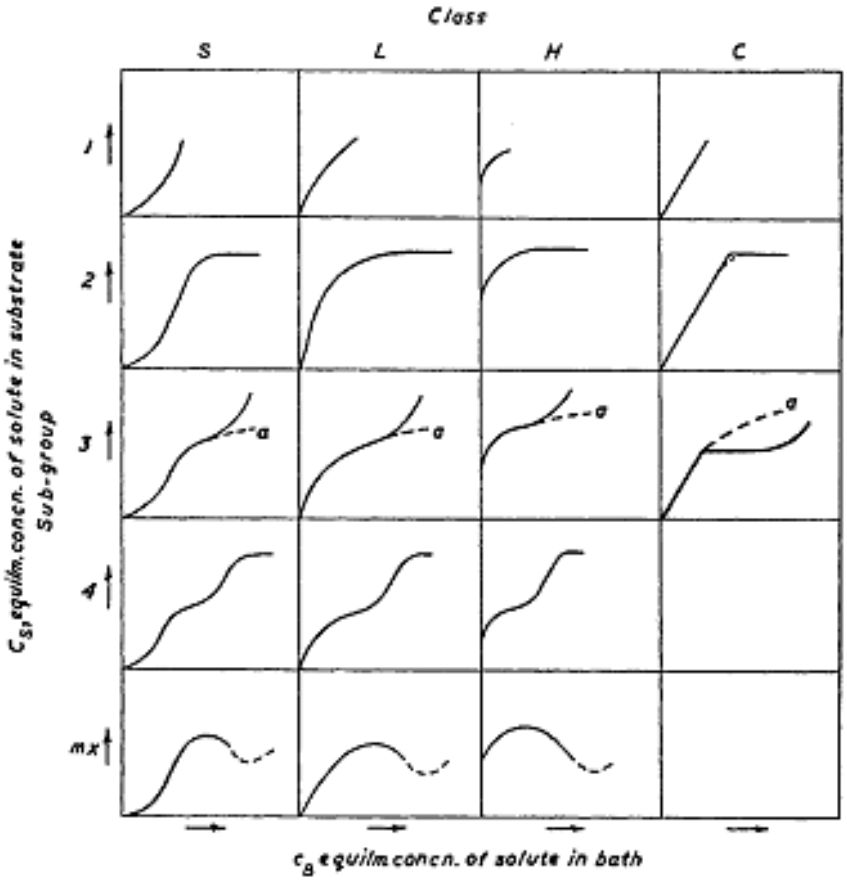

Figure 2.6. Giles et al. (1960) system of isotherm classification

2.14.2.1 The *S* Curve

The initial direction of curvature shows that adsorption becomes easier as concentration rises (Giles et al., 1960). In practice, the *S* curve usually appears when three conditions are fulfilled by the solute molecule:

(a) monofunctionality,
(b) moderate inter-molecular attraction, causing it to pack vertically in regular array in the adsorbed layer, and
(c) strong competition for sorbent sites from molecules of the solvent or of another adsorbed species.

The definition of "monofunctional" in this context is that the solute molecule has a fairly large hydrophobic residue ($>C_5$) and a marked localization of the forces of attraction for the substrate over a short section of its periphery, and that it is adsorbed as a single unit and not in the form of a micelle. Thus, phenol is monofunctional in its attraction towards a polar substrate, e.g., alumina, because the attraction arises from its hydroxy-group, but it is initially not monofunctional towards either graphite or powdered water-insoluble vat dyes with large planar assemblages of aromatic nuclei. With these it does not give an *S* isotherm, because its attraction for the substrate lies probably in non-polar forces operating over the whole phenol nucleus. Aromatic sulphonic acids appear to be monofunctional towards graphite in water, probably because the very high attraction of the sulphonate group for water draws this group as far as possible into the water phase, and thus only the opposite unsulphonated end of the nucleus is in contact with the graphite (Giles et al., 1960).

It might be thought from the above definition that all surface-active substances, being, as they are, monofunctional under the above definition, would give *S* isotherms, but in practice this is not so. Possible reasons are that they are adsorbed as ionic micelles, or that their intermolecular attraction is very high. Sometimes high salt concentration promotes S-curve formation with surface-active solutes (Giles et al., 1960).

As a working hypothesis it may be said that whenever an *S* curve is obtained with any aromatic solute, or an aliphatic solute with more than about five carbon atoms, the

adsorbed molecules are oriented perpendicularly to the surface. The converse is not always true: not all systems with perpendicularly oriented adsorbed molecules give *S* curves, especially some with strong solute intermolecular attractions.

2.14.2.2 The *L* Curve

Here the initial curvature shows that as more sites in the substrate are filled it becomes increasingly difficult for a bombarding solute molecule to find a vacant site available. This implies either that the adsorbed solute molecule is not vertically oriented (like argued for the S curve) or that there is no strong competition from the solvent (Giles et al., 1960). The types of system which give this curve do in fact fulfill these conditions. Thus they have one of the following characteristics:

(i) the adsorbed molecules are most likely to be adsorbed flat, eg. resorcinol and terephthaldehyde on alumina, or

(ii) if adsorbed end-on, they suffer little solvent competition; examples include

(a) systems with highly polar solute and sorbent, e.g. phenol and alumina, and a non-polar solvent, e.g., benzene or 2,2,4-trimethylpentane, and

(b) systems in which monofunctional ionic substances with very strong intermolecular attraction, eg. long paraffin-chain sulphate esters;

are adsorbed from water by ion-ion attraction. It is possible that in these cases in systems *b,* the adsorbed ions may have become associated into very large clusters just before adsorption takes place (Giles et al., 1960).

2.14.2.3 The *H* Curve

This is a special case of the L curve, in which the solute has such high affinity that in dilute solutions it is completely adsorbed, or at least there is no measurable amount remaining in solution. The initial part of the isotherm is therefore vertical. The adsorbed species are often large units such as ionic micelles or polymeric molecules, but sometimes they are apparently single ions which exchange with others of much lower affinity for the surface. These include sulphonated dye ions which exchange with chloride ions on alumina, and cyanine dye cations adsorbed by ion-ion attraction on silver halides. In the

most extreme form, the curve is a horizontal line running into the vertical axis. This was found for chemisorption of fatty acids on Raney nickel (Giles et al., 1960).

2.14.2.4 The *C* Curve

The *C* curve is characterized by the constant partitioning of solute between solution and substrate, up to the maximum possible adsorption, where an abrupt change to a horizontal plateau occurs (Giles et al., 1960). The *C* curve is usually obtained when a solute is partitioned between two immiscible solvents. The phase "adsorption without solvent" has been used to describe such adsorptions because the conditions favouring the *C* curve appear to be

(a) a porous sorbent with flexible molecules and regions of differing degrees of crystallinity; and a solute with
(b) higher affinity for the sorbate than the solvent has; and with
(c) better penetrating power, by virtue of condition (b) and of molecular geometry, into the crystalline regions of the sorbent.

Fundamentally, the linearity shows that the number of sites for adsorption remains constant; that is, as more solute is adsorbed more sites must be created. Such a situation could arise where the solute has a higher attraction for the sorbent molecules than the solvent itself has. The solute could then break inter-substrate bonds more readily than the solvent could, and if its molecular dimensions are suitable, could penetrate into the structure of the substrate in regions not already penetrated by the solvent. The action stops abruptly when more highly crystalline regions of the substrate are reached. In fact the isotherms usually do suddenly change direction to give the horizontal plateau. Thus a linear isotherm indicates that the solute is penetrating regions inaccessible to the solvent. Partition of a solute of limited solubility between two immiscible solvents is a special case of this behaviour; neither solvent penetrates between the molecules of the other but the solute penetrates both solvents (Giles et al., 1960).

Some additional characteristics of the *C* Curve

(i) Indications of the Monolayer – Nearly all sufficiently complete curves have either a plateau or an inflection ("knee"). Those that do not (sub-group 1) are clearly

incomplete: saturation of the surface has not been reached. The plateau or the beginning of the linear portion above the "knee" must represent "first degree saturation" of the surface, that is, the condition in which all possible sites in the original surface are filled and further adsorption can take place only on new surfaces. For convenience, this degree of coverage may be called the formation of a complete "monolayer" but this does not necessarily imply that it is a close-packed layer of single molecules or ions. It may be so in some cases, and when it is, specific surface area determinations can readily be made. Generally, however, the layer may

(a) contain solvent as well as solute molecules,

(b) consist only of isolated clusters of solute molecules adsorbed on the most active sites,

(c) consist of ionic micelles, either packed closely or well separated.

(ii) Significance of plateau length – In practice the precision of the value of the 'monolayer' capacity determined from the curve varies widely. At one extreme there are curves with a long flat plateau, and, at the other, those with only a very small change of slope at the beginning of broken lines. Indeed, in some cases the position of this point is not very clear. The significance of a long plateau must be that a high energy barrier has to be overcome before additional adsorption can occur on new sites, after the surface has been saturated to the first degree. The solute has high affinity for the solvent, but low affinity for the layer of solute molecules already adsorbed. It is perhaps significant that adsorptions of ionic micelles give curves with long plateau; in these cases the surface of the solid, when covered, will tend to repel other micelles holding the same charge. A short plateau must mean that the adsorbed solute molecules expose a surface which has nearly the same affinity for more solute as the original surface had (Giles et al., 1960).

(iii) Second rise and second plateau – These are attributed to the development of a fresh surface on which adsorption can occur, the second plateau (sub-group 4) representing the complete saturation of the new surface, though this stage is not always realizable, and the curve then appears as in sub-group 3. The fresh surface may be:

(a) the exposed parts of the layer already present; this will be the case, of course, only if there is room for a second layer; or

(b) new, probably more crystalline regions of the substrate structure into which the solute begins to penetrate; or

(c) part of the original surface which may be uncovered by re-orientation of the molecules already adsorbed. Alternatively, the second plateau may, apparently, in many cases represent a second condensed monolayer formed on top of the first.

Maxima – Occasionally a fall in slope occurs after the first inflection, that is, the isotherm has a maximum (sub-group *mx*). This is probably due to association of the solute in solution, that is, with increase in concentration the solute–solute attraction begins to increase more rapidly than the substrate-solute attraction.

2.15 Adsorption models

The curve relating the sorbed materials at a fixed temperature is called the sorption isotherm which invariably is used to express the sorption process. Several mathematically and fundamentally different sorption models have been employed to quantify and mechanistically explain the equilibrium distributions of sorbates between aqueous phase and soils/sediments. The most common of them are discussed below.

2.15.1 Langmuir adsorption isotherm model

In 1916, Langmuir (1916) published a new isotherm for gases adsorbed on solids, which retained his name. It is an empirical isotherm derived from proposed kinetic mechanism.

A sorbing system has a sorption capacity, q_e, defined as the ratio of the mass of sorbate to the unit mass of the sorbent. The total sorption capacity is therefore ($q_e m$), where m equals the mass of the sorbent. The rate of sorption is assumed to be proportional to the dissolved concentration of the chemical C_o and to the difference between the total capacity, $q_e m$, and the amount sorbed, q_e, where q is the actual concentration of the sorbate in the solid phase. Thus the kinetic equation may be written as shown in equation 2.7.

$$\frac{dC}{dt} = -k_1 m C_o (q_e - q) + k_2 q m \qquad 2.7$$

where k_1 and k_2 are the constants for the sorption and desorption, respectively. At equilibrium, the equation reduces to the Langmuir isotherm in equation 2.8.

$$q_e = \frac{Q_O b C_e}{1 + b C_e} \qquad 2.8$$

or its linear form in equation 2.9

$$\frac{C_e}{q_e} = \frac{1}{Q_o b} + \frac{C_e}{Q_o} \qquad 2.9$$

where Q_o is the maximum sorption capacity per unit weight of sorbent, *b* is a solute–surface interaction energy-related parameter, while q_e and C_e are the sorption capacity and concentration of sorptive remaining in solution, respectively, and $b = \frac{k_1}{k_2}$

In the Langmuir model the mass of solute sorbed per unit mass of sorbent, *q*, increases linearly by increasing the solute concentration *C* at low surface coverage, approaching to an asymptotic value Q_o when adsorption sites approach saturation.

The effect of isotherm shape can be used to predict whether a sorption system is "favorable" or "unfavorable" both in fixed-bed systems and the batch processes. The essential features of the Langmuir isotherm can be expressed in terms of a dimensionless constant separation factor or equilibrium parameter K_R, which is defined by the following relationship:

$$K_R = \frac{1}{1 + K_a C_o} \qquad 2.10$$

Then the Langmuir equation can be represented by

$$\frac{C_e}{q_e} = \frac{1}{K_L q_m} + \frac{C_e}{q_m} \qquad 2.11$$

where K_R is a dimensionless separation factor, C_o is initial sorptive concentration and K_a is Langmuir constant. The parameters q_m and K_a are the Langmuir constant relating adsorption capacity and the energy of adsorption, respectively. K_R indicates the shape of the isotherm accordingly as shown below:

when $K_R > 1$; then this type of isotherm indicates unfavourable, when $K_R = 1$; then the type of isotherm is linear, if $0 < K_R < 1$; then the isotherm is favourable, but if $K_R = 0$; then the isotherm indicates irreversibility.

Three important assumptions made in deriving the Langmuir equation (Olu-Owolabi et al., 2012) are:

(i) the energy of sorption is the same for all sites and is independent of degree of surface coverage,

(ii) sorption occurs only on localized ‘‘sites,’’ with no interaction between adjoining sorbed molecules, and

(iii) the sorption maximum (Q_o) represents a monolayer coverage.

Given these restrictive assumptions, it is not surprising that the Langmuir isotherms are observed only in a few cases for the sorption of environmental pollutants in such a complex and heterogeneous media as soils.

2.15.2 The Linear adsorption isotherm model

In natural systems, Q_o is invariably an order of magnitude greater than q, and, in many cases, many orders of magnitude greater. Under this condition, the Langmuir equation reduces to a linear equation as shown in equation 2.12.

$$bq_e = K_d = q/C_e \qquad 2.12$$

The linear partitioning model is the simplest adsorption model having just a single parameter, the partitioning coefficient (K_d) as shown in equation 2.13:

$$q_e = K_d C_e \qquad 2.13$$

where q_e and C_e are the equilibrium solid-phase and aqueous-phase solute concentrations, respectively. K_d is the partition coefficient equal to the ratio of the solute (sorbate) concentration in the solid phase at equilibrium, *q* (indicated also as *x/m*, where *x* is the amount of compound sorbed on the mass m of sorbent), to the solute concentration in the aqueous phase at equilibrium C_e .

The linear partitioning model is predicated on a hypothesis that the sorbent has no limitation of ‘‘sites’’ or spaces to accommodate the sorbate molecules as the solute concentration increases. However, soils, like most sorbents, manifests capacity limited sorption as well as varied isotherm nonlinearity, slow rates of sorption and desorption, sorption-desorption hysteresis, and solute–solute competition. These non-partitioning phenomena are often observed to significantly impact the fate and transport of hydrophobic organic compounds (HOCs) in groundwater systems and are frequently invoked to explain the ineffectiveness of various technologies for remedy of contaminated sub-surface systems (Huang et al., 2003). The Langmuir model is the simplest model describing such site-limiting sorption equilibrium.

2.15.3 Freundlich model

Often the experimental data do not follow the Langmuir or linear adsorption isotherm models but may be fitted by the empirical Freundlich isotherm (Freundlich, 1906). This model usually fit data quantifying sorption equilibria for soils and sediments and other heterogeneous sorbent media. The model is shown in equation 2.14**.**

$$q_e = K_F C_e^{(1/n)} \qquad 2.14$$

Linearizing equation 2.15 gives the expression in equation 2.15

$$\log q_e = \log K_f + \frac{1}{n}\log C_e \qquad 2.15$$

where K_F and n are the Freundlich model capacity factor and the isotherm linearity parameter, respectively.

The plot of $\log q_e$ as a function of $\log C_e$ has a slope equal to $\frac{1}{n}$ and an intercept equal to $\log K_f$. $\log K_f$ equals $\log q_e$ when C_e equals unity. When $\frac{1}{n} \neq 1$, the value of K_f depends on the units with which q and C_e are expressed. Suppose q is expressed in μg/g of sorbent and C_e in μg/cm^{-3} of solution; thus, K_f (μg$^{1-1/n}$ cm$^{3/n}$ g^{-1}) is equal to q when C_e = 1 μg/cm^{-3}.

The Freundlich equation is often considered as an empirical sorption equation with n being an indicator of site energy heterogeneity. The value of $\frac{1}{n}$ represents a joint measure of both the relative magnitude and diversity of energies associated with a particular sorption process. A value of $\frac{1}{n} = 1$ indicates linear adsorption and, therefore, equal adsorption energies for all sites. Linear adsorption generally occurs at very low solute concentrations and low loading of the sorbent. A value of $\frac{1}{n} > 1$ represents a concave, curved upward, S-type (solvent affinity–type) isotherm, where the marginal sorption energy increases with increasing surface concentration. It can be interpreted also with strong adsorption of the solvent, strong intermolecular attraction within the adsorbent layers, penetration of the solute in the sorbent, and mono–functional nature of the adsorbate. S-type isotherms, characteristic of cooperative sorption, are more common for the soil fine fractions, which have a higher total amount of associated organic matter, than for the coarse fractions. A value of $\frac{1}{n} < 1$ represents a convex, curved downward, L-type (Langmuir–type) isotherm, where the marginal sorption energy decreases with increasing surface concentration. It may arise where the competition of solvent for sites is minimum

or the sorbate is a planar molecule. When $\frac{1}{n}$ values are lower than 1 the mobility of a compound in soil columns can be significantly greater for the higher concentrations. Thus, serious errors may be introduced by assuming a linear sorption isotherm (Site, 2001).

The Freundlich-type isotherms can result from the overlapping patterns of several Langmuir–type sorption phenomena occurring at different sites on complex sorbent and showing different interaction energies (Weber et al., 1992).

Of the models discussed so far, only the Freundlich model assumes that sorption is on heterogeneous surfaces, and it relatively fits sorption on soils and sediment better (Olu-Owolabi et al., 2010). However, it suffers from another setback, inability to explain the shape of most sorption curves, because sorption by soils and sediments is characterized as a multiple reaction phenomenon being neither linear nor non-linear (Weber et al., 1992).

2.15.4 The composite model

Soils and sediments are highly heterogeneous combinations of active organic and inorganic components with respect to sorption equilibria at both the microscopic and macroscopic scales. It is thus reasonable to explain the non-linear behavior of soil sorption isotherms with the concept of multiple discrete reactive minerals and SOM domains as defined by the composite distributed reactivity model (DRM) (Weber et al., 1992). Each component has its own sorption energy and sorptive property and exhibits either a nonlinear (Freundlich or Langmuir) or linear sorption with respect to a particular solute. While ‘surface adsorption’ can be used to describe the interaction between most soil minerals and organic pollutants leading to a nearly linear isotherm, the same cannot be used for SOM whose isotherms have been regarded largely as nonlinear. Interactions between most SOM and organic pollutants have been mainly classified as a non-linear partitioning process. The overall sorption reaction for a natural solid is therefore the composite of the individual sorption reactions of the active components (Equation 2.16).

$$q_e = \sum_{i=1}^{m} x_i q_{ei} \qquad 2.16$$

where q_e is the total solute mass sorbed per unit mass of bulk solid, x_i is the mass fraction of the soil comprising sorption component *i* and q_{ei} is the sorbed concentration expressed per unit mass of that component. If each of the individual contributing mechanisms of sorption yields an isotherm which is linear, then the composite isotherm will be linear:

$$q_e = \sum_{i=1}^{m} x_i K_{D_i} C_e = \left(\sum_{i=1}^{m} x_i K_D \right) C_e = K_D C_e \qquad 2.17$$

where K_{D_i} is the partition coefficient for reaction *i* expressed on a per mass of component *i* basis and K_D is the mass-averaged partition coefficient. For true partitioning processes, the equation 2.17 above is rearranged to accommodate the mass fractions of different types of organic matrices

$$q_e = \sum_{i=1}^{m} x_i \, f_{OC_i} K_{OC_i} C_e \qquad 2.18$$

where f_{OC_i} and K_{OC_i} are the organic carbon mass fraction and the organic carbon-normalized partition coefficient for the *i* sorption component, and $\sum x_i \, f_{OC_i}$ gives the organic carbon mass fraction f_{OC} of the bulk soil.

However, if one or more of the component elements of sorption is governed by a nonlinear relationship between the solution and sorbed phases, then the composite isotherm will deviate from linearity. This is often the case for soil/sediment systems with a series of near-linear absorption reactions and nonlinear adsorption reactions; hence it is better described by the composite isotherm. The nonlinear reactions may be modeled with a series of any of a number of different models such as the Langmuir and Freundlich models, though the Freundlich model is more often encountered than the Langmuir model due to the heterogeneous nature of soils/sediments (Weber et al., 1992). Since only the linear absorption contributions can be expressed in terms of a summed sorption parameter K_D, the DRM becomes

$$q_e = x_i K_D C_e + \sum_{i=1}^{m} \left(x_{nl} \right)_i K_{F_i} C_e^{ni} \qquad 2.19$$

where x_i is the summed mass fraction of solid phase exhibiting linear sorptions, K_D, is the mass-averaged partition coefficient for the summed linear components, and $(x_{nl})_i$ is the mass fraction of the *i* nonlinearly sorbing component. From a practical perspective, the number of operationally distinguishable nonlinear components, *m*, will typically be only 1 or 2.

In a limiting case of the composite DRM model incorporating a linear sorption component and a finite-capacity, homogeneous-site-energy Langmuir-type non-linear component (i.e., the dual mode model – DMM), the overall equation becomes:

$$q_{e,} = q_{e,l} + q_{e,nl} = K_{D,L} C_e + \left(\frac{Q_O b C_e}{1 + b C_e} \right) \qquad 2.20$$

where q_e, $q_{e,l}$, and $q_{e,nl}$ are the total, linear contribution, and nonlinear contribution solid-phase concentrations of DMM, respectively.

2.16 Kinetics models

Pollutants sorption and subsequent desorption from soils and sediments involve multi-step mass transfer of sorbate molecules across the solid–solution boundary and diffusion within the solid matrices. Though sorbate exchange between the bulk solution phase and external surfaces of soil aggregates can be relatively fast or even instantaneous under rapid mixing conditions, diffusion of sorbate molecules within SOM matrices and micro/meso–pores connecting the external solution phase and SOM trapped within soil aggregates can be extremely slow and often limits the overall sorption and desorption rates (Huang et al., 2003).

Various kinetic models have been applied to sorption on soils and sediments including the simplified linear equations of the Lagergren (1898) pseudo-first-order (PFO) and pseudo second-order (PSO) rate models, Elovich (Low, 1960), and intra-particle diffusion (Weber and Morris, 1963) models, which are expressed in Equations 2.22–2.32 as shown below.

2.16.1 The pseudo first-order (PFO) rate model

The differential equation for the PFO (Lagergren, 1898) is expressed as follows:

$$\frac{\mathrm{d}qt}{\mathrm{d}t} = k_1 (q_e - q_t) \qquad 2.21$$

After intergrating equation 2.21 for the limiting conditions $q_t = 0$ at $t = 0$ and $q_t = q_t$ at $t = t$, it becomes the linearized expression for the PFO in equation 2.22.

PFO
$$\log(q_e - q_t) = \log q_e - \frac{k_1}{2.303} t \qquad 2.22$$

where q_e and q_t are sorption quantity (mg/g) at equilibrium and at time t, respectively; and k_1 is the rate constants (min^{-1}) of the PFO. The q_e and rate constant were calculated from the slope and intercept of the plots of log $(q_e - q_t)$ *vs. t*.

2.16.2 The pseudo second-order (PSO) rate model

The PSO (Lagergren, 1898) is given by equation 2.23

$$q_t = kq_e^2 t + kt \qquad 2.23$$

The differential equation is as follows:

$$\frac{dqt}{dt} = k(q_e - q_t)^2 \qquad 2.24$$

Intergrating equations 2.23 and 2.24 for the limiting conditions $t = 0$ to t, and $q_t = 0$ to q_t , gives:

$$\frac{1}{(q_e - q_t)} = \frac{1}{q_e} + kt \qquad 2.25$$

Equation 2.25 can be rearranged to give equation 2.26

PSO
$$\frac{t}{q_t} = \frac{1}{k_2 q_e^2} + \frac{t}{q_e} \qquad 2.26$$

where q_e and q_t are sorption quantity (mg/g) at equilibrium and at time t, respectively; and k_2 is the rate constants (min^{-1}) of the PSO. The q_e and rate constant were calculated from the slope and intercept of the plots of *t/q vs. t* .

2.16.3 The Elovich kinetics model

The Elovich model (Low, 1960) described sorption process as a group of reaction mechanisms such as diffusion in the mass of dissolution, surface diffusion, and activated catalytic surfaces, in the form

$$\frac{dqt}{dt} = \alpha \exp(-\beta q_t) \qquad 2.27$$

Upon integrating equation 2.27 for the limiting conditions $q_t = 0$ at $t = 0$ and $q_t = q_t$ at $t = t$, and subsequently linearizing the integrated form results in equation 2.28

$$q_t = \frac{1}{\beta} In(\alpha\beta) + \frac{1}{\beta} In(t + t_o) \qquad 2.28$$

If α, β, and $t \geq 1$, then equation 2.28 can further be simplified as equation 2.29

$$q_t = \frac{1}{\beta} In(\alpha\beta) + \frac{1}{\beta} In(t) \qquad 2.29$$

Elovich

where q_t are sorption quantity (mg/g) at time t; and α is the initial sorption rate (mg/g/min) and β is the desorption constant (g/mg) during any one experiment.

The Elovich constants were obtained from the slope, $\frac{1}{\beta}$, and intercept, $\frac{1}{\beta} In(\alpha\beta)$, of the plot of plot of q_t versus $In(t)$.

The Elovich model originates from chemical reaction kinetics and suggests that if the curve of q_t verses $In(t)$ does not pass through the origin, there is some degree of boundary layer control between the hydrophobic organic pollutant molecules in solution and the heterogeneous surfaces sorption sites. This boundary layer control is predicted to be related to the rate controlling mechanism.

2.16.4 Intra–particle diffusion

The Weber and Morris (1963) intra–particle diffusion kinetics model is very useful in predicting the sorption kinetics. Predicting the mechanism of sorption of hydrophobic organic solutes on heterogeneous materials is difficult because of the several removal processes involved. A better understanding of the removal processes and the sorption mechanisms(s) will help in ascertaining which sorption step is rate determing. Sorptions of hydrophobic organic solutes on heterogeneous materials are believed to occur in three main sequential steps: film diffusion (where sorptive moves towards the external surface of the sorbent); particle diffusion (where sorbate moves within the pores of the sorbent); and the adsorption of the sorptive on the interior void surface of the sorbent (Mittal et al., 2008). Each of these steps occurs at different rates and a combination of these steps determines the rate of organics sorption in solution. In a heterogeneous material, such as

soils, the second and third steps determine to a large extent the rate limiting step because if the external transport is greater than the internal transport then rate is controlled by particle diffusion, but if external transport is less than internal transport then rate is controlled by film diffusion. When external and internal transports are equal, trans–boundary movement of the sorbate will not be significantly permissible and sorption will be concentration dependent. When the sorption is very rapid, it is assumed that the above steps do not influence the overall kinetics.

In this model, the fractional approach to the equilibrium changes according to a function:

$$\left(\frac{Dt}{r^2}\right)^{0.5} \qquad 2.30$$

where D is the diffusion coefficient within the solid adsorbent and r is the particle radius. The intra–particle diffusion rate equation can be written as follows

Intra–particle diffusion $\qquad q_t = k_1\left(t^{1/2}\right) + C \qquad 2.31$

where q_t are sorption quantity (mg/g) at time t; k_i and C are the rate parameter of the intraparticle diffusion control stage and sorbate surface concentration.

The plot of q_t versus $t^{1/2}$ may present multi–linearity indicating that any sorption process takes place in three main stages:

(i) film diffusion
(ii) intra–particle or pore diffusion
(iii) movement onto interior sites.

Generally, the intra–particle diffusion model suggests that if a plot of q_t versus $t^{1/2}$ is linear, then the sorption mechanism is via intra–particle diffusion; and intra–particle diffusion is the sole rate-limiting step when such a plot passes through the origin. For a multi–linear process, the sorption process will be controlled by more than one mechanism and a plot of q_t versus $t^{1/2}$ will be multi–linear (or a curve) in nature.

2.17 Nigeria: geography and climate

The study area for this research is Nigeria (10˚ 00′ N, 8˚ 00′ E), a country in West Africa. Nigeria lies fully in the tropical zone and occupies a total area of 923,768 km^2 between latitudes 4^o15'N (from the lagoon) and 13^o55'N (to Niger Republic) and between longitudes 2^o45'E (from Benin Republic) and 14^o40'E (to Cameroon). It thus has tropical warm climate throughout the year with the North generally hotter and drier than the South. The average annual temperature ranges and the map of Nigeria are shown in Table 2.7 and Figure 2.7, respectively (Fagbami, 1993; Fagbami and Shogunle, 1995).

Due to its large size and numerous reliefs there are varying climatic conditions in the different parts of the country which supports a wide range of vegetation, giving rise to different agro-ecological zones (AEZs). For instance, the northern parts have far lower humidity, drier land and hotter than the southern parts with higher humidity, wet lands and cooler weather. At the extreme north and extreme south, the seasons are not well defined; the regions are extremely dry with higher temperatures and wet with lower temperatures all year round, respectively. Inland, the seasons become better differentiated into either a wet season from around April to September having lower temperatures, or a dry season from around October to March having higher temperatures (Fagbami and Shogunle, 1995). In the montane climates of the Mambilla and Jos Plateaux, temperatures are lower and similar to early spring in temperate regions of the world, in the range of 3 – 25 °C.

Rainfall varies within the country, and is controlled by two types of air masses; northward–trade wind coming from the Atlantic Ocean and the dry continental air coming from the north-east. Precipitation is higher in the southern part (with a yearly average of 3800 mm) and lower in the northern end (with a yearly average of 600 mm). While the northward–trade wind brings cloudy and rainy weather, the dry continental air from the northeast is very hot and dry and carries dust from the desert causing high temperatures during the day and very cool nights.

2.17.1 The Agro-Ecological Zones (AEZs)

The four major AEZs in West Africa (Figure 2.7a) are the forest, Guinea, Sudan, and Sahel savannah regions. However in Nigeria, these AEZs have further been divided into eight subzones due to the unique relief of the country (Figure 2.7a).

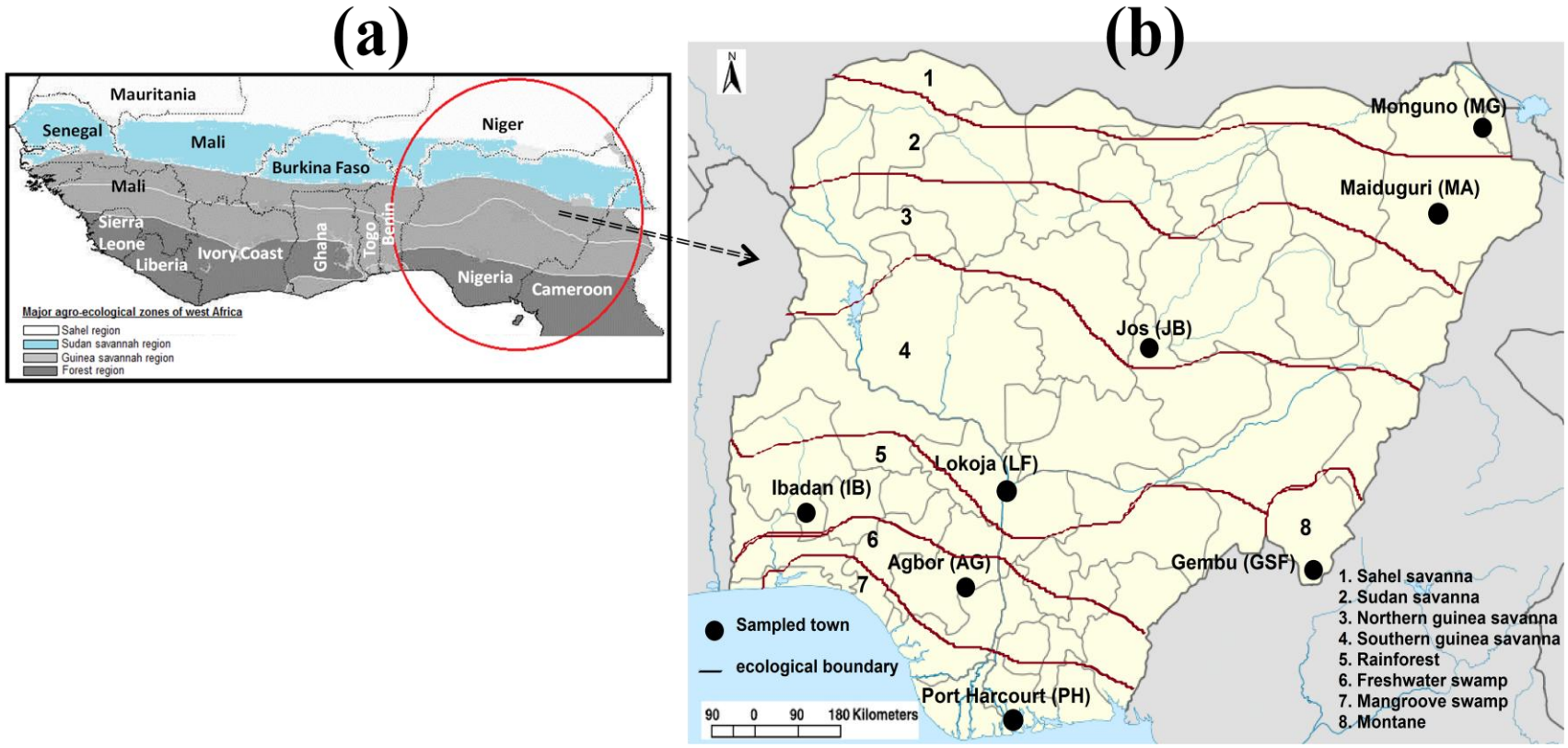

Figure 2.7. (a) map of West Africa showing the major Agro-Ecological Zones (AEZs); All AEZs in West Africa can be found in Nigeria (circled); (b) Nigeria map showing the major AEZs and the sampled towns in this study.

Table 2.7. Summary descriptions of samples

Sampling location	Sampling coordinate	AEZ*	ATR* (°C)
Lokoja (LF)	6˚ 45′ 00" E; 7˚ 49′ 00" N	Southern Guinea SV*	15 – 36
Agbor (AG)	6˚ 11′ 36" E; 6˚ 15′ 06" N	Fresh water swamp	19 – 32
Gembu (GSF)	11˚ 15′ 00" E; 6˚ 43′ 00" N	Montane	3 – 24
Jos (JB)	8˚ 52′ 00" E; 9˚ 48′ 00" N	Northern Guinea SV	6 – 28
Port Harcourt (PH)	6˚ 59′ 55" E; 4˚ 47′ 21" N	Mangrove swamp	17 – 30
Ibadan (IB)	3˚ 54′ 00" E; 7˚ 26′ 30" N	Moist lowland/Rainforest	22 – 32
Maiduguri (MA)	13˚ 09′ 42" E; 11˚ 50′ 36" N	Sudan SV	10 – 43
Monguno (MG)	13˚ 36′ 51" E; 12˚ 40′ 14" N	Sahel SV	9 – 45

ATR – Average temperature range; AEZ – Agroecological zone; SV - savanna.

The Forest zone (Mangrove swamp, freshwater swamp, and lowland rainforest), occupies a belt of 50 to 250 km wide along the coast with rainfall generally higher than 1600 mm, exceeding 2500 mm in the delta and along the eastern coast (Fagbami and Shogunle, 1995).

The semi-deciduous guinea savannah zones include: the southern guinea savannah zone, which is closer to the forest zone, with precipitation of 1150 to 1500 mm, and 4 to 5 months of no precipitation. This is followed by the northern guinea savannah zone with precipitation of 1000 to 1250 mm, and longer time (5 to 6) of no precipitation (Fagbami, 1993; Fagbami and Shogunle, 1995).

The Sudan savannah zone is next with less precipitation (500 to 1500 mm), and a greater number of months without precipitation (6 to 8).

Of all the savannahs, the Sahel has the most extreme conditions with far less precipitation (250 to 500 mm), longer months without precipitation (8 to 9) and the highest temperatures with maximum temperature of about 45 °C.

Study samples were collected from all eight agro–ecological zones (AEZs) of the country. The AEZs are the Sahel savanna, Sudan savanna, Northern Guinea savanna, Southern Guinea savanna, Moist lowland (Rain forest), Fresh water swamp, Mangrove swamp, and Montane.

2.18 Summary

Soil pollution and food security are intertwined issues of serious global concern. This is because healthy and productive agricultural soil is the world's most vital resource for food and fiber production, and as the world's population hits unprecedented figures, there is need to provide enough food of high quality.

Soil is the source of food for humans as well as the final sink for pollutants in the environment. It has been enormously degraded in recent decades due to discharges of harmful chemicals from the rapid industrial advancements. These harmful chemicals include organic and inorganic chemicals, most of which are persistent in the environment, bio–accumulative, and bio–magnify in higher trophic organisms.

Sorption is arguably the most important chemical processes governing the retention of nutrients, pollutants and other chemicals in the soil. In this literature review, the fundamental aspects of sorption on soils and some sorption studies were reviewed. However, information used for this review (especially those relating to sorption/fate of organic pollutants in soil) were mainly obtained from experiments conducted on soils from regions of the world outside Africa. Literature shows dearth of similar information on African soils especially on Nigerian soils, and hence, the need to carry out this research on Nigerian soils so as to have information on these soils as well as compare the results obtained with those reported in literature.

CHAPTER THREE
MATERIALS AND METHODS

3.1 Soil sampling and pretreatment

Soil samples were obtained from surface soils (0–30cm) from all eight AEZs in Nigeria (8˚ 00′ E; 10˚ 00′ N). Brief descriptions of the sampling locations are shown in Table 2.7 and Figure 2.7. The sampling locations and points were chosen from areas with relatively low anthropogenic activity as well as little or no history of soil pollution. Fifteen random samples were obtained from at least three different plots in each AEZ. From each sampling plot (about 200 m by 200 m), five random samples were collected using stainless steel sample grab. The samples were composited and quartering done to obtain a representative sample for each AEZ. One half of each sample was stored in aluminum foil for experiments involving organic pollutants while the other half was stored in polyethylene bag for experiments involving heavy metals. Prior to any sample treatment, the samples were air-dried, crushed gently and sieved through a 230-mesh size sieve and the fine fractions retained for these studies. Names and summary descriptions of the sampling sites are shown in Table 2.7.

3.2 Soil physical and chemical studies

The aim of these characterizations is to have precise insight into the chemical, physical, and mineralogical nature of these soils from the various AEZs.

3.2.1 Soil pH

The pH values of the soil–water solutions were measured using a pH meter which had earlier been calibrated with pH 4 and 7 buffer. The soils' pH values were determined in milipore ultra-pure water and 1.0 M KCl (both in a ratio of 1:1). This was done by weighing 10g of the properly air dried soil samples, 10 mL of the milipore ultra-pure water was added and allowed to stand for 30mins. The pH values of the samples were also determined in 1.0 M KCl in the soil–KCl solutions ratio of 1:1 following similar procedure as described for the milipore ultra-pure water (Benton, 2001).

3.2.2 Soil particle size

Particle size analysis was determined using the laser particle size analyzer (Malvern Mastersizer–2000 – Malvern Instruments Ltd., Malvern, U.K). For the analysis, each sample was diluted appropriately in distilled water in the order of 1.0 (wt%) before being analyzed 10 times. Small ultrasonic treatment is sometimes useful in breaking up loosely-held agglomerates. The ratio of soil mass to distilled water used for the measurements was chosen so that the obscurance (the fraction of light obscured by the analyzed suspension) measured by the Mastersizer 2000 at the beginning of the measurement cycle were within the recommended range (10 – 20%). At lower obscurance the quality of images reproduced on the detectors is too weak, causing a high level of measurement uncertainty. At obscurance levels >20%, the laser light beam may be subject to multiple reflections from successive soil particles, introducing errors in the results. In practice, the mass of soil samples was in the range of 0.5 to a few grams. The optimum speeds of the stirrer and the integrated pump were determined experimentally and fixed appropriately. This speed was selected to ensure that the mixture did not suffer from gravitation segregation of particles (slow speed) or formation of air bubbles in the stirred mixture (fast speed). These results were then averaged to produce the particle size distribution (Breuning-Madsen and Awadzi, 2005).

3.2.3 Soil organic carbon and organic matter

Organic carbon was determined by the Walkley and Black (1934) wet digestion method. 0.5 g of an air–dried soil sample was weighed into a 500–mL Erlenmeyer flask and 15–mL 0.267 N Potassium dichromate reagent was added. The flask was then refluxed for 30 min and the liquid cooled and flush down with milipore ultra-pure water. 3 drops of the indicator solution (*n*–phenylanthranilic acid) was added and the solution was titrated with Mohr's salt solution at room temperature. As the end point approached, a few more drops of the indicator solution were added and the colour was observed to change from violet to bright green. A blank analysis with no soil added was also carried out. The calculations have been described in Benton (2001).

3.2.4 Exchangeable bases

Exchangeable bases (Na, K, Ca and Mg) were determined by the 1.0 M Ammonium Acetate (NH_4OAC) method at pH 7.0. This was done by weighing 5.0 g of the air–soil sample into a 50–mL extraction vessel and adding 25 mL of the extraction reagent. The vessel was shaken for 10 min on a reciprocating shaker at 100 rpm, filtered immediately and the collected filtrate was analyzed for elemental determination (Benton, 2001) as described in section 3.2.7.

3.2.5 Exchange acidity

The exchange acidity of each was determined by the titration method (Benton, 2001). 10 g of the soil sample was weighed into a 100–mL beaker and 25 mL of 1.0 N KCl solution was added. The solution was mixed, allowed to stand for 30 min and filtered with a buchner filtration system using five portions of 25 mL of 1.0 N KCl solution to give a total volume of 150 mL. The filtrate was titrated with 0.1 N NaOH to the first permanent pink end point using 3 to 4 drops of phenolphthalein indicator. The obtained titer gives exchangeable acidity.

3.2.6 Cation Exchange Capacity

The cation exchange capacity (CEC) was determined by summation of the exchangeable bases (section 3.2.4) and the exchange acidity (section 3.2.5), while the percentage base saturation was determined from the percentage of cations that make up the CEC (Benton, 2001).

3.2.7 Determination of metals and metal oxides

Cations and metal oxides were determined using inductively coupled plasma optical emission spectrometry (ICP-OES, Optima 5300DV), except for Cd which was done by inductively coupled plasma mass spectrometry (ICP-MS, ELAN DRC-e). ICP-OES is an effective source of atomic emission which can, in principle, be used for the quantitative determination of all elements. Thus, a complete multi-component analysis can be undertaken in seconds and with only milliliters (mL) of samples of solution consumed. A calibration curve was established by introducing into the plasma standard analyte samples in a manner that the instrumental response was linear in typically over five orders of magnitude. ICP-OES is suitable for all concentrations, from the ultra-trace levels to major

components. Though detection limits are generally quite low for some elements falling with the range of 1 – 100 ug/L, wavelengths of varied sensitivity can be adjusted for the determination of any one element to achieve higher concentration determination.

3.2.8 Soil mineralogy

The soil samples diffractogram were obtained with a Bruker phaser diffractometer system using the whole soil procedure (randomly oriented mounts). This was done by pouring a fraction of the pretreated samples into the well of a low background sample holder and filling-up the sample holder well compactly by tapping on the bench and compressing with an etched (frosted) surface of a glass slide to avoid sample displacement which causes peak shifts. The procedure was repeated until the well is completely filled and the sample surface flattened with excess sample on the sample holder brushed off. After each measurement the sample holder was off loaded, cleaned with tap water and ethanol before reuse. Concern on trace contamination is not necessary.

3.3 Soil Treatments

3.3.1 Removal of soil organic matter

Soil organic matters (SOM) in 150g of selected samples were removed by using about 300ml of 30% hydrogen peroxide (H_2O_2) following the method described by McKeague (1978). The H_2O_2 was added in 100ml volumes and the mixture left to stand until the violent reactions and frothing stops. Another 100ml volume of H_2O_2 was again added, and the procedure above repeated. The last 100ml of H_2O_2 was added and the mixtures were heated to about 90°C. Excessive frothing was stopped by adding either cold water or methyl alcohol to avoid sample loss. High levels of depletion of the organic matter in the samples were indicated by the colour of the samples which turned reddish/brown depending on other soil components especially iron oxides. The samples were heated for more 45 minutes in order to remove excess H_2O_2, then dried in the oven for 2 hours at 105°C and later cooled in a dessicator. These soil samples were labeled as organic-matter-removed (OMR) and stored for the adsorption studies.

3.3.2 Removal of soil iron oxides

Iron oxides in 150g of selected samples were removed as described by McKeague (1978) using citrate-bicarbonate buffer and sodium hydrosulphite (dithionite – $Na_2S_2O_4$). 150ml of citrate-bicarbonate buffer was added to each beaker, stirred and 20 g of sodium hydrosulfite was gradually added as some samples may froth. The beakers were placed in a water bath at 80^{o}C and stirred intermittently for 20 minutes. About 10 g of dithionite was gradually added again to the samples until frothing stops. High levels of iron oxides depletion were indicated by the change in colour of the samples to gray depending on other soil components especially organic matter. The samples were then washed severally and filtered under vacuum until the filtrate becomes colourless. They were dried in the oven for about 2 hours at 105^{o}C and then cooled in the dessicator. These treated samples were labeled as iron oxides removed (IOR) soil samples and stored for the studies.

3.4 Sorption of Polycyclic Aromatic Hydrocarbons (PAHs)

3.4.1 Preparation of the PAHs (pyrene and fluorene)

Pyrene was dissolved in 50% acetonitrile to make a stock solution of 100 mg/L. Working solutions were prepared from this stock. The maximum concentration of pyrene used for the sorption experiments was 100μg/L to avoid precipitation or crystallization of pyrene out of water due to the low solubility in water; the solubility of pyrene in water is 130 μg/L (Chilom et al., 2005).

100 mg/L stock fluorene solution was prepared by dissolving the solid fluorene in 50 % methanol and making up with water. This was stored in a refrigerator at 4 °C to be used within 30 days of preparation. Working solutions of ≥100μg/L were prepared from this solution in 10 % (v/v) methanol-water solution. These concentrations were chosen because they were within the water solubility of fluorene at room temperature – 1980 μg/L (Chilom et al., 2005) and also a convenient concentration to study sorption on these soils.

3.4.2 Effect of time on soil sorption of PAHs

In order to determine the time it takes for equilibrium sorption of PAHs to be attained for these soils–PAHs system, 100 μg/L solution of the individual PAHs were prepared in appropriate solutions (acetonitrile/deionized water (20% v/v) for pyrene and 10 % (v/v) methanol-water solution) in 0.005 M $CaCl_2$ and 0.01 M NaN_3 as background electrolyte

and biocide to eliminate microbial degradation, respectively. Sorption experiments were carried by adding 10 mL of the appropriate PAH solution into brown vials containing 0.50 g of the soil sample and then tightly sealing the vials with Teflon lined screw caps. Aluminum foil was used to wrap the vials to minimize possible losses by photochemical decomposition. The vials were equilibrated in the dark by shaking at 100 rpm in a temperature (25 °C) controlled shaker at various time intervals ranging from 5 to 4320 min (72 h). These time intervals were different for different PAHs e.g. for pyrene the maximum time was 1440 min., while for fluorene it was 4320 min. Preliminary experiments showed that these times were long enough to reach equilibrium. These experiments were carried out for the whole and treated soils. Similar procedure has been used by Teixeira et al. (2011)

Control experiments without any soil were also prepared in the same way and used to account for possible losses due to volatilization and sorption of PAHs to the vials walls. Soil to solution ratios were chosen to ensure that between 15 to 95% of the pyrene in solution was sorbed. The losses of pyrene by photochemical decomposition, volatilization, and sorption on the brown glass vials were found experimentally to be negligible.

3.4.3 Effect of solution pH of PAHs sorptions

10 mL of the appropriate PAHs solution was measured into brown vials containing 0.50 g of the soil sample. pH of the PAHs solutions were adjusted between 3 and 9, and then the vials were tightly sealed with Teflon lined screw caps. Aluminum foil was used to wrap the vials to minimize possible losses by photochemical decomposition. Equilibration times used for the individual PAHs were as determined from previous experiments on rate of sorption – 1440 min for pyrene and 2880 min for fluorene. The vials were incubated in the dark by shaking at 100 rpm in a temperature (25°C) controlled shaker. $CaCl_2$ (0.005 M) and NaN_3 (0.01 M) were used as background electrolyte and biocide to eliminate microbial degradation, respectively. Similar procedure was repeated for the whole and treated soils.

3.4.4 Effect of PAHs concentration and temperature

Equilibrium studies were carried using 10 mL of individual PAHs solutions with concentrations of 20, 40, 60, 80 and 100μg/L and 0.50 g of the soil sample. The PAHs/soil mixtures were incubated at 25 °C while shaking at a speed of 100 rpm. $CaCl_2$ (0.005 M) and NaN_3 (0.01 M) were used as background electrolyte and biocide to eliminate microbial degradation, respectively. The incubation times used for pyrene and fluorene were 1440 min and 2880 min, respectively. The procedure was repeated at 40 °C for both pyrene and fluorene on treated and untreated soils.

At equilibrium, all vials were centrifuged at 4000 rpm for 20 minutes and concentration of PAHs in solution determined using Perkin Elmer fluorescence spectroscopy (model LS 55). All experiments were done in triplicate.

3.4.5 Desorption studies

Desorption experiments (at both temperatures) were immediately carried out after the sorption experiments by carefully decanting the aqueous solution from the equilibrium experiments and replacing with the same volume (10 mL) of fresh PAHs background solution (containing no PAHs). The vials were again equilibrated at 1440 min at 25 and 40 °C, while using $CaCl_2$ (0.005 M) and NaN_3 (0.01 M) as background electrolyte and biocide, respectively (An et al., 2010). Subsequent separation of soil and aqueous phase, and analyses were conducted as described above.

3.4.6 Competitive sorption of pyrene and fluorene, and desorption

Simultaneous sorptions of pyrene and fluorene were carried out using 0.50 g soil aliquot and equi–concentrations of pyrene and fluorene ranging from 20 through 100μg/L. The sorption experiments were incubated for 2 days and at two temperatures: 25 and 40 °C. After each sorption, desorption experiments (as similarly described above) were also carried out at both temperatures studied. These experiments were done on all soils as well as the treatments and in replicates too.

3.4.7 Determination of PAHs in solution

PAHs in solution were determined using Perkin Elmer fluorescence spectroscopy (model LS 55). These PAHs were determined in the synchronous mode following the parameters

in the Table 3.2 Similar method of PAHs determination has been reported by Ramirez et al. (2001) and Teixeira et al. (2011).

Fluorescence parameters: the concentrations of pyrene/fluorene left in solution were determined by synchronous fluorescence at wavelength difference (Δλ), scanning range, scanning speed, and excitation and emission slit widths described in Table 3.1. The synchronous peak at 335 and 264 nm were used to monitor the adsorption of pyrene and fluorene, respectively.

Table 3.1. Synchronous fluorescence scan parameters

Synchronous parameter	Pyrene	Fluorene
Wavelength difference – $\Delta\lambda$ (nm)	36	45
Scanning range (nm)	300 – 400	200 – 350
Scanning speed nm/min	500	1000
Excitation slit width (nm)	2.5	2.5
Emission slit width (nm)	20.0	20.0
Synchronous peak monitored (nm)	335	264

3.5 Sorption of Pentachlorophenol (PCP)

3.5.1 Preparation and determination of PCP

Stock PCP solution (500 mg/L) was prepared by dissolving solid PCP in 10 % ethanol and made up with milipore ultra–pure water. This was stored in a refrigerator at 4 °C to be used within 14 days of preparation. Working solutions were prepared from the stock in ethanol/deionized water (10% v/v) using 0.005 M $CaCl_2$ and 0.01 M NaN_3 as background electrolyte and biocide to eliminate microbial degradation, respectively.

3.5.2 Effect of time on PCP sorptions

Sorption time experiments were carried by adding 10 mL of 40 mg/L concentration of the PCP into brown vials containing 0.50 g of the soil sample and then tightly sealing the vials with teflon lined screw caps. Aluminum foil was used to wrap the vials to minimize possible losses by photochemical decomposition. $CaCl_2$ (0.005 M) and NaN_3 (0.01 M) were used as background electrolyte and biocide, respectively. The soil-PCP mixtures were incubated in the dark by shaking at 100 rpm in a controlled shaker at temperature of 25 °C and at various time intervals ranging from 5 to 1440 min. The procedure was repeated for the treated and untreated soils in triplicates. Similar procedure has been reported by Abdul Salam and Burk (2010).

Mass of soil to PCP solution concentration ratios were carefully chosen to ensure that at equilibrium between 10 to 90% of the PCP in solution was removed. The loss of PCP by photochemical decomposition, volatilization, and sorption on the brown glass vials were compensated for by incubating blank vials containing PCP solution with no soil sample along with the soil–PCP mixtures. Results showed that PCP losses were negligible.

3.5.3 Effect of solution pH on PCP sorption

10 mL of 40mg/L PCP solution was measured into brown vials containing 0.50 g of the soil sample. The PCP solutions' pH values were adjusted between 3 and 9, and then the vials were tightly sealed with teflon lined screw caps. The vials were protected as described in section 3.5.2 and equilibrated for 1440 min (24 h) in the dark by shaking at 100 rpm in a temperature (25°C) controlled shaker (Abdul Salam and Burk, 2010)). $CaCl_2$

(0.005 M) and NaN_3 (0.01 M) were also used. Similar procedure was repeated for all whole and treated soils, and each experiment was done in duplicate.

3.5.4 Effect of concentration and temperature on PCP sorptions

PCP equilibrium sorption studies were done by incubating 0.50 g of the soil with 10 mL solution of PCP concentrations of 20, 25, 30, 35 and 40 mg/L at the ambient soil pH and 1440 min. The PCP/soil mixtures were equilibrated at 25 °C with shaking at 100 rpm. $CaCl_2$ (0.005 M) and NaN_3 (0.01 M) were used as background electrolyte and biocide to eliminate microbial degradation, respectively. The experiments were done in duplicate.

At equilibrium, the vials were centrifuged at 4000 rpm for 20 minutes and concentration of PCP in solution before or after equilibration were determined using Perkin–Elmer Lamda 950 high performance UV-Vis-NIR spectrophotometer and 1 cm path length quartz cells. The peak at 320 nm was used to monitor the PCP sorption.

3.6 Heavy Metals Adsorption

Adsorption of three heavy metal ions (Pb(II), Cu(II) and Cd(II)) were studied on four representative soils (LF, JB, GSF, and MA) using the batch adsorption equilibrium technique.

3.6.1 Effect of time on metals adsorption

Soil and metal solution mixtures for time intervals between 30 and 1440 min, were prepared for each metal studied by weighing 1.0 g of the soil samples and adding 20 mL solution of either Pb(II) – 800 mg/L, Cu(II) – 300 mg/L, or Cd(II) – 300 mg/L. 0.01M $NaNO_3$ was used as background electrolyte at room temperature (27±1 °C) and at the soil pH. The background electrolyte is essential for these adsorption experiments to minimize non-specific sorption of the metals due to ion exchange mechanisms (Carey et al., 1996). The soil sample/metal mixtures were initially shaken for 30 minutes and thereafter agitated during the 1440 min incubation period (Olu-Owolabi et al., 2012).

3.6.2 Effect of pH on metals adsorption

Duplicate soil sample/metal mixtures, representing pH values from 3±0.2 to 7±0.2, were prepared for each metal studied by weighing 1.0 g of the soil samples and adding 20 mL

solution of the individual metals as described in section 3.6.2. pH adjustments were done with either 0.1M NaOH or 0.1M HNO_3. 0.01M $NaNO_3$ was used in preparing the metal solutions as background electrolyte. The experiments were carried out at room temperature (27±1 °C) and at incubation time of 1440 min. The soil sample/metal mixtures were then incubated by shaking as described above.

3.6.3 Effect of sorbate concentration and temperature on adsorption

Individual soil sample/metal mixtures for each metal studied were obtained by weighing 1.0 g of soil and adding 20 mL metal solution over a concentration range of 50 to 300 mg/L. 0.01M $NaNO_3$ was used as the background electrolyte and incubation was for 1440 min at room temperature (27±2 °C) and at soil pH. 0.01M $NaNO_3$ was used as background electrolyte. The soil sample/metal mixtures were agitated during the incubation as stated above. Similar procedure was repeated for the investigated soil samples at 25 and 40±2 °C.

On completion of each equilibration time, soil-metal mixtures were withdrawn from the shaker, filtered, and the filtrate analyzed for concentration of the metal left in solution using the Buck Scientific 205 Atomic Absorption Spectrometer (AAS) with air-acetylene flame on absorbance mode. Similar procedure was repeated for the investigated soil samples.

3.6.4 Effect of competition and aging on soils cation adsorption

Metal sorptions from mixed metals (cocktail) solutions containing Pb(II), Cu(II) and Cd(II) were investigated by weighing 1.0 g of the soil sample into a sample bottle and adding 20 mL of cocktail metals solution containing Pb(II), Cu(II) and Cd(II) in mole ratios of 1:1:1, 1:4:1, 1:1:4, and 4:1:1. The least and highest metal concentrations used in these ratios are 50 and 200 mg/L, respectively. The aliquots were incubated for 1, 7 and 90 days. Similar procedure was repeated for treated and untreated samples of LF, MG, GSF and JB. For incubation periods longer than 1 d, three (3) drops of chloroform ($CHCl_3$) was added, at intervals of 7 days, to the soil sample/metals mixtures to inhibit microbial activity (Agbenin and Olojo, 2004). After the incubations, filtrates were analyzed for Pb(II), Cu(II) and Cd(II) remaining in solution as described above.

3.7 Data Treatment

The amount of analyte sorbed was calculated using equation 3.1.

$$q_e = \frac{(C_O - C_e)V}{M} \qquad 3.1$$

where (C_O) and (C_e) are the initial and final sorbate concentrations in solutions; q_e, V and M are the amount of sorbate sorbed (mg/g), volume of the solution (mL) used for incubation and mass (g) of sample, respectively.

3.7.1 Sorption isotherms

Three sorption isotherm models – Langmuir (1916), Freundlich (1906), and the composite isotherm model (Weber et al., 1992), were employed in describing the sorption process. These models are described mathematically in equations 2.9, 2.14 and 2.20, respectively.

3.7.2 Sorption kinetics models

Five sorption kinetics models were employed in describing the sorption data. These are the Lagergren (1898) pseudo-first-order (PFO), pseudo second-order (PSO), Elovich (Low, 1960), and intra–particle diffusion (Weber and Morris, 1963) models. The models are described mathematically in equations 2.21, 2.26, 2.29 and 2.31, respectively.

3.7.3 Thermodynamic parameters

The thermodynamic parameters – enthalpy ($\Delta H°$), entropy ($\Delta S°$), Gibbs free energy ($\Delta G°$) and equilibrium constant (K_c) were evaluated using appropriate sorption data and equations 2.3 to 2.6.

3.7.4 Distribution coefficient

The distribution coefficients (K_d) was calculated using equation 3.2.

$$K_d = \frac{C_{ads}}{C_e} \qquad 3.2$$

where C_{ads} and C_e are the amount of sorbate sorbed and the amount remaining in solution at equilibrium, respectively.

CHAPTER FOUR

RESULTS AND DISCUSSIONS

4.1 Physicochemical parameters

The physico-chemical characteristics of the studied soils are shown in Tables 4.1(a–e). Tables 4.1(a–e) also show the locations of sample collection, their geographical co-ordinates and respective Agro-Ecological Zones (AEZs). The soils' physico-chemical properties were compared to the reference data of soils of moist lowlands in Nigeria (Fagbami and Shogunle, 1995). The values of the pH determined in water were close to neutral (6.0 – 7.5) except for GSF and JB which are acidic (5.0 – 5.5). The CEC values of the soils were low. The base saturations of these soils were high (> 85 %), and this indicated that the exchangeable bases were the main contributors to the CEC. The CEC values for LF and AG were higher than other samples, suggesting a likely higher affinity for charged molecules on these soils than others. Soil organic matter (SOM) values were high except for GSF and MA which was described as medium, and MG which is very low. These lower SOM values obtained for the GSF, MA, and MG soils was attributed to the observed sparse vegetation of the AEZs from which these samples were obtained. LF, AG and PH have the highest SOM contents, and this is not unconnected to the dense vegetative coverings of the soils in these sampled areas. The granulometric measurements showed that the soils textural classes for PH, IB, and MA are sandy loam, MG and AG are Loamy sand, GSF and JB are silt loam, while LF is loam (soil survey staff, 2006). Metal and metal oxides contents also vary with AEZ: GSF and JB had the highest percent of Fe and Al oxides, while heavy and trace metals are within concentration ranges stipulated for soils (Spark, 2003). The temperature regimes (Table 4.1c) of the soils are mainly thermic for soils in central and southern Nigeria, mesic for soils obtained with the mountain AEZs, and hyperthermic for soils obtained from northern Nigeria (soil survey staff, 2006). Table 4.1c also showed the soil types common in these AEZs as well as the clay activities of the

Table 4.1a. Physico-chemical characteristics of the soil (sampling points, pH, and CEC)

Soil symbol	*AEZ	Sampling coordinate	pH H_2O	pH 1N KCl	*EA	*CEC (meq/100g)	BS (%)
Lokoja (LF)	Southern Guinea SV*	6˚ 45′ 00"E; 7˚49′ 00" N	6.7	5.86	0.14	8.29	98.3
Agbor (AG)	Fresh water swamp	6˚11′36" E; 6˚15′06" N	6.29	5.39	0.10	5.49	98.2
Gembu (GSF)	Montane	11˚ 15′00"E; 6˚43′ 00" N	5.14	4.25	0.14	2.37	94.1
Jos (JB)	Northern Guinea SV*	8˚ 52′ 00"E; 9˚48′ 00" N	5.17	4.08	0.44	2.98	85.2
Port Harcourt (PH)	Mangrove swamp/	6˚ 59′ 55"E; 4˚ 47′ 21" N	7.66	7.24	0.06	2.50	97.6
Ibadan (IB)	Moist–lowland Rainforest	3˚ 54′ 00"E; 7˚ 26′ 30" N	6.57	5.88	0.08	2.95	97.3
Maiduguri (MA)	Sudan SV*	13˚ 09′42"E; 11˚50′36"N	6.67	5.21	0.02	4.25	99.5
Monguno (MG)	Sahel SV*	13˚36′51"E; 12˚40′14" N	7.40	6.59	0.12	3.66	96.7

AEZ – Agroecological zone; SV - savanna; BS - Base saturation; EA - Exchange acidity; CEC - cation exchange capacity

Table 4.1b. Physico-chemical characteristics of the soil (particle size and metals)

Soil	*OM (%)	Particle size analysis (%)			Oxides (wt %)		Trace elements/heavy metals (mg/kg)					
		*sand	*silt	*clay	Fe_2O_3	Al_2O_3	Cd	Cu	Mn	Ni	Pb	Zn
LF	6.25	48.3	31.1	20.6	0.16	1.69	0.02	7.64	220	0.91	16.8	24.6
AG	5.26	83.8	15.4	0.76	1.54	2.78	0.11	17.5	110	0.00	26.8	69.5
GSF	2.80	13.9	79.8	6.36	3.90	15.8	0.00	20.2	126	11.2	29.5	23.2
JB	3.57	42.3	57.1	0.63	3.13	9.12	1.02	33.1	134.	9.85	119	165.7
PH	5.29	68.0	30.5	1.45	1.09	2.96	0.09	5.82	229	4.98	8.63	20.9
IB	4.68	69.9	16.4	13.6	3.71	3.18	0.06	21.1	686	4.49	455	82.8
MA	1.67	70.4	28.9	0.67	0.99	2.23	0.10	13.6	124	0.00	45.9	6.57
MG	0.18	82.2	17.3	0.50	0.93	1.50	0.08	14.5	113	0.00	17.2	6.28

OM - Organic matter; *% sand (>50 μm); *% silt (2-50 μm); *% clay (<2 μm)

Table 4.1c. Physico-chemical characteristics of the soil (soil regime and texture)

Sampling location	ATR* (°C)	[a]Soil temperature regime	[b]Soil type	[c]Clay activity	Degree of weathering	Textural class
LF	15 – 36	Thermic	Entisols	40.2	MW	Loam
AG	19 – 32	Thermic	Ultisols	722	WW	Loamy sand
GSF	3 – 24	Mesic	Verisols	37.3	MW	Silt loam
JB	6 – 28	Mesic	Oxisols	473	WW	Silt loam
PH	17 – 30	Thermic	Inceptisols	172	WW	Sandy loam
IB	22 – 32	Thermic	Alfisols	21.6	MW	Sandy loam
MA	10 – 43	Hyperthermic	Vertisols	634	WW	Sandy loam
MG	9 – 45	Hyperthermic	Entisols	732	WW	Loamy sand

*ATR – Average temperature range; VSW – Very strongly weathered; SW – Strongly weathered; MW – Moderately weathered; WW – Weakly weathered; [a] – soil survey staff, 2006; [b] – Fagbami (1993); [c] – Westin and Brito (1969).

Table 4.1d. The mineralogical composition of the soils determined from the XRD patterns of whole soil samples

	Mineral (%)										
Soil	aragonite	Calcite	Dolomite	gibbsite	goethite	Hematite	illite	kaolinite	montmorillonite	quartz	siderite
LF	11.8	0.29	16.2	–	18.3	1.51	15.4	11.5	–	25.0	–
AG	2.49	5.37	8.70	23.5	–	1.58	–	0.68	–	57.7	–
GSF	3.84	2.17	3.42	6.06	–	1.87	–	3.97	–	78.7	–
JB	7.86	1.14	11.8	57.1	–	1.47	4.41	5.96	0.59	9.6	–
PH	6.53	7.40	10.7	4.61	–	0.88	–	1.48	–	68.4	–
IB	15.1	0.52	4.17	51.0	5.15	–	–	2.18	–	21.3	0.47
MA	9.89	2.37	11.7	3.48	–	2.19		4.62	0.14	63.2	2.38
MG	14.4	4.48	8.19	12.7	–	2.15	36.9	1.28	–	20.0	–

Table 4.1e. Physico-chemical characteristics of the soil (metals and metal oxides)

Soil	Exchangeable cations (meq/100g)				Percentage weight of metal oxides (wt %)				Micronutrients/Trace elements and Heavy metals (mg/kg)										
	Ca	Mg	K	Na	K_2O	Na_2O	MgO	CaO	Ba	Co	Cr	La	Li	Mo	P	Sc	Sr	Ti	V
LF	6.03	1.15	0.21	0.75	0.09	0.08	0.18	0.51	119.2	10.9	18.9	20.6	4.00	0.21	344	0.50	35.3	56.3	1.96
AG	4.94	0.20	0.24	0.01	0.03	0.05	0.03	0.18	24.9	7.03	59.1	3.72	2.10	0.45	1273	1.62	8.02	452	27.8
GSF	1.35	0.07	0.10	0.71	0.16	0.04	0.13	0.10	79.4	11.3	74.5	39.0	20.6	0.00	1438	7.57	25.3	454	50.8
JB	1.84	0.38	0.23	0.09	0.29	0.12	0.21	0.60	177.8	10.3	78.8	67.9	24.6	0.65	1453	6.15	23.8	694	37.2
PH	2.10	0.19	0.13	0.02	0.05	0.06	0.04	0.26	25.7	5.31	27.0	10.0	1.58	0.18	815	2.67	31.8	231	17.0
IB	2.41	0.27	0.17	0.01	0.11	0.06	0.08	0.22	105.2	18.5	127	26.3	3.77	0.00	1853	1.84	10.9	533	48.9
MA	2.67	0.66	0.14	0.76	0.08	0.05	0.09	0.19	56.7	8.84	36.2	18.7	3.87	0.51	1116	2.17	11.1	636	18.1
MG	2.62	0.59	0.33	0.00	0.22	0.05	0.28	0.24	75.8	7.31	28.4	4.79	4.12	0.36	1340	0.98	15.6	179	9.94

soils. The genetic age of a soil is an indicator of the degree of weathering in the soil (Westin and Brito, 1969). The degree of weathering of a soil was determined from the clay activity using the equation:

$$\text{Clay activity} = \frac{CEC}{Clay\ \%}\ x100$$

Results (Table 4.1c) showed that these soils are mainly weakly weathered soils.

The XRD patterns of the whole soil samples are shown in the Appendices (Figures A1 and A2). The observed peaks of the XRD patterns were analyzed using the X´Pert Highscore software. The Mineralogical compositions of the soils are shown in Table 4.1d, and the Appendices (Figures A3 to A10). The results indicate that the major minerals in the soils are aragonite, calcite, dolomite, gibbsite, goethite, hematite, illite, kaolinite, montmorillonite, quartz, and siderite. Quartz is the most common mineral in these soils, though the percentage composition varies. The abundance of quartz mineral in the studied soils was over 55% in composition for AG, GSF, PH, and MA soils. Other soils (LF, JB, IB, and MG) had between 10 and 25 % composition of quartz.

Another common mineral observed in these soils is the Al oxide mineral – gibbsite. The percentage compositions of gibbsite in these soils vary widely from major in JB and IB, to minor in other soils. Iron oxide/hydroxides minerals (goethite and hematite) were also common in these soils but were minor minerals.

Montmorillonite, the most common 2:1 expansive clay mineral, was only observed in JB and MA soils as minor minerals with values of less than 1.0%. Illite, though not a common mineral component in the studied soils, was found in the soils (LF and MG) obtained close to major water bodies such as the Rivers Niger and Benue, and the Lake Chad. Illite is a 2:1 expansive clay mineral that is widespread in weakly weathered soils. Kaolinite is another clay mineral common to the studied soils but found mainly as minor clay components. It is a 1:1 inexpansive clay mineral that is common in highly weathered soils.

Table 4.2: Comparison of selected physico-chemical characteristics of three whole and treated soils

	pH		Exchangeable cations (meq/100g)						
	H_2O	KCl	Ca	Mg	K	Na	EA[a]	CEC	OM[b]
LF	6.73	5.86	6.03	1.15	0.21	0.75	0.14	8.29	6.25
GSF	5.14	4.25	1.35	0.07	0.10	0.71	0.14	2.37	2.80
JB	5.17	4.08	1.84	0.38	0.23	0.09	0.44	2.98	3.57
LF OMR	6.08	5.57	0.41	2.18	0.30	0.33	0.04	3.26	1.96
LF IOR	7.79	7.01	1.88	0.49	0.15	15.4	0.04	17.9	3.99
GSF OMR	4.38	3.98	0.44	0.26	0.14	0.24	1.06	2.14	1.83
GSF IOR	8.06	7.26	2.87	0.14	0.42	21.3	0.08	24.8	1.23
JB OMR	4.14	3.63	2.14	0.52	0.31	0.15	0.74	3.87	0.92
JB IOR	8.00	6.98	1.31	0.30	0.38	35.9	0.08	37.9	1.72

a - Exchange acidity; b - Organic matter

One main clay mineral common to these soils are the carbonate minerals – aragonite, calcite, siderite, and dolomite. The carbonate minerals were found in all studies soils. Though they occur as minor minerals, their combined percentage compositions were usually higher than other minor mineral in these soils.

These results showed positive correlation with the report of Fagbami and Shogunle (1995). These variations in the physico–chemical properties of these soils are understandable bearing in mind the different ambient environmental conditions (vegetation, temperature, topography, rainfall, climate, soil forming minerals, biotic influence, etc) associated with these AEZs.

4.2 Comparison of selected physicochemical parameters after treatments

Selected physico-chemical characteristics of three whole soils (LF, GSF and JB) as well as their OMR and IOR treatments were compared to determine the extent of physicochemical changes associated with the respective treatments (Table 4.2). These soils were selected for this study because of their contrasting physicochemical properties (as observed in the clay, Fe_2O_3, and Al_2O_3 contents shown in Table 4.1b, as well as their clay mineralogical compositions shown in Figures A4, A6, and A7). Table 4.2 shows that removal of organic matter lowers the soils' pH in both water and 1 M KCl. As observed for the whole soils, pH values in KCl were lower than those in water. Removal of organic matter caused a reduction in the CEC value of LF and GSF soils; however, there was a significant increase (29%) in CEC for JB OMR soil. This trend has been attributed to the CEC of LF and GSF soils being contributed by exchangeable cations associated with the SOM; thus, removal of the SOM leads to reduction in these soils CEC values. For the JB soil, it can be inferred that the CEC is associated with the exchangeable cations of the clay minerals rather than the SOM. The soil organic matter masked the clay mineral exchangeable cations in the soil), hence, removal of the SOM resulted in an increase in the CEC. Unlike the removal of organic matter, removal of iron oxides in the soils caused very significant increase (> 100%) in CEC values. This increase in CEC was attributed to the increases in exchangeable bases (predominantly Na^+ ions – Table 4.2) associated with the soils' clay minerals that become available (unmasked) after the removal of iron oxide removal. Results also showed that IOR treatment caused a reduction in SOM in these soils. This is

an indication that some soil organic matter was associated with iron oxides in these soils forming an organically bound iron oxide, and hence removal of iron oxide consequently led to removal of these soil organic matters associated with the removable iron oxides.

4.3 PAHs Sorption

4.3.1 Effect of time on sorptions of pyrene and fluorene

Experimental results of the effect of time on pyrene and fluorene sorptions by the whole soils as well as the OMR and IOR samples are shown in Figures 4.1 (a–b) and 4.2 (a–b). Figure 4.1a showed that equilibrium pyrene sorptions were attained within 180 minutes for the whole soils except for MA and IB soils which attained equilibrium within 720 minutes. For these latter soils (MA and IB), there was an initial high sorption of pyrene between the 60th and 360th minutes, followed by a cycle of sorption and desorption until equilibrium was attained. Similar rate of pyrene sorption equilibrium for soils have been reported in literature (Teixeira et al., 2009; Cottin and Merlin, 2007; Teixeira et al., 2010).

Fluorene sorption reached equilibrium (Figure 4.2a) on the whole soils within 1440 min (1 day) except in PH and MG soils where equilibrium was attained in 2880 minutes (2 days) and LF with 360 minutes. The faster equilibrium sorption time observed for LF might not be unrelated to the type of organic matter in the soil. Organic sorption equilibrium is attained faster in the presence of high percentage of low polarity soft organic matter (Weber et al., 1992). At equilibrium no significant fluorene sorption and/or desorption are recorded. The varying time for attainment of fluorene equilibrium on these soils is in agreement with the results of other authors (Kohl and Rice, 1999; Chilom et al., 2005), and suggests that fluorene sorption equilibrium is dependent on soil type.

Considering the role of soil components in sorption (Kohl and Rice, 1999; Chilom et al., 2005), the effects of soil organic matter and iron oxides were also investigated for their contribution to pyrene and fluorene sorptions in selected soils. Results of the effect of time on the treated soils are shown in Figures 4.1b and 4.2b. It shows that the times of attainment of pyrene sorption equilibria were faster with the removal of iron oxides and organic matter in these samples, and equilibria were attained within 60 minutes. However, two exceptions to the present observations are the LF OMR and GSF IOR samples which

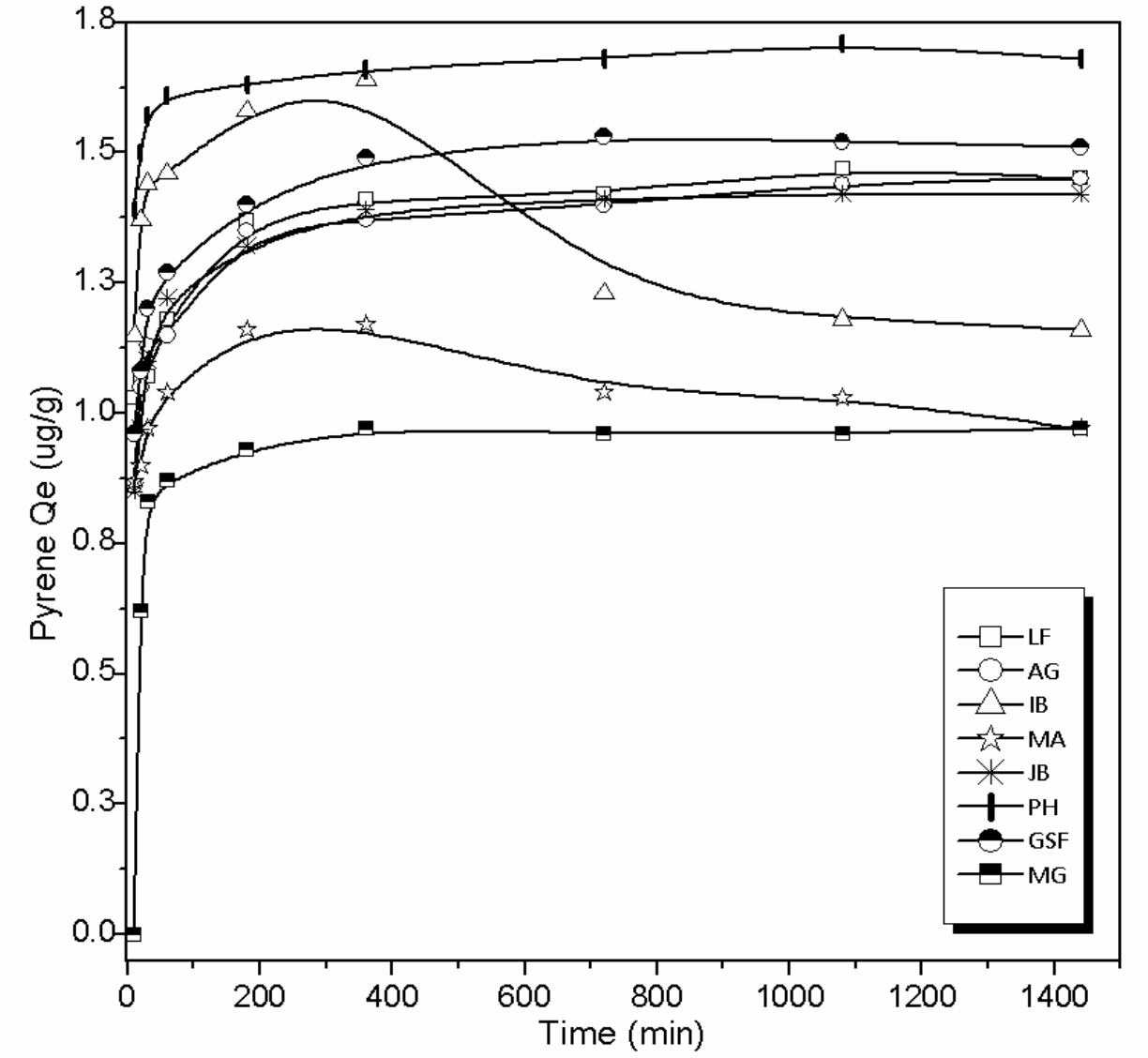

Figure 4.1a. Effect of time on pyrene sorption on whole soils

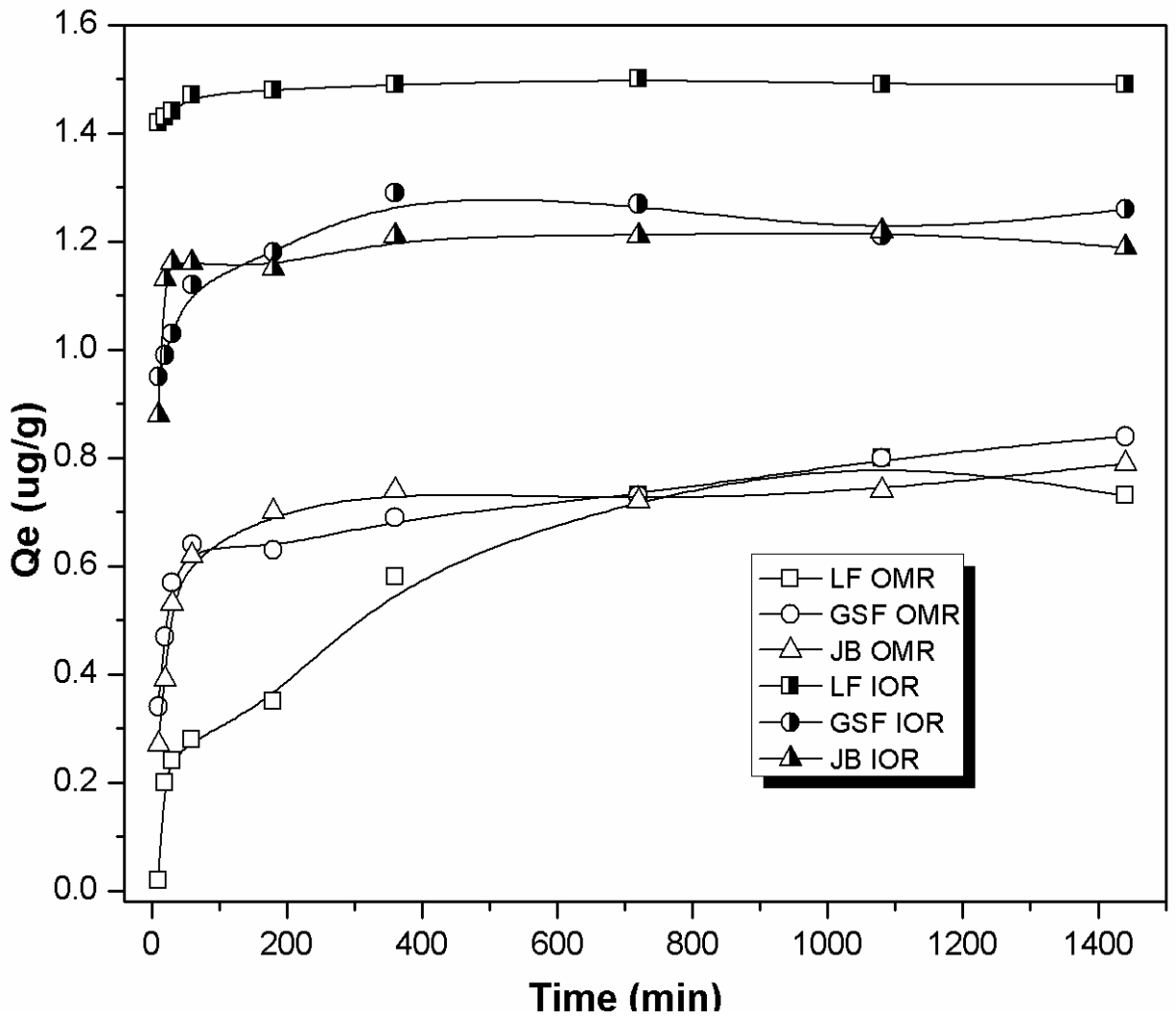

Figure 4.1b. Effect of time on pyrene sorption on OMR and IOR treated soils

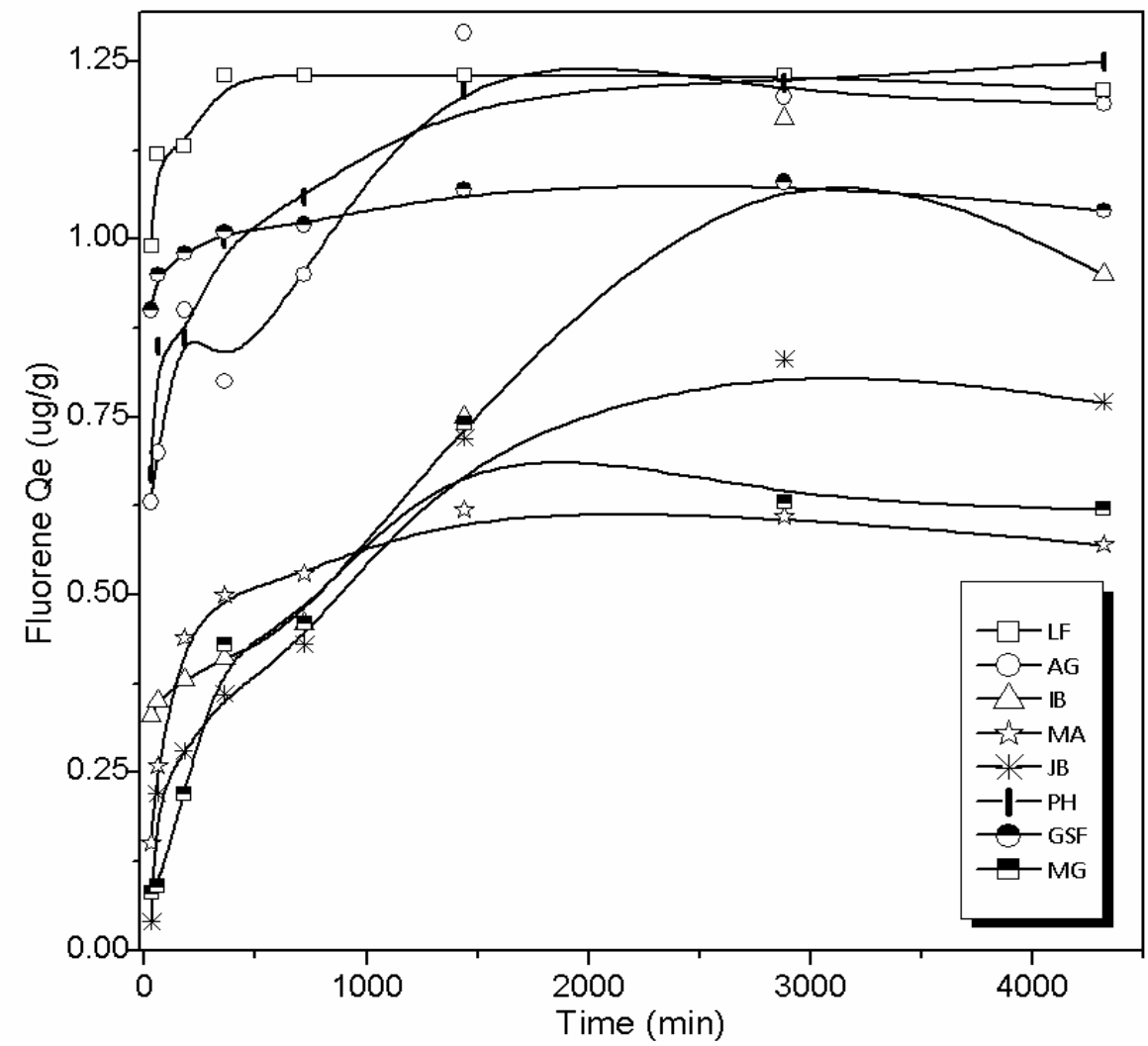

Figure 4.2a. Effect of time on fluorene sorption on whole soils

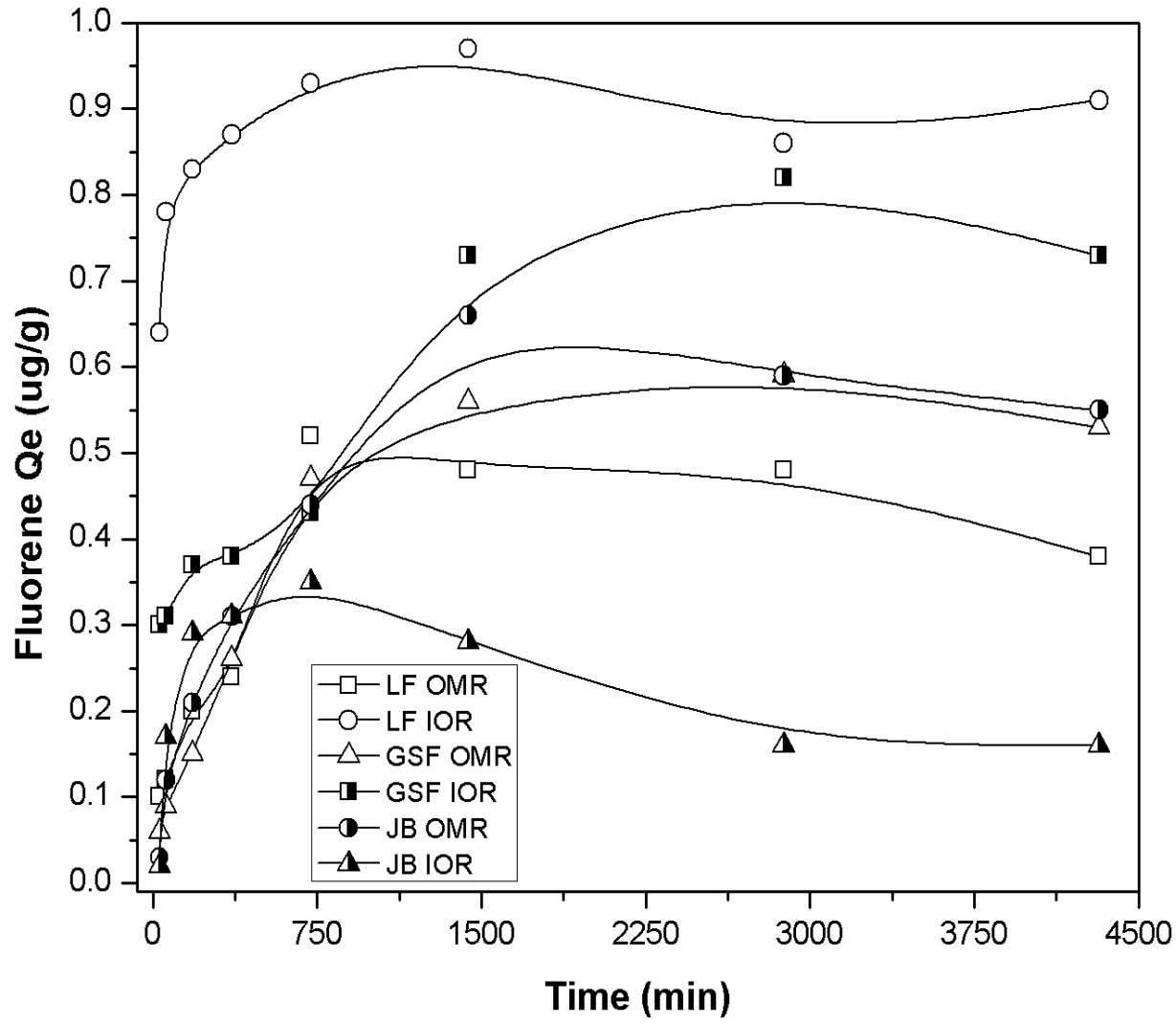

Figure 4.2b. Effect of time on fluorene sorption on OMR and IOR treated soils

took more time in attaining equilibrium sorption. The delay might be an indication that the sorption of pyrene on these treated soils was time-dependent especially as the relative ratio of expansible clay minerals to other soil components increased.

Comparisons of pyrene sorptions on OMR and IOR samples with those of whole soils showed that organic matter in these soils contributed ≥ 50 % of the soils' sorption capacities while iron oxides contributed only a little fraction, ≈ 15 %, for GSF and JB. LF IOR showed a different trend: iron oxides removal caused an increase, ≈ 5%, in the pyrene sorption, an indication that some of the pyrene sorption sites might have been masked by the presence of iron oxides leading to lower sorption on the whole soil.

It was also observed (Fig. 4.2b) that the removal of both organic matter (GSF OMR) and iron oxides (GSF IOR) in the GSF soil led to delay in attainment of fluorene sorption equilibrium when compared with the whole soil (from 720 to 1440 min). Similar trend was observed in the JB and LF soils where removal of organic matter led to increase in equilibrium time from the initial 1440 and 360 min to 2880 and 1440 min, respectively. However, removal of iron oxides in the soils did not affect the fluorene sorption equilibrium attainment in LF IOR, while it reduced the time for JB IOR (720 min). By comparing the quantities of fluorene sorbed on whole and treated soils, it is observed that ≈ 50 % of the fluorene sorption was on the organic matter component. Analysis of the result also showed sorbate exchange between the bulk solution phase and external surfaces of soil aggregates and/or SOM was relatively fast or even instantaneous under rapid mixing conditions. Hence, removal of organic matter in these soils will imply that sorption will take a longer time to occur on other soil constituents (such as expansible and pore containing in–expansible clay minerals) whose sorption is time–dependent, resulting in the increased time with removal of organic matter. This is so because the diffusion of sorbate molecules within mineral matrices and micro/meso–pores connecting the external solution phase and pores within soil aggregates was extremely slow and often limits the overall sorption and desorption. Removal of iron oxides in these soils also implied higher percentage of available organic matter both in the bound and dissolved forms, hence, the faster equilibrium attainment.

Results also showed that the role of one soil components in pollutant sorption could be masked by the presence of another soil component (Site, 2001). Hence, while removal of organic matter from these soils always led to lower pyrene sorptions, removal of iron oxides did not always decrease sorptions. The lowered sorption of pyrene on the organic matter removed soils was in contrast to what An et al. (2010) reported for Canadian soil. This suggested that organic matter was more important in the sorption of PAHs in these soils than other soil components.

4.3.2 Kinetics of pyrene and fluorene sorption

The data generated from the effect of time sorption experiments were fitted into four kinetics models: Lagergren pseudo–first and second order, Elovich and intra-particle diffusion kinetics models. The estimated parameters on these models were presented in Tables 4.3 to 4.6. These models were used to correlate the data of PAHs sorptions as well as suggest the mechanisms involved in their removal from solution. Tables 4.3 and 4.5 showed the kinetics models parameters for PAHs sorptions on the whole soils. Comparison of the correlation coefficients (r^2) and the estimated model sorption capacity (q_e) values of the Lagergren pseudo–first and second–order kinetics showed that the sorption was better described by the pseudo–second order kinetics model; the r^2 values closer to unity (0.999–1.000) and the model q_e values were better correlated to experimental values. The small deviations observed in the pseudo–second order kinetics model q_e values were attributed to the uncertainties inherent in obtaining the experimental q_e values (Olu-Owolabi et al., 2012).

The estimated q_e values from the Elovich model showed that the sorption could be explained by this model. The Elovich model originated from chemical reaction kinetics, and since the curves did not pass through the origin (Appendix – Figure A11 and A12), it suggested there was a degree of boundary layer control between pyrene and fluorene molecules in solution and the soils' surface active sorption sites. This boundary layer control is related to the rate controlling mechanism and involves π–π interactions between these PAH molecules in solution and active sorption sites at the soil surface (Mittal et al., 2008).

Table 4.3. Kinetics model parameters for whole soils

Kinetics model	Model parameters	Soil samples							
		LF	AG	IB	MA	JB	PH	GSF	MG
pseudo-first-order	q_e (μg g^{-1})	0.318	0.873	0.221	0.594	0.285	0.244	0.330	0.275
	k_1 (min^{-1})	1.7x 10^{-3}	3.9x 10^{-4}	5.8x 10^{-4}	8.3x 10^{-3}	2.5x 10^{-3}	7.6x 10^{-4}	1.5x 10^{-3}	1.1x 10^{-3}
	r^2	0.783	0.659	0.159	0.004	0.822	0.654	0.674	0.453
pseudo-second-order	q_e (μg g^{-1})	1.46	1.46	1.16	0.99	1.43	1.70	1.52	0.99
	k_2 (g μg^{-1} min^{-1})	0.06	0.05	0.03	0.07	0.07	0.15	0.08	0.23
	r^2	0.999	0.999	0.995	0.997	1.000	0.999	0.999	0.999
Elovich	q_e(μg g^{-1})	1.43	1.42	1.34	1.06	1.41	1.69	1.43	1.00
	β	10.3	9.26	71.4	34.4	9.01	19.2	9.01	7.63
	r^2	0.948	0.933	0.020	0.272	0.914	0.854	0.933	0.580
Intra-particle diffusion	C (μg g^{-1})	1.06	1.01	1.45	0.98	1.00	1.50	1.10	0.55
	k_{id}	0.012	0.013	0.005	0.002	0.013	0.006	0.013	0.014
	r^2	0.805	0.756	0.153	0.075	0.707	0.654	0.735	0.363

Table 4.4. Kinetics model parameters for OMR and IOR treated soils

		Soil samples					
Kinetics model	Model parameters	LF OMR	GSF OMR	JB OMR	LF IOR	GSF IOR	JB IOR
pseudo-first-order	q_e (μg g^{-1})	0.59	0.37	0.28	0.06	0.17	0.11
	k_1 (min^{-1})	$2.1x10^{-3}$	$2.0x10^{-3}$	$2.1x10^{-3}$	$8.8x10^{-4}$	$1.3x10^{-2}$	$1.1x10^{-3}$
	r^2	0.768	0.930	0.807	0.525	0.343	0.436
pseudo-second-order	q_e (μg g^{-1})	0.853	0.838	0.781	1.497	1.252	1.203
	k_2 (g μg^{-1} min^{-1})	0.007	0.032	0.056	1.223	0.173	0.540
	r^2	0.966	0.995	0.998	1.000	0.999	0.999
Elovich	q_e (μg g^{-1})	0.670	0.797	0.752	1.48	1.27	1.18
	β	6.80	12.2	11.1	66.7	15.63	24.4
	r^2	0.952	0.915	0.862	0.911	0.881	0.545
Intra-particle diffusion	C (μg g^{-1})	0.096	0.450	0.425	1.44	1.01	1.06
	k_{id}	0.020	0.011	0.011	0.002	0.008	0.004
	r^2	0.905	0.816	0.651	0.709	0.684	0.358

Table 4.5. Kinetics model parameters for fluorene sorption on whole soils

Kinetics model	Model parameters	Soil samples							
		LF	AG	IB	MA	JB	PH	GSF	MG
pseudo-	q_e (μg g^{-1})	0.07	0.36	0.84	0.28	0.63	0.41	0.12	0.46
first-	k_1 (min^{-1})	3.2x	4.6x	5.3x	3.0x	5.1x	5.5x	3.2x	3.5x
order		10^{-4}	10^{-4}	10^{-4}	10^{-4}	10^{-3}	10^{-4}	10^{-4}	10^{-4}
	r^2	0.249	0.242	0.539	0.438	0.781	0.840	0.443	0.388
pseudo-	q_e (μg g^{-1})	1.22	1.22	1.09	0.59	0.88	1.26	1.05	0.68
second-	k_2 (g μg^{-1} min^{-1})	0.97	0.01	0.00	0.04	0.00	0.01	0.21	0.01
order	r^2	0.999	0.996	0.944	0.996	0.981	0.999	0.999	0.988
Elovich	q_e (μg g^{-1})	1.16	1.10	0.89	0.57	0.64	1.15	1.02	0.66
	β	24.39	7.94	6.54	11.24	6.45	8.70	31.25	7.46
	r^2	0.724	0.847	0.745	0.874	0.938	0.959	0.879	0.888
Intra-	C (μg g^{-1})	1.09	0.68	0.21	0.29	0.10	0.77	0.94	0.12
particle	k_{id}	0.00	0.01	0.01	0.01	0.01	0.01	0.00	0.01
diffusion	r^2	0.443	0.754	0.867	0.605	0.887	0.829	0.672	0.729

Table 4.6. Kinetics model parameters for fluorene sorption on OMR and IOR treated soils

Kinetics model	Model parameters	Soil samples: LF OMR	GSF OMR	JB OMR	LF IOR	GSF IOR	JB IOR
pseudo-first-order	q_e (μg g^{-1})	0.30	0.33	0.68	0.15	0.53	0.13
	K_1 (min^{-1})	2.1x10^{-4}	7.4x10^{-4}	2.8x10^{-4}	1.8x10^{-4}	3.9x10^{-4}	1.1x10^{-4}
	r^2	0.211	0.515	0.485	0.137	0.707	0.068
pseudo-second-order	q_e (μg g^{-1})	0.42	0.60	0.62	0.90	0.62	0.16
	K_2 (g μg^{-1} min^{-1})	0.04	0.01	0.01	3.31	0.01	0.04
	r^2	0.973	0.983	0.983	0.998	0.980	0.975
Elovich	q_e (μg g^{-1})	0.41	0.48	0.65	0.84	0.63	0.21
	β	12.2	8.40	8.13	21.3	9.26	52.6
	r^2	0.744	0.913	0.908	0.665	0.825	0.100
Intra-particle diffusion	C (μg g^{-1})	0.15	0.08	0.10	0.77	0.25	0.22
	K_{id}	0.01	0.01	0.01	0.00	0.01	0.00
	r^2	0.541	0.787	0.748	0.385	0.868	0.000

Mechanism of hydrophobic organic hydrocarbon sorption on soil is a complex process and it is difficult to predict. A better understanding of sorption mechanisms will help in ascertaining which sorption step is rate-limiting. PAHs sorption process in soils are thought to occur in three main sequential steps: film diffusion (where sorbate moves towards the external surface of the sorbent); particle diffusion (where sorbate moves within the pores of the sorbent); and the adsorption of the sorbate on the interior void surface of the sorbent (Mittal et al., 2008). Each of these steps occurs at different rates and their combination determines the rate of organics sorption in solution. In soils, however, the second and third steps determine to a large extent the rate limiting step because if the external transport is greater than the internal transport then rate is controlled by particle diffusion, but if external transport is less than internal transport then rate is controlled by film diffusion. When external and internal transports are equal, trans–boundary movement of the sorbate will not be significantly permissible and sorption will be concentration dependent. Since the sorption step is very rapid, it is assumed that the mechanisms of the above steps do not influence the overall kinetics. The overall sorption rate is controlled either by surface diffusion or intra–particle diffusion. Hence, the Weber and Morris (1963) intra–particle diffusion kinetics model was employed in this study to ascertain whether the film diffusion or intra–particle diffusion is the rate limiting step in these PAHs sorptions. The calculated model parameters are shown in Tables 4.3 to 4.6. The intra–particle diffusion kinetics model suggest that if the sorption mechanism is via intra–particle diffusion then a plot of q_t versus $t^{1/2}$ will be linear; and when such linear plot passes through the origin, then intra–particle diffusion is the sole rate-limiting step. When the sorption process is controlled by more than one mechanism, then a plot of q_e versus $t^{1/2}$ will be multi–linear. Given the multi–linear nature (Figure 4.3 and Appendix Figures A13 and A14) of the plots of these PAHs sorptions, it was observed that sorptions occurred in three phases. The initial steep phase (first segment of Figure 4.3 and Appendix Figures A13 and A14) represented surface diffusion of the PAHs species to the soil surfaces; the second less steep phase (second segment of Figure 4.3 and Appendices Figure A13 and A14) indicated gradual sorptions of the PAHs species (where intra–particle diffusion within the pores is the rate-limiting step); and the third phase (last segment of Figure 4.3 and Appendices Figure A13 and A14) where equilibrium have been attained (and the rates

of sorption and desorption are constant). Since the plot did not pass through the origin, intra–particle diffusion was not the sole rate-limiting step. Film diffusion and adsorption on interior void surfaces played significant roles in these PAHs sorption. These processes controlled the sorption of these species but only one predominates at any particular time phase.

The values of the intra–particle diffusion model constants are shown in Tables 4.3 to 4.6. The C (μg g^{-1}) values indicate the amount of sorbate adsorbed on the surface. If the PAHs species sorptions are solely a surface phenomenon then the C (μg g^{-1}) values will be approximately equal to q_e values, but if otherwise the C (μg g^{-1}) values will be less than the q_e values. It was observed that the C (μg g^{-1}) values were less than q_e values for these soils; and hence, these C values suggested that surface diffusion played an important role as the rate-limiting step in the overall sorption process, but the contribution of partitioning within inherent internal soil voids were also significant.

Due to the conjugated spatial arrangement of the benzene rings in the fluorene molecule, sorption by π–π interactions are thought to play less significant role in fluorene sorption unlike in the PAHs species with more condensed benzene rings such as those found in pyrene. Zeledon-Toruno et al. (2007) has also argued that the structure of fluorene may govern its apparent sorption on adsorbent matrix.

The C (μg g^{-1}) values for fluorene sorptions indicated that the amount of the fluorene molecules adsorbed on the soils' surface were generally smaller (0.12 – 1.09; 0.08 – 0.77) than those observed with the pyrene (0.55 – 1.50; 0.10 – 1.44) for whole and treated soils, respectively. These lower C values suggested that intra-particle diffusion was a significant rate–limiting step for fluorene sorption and unlike pyrene sorption, the lower π–π interactions associated with the fluorene molecules consequently led to reduced C values and hence reduced fluorene sorption.

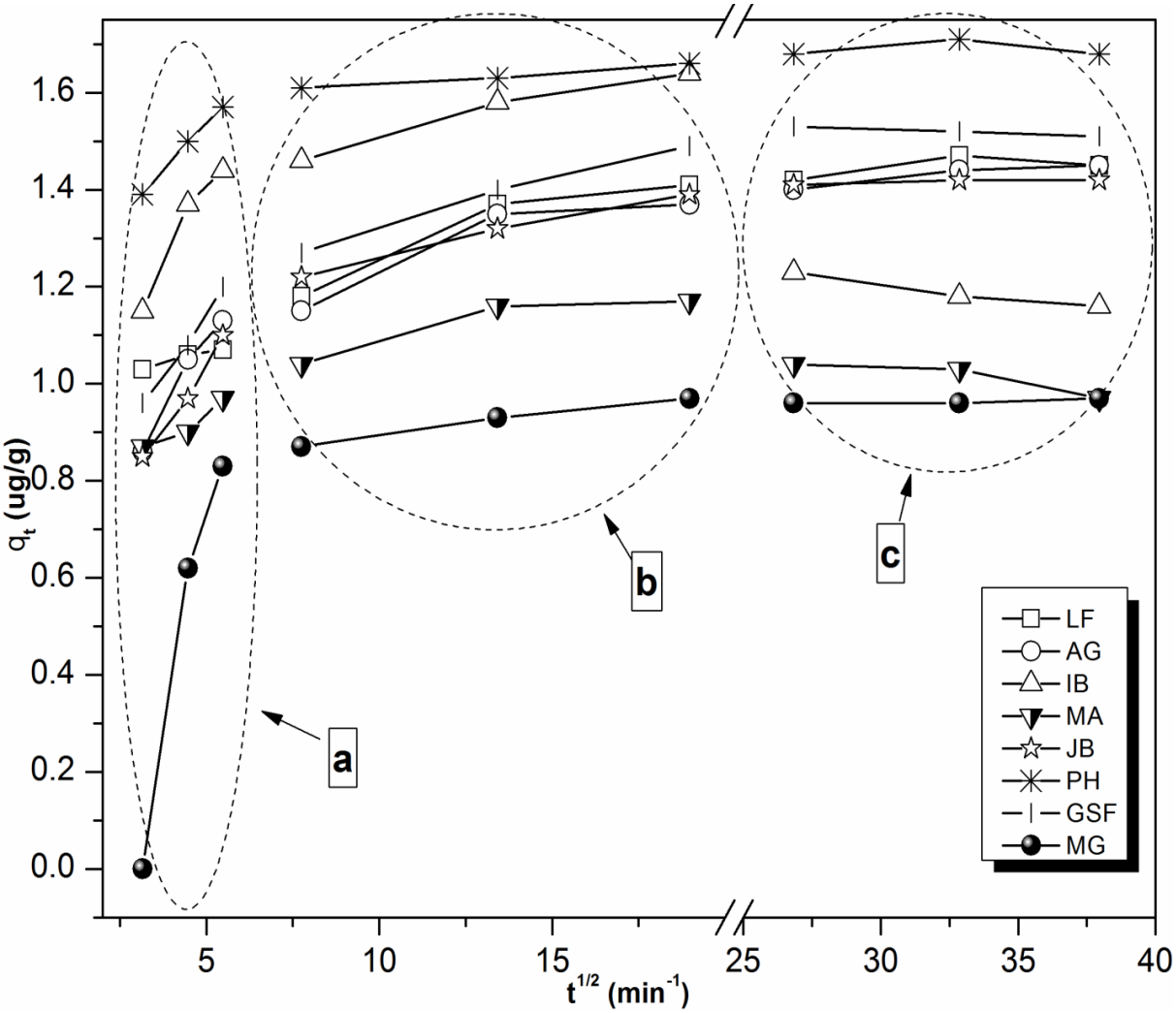

Figure 4.3. Intraparticle diffusion model plots for pyrene sorption on whole soils

4.3.3 Effect of pH on pyrene and fluorene sorptions

Sorption behaviors of PAHs can be significantly influenced by soil properties. It has been recognized that pH plays a profound role on PAHs sorptions in soils because of the influence of solution pH on soil physical and chemical properties especially the nature of the surface sorption sites (An et al., 2010). In this study, soil solution pH values were varied between 3 and 9 in order to investigate the extent to which pyrene and fluorene sorptions are dependent on solution pH using these soils of contrasting physico–chemical properties.

Figures 4.4 and 4.5 (and Appendix Figure A15) showed pyrene and fluorene sorptions with respect to soil solution pH. Pyrene and fluorene sorptions were significantly affected as the soil solution pH was varied between 3 and 9. These PAHs sorptions (Figure 4.4) were relatively high at low solution pH but then decreased with the increasing pH until around pH 6.0 where there were no significant changes in pyrene and fluorene sorbed. Irrespective of the soil, higher amounts of PAHs were sorbed at lower soil solution pH, but the amount sorbed at anytime, depends on soil properties such as organic matter content. The higher the soil organic matter content, the higher the pyrene sorption at any pH. The lower sorptions observed at higher pH values, especially close to neutrality, was a reflection of the true sorption capacity of these soils in the unaltered/normal environment since the natural ambient pH values of these soils are close to neutrality. Similar findings have been reported by An et al. (2010) and Zeledon-Toruno et al. (2007).

The observed PAHs sorption trend with variation in solution pH values was attributed to the sorption behavior of the hydrophobic functional groups of aliphatic and aromatic compounds as well as phenols in the organic matter of these soils. The increased sorption of these PAHs at low pH values was attributed to the fact that at low pH there was reduced polarity of the charged surfaces at adsorption sites on the soil especially those sites associated with the aromatic–hydrocarbon–rich soil organic matter. This resulted from the displacement of charged atoms by protons in solution leading to reduced ionization, increased association, and increased hydrophobicity, thus leading to shrinking of the constituent organic matter aromatic compounds (a typical occurrence for polymers at such pH in order to shield off water and other polar compounds from the hydrophobic

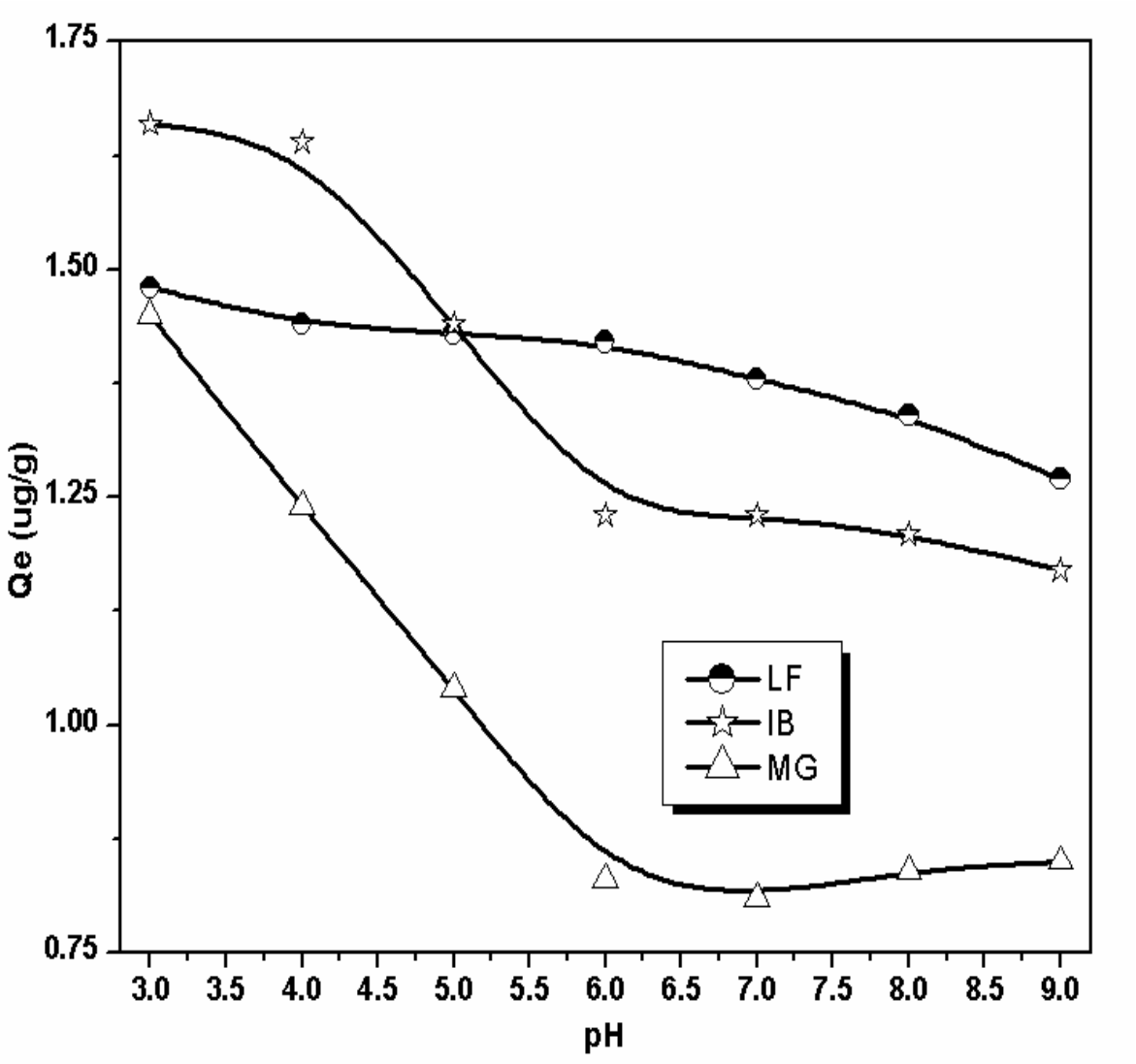

Figure 4.4. Effect of pH on pyrene sorption on LF, IB, and MG soils

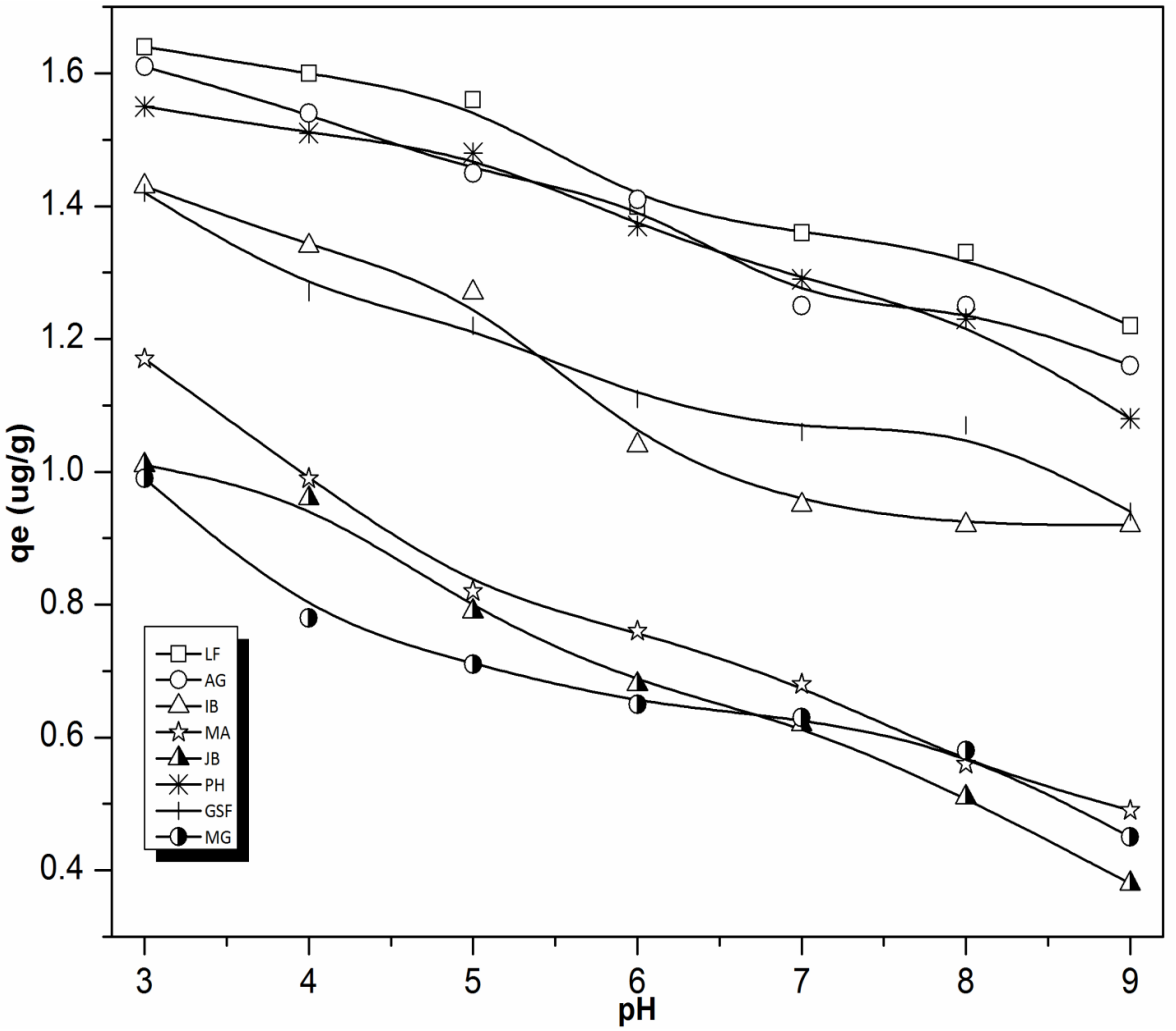

Figure 4.5. Effect of pH on fluorene sorption on whole soil samples

functional groups of these compounds). This increase soil hydrophobicity ultimately led to increased affinity for hydrophobic compounds like pyrene and fluorene. However, with increase in soil solution pH values, the competition for charged sites on the soil organic matter and clay minerals by the protons in solution drops correspondingly due to increase in ionization and dissociation resulting in increased polarity and reduced hydrophobicity; and hence, the acquired affinity for hydrophobic compounds is lost resulting in the reduced pyrene sorption observed. Similar results have been reported in literature (An et al., 2010; Zeledon–Toruno et al., 2007).

The higher quantities of pyrene sorbed in comparison to fluorene has been attributed to the chemical nature of both PAHs. Though both pyrene and fluorene molecules have equal numbers of cyclic hydrocarbons as part of their structures, the higher number of aromatic benzene rings in pyrene increased the number of π–π interactions between pyrene and other aromatic molecules when compared with fluorene, thus, the higher sorption of pyrene. Also, the conjugated spatial arrangement of the benzene rings in the fluorene molecule is also thought to reduce its strength of the π–π interactions with other aromatic molecules, resulting in its lower sorption.

4.3.4 Equilibrium sorption of pyrene and fluorene

Study of sorption equilibrium isotherms is an important method for investigating soil sorption and desorption processes because the relationship between the quantity of sorbate (sorbed pyrene or fluorene) and amount of pyrene or fluorene still in soil–water solution at equilibrium can be ascertained using the isotherms, that is, the relationship between the sorbate–equilibrium concentration. Hence, the effect of varying solution pyrene or fluorene concentration (20 – 100 μg/L) was studied at two temperatures (25 and 40 °C), ambient soil pH and incubation for 24 h.

Figures 4.6a, b, c, and Appendix Figures A16*i–xiii* showed the isotherm curves and sorption trends of pyrene and fluorene with increase in temperature (at 25 and 40 °C). Figure 4.6 showed that for all the soil samples studied, increasing the solution concentration of pyrene resulted in higher sorption of pyrene from solution. Teixeira et al. (2011) have reported that pyrene sorption on Brazilian soils is concentration dependent;

the amount adsorbed was found to increase with increasing pyrene concentration. Similar trend was also observed for fluorene sorption on these soils. Table A1 showed the type of isotherm curve for pyrene and fluorene sorptions at 25 and 40 °C. It suggested that the sorptions fitted different isotherm types under different sorption conditions.

The concentration dependence of pyrene and fluorene sorptions on these soils were attributed to the fact that as maximum sorption is attained in the soil and PAHs concentration increases, the tendency for multi–layer adsorption (enhanced by π–π interactions) on the already adsorbed PAHs on the soil's surfaces increases, leading to the observed increase in sorption as concentration increases. Thus, at equilibrium when the transport of each PAHs from the soil external surface into the internal pores and vice versa are equal, the trans–boundary movement of the sorbate will not be significantly permissible and sorption can only be 'forced' by higher concentration, hence the concentration dependence (Mittal et al., 2008).

The figures 4.6, A6 and A7 showed that increasing the soil solution temperature from 25 to 40 °C reduced the soils' sorptions of pyrene and fluorene. This observation suggested that the removal of these PAHs from solution will not require high temperature. It also implied that the sorptions are via weak hydrophobic forces (requiring low sorption energy, such as the π–π interactions and van der Waal's forces) of interaction between the soil sorption sites and the PAHs species in solution. Similar reduction in organic pollutants sorption as temperature increased has been reported by Abdel-Salam and Burk (2009) and Shu et al. (2010). The reduced sorption that occurs as solution temperature increases is not significant at low concentration of PAHs in solution due to the presence of unoccupied sorption sites in the soils, and thus the sorption of nonpolar organic compounds is in general, adequately described by linear isotherms over the lower range of equilibrium aqueous concentrations (Weber et al. 1992). However, the negative effect of temperature on PAHs sorptions becomes progressively and significantly higher with fewer sorption sites left on the soil and increase in solution PAHs concentration. This is because increase in the solution temperature increases PAHs solubility as well as its mobility in solution. Increased PAHs solubility will imply that the thin surface film of pyrene or fluorene on the soils surface will re-dissolve in solution, and the individual PAHs will acquire enough

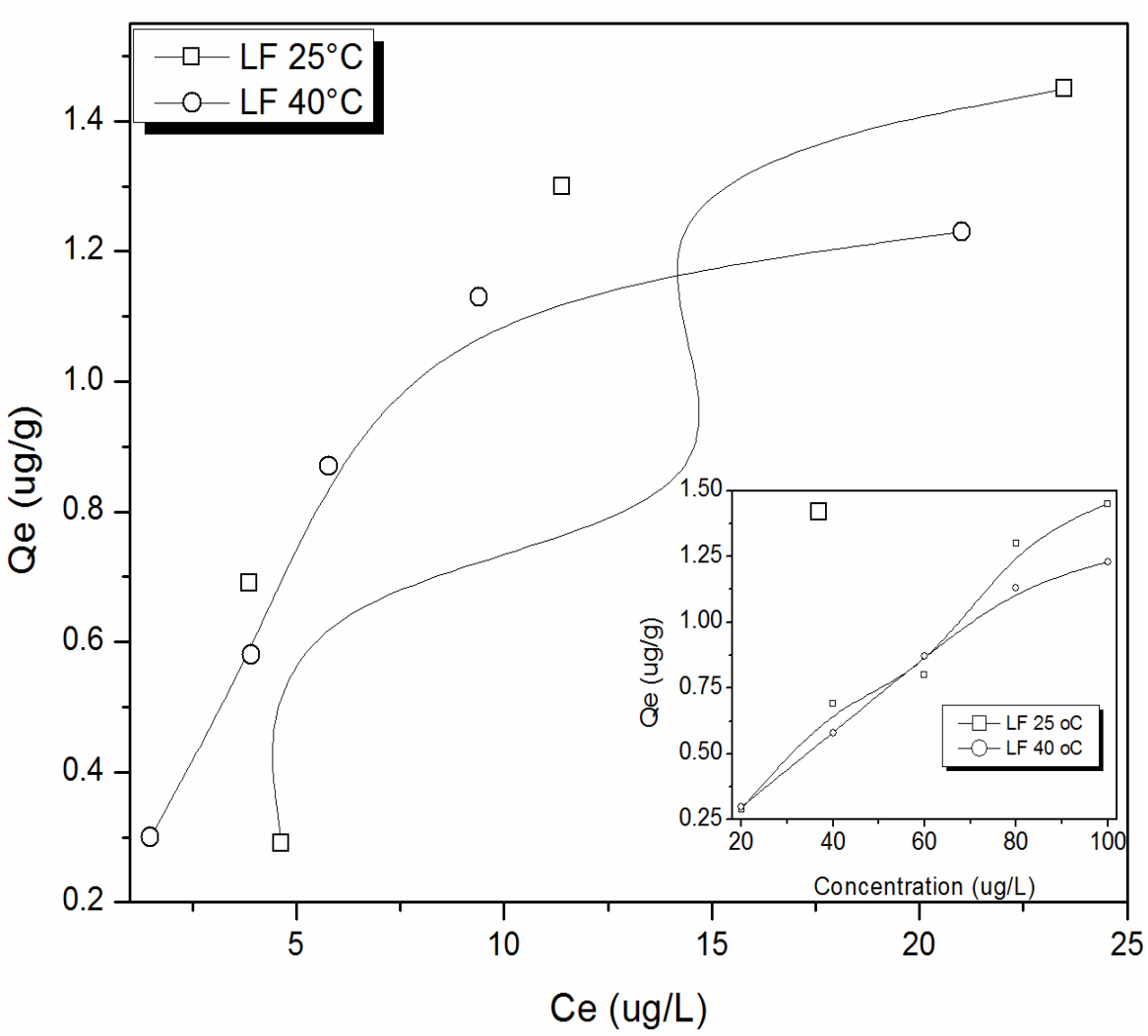

Figure 4.6 *a*. Pyrene sorption isotherm for LF soil (Insert: pyrene sorption trend as concentration varied at 25 and 40 °C)

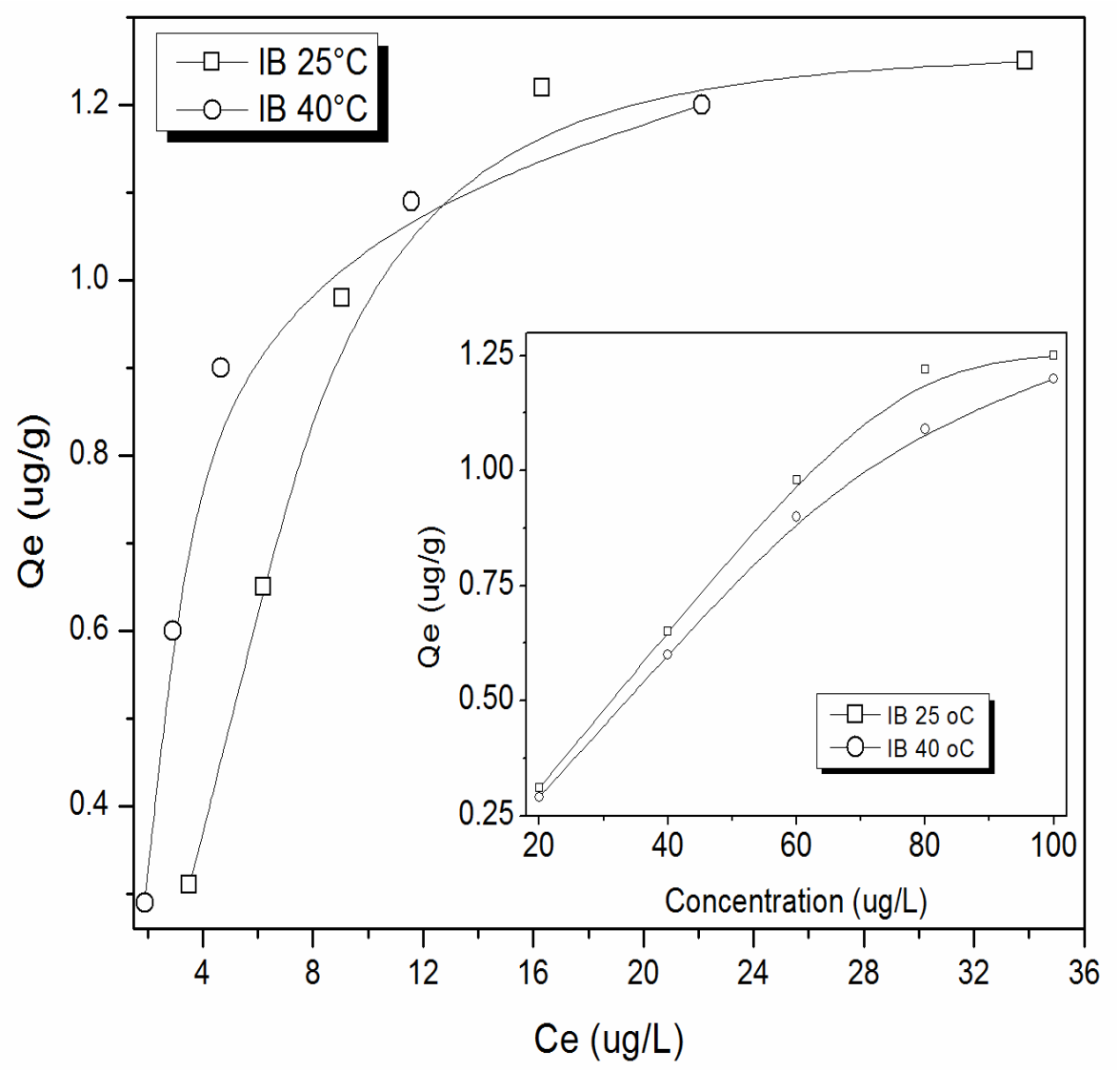

Figure 4.6 *b*. Pyrene sorption isotherm for IB soil (Insert: pyrene sorption trend as concentration varied at 25 and 40 °C)

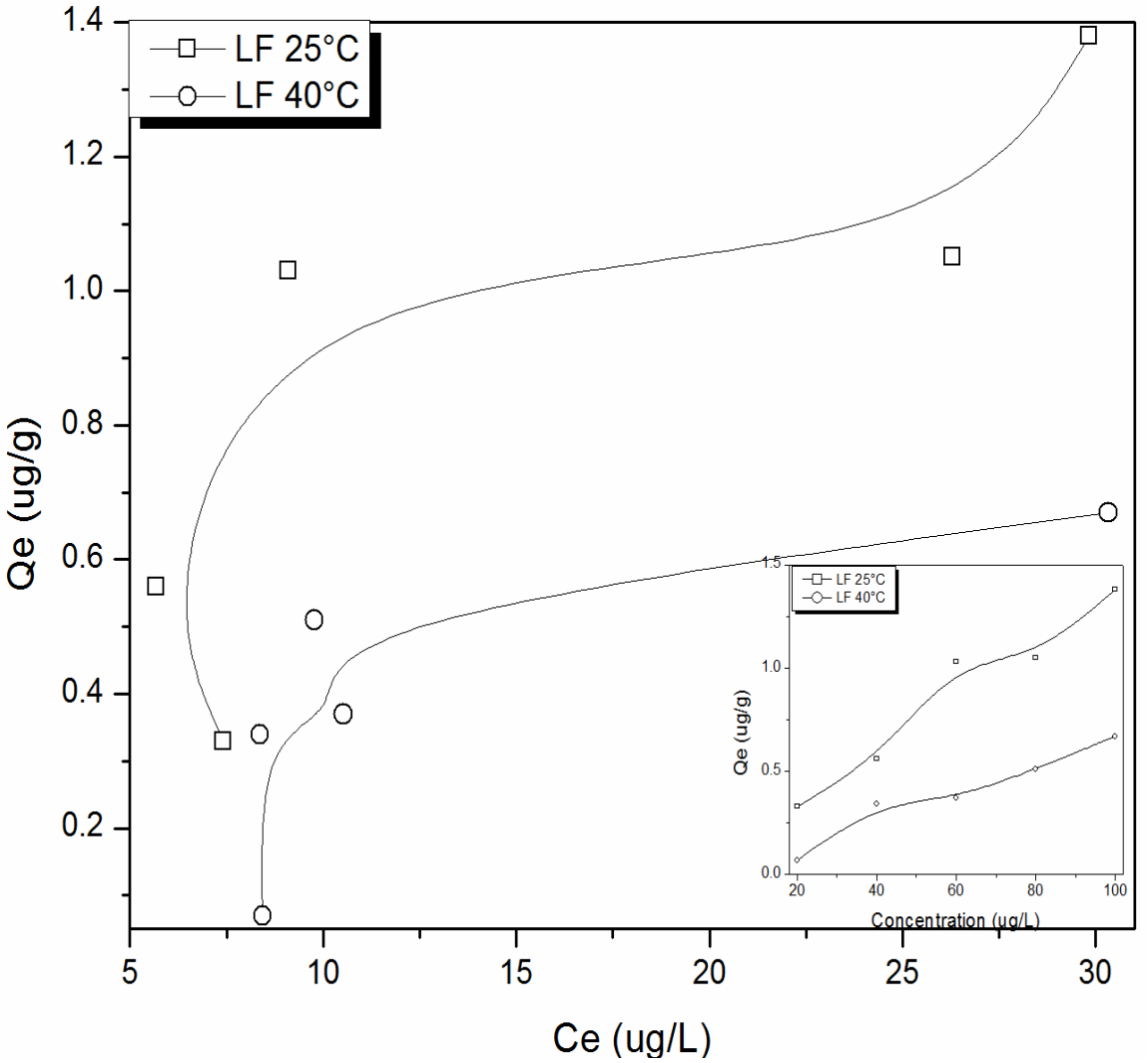

Figure 4.6c. Fluorene sorption isotherm for LF soil (Insert: fluorene sorption trend as concentration varied at 25 and 40 °C)

heat to facilitate their migration away from the sorption sites on soil surfaces; hence the reduction of PAHs sorptions on these soils.

It was observed that in the MA, JB, and MG soils, high temperature led to higher sorption of fluorene at low concentration. Though these soils had the lowest organic matter content of all the studied soils, this observation may not be unconnected to the presence of 2:1 expansive clays: illite in JB and MG and montmorillonite in JB and MA. The presence of these soils in aqueous solution as well as increase in temperature led to expansion of these clay minerals which resulted in increased sorption. However, for these soils, as concentration increased, the pores of the expansive clays become saturated and fluorene sorption on the soils does not increase correspondingly when compared with sorption at 25 °C. This reduction in fluorene sorption at 40 °C was attributed to the increased solubility and mobility of fluorene induced by the increase in temperature. Other soils (AG, IB, PH, GSF, and LF) with higher organic matter contents, this 'expansible minerals effect' is masked and sorption at all fluorene concentrations is lower at the higher temperature (40 °C), hence an exothermic process.

Similar pyrene sorptions trends were also observed for the OMR and IOR treated soils but with a significant variation in the amounts of pyrene sorbed per soil. Results showed that the OMR soils had the lowest pyrene sorption capacities when compared with the IOR and the whole soils (Figure 4.7 and Figures A6 *xiv* and *xv*). Pyrene sorption trend for the whole and treated soils was OMR > IOR > whole soils. Low sorption of pyrene observed for OMR soils was an indication of the contribution of soil organic matter in the sorption process. Polarity of the soil organic matter in any soil is an important parameter for sorption of hydrophobic organic pollutants because the sorption capacity of soil organic matter, especially the humic materials, is directly proportional to its polarity: the lower the polarity, the higher the affinity for hydrophobic organic pollutants (Guo et al., 2010; Site, 2001; Huang et al., 2003). Hence, sorption of hydrophobic organic chemicals by soils and sediments is driven by hydrophobic interactions.

Fluorene sorptions on the OMR and IOR treated soils also showed similar sorptions trend. The sorptions were concentration dependent. It was also observed that the whole soils

nearly always had higher fluorene sorptions at 25 °C than the treated soils, while increase in the sorption medium temperature lead to a general decrease in the fluorene sorptions on the treated soils. An exception to this trend is the JB soil. One reason for this trend might be due to the fact that fluorene sorptions on LF and GSF soils are mainly on soil constituents other than the soil mineral components, especially the organic matter. Thus, removal of these soil components led to reduced fluorene sorption. However, fluorene sorptions on JB soil (whole and treated) are mainly on the clay minerals. The higher fluorene sorption observed in the treated JB soils at lower solution fluorene concentrations at 40 °C was attributed to the presence of the 2:1 expansive clays, illite and montmorillonite, which absorb water and swell as temperature increased. This expansion creates new surfaces for fluorene sorption on the expanded pores of treated JB soils. These new surfaces, though present in the whole JB soil, were masked by the presence of iron oxides and organic matter. These surfaces are few and are easily saturated; hence, their effect is felt mainly at low solution fluorene concentration. However, due to the concentration dependent nature of fluorene sorption, increase in the solution concentration of fluorene will mean that the movement of fluorene towards the external surface of the sorbent (film diffusion) will surpass the fluorene movement within the pores of the sorbent (particle diffusion); hence, increase in fluorene concentration will result in '*forced*' sorption of fluorene on the soil external surface especially on the whole soil having more sorption surfaces, thus the observed higher sorption at higher concentration. Mittal et al. (2008) have reported similarly.

Removal of iron oxides and organic matter in these soils showed the contributions made by these constituents to fluorene sorption: organic matter contributed ≥ 50 % while iron oxides contributed < 50 % to fluorene sorption. The arguments that expansible clays played the major role in fluorene sorption at higher temperatures, and that some soil constituents masked the soil fluorene sorption sites were supported by the JB IOR which exhibited higher fluorene sorption than that of the untreated soils at 40 °C. Fluorene sorption trend at both temperatures for the whole and treated soils was OMR > IOR > whole soils. Fluorene sorption on the JB IOR sample at 40 °C is an exception: IOR > whole soil > OMR.

Most sorption processes, especially with PAHs, are reversible, but often a 'hysteresis' effect is observed. Hysteretic desorption phenomenon is practically important because the low desorption corresponds to a lowered chemical activity of the sorbed chemical, suggesting a reduced biological reactivity and decreased toxicity of the chemical (Huang et al., 2003). Hence, desorption studies on these soils were carried out immediately after the sorption experiments. Results in Figures 4.7, Appendix A16*xiv–xix*, A17, and A18 showed desorption studies using untreated and treated soils. The quantities of pyrene and fluorene desorbed from these soils were dependent on the quantities of each PAH sorbed – the higher the sorption the more desorption. Hysteresis was observed for all soils. However, the degree of hysteresis was higher in soils with high organic matter contents and lower in soils with low organic matter contents. This was in line with the earlier observation that organic matter had higher contribution to these PAHs sorptions than other soil components.

Whole soils with relatively high contents of organic matter showed lower pyrene and fluorene desorptions (high hysteresis) when compared to the treated soils. This also supported the earlier observation that soils with high quantity of low polarity organic matter have high affinity for hydrophobic organic pollutants which will logically result in low desorption. Hence with the higher sorptions of pyrene and fluorene in the higher organic matter soils (LF, AG, IB, and PH), these soils exhibited the highest desorption hysteresis (lowest desorption). Site (2001) has reported similar results of high hysteresis for high organic matter soils.

Desorptions of fluorene from these soils also showed similar trend as the pyrene desorptions. Fluorene desorption hysteresis were higher in soils with high organic matter content; and hysteresis were very low (very high desorptions) at higher temperature. Increase in temperature increased desorption because increase in temperature increased the solubility and mobility of fluorene in solution and this tends to increase the kinetic energy of the fluorene molecules which are weakly sorbed on the soil surface sorption sites. Increase in kinetic energy will ultimately induce the surface adsorbed fluorene molecules to migrate away from these sorption sites, hence the desorption.

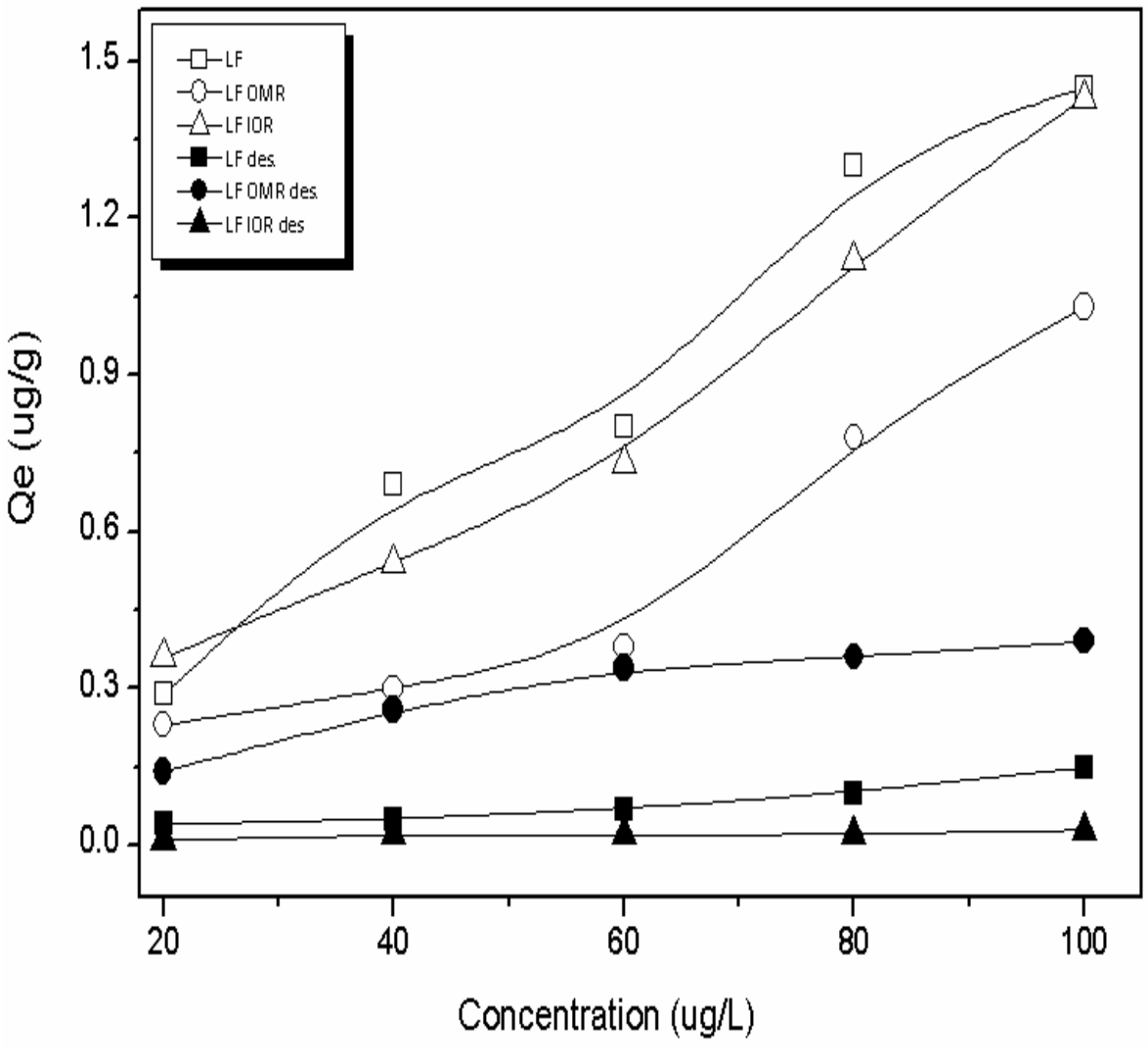

Figure 4.7. Sorption (empty symbols) and desorption (filled symbols) trend of pyrene on whole and treated LF soils.

For soils with low organic matter content, desorption was more pronounced than for those with high organic matter contents. Treatments of the soils also showed the contributions of organic matter and iron oxides to desorption or retention of fluorene by the soils. Results in Figure 4.8a, b, and Appendix A6*xiv–xix* also showed that removal of any of these soil constituents increased desorption of fluorene from the soils. Lower hystereses were observed in the treated soils than the whole soils. Desorption on the soils followed a reverse trend as the sorption of fluorene – OMR < IOR < whole soils. This trend follows from the fact that the higher the organic matter in the soil the lower the desorption.

One major mechanism that has been proposed for the observed pyrene and fluorene desorption hysteresis in soils with higher organic matter contents is the entrapment of these PAHs within inorganic and organic matrices causing the slower rate of desorption than the sorption (Huang et al., 2003; Site, 2001). Entrapment of sorbed molecules within the meso/micro-porous structures of the inorganic aggregates (such as the 2:1 expansive clays: illite and montmorillonite) was thought to be the main factor responsible for the hysteresis observed in MA, JB, and MG soils with lower organic matter contents. Huang et al. (2003) have also proposed that the irreversible chemical binding of organic pollutants to humic acids may also be implicated in hysteresis, but this may be of less significance in this study because of the uncharged nature of the PAHs of interest.

Desorption in the treated soils followed the same trend for both PAHs: OMR > IOR > whole soils. The high desorptions observed in the low organic matter containing soils implied high availability of these PAHs in the soil water solution, bioavailability to biota, and subsequent contamination of the water aquifer.

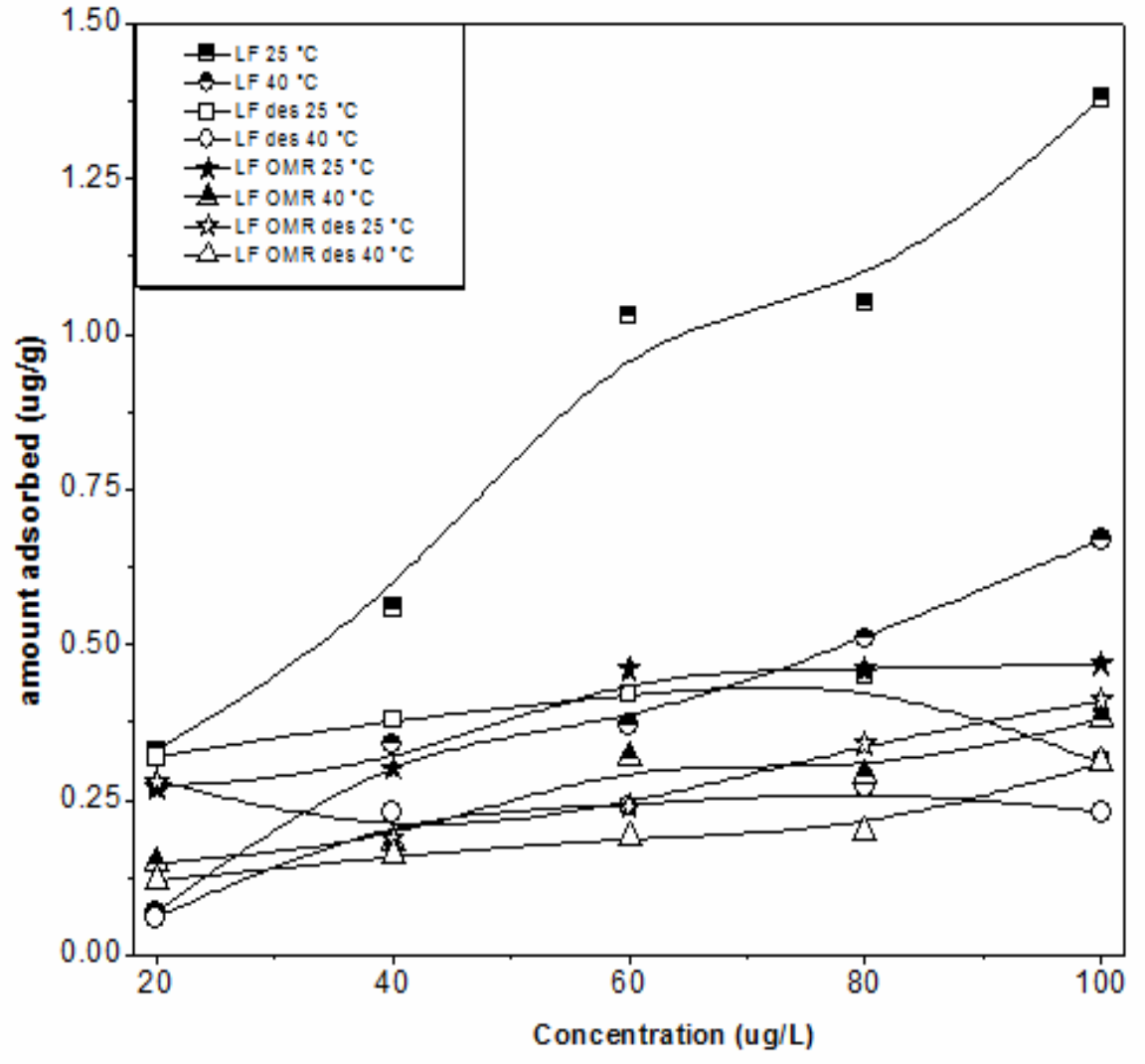

Figure 4.8 *a*. Sorption (half–filled symbols) and desorption (empty symbols) of fluorene on LF whole and treated soil (OMR) at 25 and 40 °C

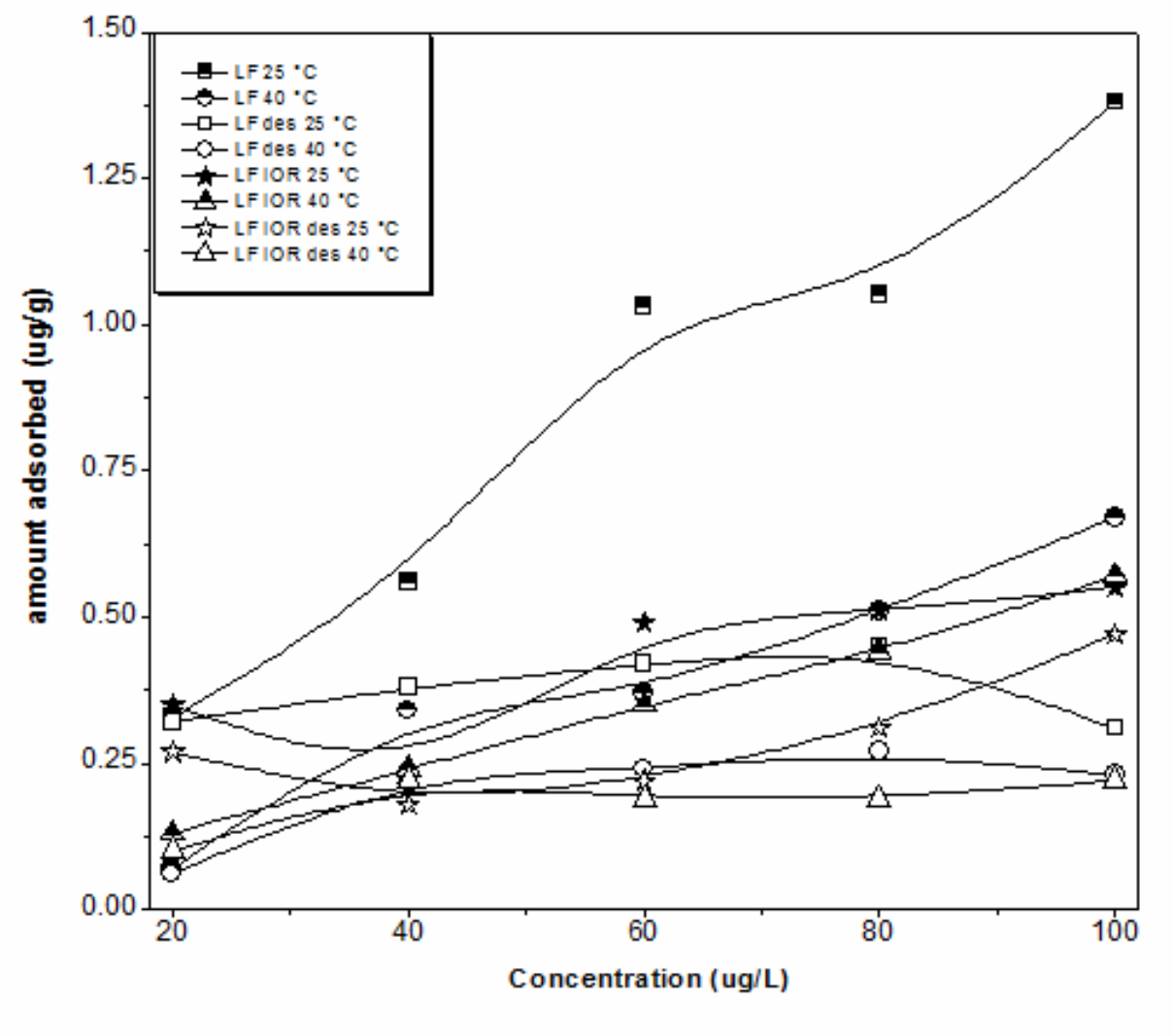

Figure 4.8 *b*. Sorption (half–filled symbols) and desorption (empty symbols) of fluorene on LF whole and treated soil (IOR) at 25 and 40 °C

4.3.5 Thermodynamics of pyrene and fluorene sorptions

The thermodynamic parameters – standard free energy ($\Delta G°$), enthalpy change ($\Delta H°$), and entropy change ($\Delta S°$) – were calculated using equations 2.3–2.6 and the calculated parameters were used to evaluate the feasibility and the energetics of the PAHs sorption processes. Tables 4.7 and 4.8 showed the thermodynamic parameters for pyrene and fluorene sorptions on the whole soils. The $\Delta H°$ and $\Delta S°$ values for pyrene sorptions were in the range of −67.51 to 63.70 kJ mol^{-1} and −0.21 to 0.23 kJ mol^{-1} K^{-1}, respectively. The $\Delta H°$ and $\Delta S°$ values were negative with the exception of PH, GSF, and MG soils. The negative $\Delta H°$ values conform to the observed exothermic nature of the pyrene sorption process, while negative $\Delta S°$ values indicated a decrease in the randomness at the solid–liquid interface as the pyrene sorption process proceeded towards equilibrium implying accumulation of the pyrene molecules on the soil.

The $\Delta H°$ values for the fluorene sorptions are in the range of −43.89 to 95.45 $kJmol^{-1}$. The $\Delta H°$ values showed that the sorptions were endothermic (positive) except for MA, JB, and MG soils which were exothermic (negative). The negative $\Delta H°$ values conform to the observed exothermic nature of fluorene sorption process on the MA, JB, and MG soils. However, for other soils, calculated $\Delta H°$ values showed that the fluorene sorption was endothermic, requiring heat energy, but experimental results indicated otherwise. Input of heat energy was expected to increase the sorption of fluorene by breaking the energy barrier (activation energy) required to be surpassed for sorption to occur. However, increased energy led to increase in solubility as well as the mobility of fluorene in solution. These later effects affected the sorption process more than the former as observed in the calculated $\Delta S°$ (increased entropy); and this led to reduced fluorene sorption. The $\Delta S°$ values were in the range of -0.10 to 0.34 $kJmol^{-1}K^{-1}$. The increase in $\Delta S°$ values implied increased randomness of the fluorene molecules in solution as temperature increased. This was attributed to increased fluorene solubility and increased kinetic energy acquired from the higher temperature. However, MA, JB, and MG soils had decreased entropy of the molecules with increase in temperature. This was attributed to the presence of the 2:1 expansive clays, illite and montmorillonite, in these soils.

Table 4.7: Thermodynamic parameters for pyrene sorption on the whole soils

Soil	ΔH^{o}	ΔS^{o}	ΔG^{0} (kJ mol^{-1})	
	(kJ mol^{-1})	(kJ mol^{-1}K^{-1})	298 K	313 K
LF	-67.5	-0.21	-6.30	-3.22
AG	-17.4	-0.04	-5.06	-4.44
IB	-40.5	-0.12	-4.96	-3.17
MA	-31.0	-0.07	-9.79	-8.72
JB	-65.4	-0.19	-8.80	-5.95
PH	10.9	0.06	-8.42	-9.39
GSF	63.7	0.23	-5.95	-9.45
MG	27.4	0.10	-3.85	-5.42

Table 4.8: Thermodynamic parameters for the sorption of fluorene on the whole soils

Soil	ΔH^o (kJ mol^{-1})	ΔS^o (kJ mol^{-1}K^{-1})	ΔG^o (kJ mol^{-1}) 298 K	313 K
LF	95.5	0.34	-6.35	-11.5
AG	28.2	0.13	-10.9	-12.9
IB	12.5	0.08	-10.3	-11.4
MA	-25.8	-0.04	-14.3	-13.7
JB	-26.8	-0.04	-15.5	-14.9
PH	40.4	0.17	-9.01	-11.5
GSF	88.9	0.33	-8.73	-13.6
MG	-44.0	-0.10	-14.5	-13.0

Increase in temperature caused the expansion of these clays leading to sorption of fluorene in solution onto the interstitial spaces on these clays, and hence the reduced entropy. The effect of the presence of these clays on fluorene sorption was especially noticed at lower solution concentration of fluorene. Sorption of fluorene leading to its removal from solution caused reduction in randomness at the soil–solution interface as the sorption process progressed towards equilibrium.

The values of the ΔH^o can give insight to the type of interaction(s) associated with the sorption process. In this study, the ΔH^o values of both pyrene and fluorene sorptions suggested that the forces of interaction between the PAHs and the soil sorption sites were weak hydrophobic forces such as the van der Waals and π–π interactions which are common forms of interaction for hydrophobic organic compounds with weak or no polar groups.

Negative $\Delta G°$ values were observed for pyrene and fluorene sorptions in all the studied soils at both temperatures. The negative values of $\Delta G°$ indicated that the sorptions of both PAHs on these soils are feasible and spontaneous. The size range of the ΔG^o values implied that the initial sorption barrier needed to be surpassed before sorptions occurred was very small; thus confirming the sorptive forces involved in these PAHs sorption were weak.

The calculated thermodynamic parameters for pyrene sorption on PH, GSF, and MG (Table 4.7) suggested endothermic sorption, though experimental sorption data of pyrene on these soils indicated exothermic reactions (Figures 4.6 e – h). The reason for the above observations could be attributed to small errors associated with linear model calculations of the thermodynamic parameters which may become significant when dealing with low energy sorption surfaces leading to slight shifts of values from the border of one extreme to another. When this occurs, sorption processes with thermodynamic parameters having small negative values could shift to positive values (Unuabonah et al., 2008).

Thermodynamics of the sorption of fluorene on the whole and treated soils was compared for the LF, GSF, and JB soils to ascertain if the thermodynamic trends for the whole and

treated soils are similar. The values of the thermodynamic parameters are shown in Table 4.9.

$\Delta G°$ values for both whole and treated soils at both temperatures were negative. This implies that the sorption of fluorene on these soils was feasible and spontaneous, and the size range of the sorption energy involved were of the type associated with the weak hydrophobic interactions such as the van der Waal's forces and $\pi - \pi$ interactions.

The ΔS^o values are in the range of −0.00 to 0.34 kJmol^{-1}K^{-1}. The ΔS^o values were mainly negative and indicated that sorption of fluorene from solution led to decrease in randomness of fluorene molecules in solution. Though some exceptions were observed, the values were low, and this might be due to minor errors associated with linear model calculations of the thermodynamic parameters which could become significant when dealing with low energy sorption surfaces like this one. When this happens, there may be slight shifts of values from the border of one extreme to another (Unuabonah et al., 2008).

The ΔH^o values showed that the sorptions were mainly exothermic (negative), with few exceptions – LF, LF OMR, and JB IOR. The negative ΔH^o values confirmed the exothermic nature of sorption processes. Like the ΔS^o values, the few variations from the exothermic sorption process were attributed to minor errors associated with linear model calculations of the thermodynamic parameters.

4.3.6 Sorption Isotherm Models

The equilibrium sorptions data of pyrene and fluorene on all whole soils at 25 °C were fitted to two different sorption isotherm models – the Langmuir and Freundlich – to ascertain which of these models better correlates the sorption data. These isotherm models are the most commonly used in sorption experiments.

Table 4.10 and 4.11 showed the values of the isotherm parameters for both models for pyrene and fluorene sorptions, respectively. Table 4.10 showed that the correlation coefficients (r^2) values were poor and the estimated q_e values did not show correlation with experimental values obtained for pyrene sorption. Similar observations were

Table 4.9: Thermodynamic parameters for the sorption of fluorene on the treated soils

Soil	ΔH^o	ΔS^o	ΔG^o (kJ mol^{-1})	
	(kJ mol^{-1})	(kJ mol^{-1}K^{-1})	298 K	313 K
LF	95.5	0.34	-6.35	-11.5
GSF	88.9	0.33	-8.73	-13.6
JB	-26.8	-0.04	-15.5	-14.9
LF OMR	108	0.38	-5.97	-11.7
GSF OMR	-88.2	-0.24	-15.8	-12.2
JB OMR	-17.1	0.00	-17.1	-17.1
LF IOR	-5.01	0.01	-9.07	-9.28
GSF IOR	-107	-0.31	-14.7	-10.0
JB IOR	41.8	0.17	-7.37	-9.85

Table 4.10. Isotherm model parameters for pyrene sorption on whole soils

soil	Langmuir sorption model			Freundlich sorption model				Distributed Reactivity Model (DRM)	
	Q_O (mg/g)	b	r^2	q_e (mg/g)	n	K_f	r^2	$q_{T(l+nl)}$ (mg/g)	r^2
LF	2.22	0.05	0.340	1.32	0.58	0.21	0.528	1.45	1.000
AG	2.19	0.08	0.639	1.57	0.60	0.24	0.676	1.45	0.992
IB	1.73	0.09	0.908	1.60	0.59	0.20	0.805	1.25	0.984
MA	1.42	0.02	0.225	0.80	0.65	0.07	0.651	0.95	0.988
JB	0.90	0.19	0.400	0.83	0.64	0.12	0.449	1.50	0.983
PH	1.15	0.13	0.346	0.96	0.77	0.11	0.439	1.58	0.994
GSF	2.12	0.06	0.419	1.27	0.65	0.17	0.822	1.49	0.957
MG	1.05	0.15	0.948	0.99	0.32	0.29	0.672	0.94	0.931

$q_{T(l+nl)}$ (mg/g) – Total linear (l) and non–linear (nl) sorption, its values are exactly equal to the experimental q_e values

Table 4.11. Isotherm model parameters for fluorene sorption on whole soils

soil	Langmuir sorption model			Freundlich sorption model				Distributed Reactivity Model (DRM)	
	Q_O (mg/g)	b	r^2	q_e (mg/g)	n	K_f	r^2	$q_{T(l+nl)}$ (mg/g)	r^2
LF	2.27	0.041	0.446	1.28	0.58	0.18	0.578	1.38	0.999
AG	12.2	0.002	0.000	1.00	0.69	0.10	0.063	1.41	0.998
IB	1.49	0.011	0.472	1.02	1.37	0.01	0.935	1.21	0.992
MA	0.19	0.014	0.631	0.42	2.25	0.00	0.911	0.66	0.999
JB	0.07	0.017	0.728	0.55	3.20	0.00	0.935	0.75	0.999
PH	10.5	0.003	0.016	1.09	0.68	0.04	0.676	1.24	0.997
GSF	2.09	0.021	0.493	0.90	0.69	0.08	0.655	1.02	0.991
MG	0.32	0.010	0.347	0.72	1.73	0.00	0.789	0.52	0.962

$q_{T(l+nl)}$ (mg/g) – Total linear (l) and non–linear (nl) sorption, its values are exactly equal to the experimental q_e values

noticed for fluorene sorptions (Table 4.11) on these soils. Thus, the equilibrium sorption data of pyrene and fluorene did not fit both the Langmuir and Freundlich adsorption isotherms, and so the isotherms could not be used to explain their sorptions on these soils. This implies that pyrene and fluorene sorption were neither monolayer adsorption on similar surface adsorption sites of nearly equal energy (as suggested by the Langmuir model), nor where they strictly on heterogeneous surface sites of dissimilar energy having tendency of formation of PAHs multi–layer on the sorbent surface(s) at saturation (as suggested by the Freundlich model). However, comparing both isotherm models shows that the Freundlich isotherms described these PAHs sorptions, relatively, better than the Langmuir isotherms. The small *n* values of the Freundlich isotherm indicated the non–linearity of the isotherms and represented PAHs sorptions on predominantly heterogeneous sorption sites. This is in line with the argument that the Langmuir type isotherm is rarely encountered in soils because of its highly heterogeneous nature (Weber et al., 1992). The Freundlich type isotherm is mostly encountered. However, PAHs sorptions on these soils rarely adhere strictly to any of these isotherm models and this could be attributed to the fact that most natural soils are intrinsically heterogeneous and variable in composition even at the microscopic level scale. Hence, PAHs sorptions on these soils might be characterized by multiple sorption processes as proposed by Weber et al. (1992).

The Weber et al. (1992) distributed reactivity model was used to fit the sorption data of both pyrene and fluorene on these soils. The model assumes that there are several individual linear and non–linear isotherms that make up the final soil isotherm. These individual isotherms were treated as a composite of the general linear and non–linear isotherms observed in the soil for a particular sorption process.

For a system comprising both the linear and non–linear sorptions, the composite of these sorption isotherms models will give an equation as stated in equation 2.19.

$$q_e = x_i K_D C_e + \sum_{i=1}^{m} \left(x_{nl}\right)_i K_{F_i} C_e^{ni} \qquad 2.19$$

where x_i is the summed mass fraction of solid phase exhibiting linear sorptions, K_D, is the mass-averaged partition coefficient for the summed linear components, $\left(x_{nl}\right)_i$ is the mass fraction of the *i* nonlinearly sorption component, , K_{F_i}, and C_e^{ni} are the Freundlich constant and the nonlinear component of the amount of sorptive left in solution at equilibrium. The first part of equation 2.17 ($x_i K_D C_e$) represents the linear components of the sorptions, while the second part ($\sum_{i=1}^{m}\left(x_{nl}\right)_i K_{F_i} C_e^{ni}$) represents nonlinear components.

The results of the Distributed Reactivity Model (DRM) fittings of the equilibrium sorptions data of pyrene and fluorene on all whole soils at 25 °C are shown in Table 4.10 and 4.11. It was observed from Table 4.10 that the sorptions of pyrene fitted the DRM with correlation coefficients (r^2) in the range of 0.957–1.000. Similar results were observed for the fitting of fluorene sorption data using DRM with r^2 values in the range of 0.962 – 0.999. The calculated q_e (mg/g) values were in close agreement with the experimental q_e (mg/g) values. These results suggested that the sorption isotherms of pyrene and fluorene were composed of several linear and non–linear isotherms of the Freundlich type.

The small *n* values, especially those less than 1, (ranging from 0.58 to 0.77) also suggested non–linearity of the isotherms (Tables 4.10 and 4.11). *n* values may be regarded as an index of surface site energy distribution (Weber et al., 1992), where small *n* values represent sorption on predominantly heterogeneous sorption sites. This corroborated the earlier predicted mechanisms for the sorptions of PAHs on these soils being governed by sorption onto specific sorption sites, partitioning within the interstitial spaces of soil clay minerals and organic matter, as well as by weak hydrophobic forces of interaction between soil sorption surfaces and the PAHs molecules.

Table 4.12 showed that soil treatments could change the fitting of the sorption data on isotherm models that initially described fluorene sorption on the whole soils. For instance, fluorene sorption on the LF whole soil could not be described by the Langmuir or the Freundlich isotherm. However, fluorene sorption on the LF OMR was well described by

all three models. This observation was attributed to the fact that sorption on heterogeneous surfaces where each surface obeys the Langmuir type isotherm model, combination of these various Langmuir type isotherm model results in a Freundlich type isotherm (Weber et al., 1992). Similar trends were observed for other treatments except for the LF IOR, JB OMR and GSF OMR, whose fluorene sorptions followed similar trend as observed in the whole soil and mainly fitted the DRM.

4.4 Competitive Sorption of Pyrene and Fluorene

4.4.1 Equilibrium sorption of Pyrene and Fluorene mixtures

Competitive sorptions of fluorene and pyrene were carried out and sorption isotherms are shown in Figures 4.9 and 4.10, respectively (expanded isotherms are shown in Figures A17 *i* and *ii*). The isotherms showed that the sorptions of both PAHs were concentration dependent and increased with increase in concentration. The data generated from the single PAHs solution studies were compared with those from the mixed PAHs solutions studies – Figures 4.11 and 4.12 (and Figures A17 *iii* and *iv*). It was observed that pyrene sorptions from single PAHs solutions were higher than from the mixture solutions. However, for soils with relatively higher organic matter contents – LF, AG, IB, and PH, the amounts of pyrene sorbed in the single and mixed PAHs solutions were nearly the equal. The reason for this observation can be due to the high affinity of pyrene for organic matter on these soils as well as multi–layer adsorptions of the pyrene on already adsorbed pyrene on the soils' surface.

Similarly, higher fluorene sorption on soils was observed from the single component solutions than the mixed component solutions. Exceptions to the present observation are the LF and MG soils. Unlike the pyrene sorptions which showed a specific trend – higher sorptions for soils with relatively high organic matter, fluorene sorptions did not show such trend since one of the two exceptions has relatively high organic matter contents. This observation in LF and MG soils was attributed to the presence of relatively high quantities of the 2:1 expansive clay, illite (≈15 and 36 %, respectively). The clay absorbs water and swell, creating larger voids in the interstitial spaces within the soils and allowing more PAHs sorption to occur.

Table 4.12. Isotherm model parameters for fluorene sorption on treated soils

Soil	Langmuir sorption model			Freundlich sorption model				DRM	
	Q_O (mg/g)	b	r^2	q_e (mg/g)	n	K_f	r^2	$q_{T(l+nl)}$ (mg/g)	r^2
LF OMR	0.55	0.09	0.986	0.40	0.31	0.13	0.900	0.47	0.995
GSF OMR	0.10	0.01	0.412	0.51	2.17	0.001	0.807	0.53	0.990
JB OMR	0.05	0.01	0.685	0.61	2.83	0.001	0.948	0.44	0.985
LF IOR	0.73	0.04	0.640	0.46	0.24	0.18	0.307	0.55	0.979
GSF IOR	0.16	0.01	0.872	0.68	2.25	0.001	0.935	0.67	0.999
JB IOR	0.45	0.05	0.958	0.34	0.32	0.09	0.909	0.39	0.980

$q_{T(l+nl)}$ (mg/g) – Total linear (l) and non–linear (nl) sorption, its values are exactly equal to the experimental q_e values; DRM – Distributed Reactivity Model

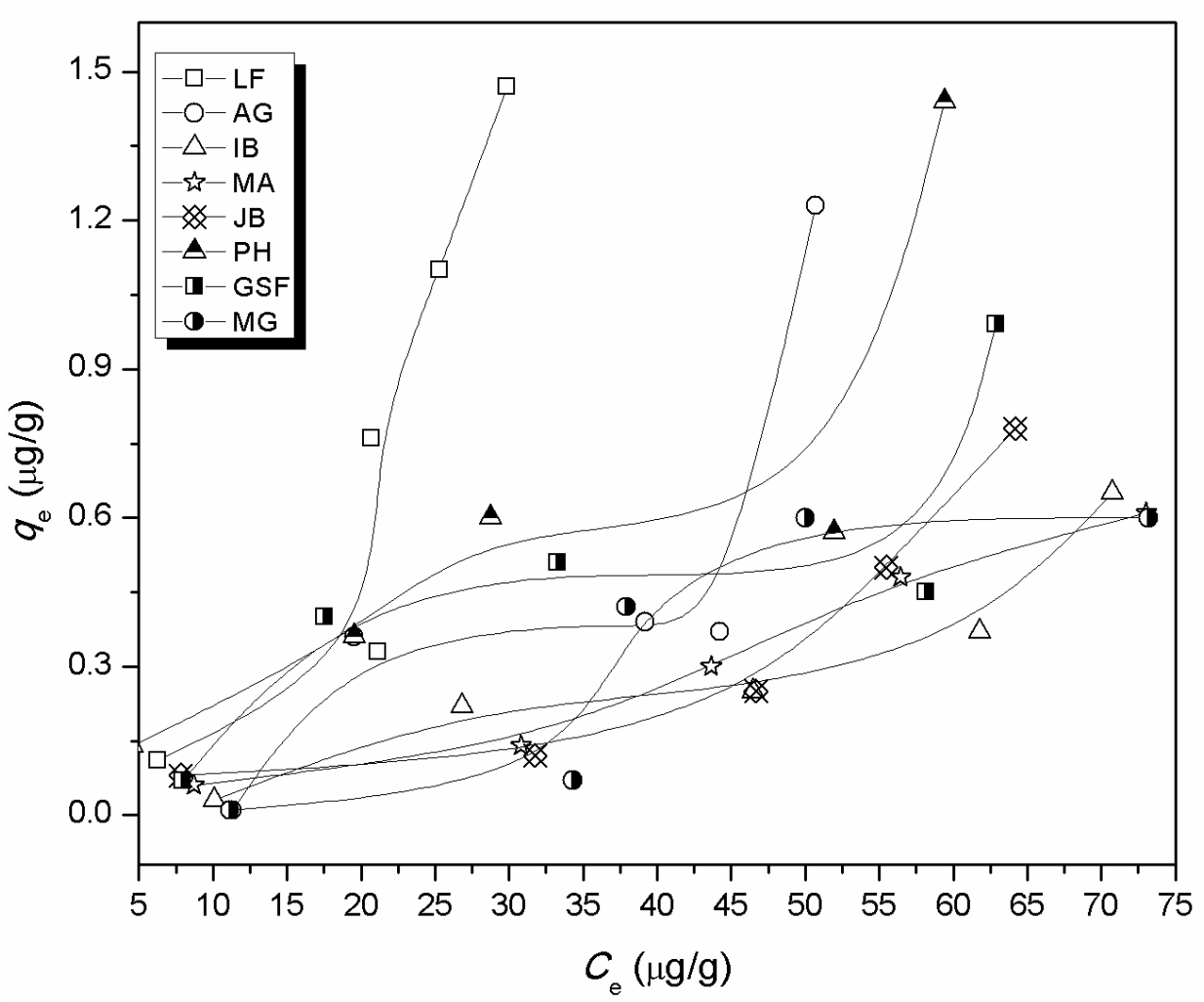

Figure 4.9. Competitive fluorene sorptions isotherms (expanded isotherms are in Figure A17 *i*)

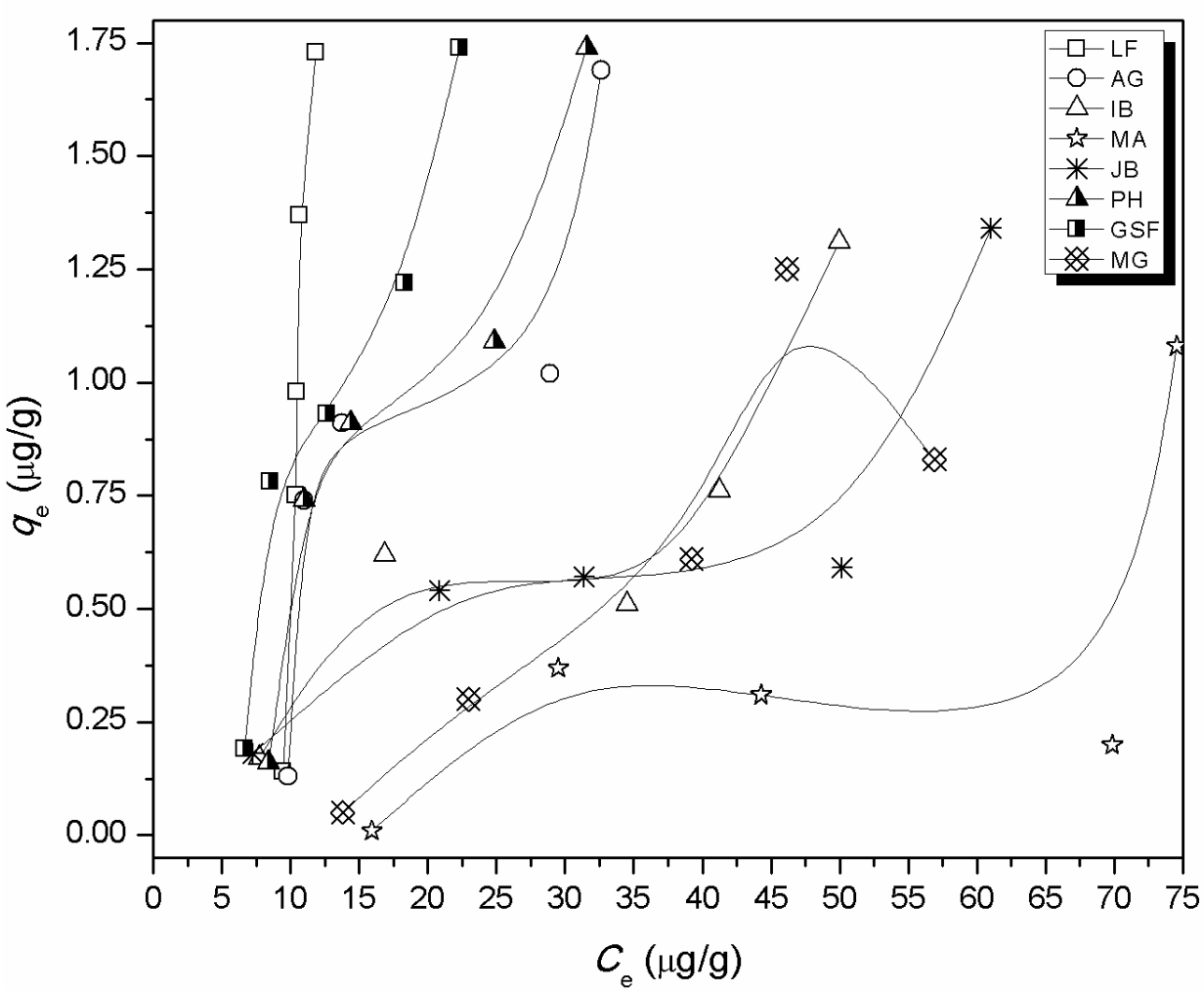

Figure 4.10. Competitive pyrene sorptions isotherms (expanded isotherms are in Figure A17 *ii*)

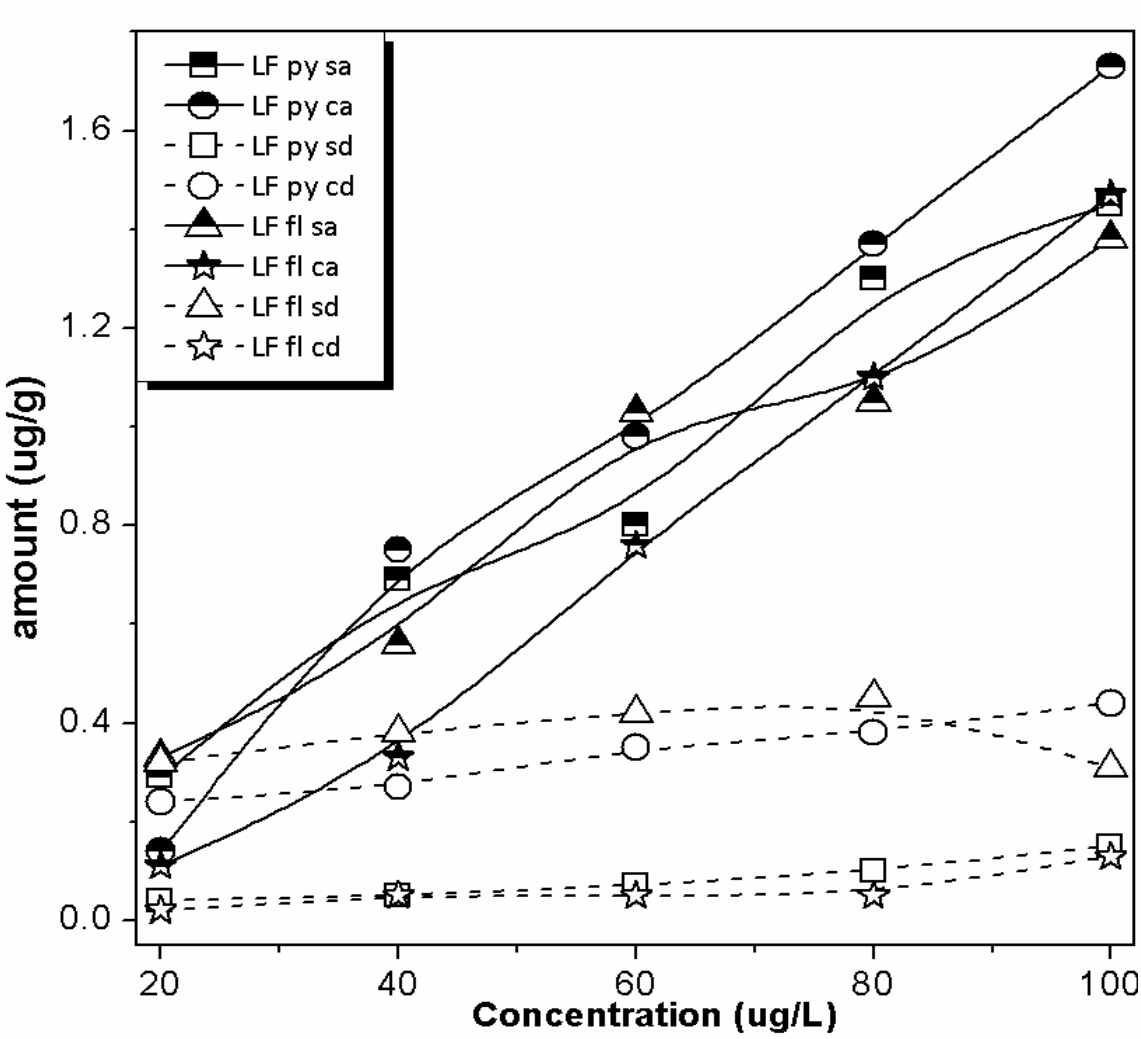

Figure 4.11. Single (solid lines and half filled symbols) and competitive sorptions (solid lines and half filled symbols) and desorption (broken lines and empty symbols) of pyrene and fluorene on the LF whole soils. Codes in figure: sa – single adsorption, ca – competitive adsorption, sd – single desorption, cd – competitive desorption.

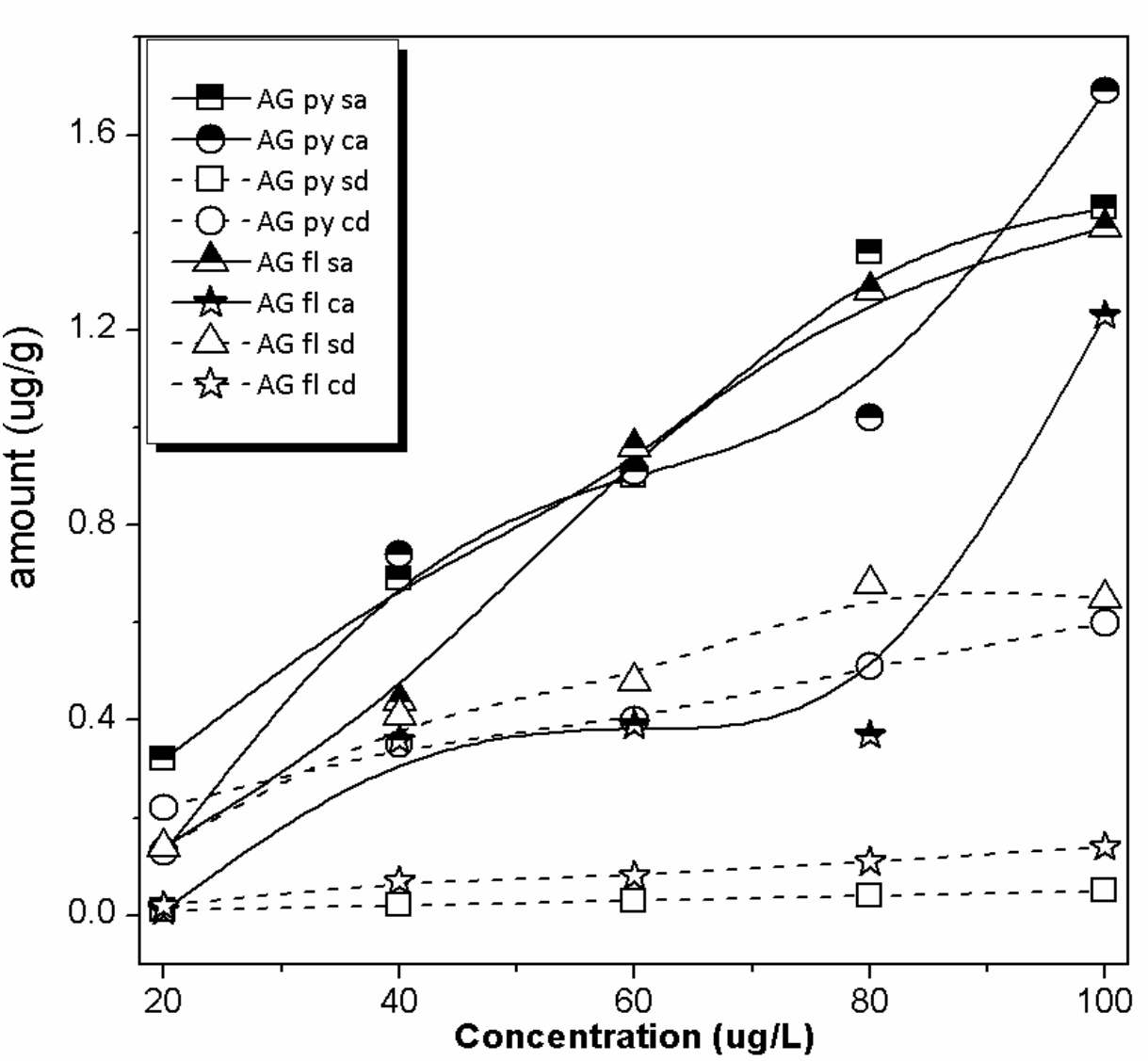

Figure 4.12. Single (solid lines and half filled symbols) and competitive sorptions (solid lines and half filled symbols) and desorption (broken lines and empty symbols) of pyrene and fluorene on AG whole soils. Codes in figure: sa – single adsorption, ca – competitive adsorption, sd – single desorption, cd – competitive desorption.

For the LF soil however, this observation could also be attributed to the relatively high organic matter content. Since similar trend was not observed for other soils of relatively high organic matter contents (such as AG, PH, and IB), this was related to the type of organic matter present in these soils – soft and hard organic matter. Soft organic matters are rich in aromatic functionalities while hard organic have far less aromatic functionalities (Weber et al., 1992). Soft organic matter with the abundance of aromatic functionalities may increase fluorene sorption by two suggested mechanisms: abundance of the aromatic functionalities can directly increase fluorene sorption via hydrophobic and π–π interactions between benzene rings in PAHs; and the formation of secondary PAHs layer on the already sorbed (initial) PAHs layer on the soil surface (multi–layer). Since, the LF soil sample has been obtained from a location with relatively young deposits of organic matter (near the River Niger bank of the Southern Guinea savanna) and abundance of aromatic functionalities, the soft organic matter is a dominant part of its organic matter content, and hence, its fluorene sorption trend. Other soils with relatively high organic matter contents are assumed to have the hard organic matter with far less aromatic functionalities (Weber et al., 1992) since they are not supplied by the fresh organic matter deposits like the LF soil.

Figures 4.11 and 4.12 (and Figures A17 *iii* and *iv*) also showed that at lower solution PAHs concentrations, sorption of pyrene was more favoured than fluorene for the organic matter rich soils. As concentration increased, the extent of this trend decreased because concentration is a positive driving force for PAHs sorption. For soils with relatively lower organic matter contents, pyrene sorptions were higher than fluorene for all concentration range. Besides concentration, presence of expansive clays, aromatic functionalities of organic matters, molecular size, steric hindrance and the structural relationship between PAHs in solution play vital roles in the sorption of hydrophobic organic pollutants from solution. The higher the quantity of expansive clays and aromatic functionalities of organic matters in the soil, the more the PAHs sorptions.

The molecular sizes and structures are important features that determine which of either pyrene or fluorene is sorbed more. Pyrene and fluorene have nearly similar molecular sizes and structures, and their unique differences affect the extent of their soil sorptions.

For instance, fluorene has less number of aromatic benzene rings than pyrene (ratio 2:4), and this reduces its affinity to aromatic functionalities in soil organic matter due to reduced amount of hydrophobic as well as reduction in the π–π interactions that can be formed with fluorene when compared to pyrene; thus, the reduction of sorption for fluorene on these soils.

Desorption experiments were investigated to ascertain how concentration and the number of PAHs in the solution mixture affect desorption and hysteresis. Results are shown in Figures 4.13 and 4.14 (and Figures A17 *v* and *vi*). It was observed that pyrene desorptions were higher (lower hysteresis) in competitive sorption than single sorptions for all soils.

The observation above was not unexpected because competitive sorption left more pyrene molecules loosely bound to the soil surfaces and vulnerable to easy desorptions. However, the reverse case was observed for fluorene desorptions from these soils – fluorene desorptions were lower in competitive sorptions than in single sorptions for all soils. This was unexpected, but could mean that simultaneous sorption of pyrene along with fluorene on soils enhanced the sorption between fluorene and the soil sorption surfaces. This enhancement was thought to be via hydrophobic and π–π interactions on the soil surface sites. Sorption of pyrene onto the soil surface sites increases the chances of formation of hydrophobic and π–π bonds between surface molecules and fluorene species in solution. When this occurs, multi–layer adsorption is established on the soil surface. It is suggested that the reason for the higher desorption of pyrene than fluorene was associated with the size of both molecules. If it is assumed that all desorbed PAHs molecules are from the multi–layer on the soil surfaces, then it is believed that pyrene will desorb easily when compared with fluorene because the magnitude of hydrophobic and π–π interactions holding both molecules in place in a multi–layer position will be more effective for a relatively smaller molecule such as fluorene. Thus, the lower fluorene desorption or higher hysteresis after competitive sorption.

The effect of temperature on the equilibrium sorptions of PAHs from binary PAHs solutions was investigated at 25 and 40 °C. It was observed that the sorption of these PAHs were higher at 40 °C than at 25 °C. This was in contrast to the results obtained for the sorption of PAHs from single PAHs solutions where increase in temperature led to

decrease in PAHs sorption. This trend was partly due to the increase/expansion in inherent pore spaces of expansive clays and organic matter in soils as temperature increases. This expansion in inherent pore spaces led to higher sorption of PAHs because more PAHs were trapped within the larger pore spaces. Another reason adduced for this trend was that increase in temperature increases PAHs solubility in water as well as the entropy. Since film diffusion is a rate limiting step in the initial fast phase of PAHs sorption on soils as observed from the intra–particle diffusion kinetics model, increase in entropy might have enhanced film diffusion which led to multi–layer adsorption via π–π stacking of the PAHs on one another at the soil surface; hence, the observed trend. Similar observation has been noted in the report of Javier Rivas et al. (2008) on sorption of PAHs from PAHs mixture solutions. Similar observation was not seen in single PAHs sorption, and this might be due to higher degree of freedom in single PAHs solutions.

Desorption experiments carried out at both temperatures (Figures 4.13 and 4.14) showed that fluorene desorptions were very low (high hysteresis) at both temperatures. High hysteresis was also observed for pyrene at the higher temperature studied, but lower hysteresis were observed at the lower temperature. The high hysteresis observed for fluorene sorption on these soils may be attributed to the fact that π–π interactions were very effective interactions associated with the removal of PAHs from solution. Bearing in mind that the medium used for desorption is hydrophilic, it is assumed that these hydrophobic PAHs would rather prefer to remain in their hydrophobic associations on the surfaces as well as the pores of the soils than go into a hydrophilic solution; hence, the high hysteresis. The reason above could be adduced for pyrene desorption at 40 °C. However, it was observed that hysteresis was lower at 25 °C, and this could be attributed to the fewer amounts of hydrophobic interactions, especially π–π stacking, that occurs at lower temperatures. Since the contributory energies associated with holding the PAHs together on these soil sorbents were smaller at lower than higher temperatures, and pyrene being a larger molecule than fluorene, then the high pyrene desorption observed becomes reasonable.

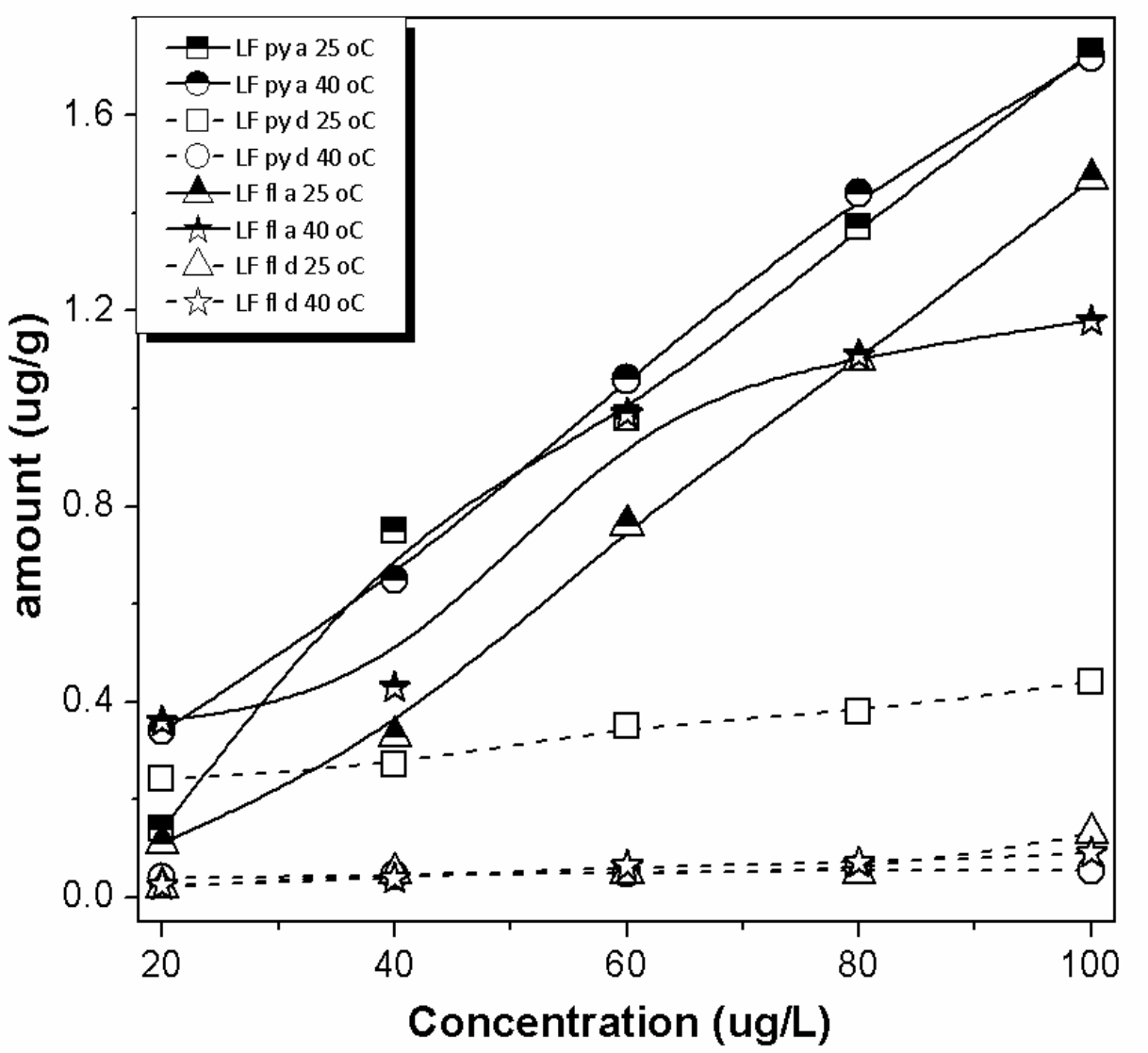

Figure 4.13. Competitive sorptions (solid lines) and desorption (broken lines) of pyrene and fluorene on the LF whole soil at 25 and 40 °C. Codes in figure: a = adsorption, d = desorption

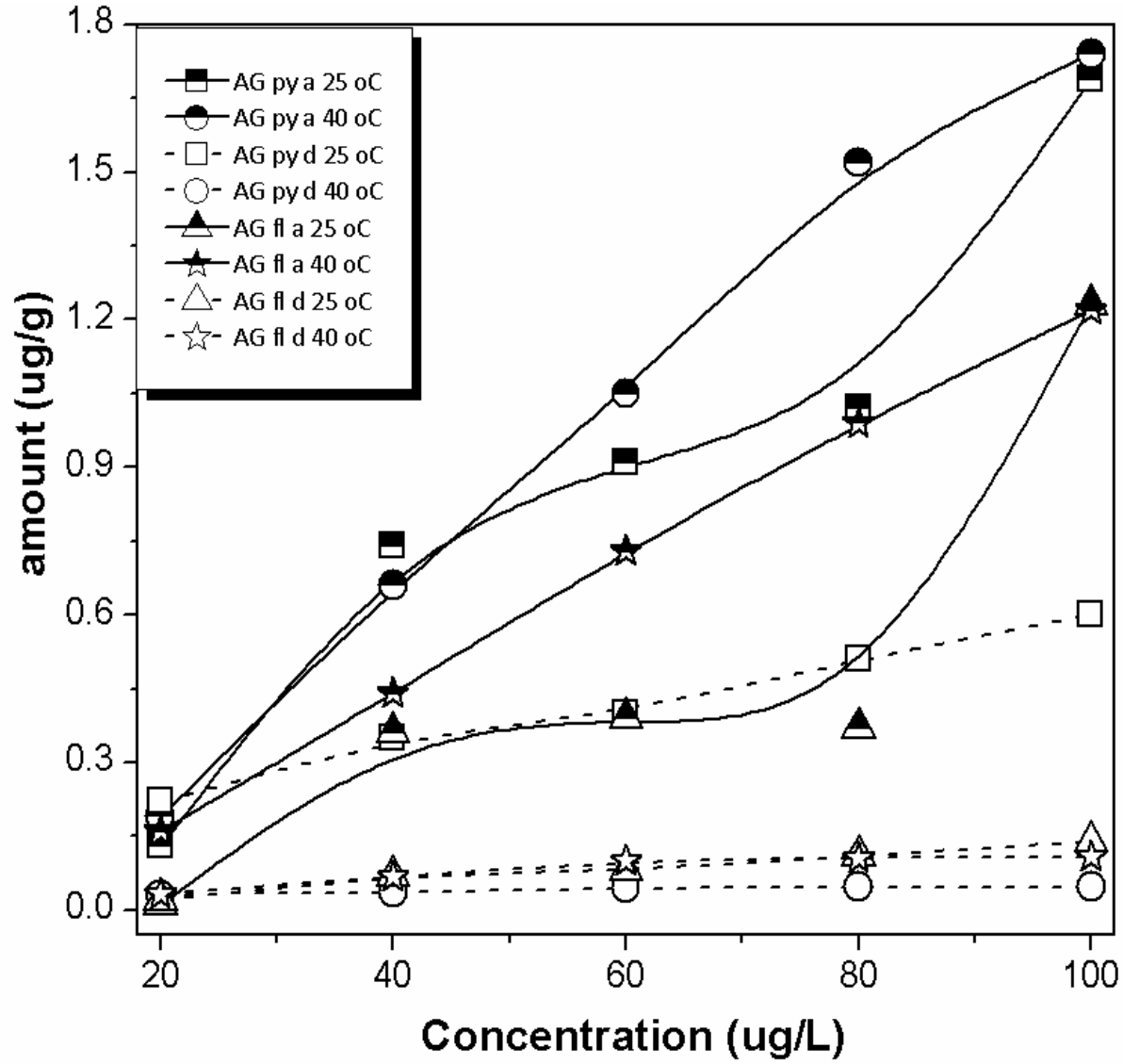

Figure 4.14. Competitive sorptions (solid lines) and desorption (broken lines) of pyrene and fluorene on the AG whole soil at 25 and 40 °C. Codes in figure: a = adsorption, d = desorption

4.4.2 Simultaneous sorption isotherm models

The linear forms of the Langmuir and Freundlich adsorption isotherm models were used to evaluate the generated simultaneous sorption data of fluorene and pyrene on the whole soils at 25 °C. The calculated isotherm model parameters are shown in Tables 4.13 and 4.14 for fluorene and pyrene, respectively.

Values of the correlation coefficients (r^2) and the estimated maximum sorption capacities (Q_o) suggested that the Langmuir isotherm could not describe the sorption of these PAHs from a multi–PAHs solution. Nearly similar results were observed with the Freundlich isotherm, but a closer examination of the Freundlich isotherm parameters indicated that the sorptions on these soils tended towards the Freundlich type isotherm (small n values and relatively higher r^2 values). This was due to the heterogeneous nature of soils and the affinity of hydrophobic compounds towards other hydrophobic compounds, and the consequent formation of multi–layer adsorption.

Hence, the Weber et al. (1992) distributed reactivity model depicted in equation 2.17 was further used to evaluate the competitive sorptions data. The model describes sorption on heterogeneous system such as soil where different isotherm models are involved simultaneously and the final isotherm is a combination of all the models involved.

The isotherm parameters obtained from the distributed reactivity model are shown in Table 4.13 and 4.14. From the r^2 values (0.958–0.999) of this model for fluorene and pyrene sorptions, it was observed that the equilibrium sorptions data were sufficiently described by the model. The estimated model q_e values were also significantly correlated with the experimental values. Hence, the simultaneous sorptions isotherms of pyrene and fluorene on these soils were described as composite of several linear and non–linear isotherms, and hence the inability of the sorptions data to fit into either the Langmuir or Freundlich type isotherms.

Table 4.13. Competitive sorption isotherm parameters of fluorene on whole soils

Soil	Langmuir sorption model			Freundlich sorption model			Distributed Reactivity Model (DRM)	
	Q_O (mg/g)	b	r^2	q_e (mg/g)	n	r^2	$*q_{T(l+nl)}$ (mg/g)	r^2
LF	0.605	0.023	0.493	1.16	1.59	0.860	1.47	0.965
AG	0.049	0.019	0.365	0.45	2.29	0.613	1.23	0.958
IB	0.436	0.008	0.494	0.55	1.39	0.941	0.65	0.973
MA	1.15	0.005	0.262	0.54	1.11	0.940	0.61	0.987
JB	0.001	3.858	0.041	0.46	0.98	0.753	0.78	0.979
PH	0.941	0.052	0.475	0.64	0.75	0.668	1.44	0.984
GSF	2.97	0.005	0.039	0.73	1.01	0.768	0.99	0.978
MG	0.070	0.015	0.658	0.90	2.31	0.868	0.60	0.999

$q_{T(l+nl)}$ (mg/g) – Total linear (l) and non–linear (nl) sorption, its values are exactly equal to the experimental q_e values

Table 4.14. Competitive sorption isotherm parameters of pyrene on whole soils

Soil	Langmuir sorption model			Freundlich sorption model			Distributed Reactivity Model (DRM)	
	Q_O (mg/g)	b	r^2	q_e (mg/g)	n	r^2	$q_{T(l+nl)}$ (mg/g)	r^2
LF	0.04	0.087	0.602	2.74	10.90	0.795	1.73	0.999
AG	2.00	0.014	0.020	0.61	1.05	0.211	1.69	0.997
IB	1.97	0.017	0.145	0.76	0.88	0.662	1.31	0.985
MA	0.05	0.016	0.324	0.30	2.28	0.504	1.08	0.991
JB	0.98	0.052	0.465	0.66	0.76	0.602	1.34	0.992
PH	1.50	0.021	0.056	0.62	1.28	0.326	1.74	0.991
GSF	1.14	0.034	0.133	0.90	1.51	0.485	1.74	0.999
MG	0.001	5.614	0.108	0.86	0.99	0.205	0.83	0.999

$q_{T(l+nl)}$ (mg/g) – Total linear (l) and non–linear (nl) sorption, its values are exactly equal to the experimental q_e values

4.4.3 Thermodynamics of the competitive sorptions of pyrene and fluorene

Thermodynamics of the competitive sorption of fluorene and pyrene on the soils were investigated. Data generated from the equilibrium experiments were used to determine the thermodynamic parameters – standard free energy (ΔG^o), entropy change (ΔS^o), and enthalpy change (ΔH^o). The values of these parameters are shown in Tables 4.15 and 4.16 for fluorene and pyrene, respectively.

Values of ΔG^o were all negative for pyrene and fluorene sorptions and at both temperatures (25 and 40 °C). This indicates that the sorptions of fluorene and pyrene on these soils were feasible and spontaneous. The ΔS^o values were mainly negative and suggested that the adsorption of these PAHs species from solution led to a decrease in randomness as a result of few PAHs species left in solution after adsorption.

Calculated ΔH^o values showed that the sorptions of these PAHs were exothermic (negative). Exceptions to this are fluorene sorptions on MA and GSF soils which had small positive values. This was attributed to minor errors associated with linear model calculations of the thermodynamic parameters which can become significant when dealing with low energy sorption surfaces (Unuabonah et al., 2008). The magnitudes of the ΔH^o values were in the range associated with the weak hydrophobic interactions such as the van der Waal's forces and $\pi - \pi$ interactions, and an indication that these forces might be involved in the sorptions of these PAHs species from solution.

Table 4.15: Thermodynamic parameters for the competitive sorption of fluorene at 25 and 40 °C

Soil	ΔH^o	ΔS^o	ΔG^o (kJ mol^{-1})	
	(kJ mol^{-1})	(kJ mol^{-1}K^{-1})	298 K	313 K
LF	-180	-0.57	-10.3	-1.94
AG	-99.5	-0.28	-15.2	-11.0
IB	-26.2	-0.04	-13.8	-13.1
MA	7.60	0.07	-13.0	-14.0
JB	-38.9	-0.09	-13.0	-11.7
PH	18.5	0.10	-10.2	-11.7
GSF	3.57	0.05	-11.5	-12.2
MG	-33.0	-0.06	-16.4	-15.6

Table 4.16: Thermodynamic parameters for the competitive sorption of pyrene at 25 and 40 °C

Soil	ΔH^o	ΔS^o	ΔG^o (kJ mol^{-1})	
	(kJ mol^{-1})	(kJ mol^{-1}K^{-1})	298 K	313 K
LF	-76.8	-0.22	-10.0	-6.67
AG	-22.6	-0.04	-10.5	-9.90
IB	-80.8	-0.24	-10.2	-6.60
MA	-125.6	-0.37	-15.9	-10.4
JB	-117.9	-0.36	-10.4	-4.96
PH	-17.1	-0.02	-9.91	-9.55
GSF	-36.1	-0.09	-8.85	-7.48
MG	-123	-0.37	-13.8	-8.31

4.5 Sorption of Pentachlorophenol

4.5.1 Effect of time on PCP sorption

The fate of most organic pollutants in the environment is controlled by sorption onto soil constituents, and a study of the sorption rate is beneficial for ascertaining the likelihood of the pollutant being present in the aquifer. Hence, the effect of time on the sorption of pentachlorophenol (PCP) as well as the kinetics of the reactions was studied in these soils using batch experiments over a period of 1440 minutes. The effect of time on PCP sorptions is shown in Figure 4.15a for the whole soil samples. It was observed that equilibria were attained in 1080 minutes (18 h) for most soils except for PH and MG soils which had higher equilibrium time – 1440 minutes (24 h). The sorptions were relatively fast in the first 180 minutes (3 h) with ≥ 75 % sorption as shown in the nearly vertical rise in Figure 4.15a. This portion of the sorption curve represents sorptions on charged sorption sites and soil components such as soft organic matter whose PCP sorptions are nearly instantaneous. PH and MG soils, however, were exceptions to this as less than 50 % of their sorptions have occurred at this point. This initial rapid PCP sorption region was followed by a gentle steep in the curve which represented the portions of gradual sorptions. The curve portion may be attributed to sorptions on expansive clay minerals as well as the hard organic matter components of the soils whose interactions with PCP are time dependent. This portion of the curve was then followed by the last portion of almost equal rates of sorption and desorption noticeable at equilibrium.

The effects of the removal of organic matter and iron oxides on the sorption of PCP on selected soils were investigated. Soil organic matter and clay minerals have been reported to play major roles in the sorption of non–ionic/non–polar organic compounds in the environment (Site, 2001; Huang et al., 2003). Though these authors reported that removal of these soil constituents usually decreases the soils' sorption capacity (Site, 2000; Wang et al., 2008), the present study seeks to ascertain the trend for these Nigerian soils. Figure 4.15b shows the PCP sorption trend after the removal of organic matter and iron oxides.

Comparing the sorptions of PCP on the whole and OMR soils of LF, GSF, and JB showed that removal of organic matter did not affect the equilibrium time (1080 minutes – 18 h). It was also observed that though the organic matter content of the LF whole soil was far

greater than those of the GSF and JB whole soils, this did not play any significant role in the amount of PCP sorbed by the GSF and JB whole soils (Figure 4.15 *c*). For instance, there was no significant difference in the amount of PCP sorbed in the LF and JB soils, while the amount of PCP sorbed by GSF was almost 100 % more than that sorbed by the LF with over twice organic matter. This indicated that organic matter played an insignificant role in the sorption of PCP in some of these soils. This finding was also supported by the fact the q_e (μg/g) values after removal of organic matter showed that organic matter in the organic–matter–rich of LF soil contributed ≤ 55 % to PCP sorption while it contributed ≤ 5 % in the lower–organic–matter soils of GSF and JB as shown in Figure 4.15a.

Removal of iron oxides in these soils reduced the time required for equilibrium to be attained in all treated soils from 1080 minutes (18 h) to 180 minutes (3 h). This was due to the fact that after the removal of iron oxides and its bound constituents, charged sorption surfaces previously masked by the presence of these components becomes unmasked and there is the presence of more organic matter per gram depending on the soil. Sorptions of PCP on these surfaces were faster than on the whole soils; hence, the reduced equilibrium sorption time. The extent of the role of iron oxides in PCP sorption was observed in the reductions of PCP sorbed when iron oxides were removed: Figure 4.15*b* showed that the q_e (μg/g) values reduced by ≈ 71 % (100.7 μg/g) reduction in the LF IOR soil, while by ≈ 85 % (261.7 and 133.9 μg/g) reductions in the GSF and JB IOR soils, respectively. The result obtained in this study showed that iron oxides played a major role in the sorption of PCP on these soils.

Two reasons might be adduced for this observation: the ionic state of PCP in the prevailing environmental conditions in the soils, and the specific clay mineralogy of the soils.

PCP is a hydrophobic weak organic acid (pKa = 4.75) and exists as either neutral or ionized species. The neutral and strongly hydrophobic species represents more than 99% of all PCP when the solution pH is below 2, whereas more than 95% of all PCP is present as the anion when the pH is above 6 (Li et al., 2009). Both ionized and unionized PCP

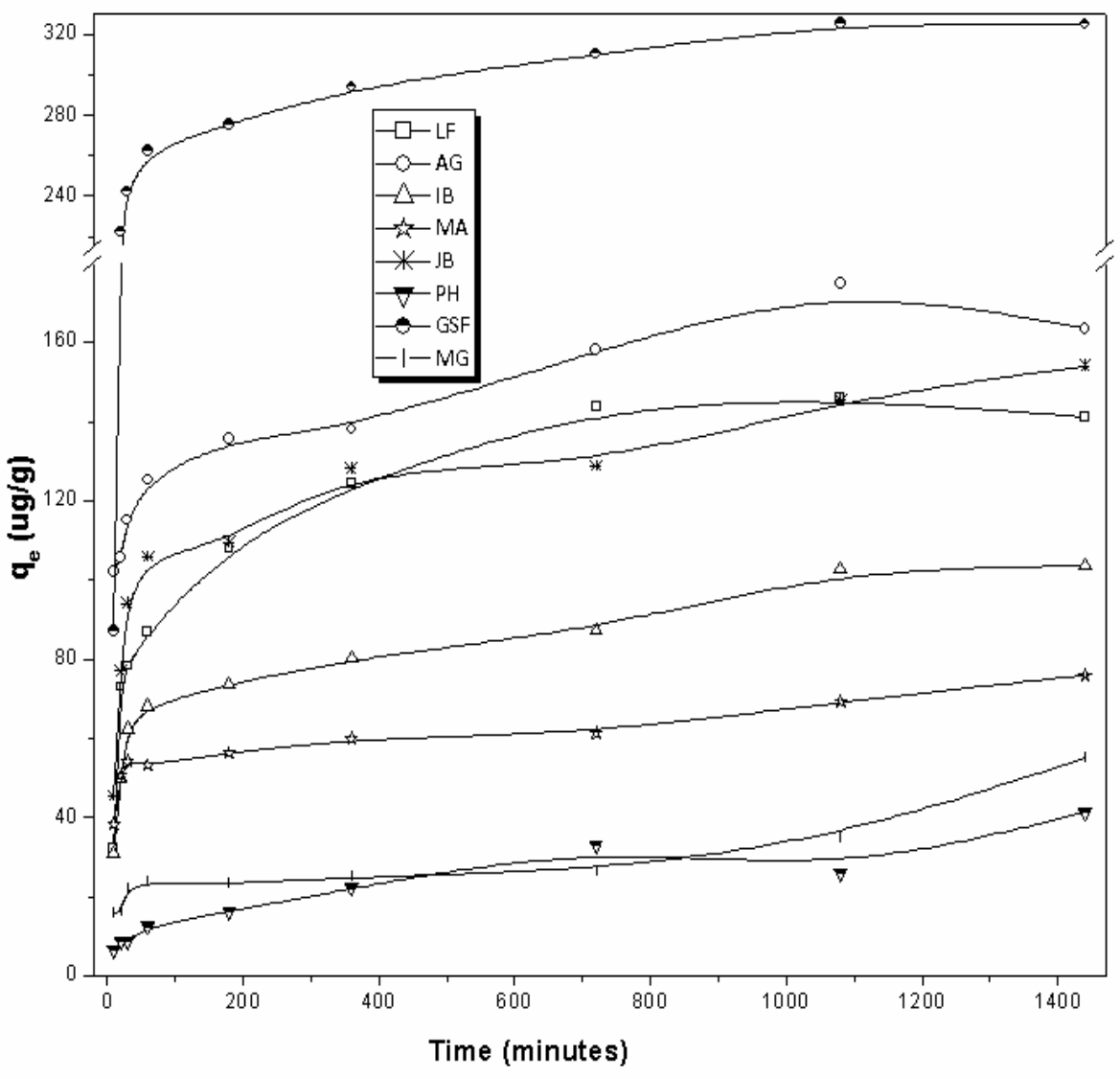

Figure 4.15 *a*. Effect of time on sorption of pentachlorophenol on whole soils

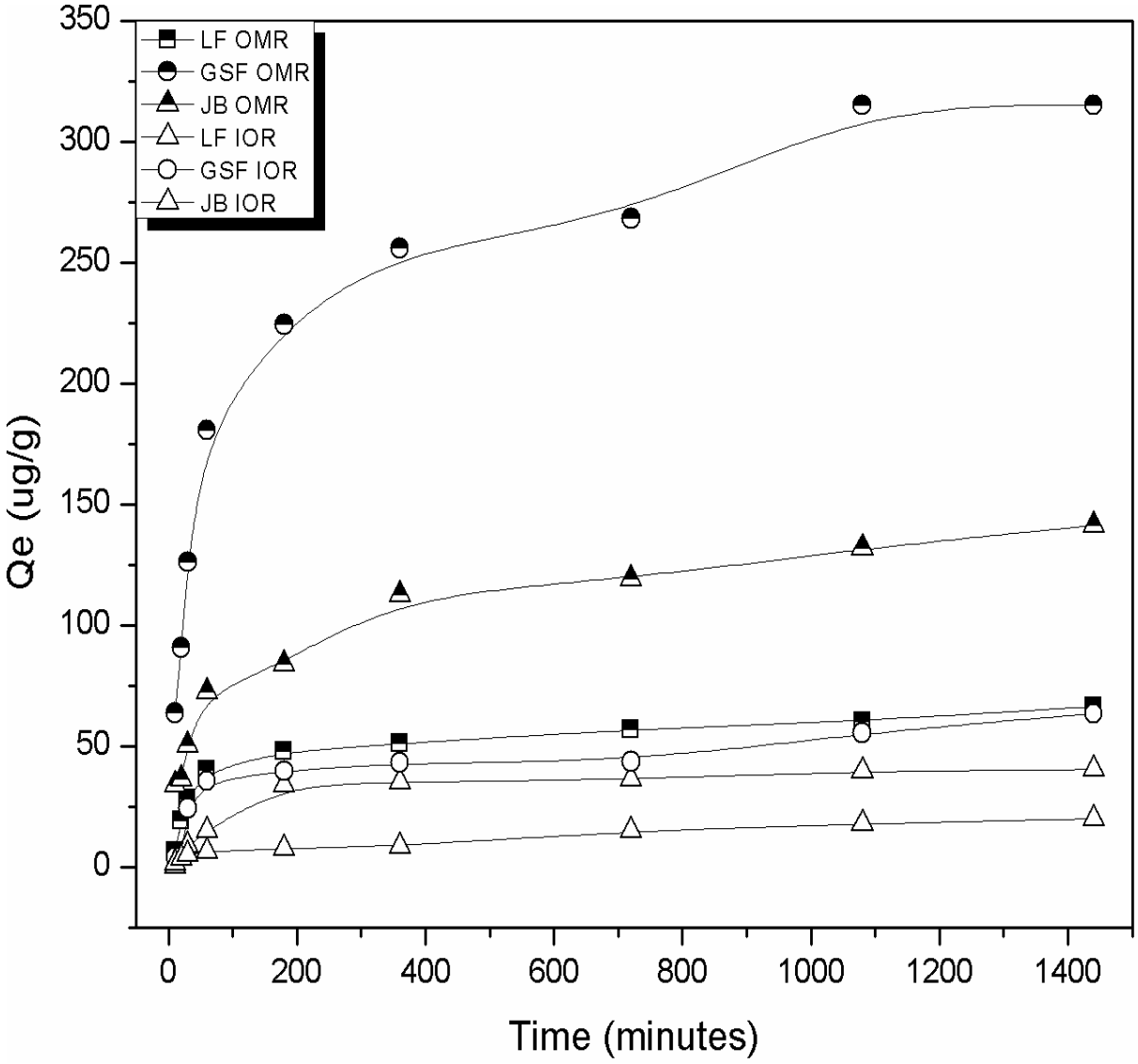

Figure 4.15 *b*. Effect of time on sorption of pentachlorophenol on OMR and IOR treated soils

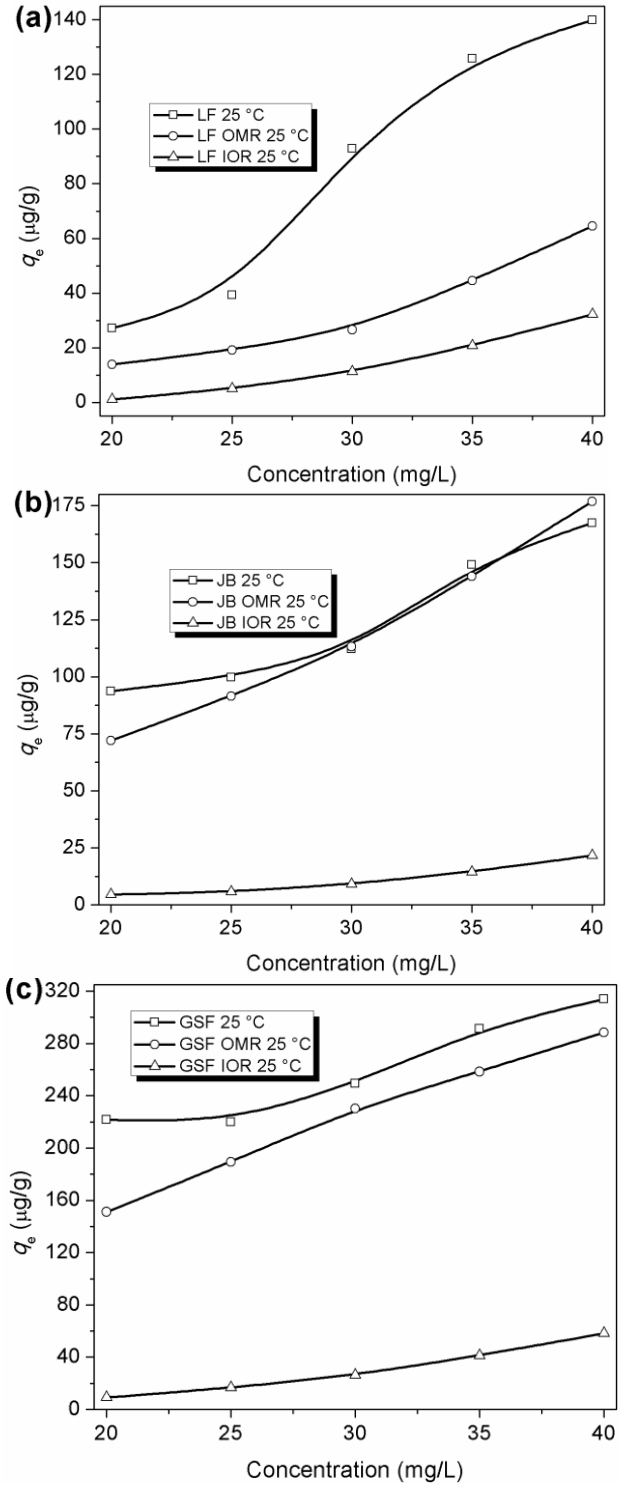

Figure 4.15 *c*. q_e sorption trend on the whole and treated soils

species are present in solution at any given time, but the amounts are dependent on solution pH. Thus, bearing in mind the pH of the studied soils (near neutrality), sorption of PCP on these soils is assumed to involve π–π interactions involving unionized PCP species and some degree of electrostatic interactions between ionized PCP molecules in solution and charged active sorption sites at the soil surface. The degree of electrostatic interactions in these soils was significant at the pH of these soils because the PCP are in the anion form – pentachlorophenolate (Li et al., 2009), and the electrostatic interactions were mainly on the numerous charged surfaces on the iron oxide components of the soils. In an earlier sorption study of pyrene (an uncharged molecule) on the same soils, it was observed that pyrene sorption is directly proportional to the amount of organic matter present in the soil. It may be implied from this relationship that the organic matter in these Nigerian soils are aromatic in nature and sorption is mainly controlled by π–π interactions (Weber et al., 1992). This was corroborated by the fact that sorption of pentachlorophenolate (a charged molecule) was not favored in the presence of the highly aromatic organic matter content in the soils. However, pentachlorophenolate sorption became favored in the presence of the charged iron oxides of the soils as solution pH increased. Since PCP is in a charged form in the prevailing soil solution pH and π–π interactions cannot be the determining factor in the removal of the PCP species from solution, these results suggested that the prevalent mechanism of PCP uptake by these soils was electrostatic interactions between the pentachlorophenolates in solution and the charged surface sorption sites (Li et al., 2009).

Clay mineralogy is another factor for the observed trend in pentachlorophenolate sorption. Presence of expansive (such as illite and montmorillonite) and charged clay surfaces in these soils have been observed to favor sorption of pentachlorophenolate. Expansive clays swell when in water resulting in larger surface areas (Diagboya et al., 2014), and consequently more surface sorption sites are made available. Presence of highly aromatic organic matter in the soil tends to mask some of the charged sorption surfaces of the soil components (depending on the quantity of organic matter). Thus removal of organic matter (while keeping the ambient soil pH constant or close to neutrality) might affect the sorption of PCP depending on other soil components. However, removal of iron oxides

implied the removal of the numerous surface sorption sites as well as the charged surfaces provided by this component and consequently, the observed reduction in sorption.

4.5.2 PCP sorption kinetics study

Sorption of organic pollutants is a complex process involving adsorption, partitioning of the pollutants inside the soil constituents (Site, 2001), as well as other non–specific complex interactions between adsorbate–adsorbate and adsorbate–adsorbent. Hence, understanding these processes is necessary for predicting the mechanism(s) involved in organics sorption. Thus, the data generated from the effect of time on PCP sorption experiments was evaluated using four kinetics models: Lagergren pseudo–first and second order, Elovich and intra-particle diffusion kinetics models. The model parameters for the whole and treated soils are shown in Tables 4.17 and 4.18. Comparison of the correlation coefficients (r^2) and the estimated model sorption capacity (q_e) values of the pseudo–first–order and pseudo–second–order kinetics showed that the PCP sorptions were better described by the pseudo–second order kinetics model. The r^2 values of the pseudo–second–order model (0.847 – 0.999) were closer to unity than those of the pseudo–first–order model (0.510 – 0.942) and q_e values showed better correlation with the experimental maximum sorption capacities.

The Elovich kinetics model parameters (q_e and r^2) values suggested that PCP sorption on these soils could be explained by the model. Figures 4.16a (whole soils) and 4.16b (treated soils) showed that the plot of q_t verses $In(t)$ did not pass through the origin suggesting that there was some degree of hindrance in the movement of PCP molecules from the soils' surface into the pore of the soils'. This hindrance was assumed to be related to the rate controlling mechanism and involves mainly electrostatic interactions between ionized PCP molecules in solution and active sorption sites at the soil surface as well as some degree of π–π interactions involving un–ionized PCP molecules (the degree of π–π interactions is limited at the ambient soil pH).

The intra–particle diffusion kinetics model has been employed to predict the rate limiting step of PCP sorption on these soils. The model parameters for the whole and treated soils are shown in Tables 4.17 and 4.18, respectively.

Table 4.17. Kinetics model parameters for pentachlorophenol sorption on whole soils

Kinetics model	Model parameters	Soil samples							
		LF	AG	IB	MA	JB	PH	GSF	MG
pseudo-first-order	q_e (μg g^{-1})	65.7	63.1	56.8	31.8	78.9	37.2	114	45.8
	K_1 (min^{-1})	2.7x 10^{-3}	2.5x 10^{-3}	2.6x 10^{-3}	1.4x 10^{-3}	2.2x 10^{-3}	1.5x 10^{-3}	3.3x 10^{-3}	1.3x 10^{-3}
	r^2	0.754	0.51	0.942	0.887	0.916	0.815	0.917	0.694
pseudo-second-order	q_e (μg g^{-1})	167	200	111	76.9	167	38.5	333	47.62
	K_2 (g μg^{-1} min^{-1})	1.4x 10^{-4}	1.6x 10^{-4}	1.6x 10^{-4}	3.1x 10^{-4}	1.2x 10^{-4}	1.8x 10^{-4}	1.3x 10^{-4}	1.5x 10^{-4}
	r^2	0.998	0.996	0.992	0.989	0.993	0.904	0.999	0.847
Elovich	q_e (μg g^{-1})	146	163	98.4	68.6	146.0	33.5	332	37.2
	β	0.048	0.073	0.080	0.183	0.056	0.164	0.028	0.195
	r^2	0.953	0.947	0.94	0.85	0.925	0.865	0.77	0.622
Intra-particle diffusion	C (μg g^{-1})	58.5	104	45.0	44.8	70.2	4.62	186	13.5
	K_{id}	2.70	1.90	1.68	0.76	2.36	0.88	4.35	0.80
	r^2	0.816	0.919	0.857	0.848	0.812	0.917	0.588	0.765
	q_e (μg g^{-1})	147	166	100	69.9	147.8	33.7	331	39.7

Table 4.18. Kinetics model parameters for pentachlorophenol sorption on OMR and IOR treated soils

Kinetics model	Model parameters	Soil samples					
		LF OMR	GSF OMR	JB OMR	LF IOR	GSF IOR	JB IOR
pseudo-first-order	q_e (μg g^{-1})	42.8	219	101	27.0	54.3	19.2
	K_1 (min^{-1})	2.1x 10^{-3}	3.5x 10^{-3}	2.5x 10^{-3}	2.2x 10^{-3}	2.7x 10^{-3}	1.5x 10^{-3}
	r^2	0.916	0.92	0.948	0.863	0.808	0.982
pseudo-second-order	q_e (μg g^{-1})	71.4	333	143	52.6	66.7	21.3
	K_2 (g μg^{-1} min^{-1})	1.8x 10^{-4}	4.5x 10^{-5}	9.2x 10^{-5}	5.6x 10^{-5}	9.4x 10^{-5}	2.3x 10^{-4}
	r^2	0.994	0.994	0.993	0.735	0.959	0.930
Elovich	q_e (μg g^{-1})	63.6	307	132	41.4	59.5	16.4
	β	0.093	0.020	0.045	0.115	0.094	0.298
	r^2	0.956	0.983	0.980	0.950	0.901	0.897
Intra-particle diffusion	C (μg g^{-1})	18.7	91.6	36.3	5.02	11.3	1.41
	K_{id}	1.39	6.73	3.02	1.12	1.41	0.49
	r^2	0.812	0.874	0.925	0.793	0.801	0.974
	q_e (μg g^{-1})	64.3	313	136	41.8	57.7	17.5

Figures 4.16c (whole soils) and 4.16d (treated soils) showed that the plot of q_t verses $t^{1/2}$ was not linear, indicating that several mechanisms are involved in the sorption. A linear plot is an indication that the sorption mechanism is majorly intra–particle diffusion, and if such a plot passes through the origin then intra–particle diffusion is the sole rate–limiting step. This is usually the case for adsorption surfaces with similar adsorption sites (adsorption sites of almost equal energy). However, for sorptions on complex media such as soil, the mechanism is usually not controlled by a single rate–limiting step, as observed in the Figures 4.16c and 4.16d. The circled portions of the intra–particle diffusion plots in Figures 4.16c and 4.16d showed an initial rapid steep (phase) indicating the film diffusion (initial migration of PCP molecules towards the external surface of the soils), as well as the initial particle diffusion (movement of the molecules within the soil pores). This rapid phase is short timed when compared to the remaining (latter) portions of the intra-particle diffusion plot – equilibrium mechanism. Hence, sorption of PCP on these soils was controlled by two rate-limiting steps/mechanisms: an initial (short time) film diffusion, and a latter (longer time) equilibrium diffusion (less dynamic) mechanism which occurred around equilibrium or when the rates of sorption and desorption were equal.

Tables 4.17 and 4.18 showed the values of intra–particle diffusion model parameters. The magnitudes of the C (μg g^{-1}) values indicated the thickness of the PCP molecules at the boundary layer. When the C values are equal to the q_e values, then the PCP removal from solution is solely adsorption and mainly on the soil's surfaces; but if the C values are less than the q_e values, then the PCP removal from solution is partly adsorption on surface sites and partly partitioning within the soil clay mineral and organic matter voids. Thus, since the observed magnitudes of C (μg g^{-1}) values for each individual soil were less than the PCP maximum sorption capacity (q_e) of the corresponding soils, PCP sorptions were partly adsorption and partly partitioning within interstitial spaces in the soil minerals.

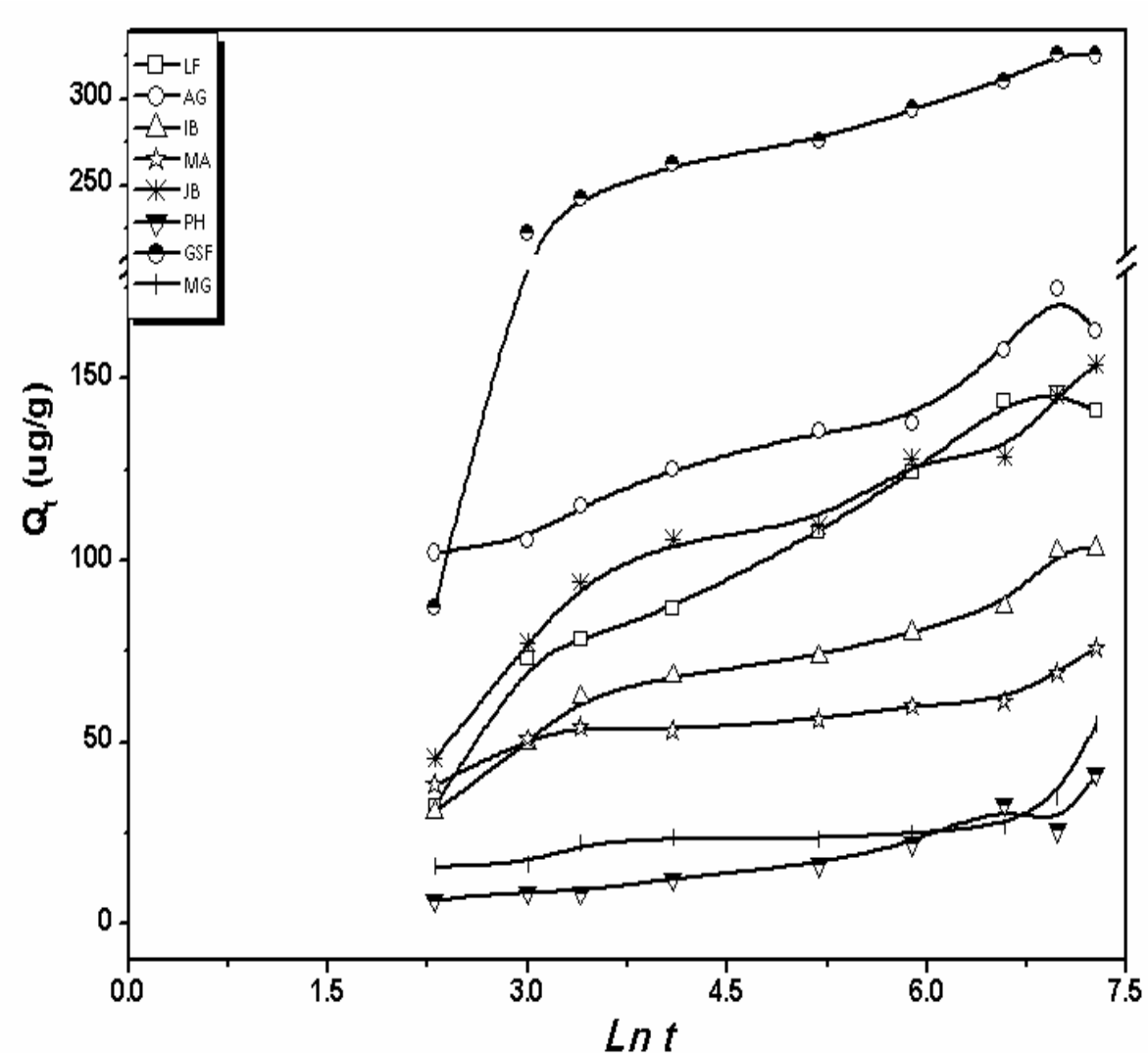

Figure 4.16 a. Elovich kinetics model plots for pentachlorophenol sorption on whole soils

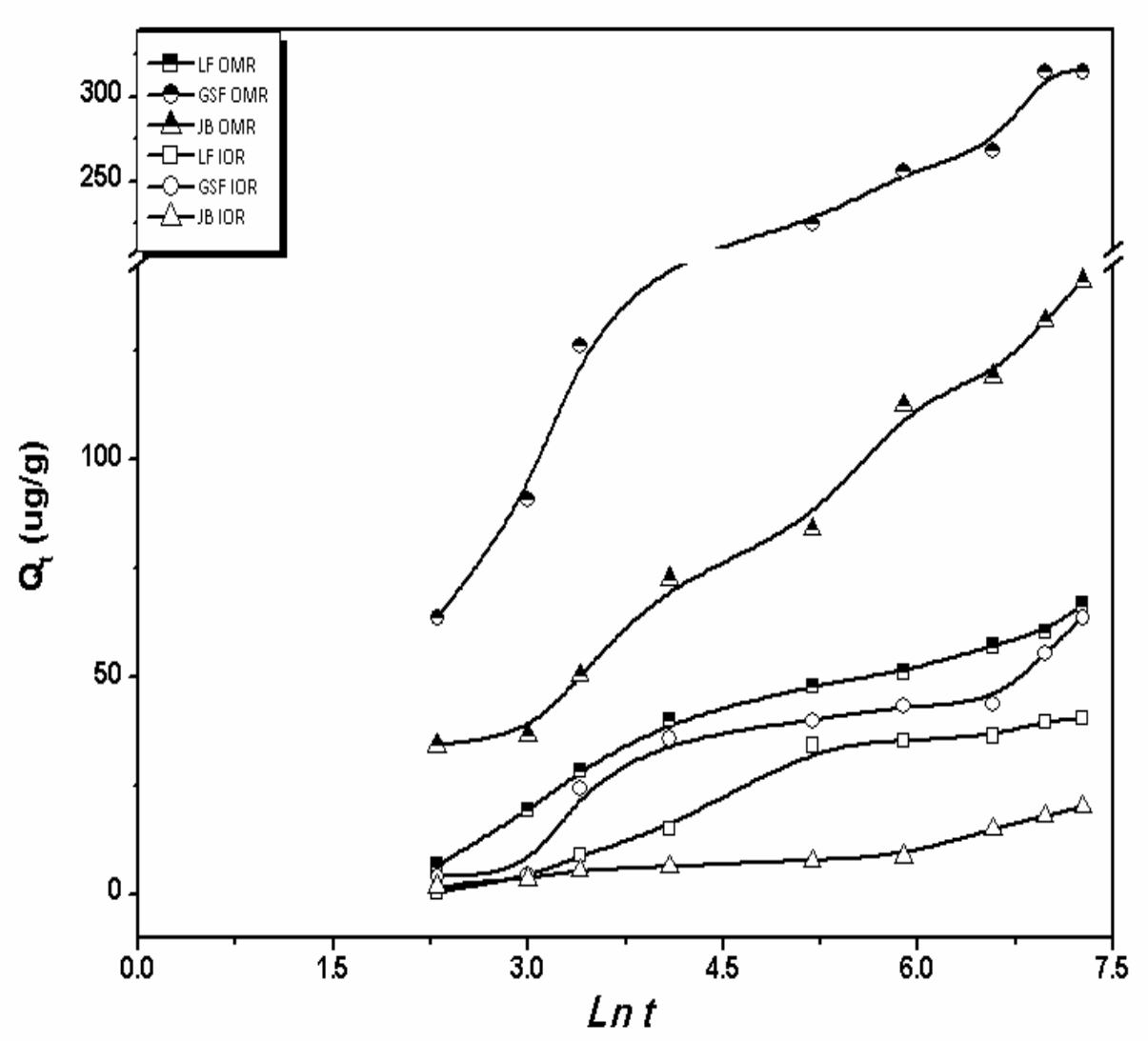

Figure 4.16 b. Elovich kinetics model plots for pentachlorophenol sorption on treated soils

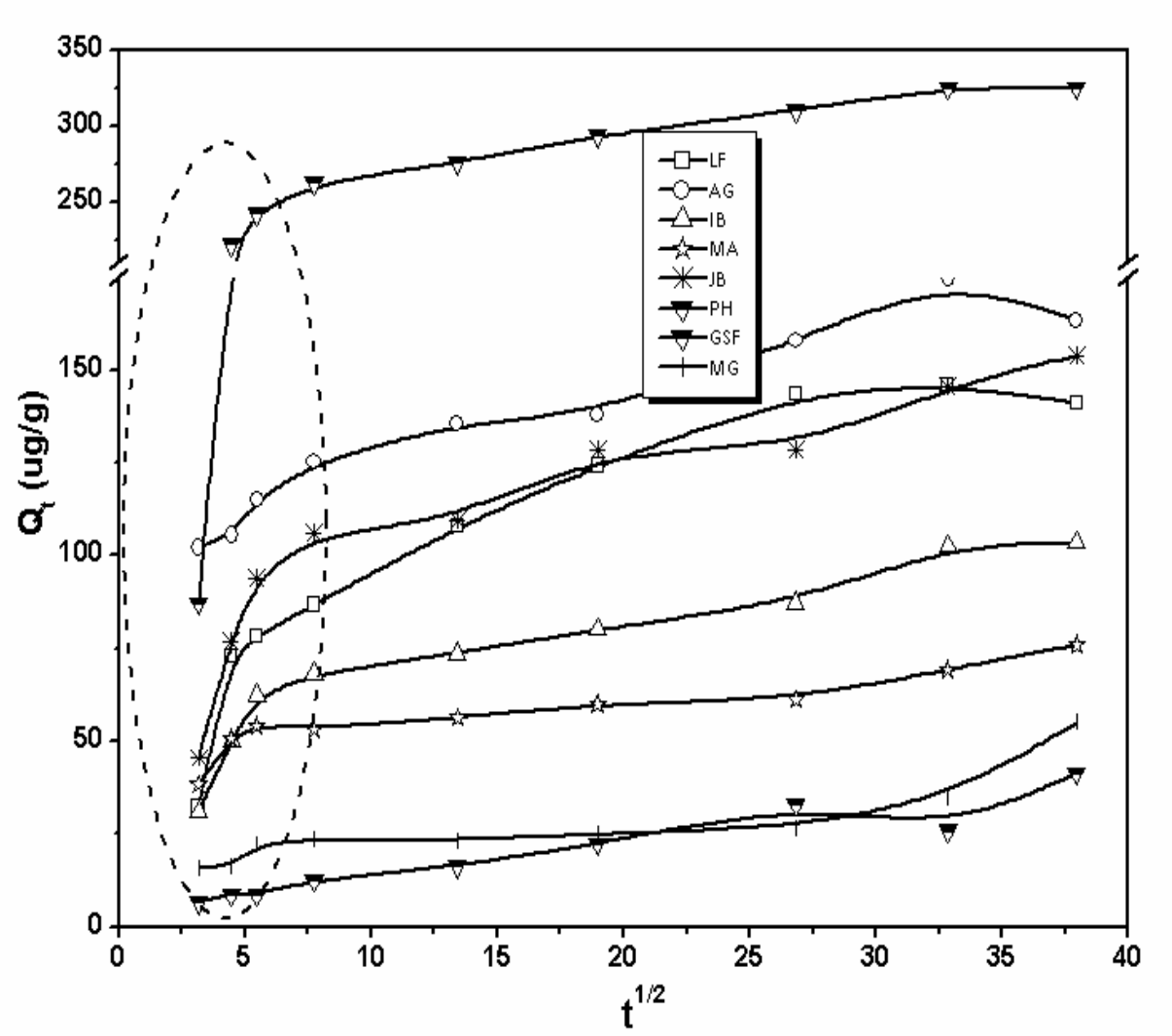

Figure 4.16 c. Intraparticle diffusion model plots for pentachlorophenol sorption on whole soils

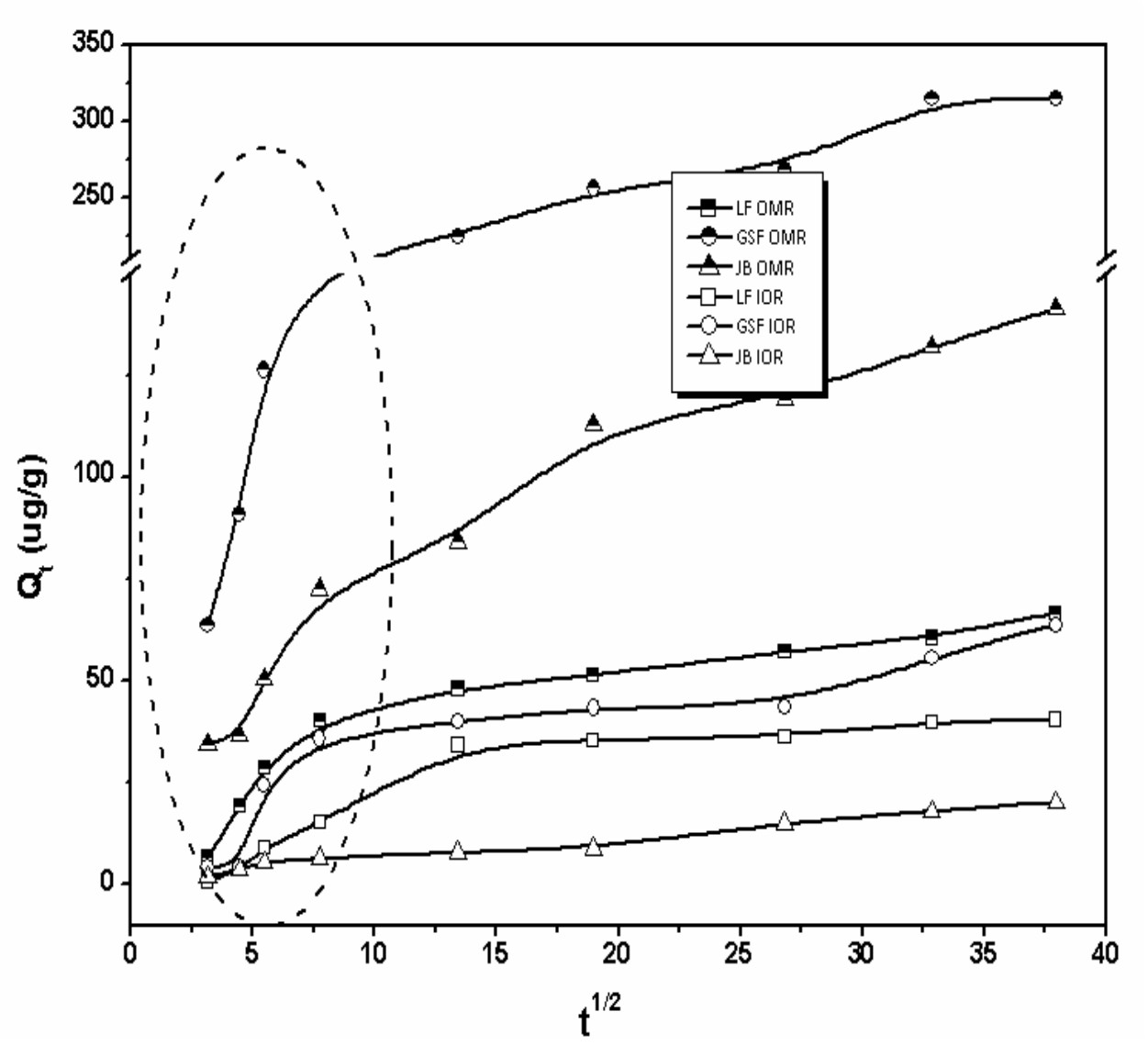

Figure 4.16 d. Intraparticle diffusion model plots for pentachlorophenol sorption on treated soils

4.5.3 Effect of pH on pentachlorophenol sorption

pH plays a major role in the sorption of PCP from soil water solution because of its effects on the ionization state of PCP in solution as well as the soil components responsible for sorption. PCP sorption has been reported to be largely dependent on the ionization of PCP as well as the soil components. For instance, at pH value of 7.0 approximately 95 % of PCP in solution exist in the anionic form while most soil components are in their charged forms. The reverse is obtainable at pH value of 2.0 when the soil surface sorption sites are uncharged (low polarity) as well as the PCP molecules due to stiff competition for these sites by protons in solution (Li et al., 2009; Wang et al., 2008). Thus, depending on the soil components responsible for sorption of PCP in a particular soil and the prevailing pH condition, sorption of PCP is expected to vary. The effect of pH on the sorption of PCP on selected soils was investigated from pH 3 to 9. Figure 4.17 (and Appendix A9) showed the amounts and percentages of PCP sorbed on the soils with variation in the soil water solution pH.

It was found that sorption was most favourable in the acidic pH zone and dropped off in the neutral and basic pH zones. That is, highest PCP sorptions were observed at the lower soil water pH values. Sorptions decreased continuously with increase in soil water pH values. This trend was similar for the studied soils irrespective of the inherent soil properties or the applied soil treatment, though the quantities of PCP sorbed at any particular pH is dependent on specific soil compositions. The amounts of PCP sorbed by these soils at pH values close to neutrality (or actual soil pH values) were in agreement with the observed quantities sorbed using the same soils which have not been pH–amended. Similar PCP sorption trend at varying water solution pH levels have been observed by other workers for soils and sediments (Li et al., 2009; Wang et al., 2008; Viraraghavan and Slough, 1999).

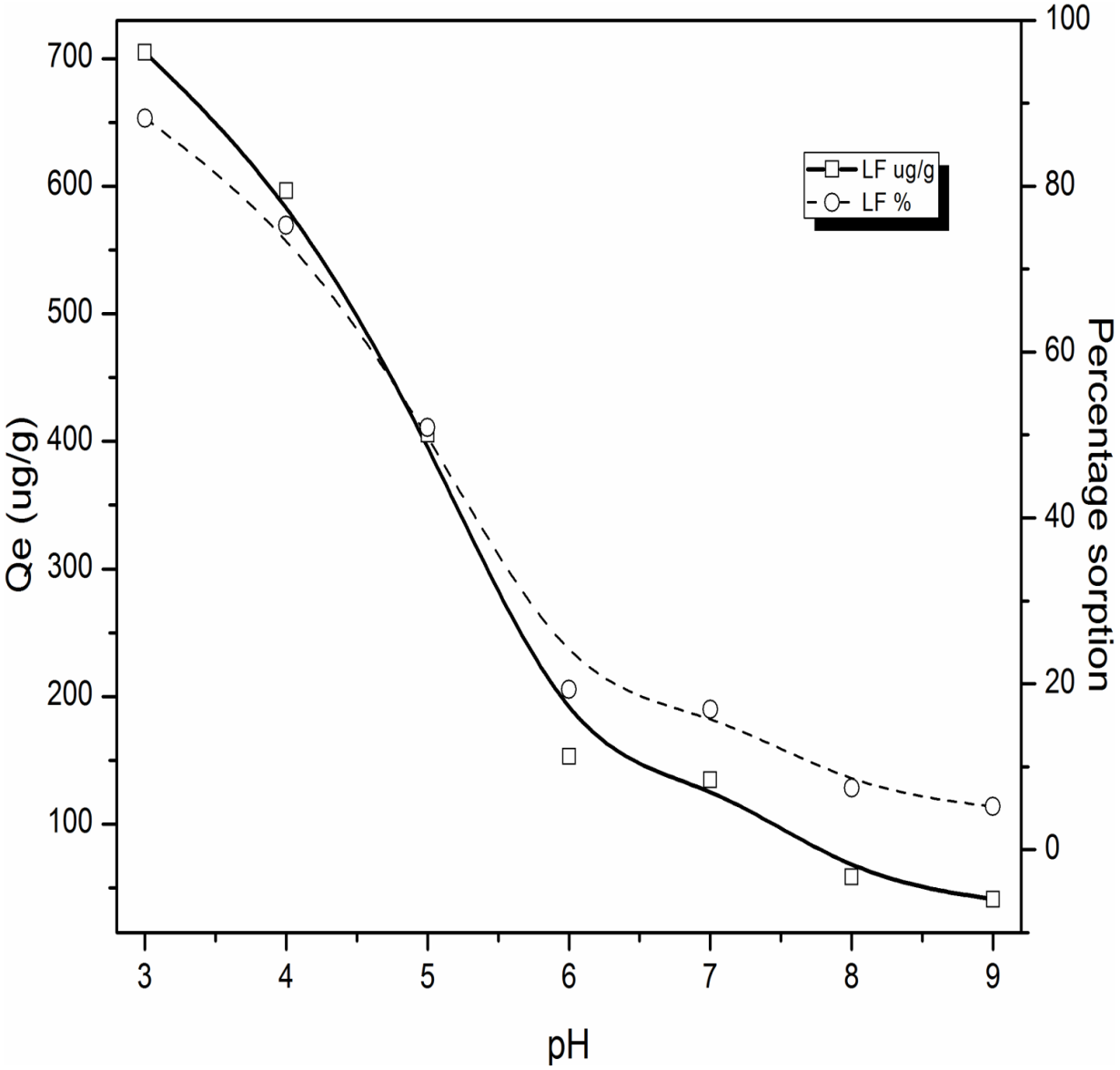

Figure 4.17 a. Effect of pH on the amount of PCP sorbed (full lines) and percentage sorbed (broken lines) on LF whole soil

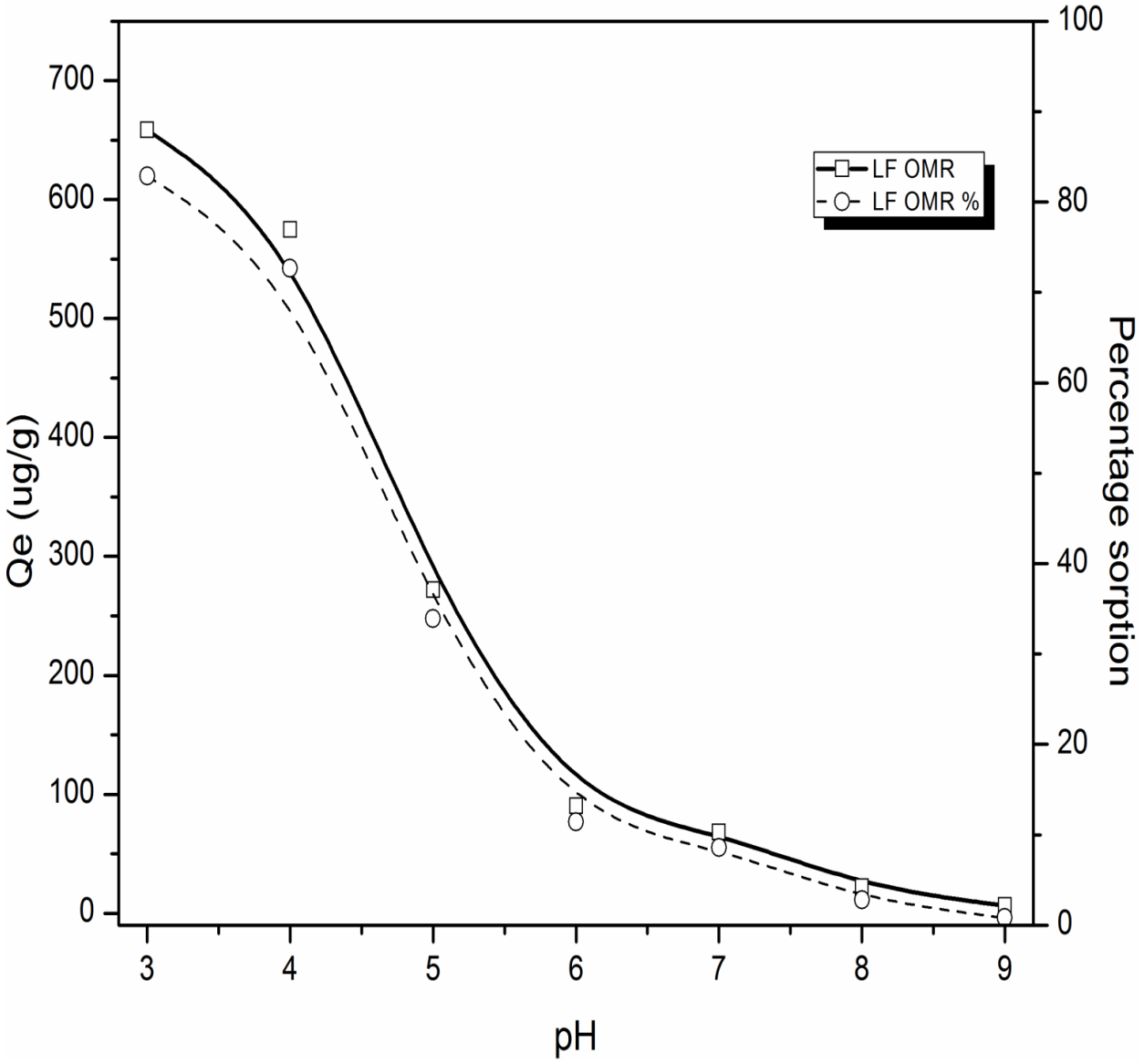

Figure 4.17 b. Effect of pH on the amount of PCP sorbed (full lines) and percentage sorbed (broken lines) on LF OMR soil

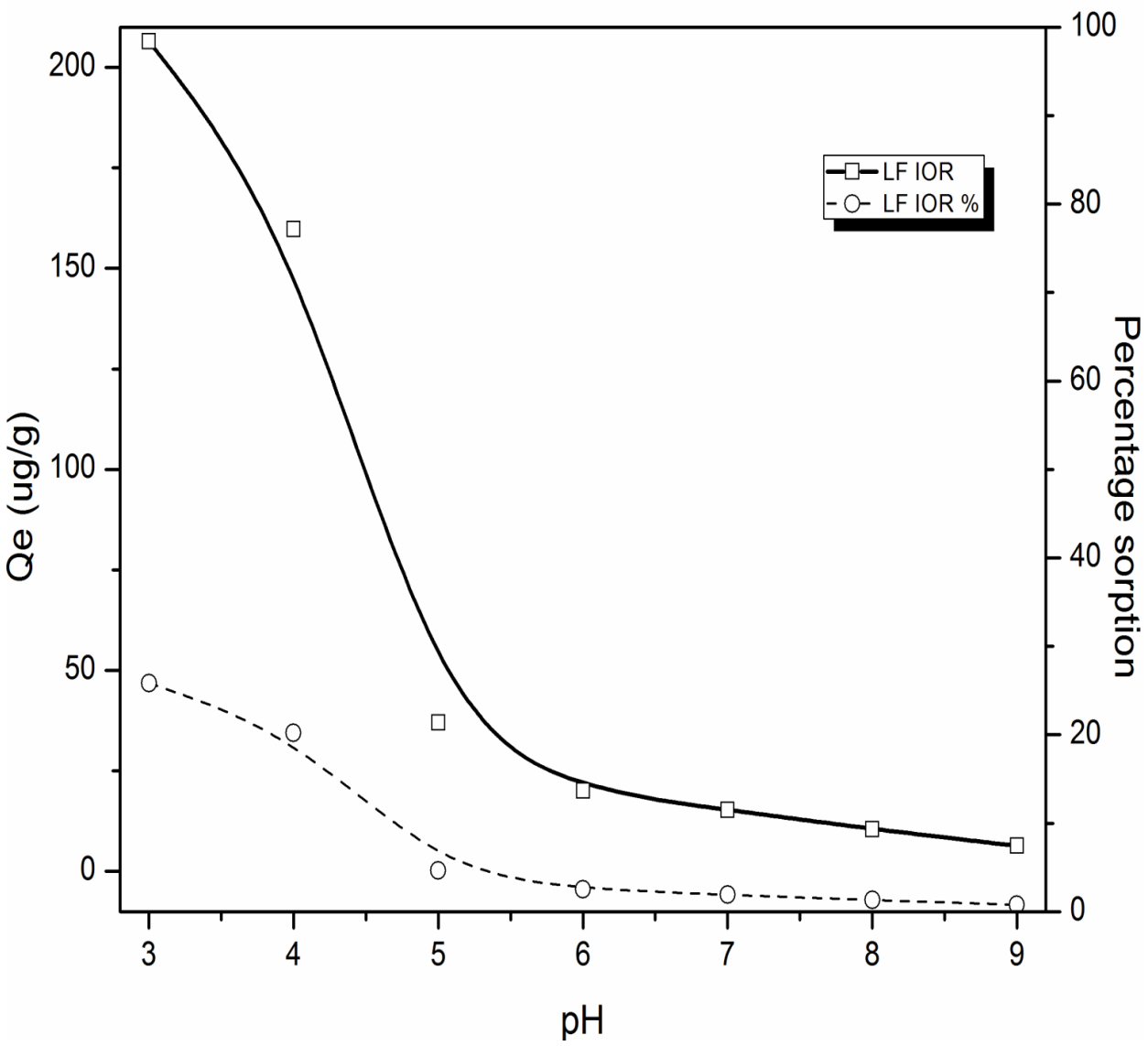

Figure 4.17 c. Effect of pH on the amount of PCP sorbed (full lines) and percentage sorbed (broken lines) on LF IOR soil

The PCP sorption trend on these soils has been attributed to the surface chemistry of the soil components (the nature of the charges available on the sorption sites of the soils at acidic, neutral, and basic pH values), the expansivity of the soil clay minerals, as well as the ionization state of the PCP molecules in solution at prevailing soil solution pH conditions. At the acidic pH regions, organic matter (especially those containing phenolic and other aromatic groups) shield off water by shrinking and they become less polar. Also, the positive cations associated with soil components that contribute the bulk of the soil's cation exchange capacity are uncharged due to stiff competitions from protons in solutions. These conditions led to the increased hydrophobic interactions resulting from increased π–π interactions (between the aromatic compounds of organic matter and the uncharged PCP species as well as between multiple PCP species in solution leading to multi–layer adsorptions). This along with sorption of PCP species onto specific sorption sites on the soils, and partitioning of PCP in the voids of expansive clays and organic matter resulted in the observed high PCP sorptions at the acidic pH range (Li et al., 2009).

At the neutral and basic pH regions, organic matter (especially those containing phenolic and other aromatic compounds) absorbs water, swells and becomes less polar, and the positive cations associated with the soil components become charged. These new conditions drastically reduces/eliminates π–π interactions; and electrostatic interactions between the charged soil surface sites and the anionic PCP species become predominant as the major route of PCP removal from solution. Sorption of PCP species onto specific sorption sites and the partitioning of PCP in the voids of soil components are usually less affected by changes in the pH of the medium. The reduced PCP sorptions observed was attributed to reductions in the number of π–π interactions between the PCP species and aromatic components of the soil as soil medium pH increased. Hence, π–π interactions were the major route of PCP removal from solution when the solution is acidic (Li et al., 2009; Wang et al., 2008).

4.5.4 Equilibrium sorption of pentachlorophenol

A study of the sorption of PCP on the eight soils as well as the selected treated soils at different temperatures (25 ºC and 40 ºC), ambient soil pH, incubation time (24 h), and varying concentration range (20000 – 40000 μg/L) was investigated and the sorption curves are presented in Figures 4.18a–c (and Appendice A10). Figure 4.18a–c showed that PCP sorption increased with increase in concentrations. At higher temperature (40 ºC), similar trend in PCP sorption was observed. Thus, PCP sorption is concentration dependent. The observed increase in PCP sorptions with increase in concentration was attributed to the fact that at any particular PCP concentration when the transport of PCP from the soil external surface and out of internal pores are equal, the trans–boundary movement of PCP becomes insignificant, and increase in PCP concentration will lead to higher sorption of PCP due to multi–layer adsorption. This trend was observed in all soils studied (Appendice A10). Similar PCP sorption trend has been reported on whole soils and individual clay minerals (Abdel Salam and Burk, 2009; He et al., 2006; Li at al., 2009).

It was observed in Figures 4.18a–c (and Figure A20) that increasing the sorption medium temperature from 25 to 40 °C caused significant decrease in the sorption of PCP on the whole and treated soils. This showed that PCP sorptions on these soils were exothermic and not favoured by high temperature. Only sample PH showed a contrary trend at low solution concentration of PCP where increase in temperature caused an increase in sorption. Temperature can affect PCP sorption equilibrium in two different ways – increase in disorder of PCP species in solution and increase in solubility and re–dissolution of sorbed PCP species. Increase in the rate of disorder of the PCP species in solution drives the species further away from the soil's external surface film as well as out of the internal voids of clay minerals and organic matter. For very low solubility organic pollutants such as PCP, increase in temperature increases the solubility in aqueous solution (or re–dissolves sorbed PCP species in solution) and this enhances the entropic effect caused by increase in temperature. Hence, the decrease in sorption observed. The decrease in sorption observed with increase in temperature is also an indication of the strength of the interaction forces involved in the sorption. It implied that the forces involved in the sorption of PCP are mainly weak electrostatic interactions requiring low

sorption energies which are easily broken. π–π interactions and van der Waal's forces, to a lesser degree, may be implicated in PCP sorption at prevailing pH. Similar negative effect of temperature on PCP sorptions has been observed by Abdel Salam and Burk (2009).

The PCP sorption trend is GSF > JB > LF ≥ AG > IB > MA > MG > PH. Unlike the earlier sorption study using PAHs, this trend did not follow organic matter quantity in the soil but rather the type of clay minerals. This argument holds true especially in JB and GSF soils with low soil organic matter content but high sorption capacities for PCP.

4.5.5 PCP sorption thermodynamics

Thermodynamic parameters – standard free energy (ΔG^o), enthalpy change (ΔH^o), and entropy change (ΔS^o) – were calculated from variation in thermodynamic equilibrium constant using experimental data obtained at the different temperatures. Data from these thermodynamics study were used in evaluating the feasibility and energetics of the PCP sorption process. These thermodynamic parameters are shown in Tables 4.19 and 4.20 for the whole and treated soils, respectively.

The ΔG^o values for the studied whole soils at both temperatures were all negative, an indication that PCP sorptions on these soils were spontaneous and feasible.

The ΔH^o values range from −81.7 to 374 kJmol^{-1}. These values of ΔH^o indicated that the sorptions were endothermic (positive). The AG, PH, and GSF soils were exceptions to this as they showed exothermic (negative) values. The exothermic nature of the PCP sorption process observed for AG, PH, and GSF soils confirmed the experimental observation that increase in temperature did not favour PCP sorptions on these soils. However, the ΔH^o values for other soils showed endothermic PCP sorptions. This observation was attributed to the theoretical fact that input of heat energy broke up the energy barrier required to be surpassed for PCP sorption to occur. The excess energy increased the solubility as well as the mobility (entropy) of PCP in solution. Thus, though the energy barrier required to be crossed for the sorption to occur was surpassed easily, the rapid movement of the molecules in solution did not favour sorption, and this consequently led to the decreased PCP sorption observed. The magnitudes of the $\Delta H°$ values indicated that the

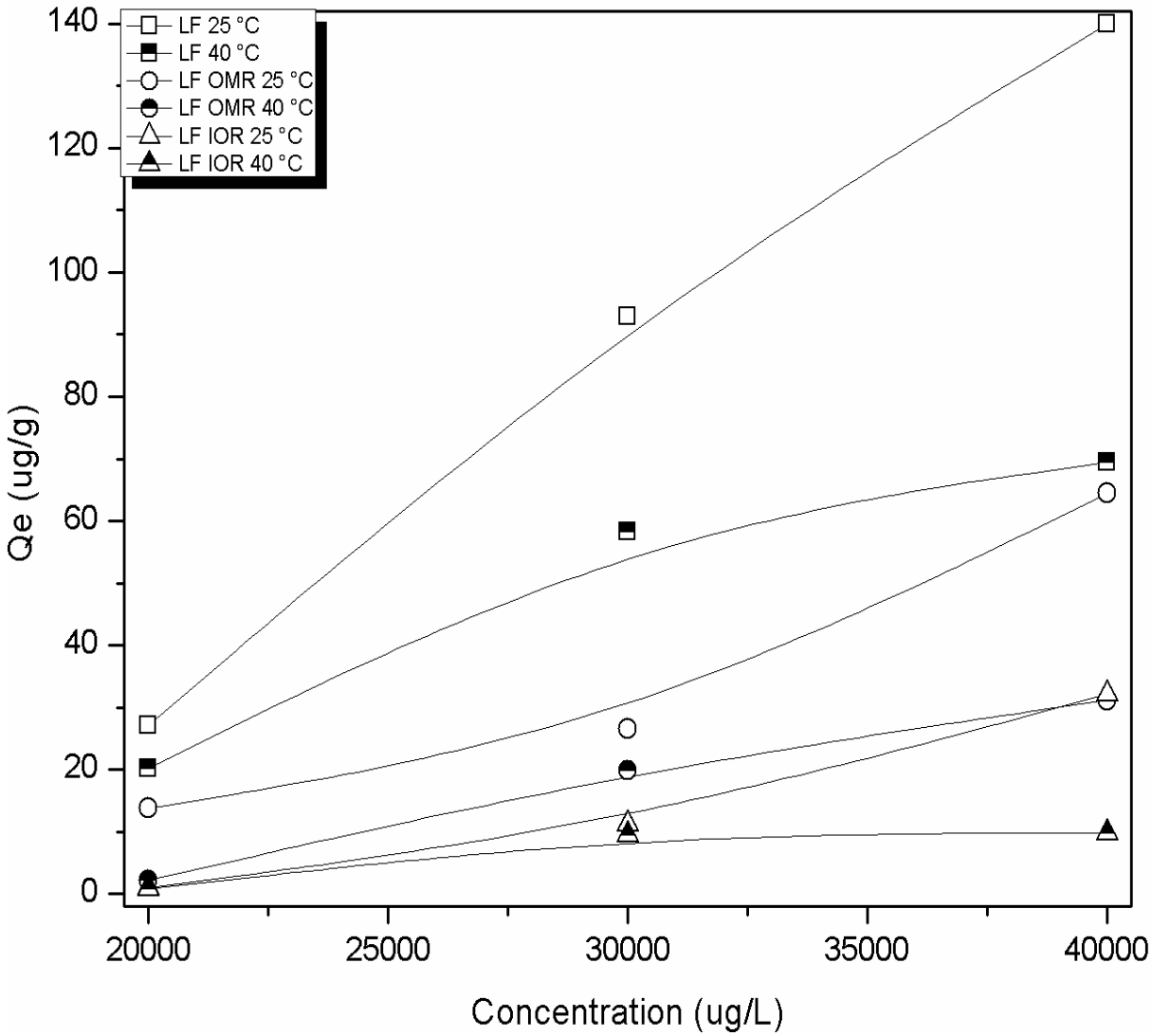

Figure 4.18*a*. Equilibrium sorption of PCP on the LF whole soils (square symbols), OMR treated soils (circular symbols) and IOR treated soils (triangular symbols) at 25 °C (half filled symbols) and 40 °C (unfilled symbols)

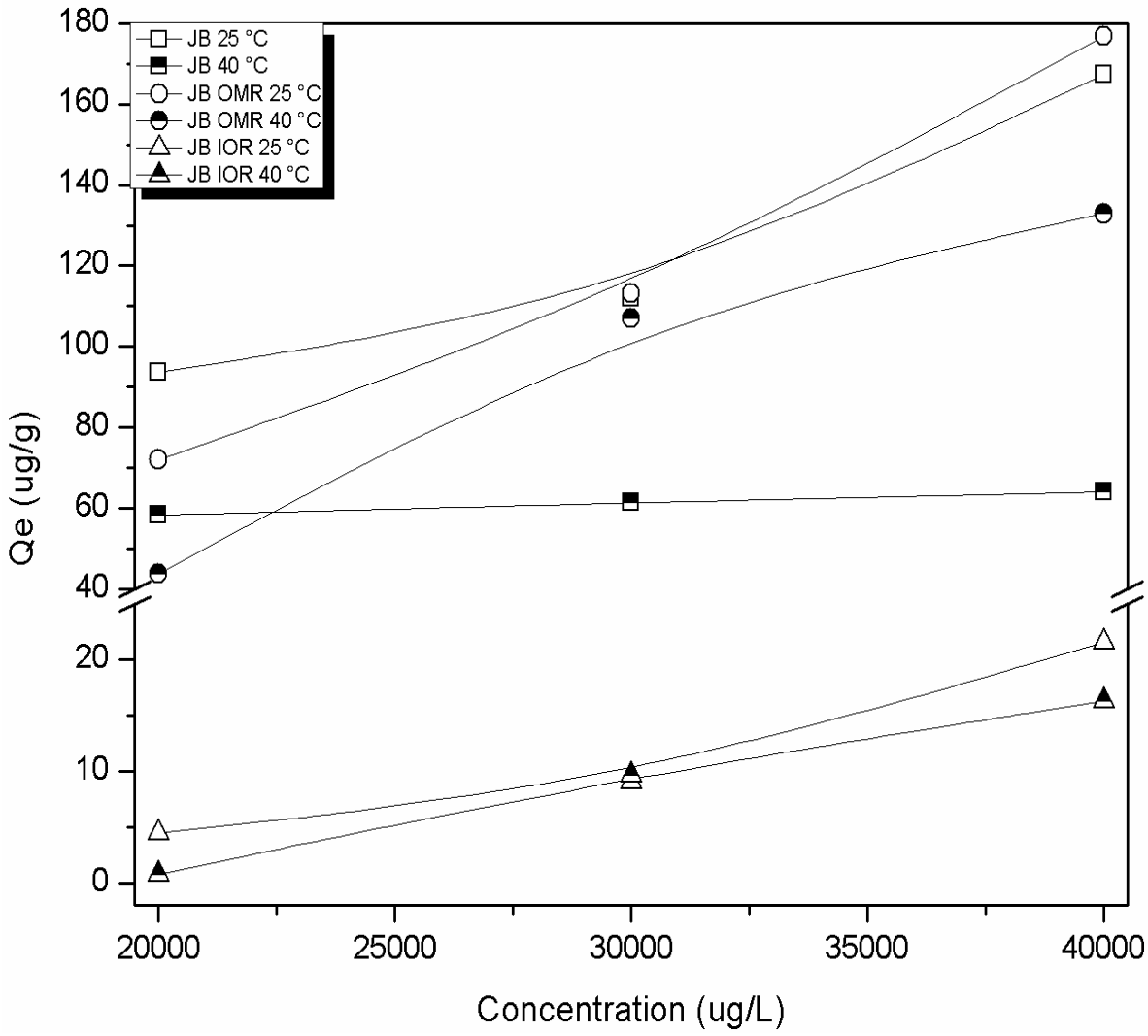

Figure 4.18*b*. Equilibrium sorption of PCP on the JB whole soils (square symbols), OMR treated soils (circular symbols) and IOR treated soils (triangular symbols) at 25 °C (half filled symbols) and 40 °C (unfilled symbols)

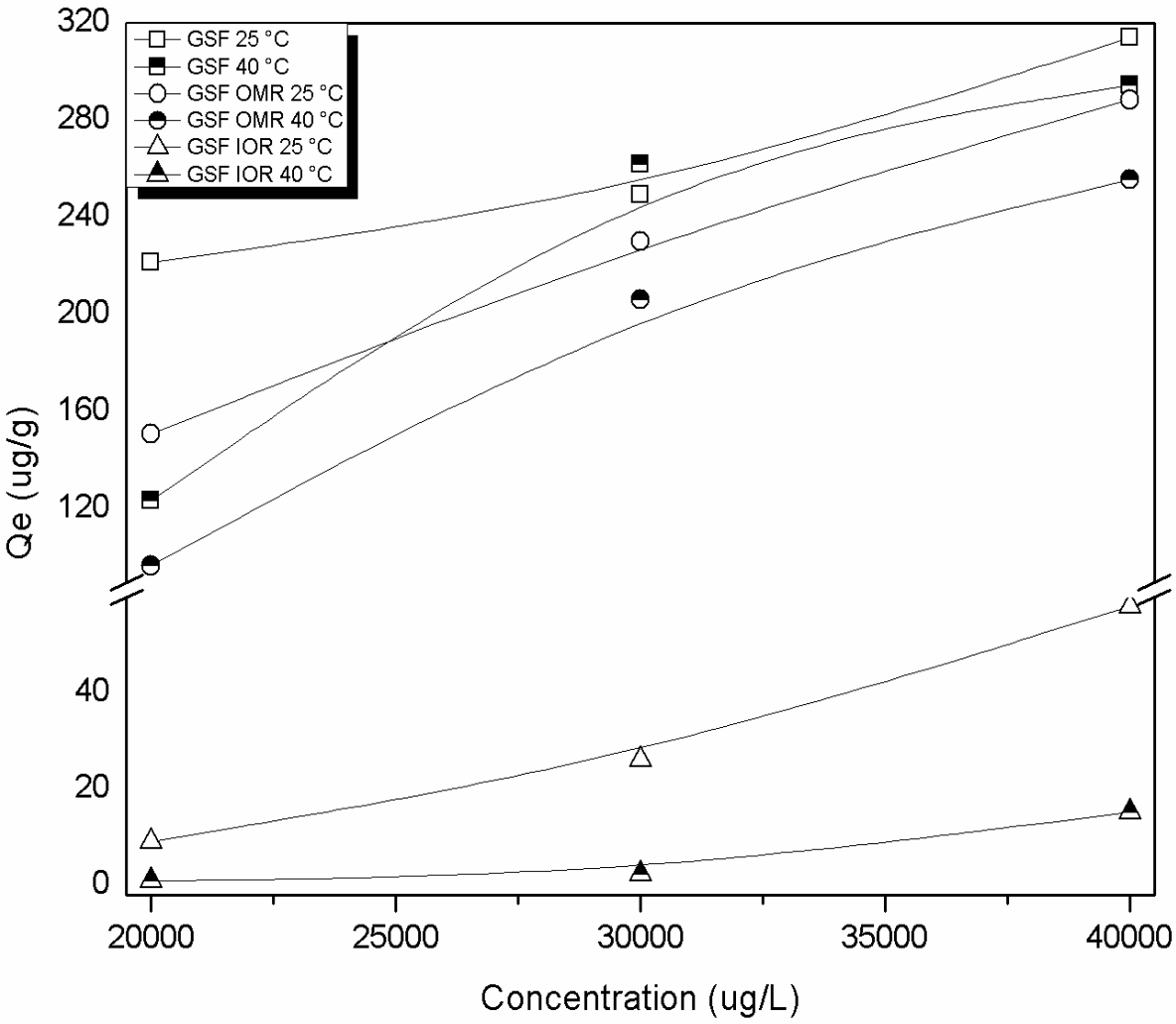

Figure 4.18*c*. Equilibrium sorption of PCP on the GSF whole soils (square symbols), OMR treated soils (circular symbols) and IOR treated soils (triangular symbols) at 25 °C (half filled symbols) and 40 °C (unfilled symbols)

Table 4.19: Thermodynamic parameters for PCP sorption on the whole soils

Soil	ΔH^o	ΔS^o	ΔG^o (kJ mol^{-1})	
	(kJ mol^{-1})	(kJ mol^{-1}K^{-1})	298 K	313 K
LF	5.27	0.02	-0.01	-0.28
AG	-16.2	-0.05	-1.94	-1.23
IB	33.8	0.12	-0.70	-2.44
MA	4.96	0.02	-2.09	-2.44
JB	374	1.27	-3.52	-22.5
PH	-81.7	-0.26	-3.94	-0.02
GSF	-70.4	-0.21	-8.66	-5.55
MG	8.22	0.03	-1.92	-2.43

Table 4.20: Thermodynamic parameters for PCP sorption on the treated soils

Soil	ΔH^o	ΔS^o	ΔG^o (kJ mol^{-1})	
	(kJ mol^{-1})	(kJ mol^{-1}K^{-1})	298 K	313 K
LF	5.27	0.02	-0.01	-0.28
GSF	-70.4	-0.21	-8.66	-5.55
JB	374	1.27	-3.52	-22.52
LF OMR	77.7	0.27	-1.78	-5.78
GSF OMR	-20.0	-0.05	-5.20	-4.46
JB OMR	-14.1	-0.04	-2.49	-1.90
LF IOR	30.1	0.12	-6.71	-8.56
GSF IOR	110	0.38	-2.54	-8.18
JB IOR	67.5	0.24	-4.56	-8.19

energies involved in these sorption processes were of the types associated with the weak forces of interactions such as the electrostatic and van der Waal's interactions. The ΔS^o values also showed that the entropies increased in AG, PH, and GSF soils, while it decreased in other soils. These trends are in line with the above arguments.

Thermodynamic parameters for PCP sorption on OMR and IOR soils are shown in Table 4.20. The $\Delta G°$ values were all negative at both temperatures as observed for the whole soils, indicating the spontaneity of the PCP sorption process on the treated soil. The values of the $\Delta S°$ were negative (or very close to negative) and implied that as sorption occurred PCP in solution entered a state of decreased randomness. The ΔH^o values for the treated soils indicated mainly endothermic processes. The magnitudes of the ΔH^o values also indicated weak forces of interactions between the PCP and soil components.

4.5.6 PCP sorption isotherm models

The PCP equilibrium sorption data for the whole soils at 25 °C were fitted with the Langmuir and Freundlich models. The Langmuir model suggests a rarely observed monolayer sorption on similar surface sorption sites; while the Freundlich model suggests sorption on heterogeneous surface sites as well as possible formation of multi–layer of the sorbent on the sorption surface(s) at saturation. Table 4.21 showed the values of the PCP sorption isotherm parameters for these soils. It was observed that because of the heterogeneous nature and variable composition of soils, the data did not fit well to the Langmuir model unlike the Freundlich which gave r^2 values that were closer to unity. The models' estimated PCP sorptions q_e (μg g^{-1}) values were closer to the experimental values for the Freundlich than for the Langmuir isotherm. The small *n* values of the Freundlich isotherms indicated non–linear PCP sorption on predominantly heterogeneous sorption sites. These results suggested that sorption of PCP on these soils occurred on heterogeneous surface sorption sites with possible multi–layer adsorption of PCP on the surface sorption sites of these soils. Partitioning of the PCP species in solution onto interstitial voids of the soil variable components has been implicated too as a means of PCP removal from solution according to observations discussed above, and hence, the good fitting of the PCP sorption data to the Freundlich isotherm model.

Table 4.22 showed that soil treatments affected the PCP adsorption isotherm model originally obeyed by the soil. With the exception of GSF OMR, all other soils were dominated by the Langmuir type models. The combination of several Langmuir type isotherms for sorption of a particular pollutant by the individual soil components in a soil can give a very good approximation to the Freundlich type isotherm (Weber et al., 1992) as observed for these treated soils. Hence, sorption data on these treated soils were well fitted to both the Langmuir and Freundlich adsorption isotherms.

Table 4.21. PCP sorption isotherm parameters for the Langmuir and Freundlich models for whole soils

soil	Langmuir sorption model			Freundlich sorption model			
	Q_o (μg/g)	b	r^2	q_e (μg/g)	n	K_f	r^2
LF	20.8	0.027	0.695	162	3.97	0.0001	0.876
AG	8.33	0.203	0.948	164	2.27	0.065	0.997
IB	21.3	0.025	0.615	119	3.27	0.001	0.811
MA	15.4	0.024	0.367	97.8	2.97	0.002	0.451
JB	0.00	0.0001	0.079	157	1.08	3.78	0.910
PH	4.35	0.025	0.758	48.0	4.17	0.0001	0.926
GSF	1000	0.029	0.872	302	0.50	62.4	0.916
MG	26.3	0.017	0.460	49.3	2.02	0.032	0.767

Table 4.22. PCP sorption isotherm parameters for the Langmuir and Freundlich models treated soils

Soil	Langmuir sorption model			Freundlich sorption model			
	Q_O (μg/g)	b	r^2	q_e (μg/g)	n	K_f	r^2
LF OMR	13.2	0.023	1.000	60.1	3.18	0.001	0.979
GSF OMR	1000	0.008	0.404	300	1.31	4.30	0.935
JB OMR	125	0.018	0.966	175	1.98	0.20	0.998
LF IOR	0.71	0.027	0.771	39.2	6.98	0.0001	0.965
GSF IOR	7.63	0.025	0.912	59.6	3.87	0.0001	0.998
JB IOR	4.67	0.021	0.992	20.7	3.04	0.0001	0.991

4.6 Heavy Metals Sorption

4.6.1 Effect of Time on metals sorption

The rate of a metal sorption in soil can be directly related to its bioavailability. The higher the sorption rate the lower the mobility and consequently the bioavailability of the metal (Lu et al., 2005). The sorption rate depends on soil-metal interactions such as adsorption, intra/inter–particle diffusion in the soil mineral and/or organic matter internal voids, complexation and in some cases precipitation. Hence, the effect of time on the adsorption of Pb(II), Cu(II), and Cd(II) was investigated on these soils and results are shown in Figures 4.19 (*a*–*d*). It was observed that the LF soil had the highest adsorption rate for all three metal ions (comparing Figures 4.19 (*a*–*d*)). The metals adsorptions on this soil were nearly completed in 60 min (Figure 4.19*a*). The amounts of metals adsorbed decreased with decrease in organic matter contents and, to an extent, the percentage content of Fe_2O_3 in the soils. Thus, the effect of time on sorption of these metals followed the trend: LF (60 min) > GSF (720 min) ≥ JB (720 min) > MA (1440 min). MA soil exhibited a relatively high sorption rates between the 60th and 180th min for the adsorptions of Pb(II) and Cd(II) ions, but this was immediately followed by high rate of desorptions leading to lower sorption rates observed in the subsequent areas of the curve (Figure 4.19*d*). These relatively high sorption rates at this point were attributed to mutli–layer adsorptions of these metals on the soil surface but since the extra layer(s) of metals adsorbed are not held by strong adsorption forces, simple agitation or shaking of the aliquots can facilitate the desorptions as were observed.

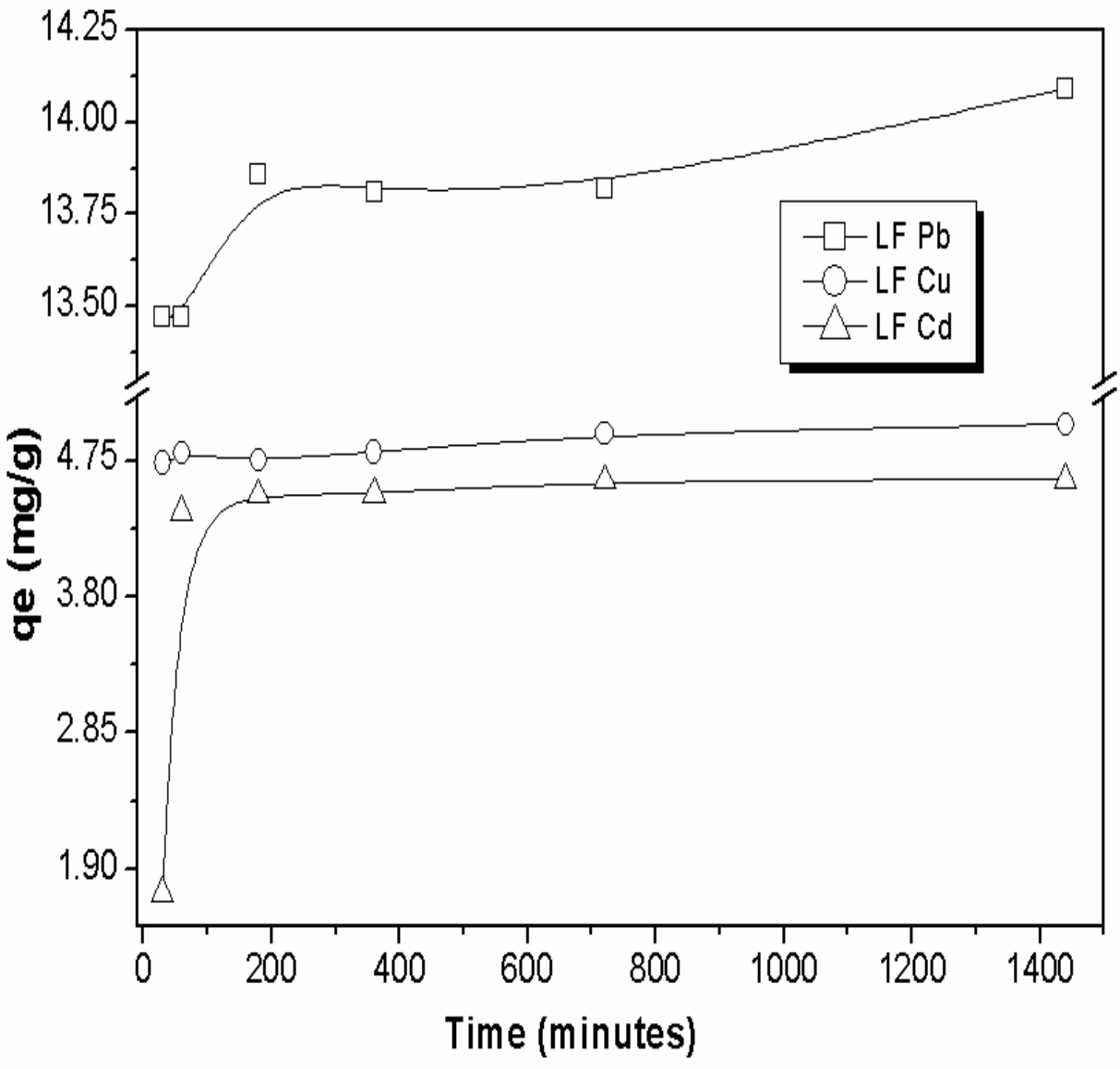

Figure 4.19 *a*. Effect of time on metals sorptions on LF soil

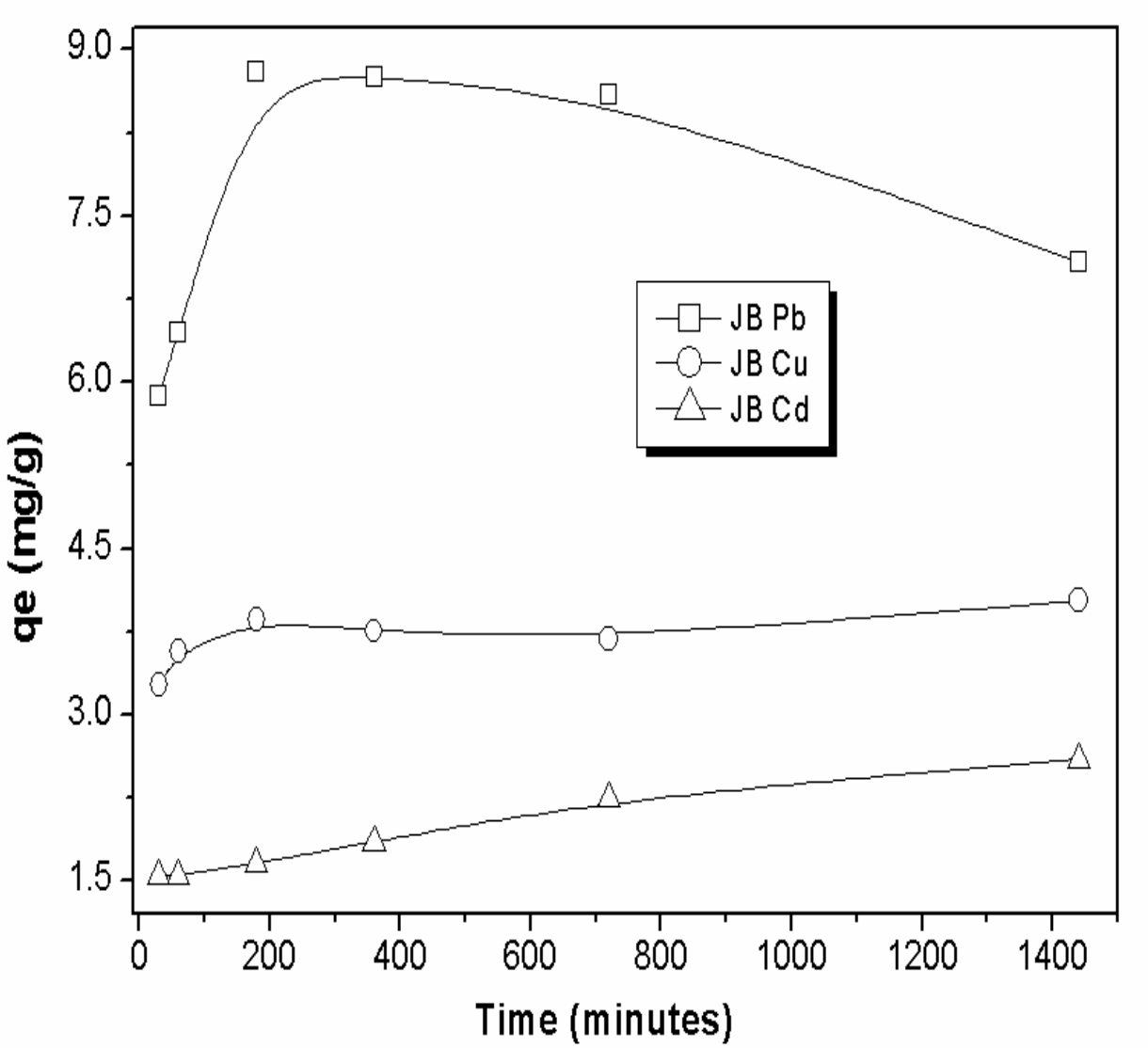

Figure 4.19 *b*. Effect of time on metals sorptions on JB soil

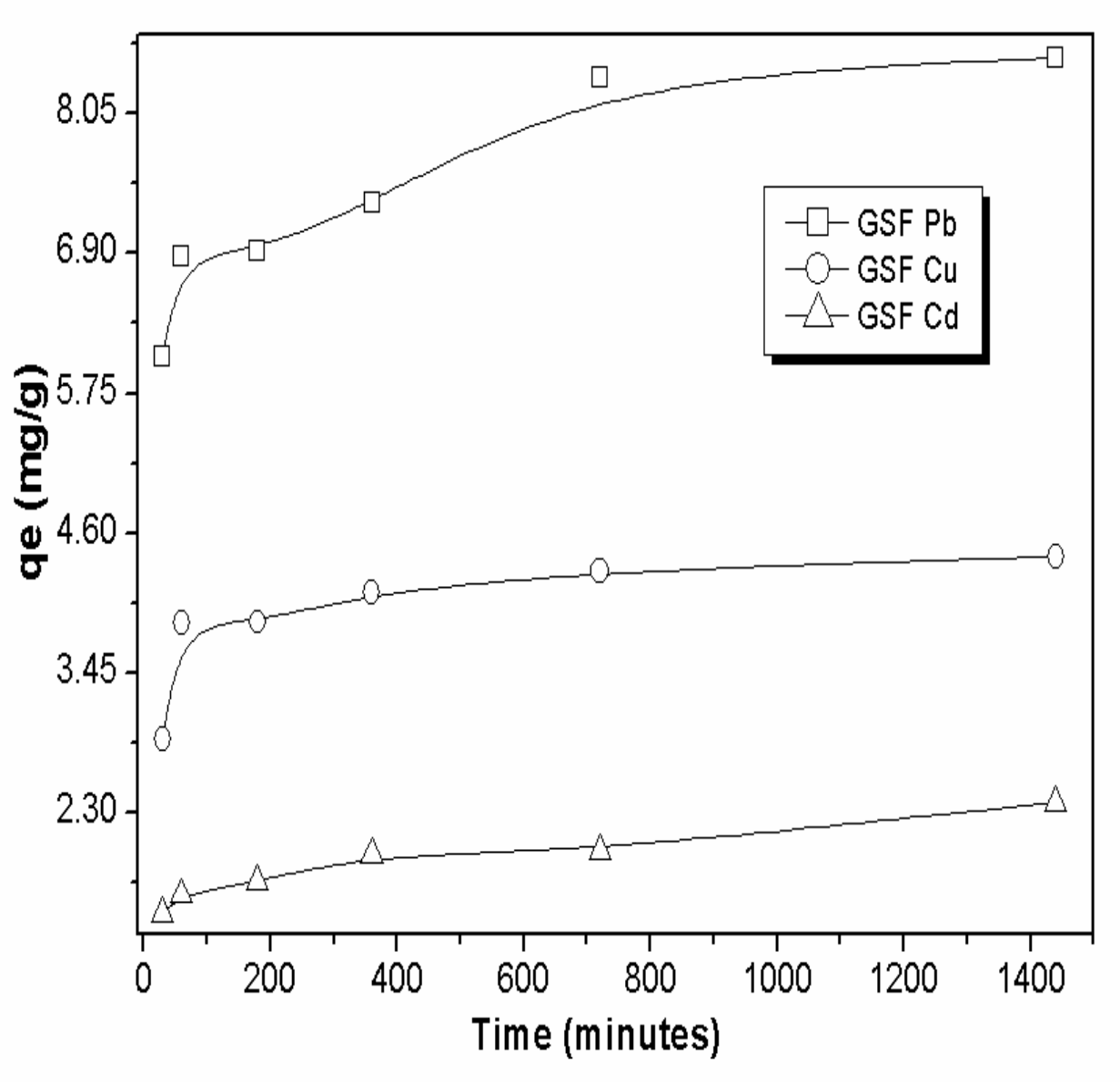

Figure 4.19 *c*. Effect of time on metals sorptions on GSF soil

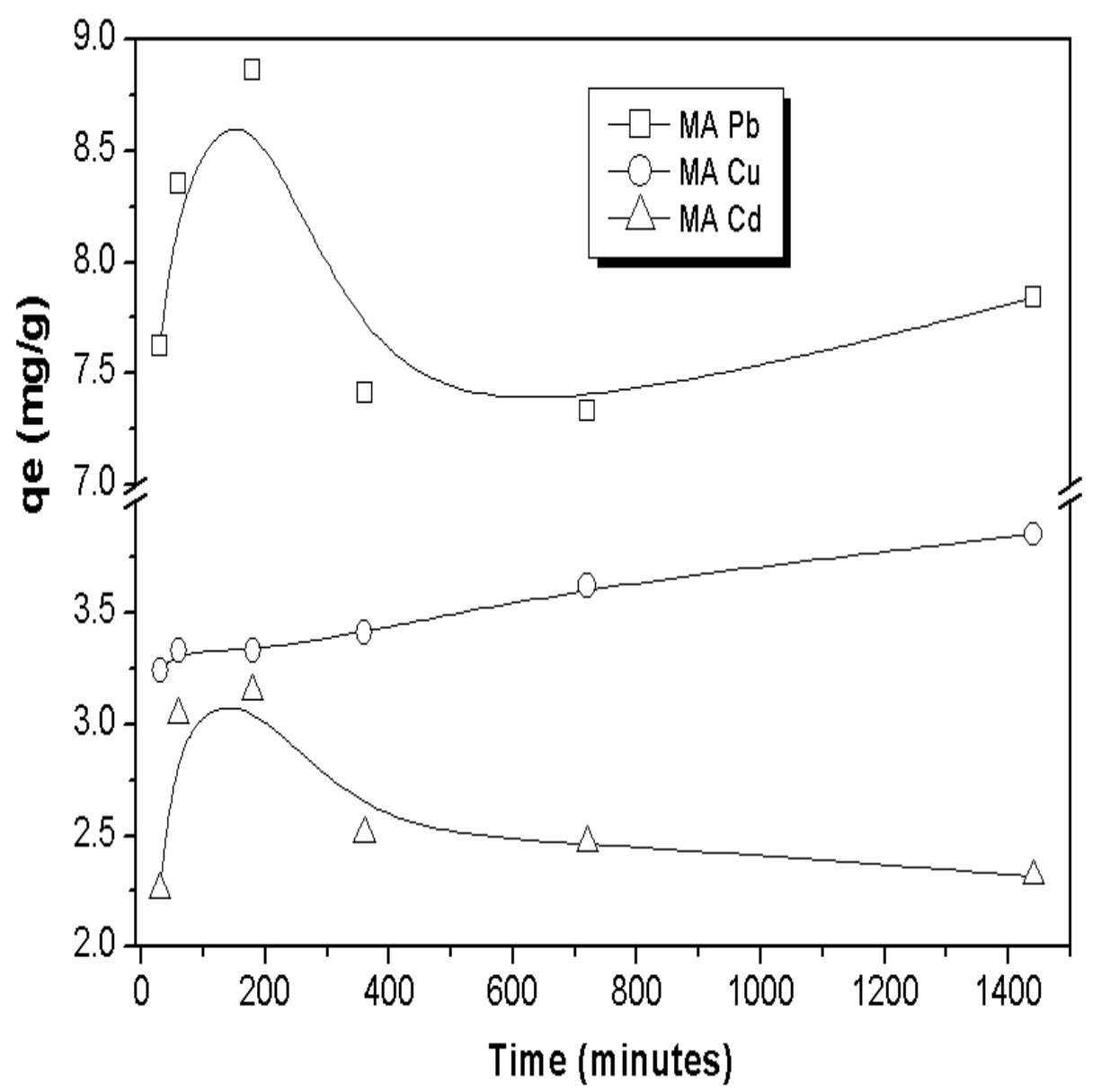

Figure 4.19 *d*. Effect of time on metals sorptions on MA soil

4.6.2 Kinetics of metals adsorption

The data generated from the effect of time experiments were evaluated using four kinetics models: Lagergren pseudo–first and second order, Elovich and intra-particle diffusion kinetics models; and the kinetics parameters are shown in Table 4.23. These models were employed to predict the possible mechanism(s) involved in the sorption of these cations from solution onto the soil surfaces and pores. Comparisons of the soils' correlation coefficients (r^2) and the estimated cation sorption capacities (q_e) for the pseudo–first and second order kinetics indicated that the sorptions were better fitted to the pseudo–second order kinetics model. The r^2 values pseudo–second order kinetics were closer to unity (0.988–0.999) and the q_e values closer to experimental results. The good fit of the metals sorption data to the pseudo–second order kinetics model suggested that sorption reactions between the cations and sorption sites on soils involved sharing or exchange of valence electrons.

The Elovich kinetics model parameters (Table 4.23) suggested that cation adsorptions on these soils could be described by the model when the adsorption behave more like a surface phenomenon as observed in the fast adsorbing organic matter rich soil of LF or the low organic matter MA soil. However, for soils whose physico–chemical parameters showed high contents of gibbsite and the 2:1 expansive clay – illite, metals sorptions were distributed between adsorption and partitioning of the cations within the expansive clay voids as observed in the JB and GSF soils and thus, their sorptions data did not fit the Elovich model. This argument was also supported by the C (μg g^{-1}) values of the intra–particle diffusion model. The C value may be related to the thickness of the adsorbed species on the soil surface: if the sorption is more of a surface–like phenomenon, the C values will be approximately equal to the q_e values since the sorptions will occur on the soil surface as was observed for all metals adsorptions on the LF and MA soils. However, if the sorption is distributed between the adsorption and partitioning processes, the C values will be significantly smaller than the q_e values because significant amount of the cations removed from solution will be distributed within the soil voids. This was the case for all metals adsorptions in the JB and GSF soils (Low, 1960).

Table 4.23. Metal adsorption kinetics model parameters for Pb(II), Cu(II), and Cd(II).

		LF			JB			GSF			MA		
		Pb(II)	Cu(II)	Cd(II)	Pb(II)	Cu(II)	Cd(II)	Pb(II)	Cu(II)	Cd(II)	Pb(II)	Cu(II)	Cd(II)
PFO*	q_e (μg g^{-1})	1.43	1.76	1.09	1.50	5.41	7.40	2.45	0.90	0.79	1.04	1.13	1.85
	K_1 (min^{-1})	0.0001	0.0001	0.001	0.0001	0.0001	0.0001	0.001	0.001	0.001	0.0001	0.001	0.001
	r^2	0.746	0.917	0.304	0.003	0.531	0.976	0.898	0.757	0.956	0.104	0.999	0.229
PSO*	q_e (μg g^{-1})	14.08	5.03	4.69	7.19	4.02	2.67	8.70	4.46	2.40	7.75	3.88	2.30
	K_2 (g μg^{-1} min^{-1})	0.015	0.026	0.011	0.005	0.014	0.004	0.004	0.011	0.007	0.052	0.010	0.017
	r^2	0.999	0.999	0.999	0.990	0.997	0.988	0.998	0.999	0.990	0.998	0.998	0.998
Elovich	q_e (μg g^{-1})	13.6	4.49	1.06	5.38	2.88	0.47	4.66	2.14	0.73	8.41	2.70	3.00
	β	6.62	15.6	1.80	1.99	6.71	3.77	1.65	3.06	4.79	8.77	7.09	14.71
	r^2	0.851	0.741	0.511	0.332	0.717	0.847	0.910	0.808	0.921	0.081	0.830	0.071
IPD*	C (μg g^{-1})	13.4	4.69	3.09	6.93	3.39	1.28	6.01	3.26	1.39	8.20	3.13	2.86
	K_{id}	0.017	0.008	0.052	0.036	0.016	0.034	0.072	0.035	0.025	0.016	0.018	0.012
	r^2	0.793	0.874	0.322	0.121	0.609	0.976	0.900	0.655	0.959	0.110	0.963	0.117

*PFO – pseudo–first–order; PSO – pseudo–second–order; IPD – Intra–particle diffusion

4.6.3 Effect of pH on metals adsorptions

Heavy metals adsorption on soils are significantly influenced by soil properties. Soil properties, especially the nature and ionization of the adsorption sites, are in turn affected by the pH condition of the ambient soil water solution; hence, the effect of pH on the adsorptions of the Pb(II), Cu(II), and Cd(II) was investigated and the results are shown in Figures 4.20 (*a*–*d*). It was observed that the sorptions were pH dependent and increased with increase in pH. At lower pH values, the quantities of metals adsorbed onto the surface adsorption sites were small. With rise in solution pH, the quantities adsorbed increased steadily until about pH values of 5.5 and 6.5 where optimum adsorptions were recorded for the various metals. Though further metals removal from solution can be noticed in the curve in Figures 4.20 (*a*–*d*) for most of the sorbed ions on the studied soils, the general trend is explained below. At the lower pH values there was stiff competition between metal ions in solution and protons for the negatively charged soil sorption sites. The competition from the protons resulted in displacement of the exchangeable cations as well as the heavy metal cations from the adsorption sites, resulting in uncharged adsorption sites, and hence the observed low adsorptions. As pH increased, the amounts of protons in solution reduced and the competition due to protons reduced; resulting in the increase in adsorptions. Adsorptions increased steadily until pH at which optimum adsorption occurred (between 5.5 and 6.5) and after this point the 'pseudo–adsorptions' were observed. This was attributed mainly to hydrolysis of the cations products leading to precipitation from solution. In aqueous solutions of pH less than 6, the cations exist as either X^{2+} or $X(OH)^{+}$ or both. However, the formation of X^{2+} hydrolysis products begins to occur at pH values after 6.5, resulting in precipitation (Olu–Owolabi et al., 2012).

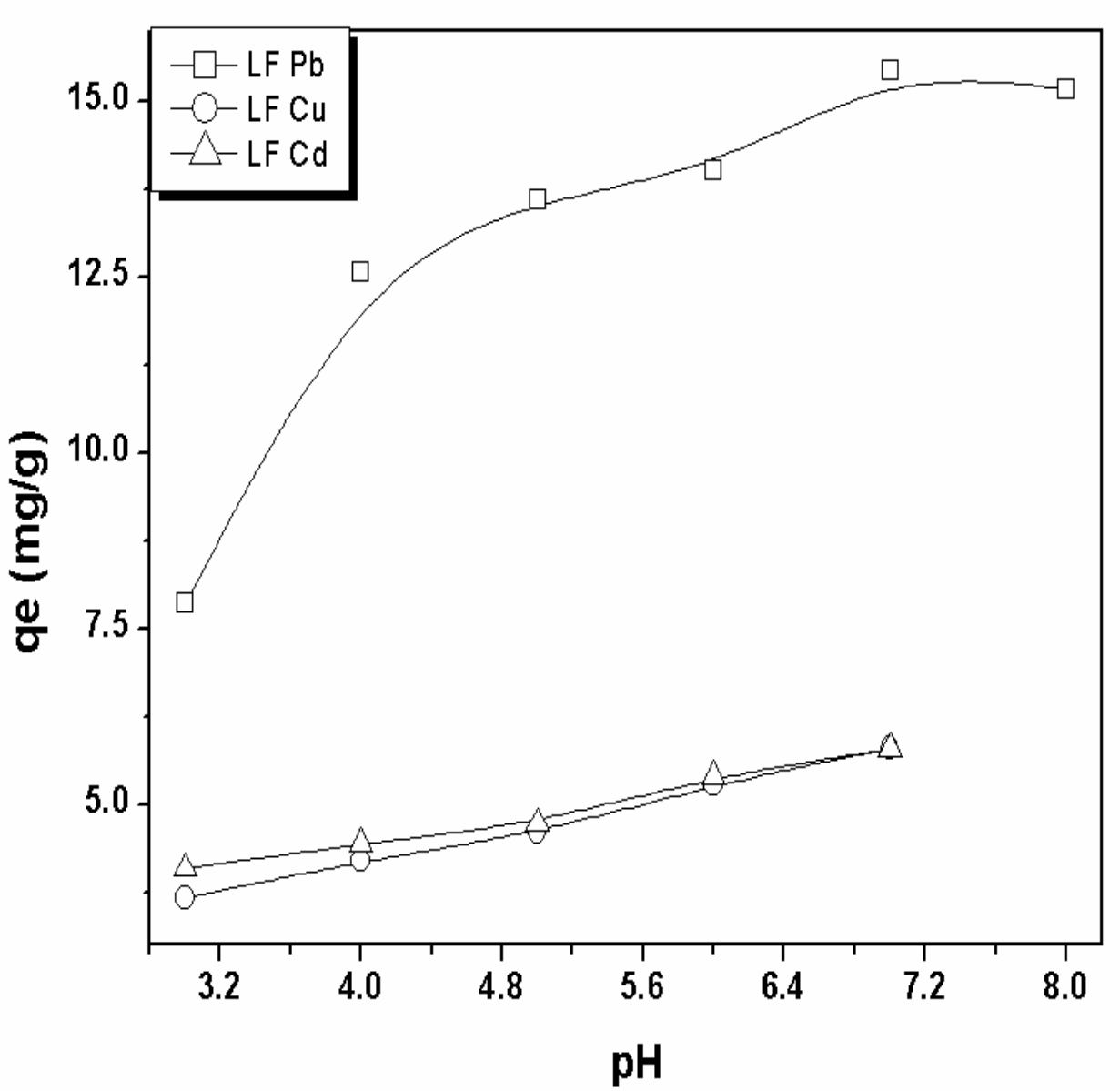

Figure 4.20 *a*. Effect of pH on metals sorptions on LF soil

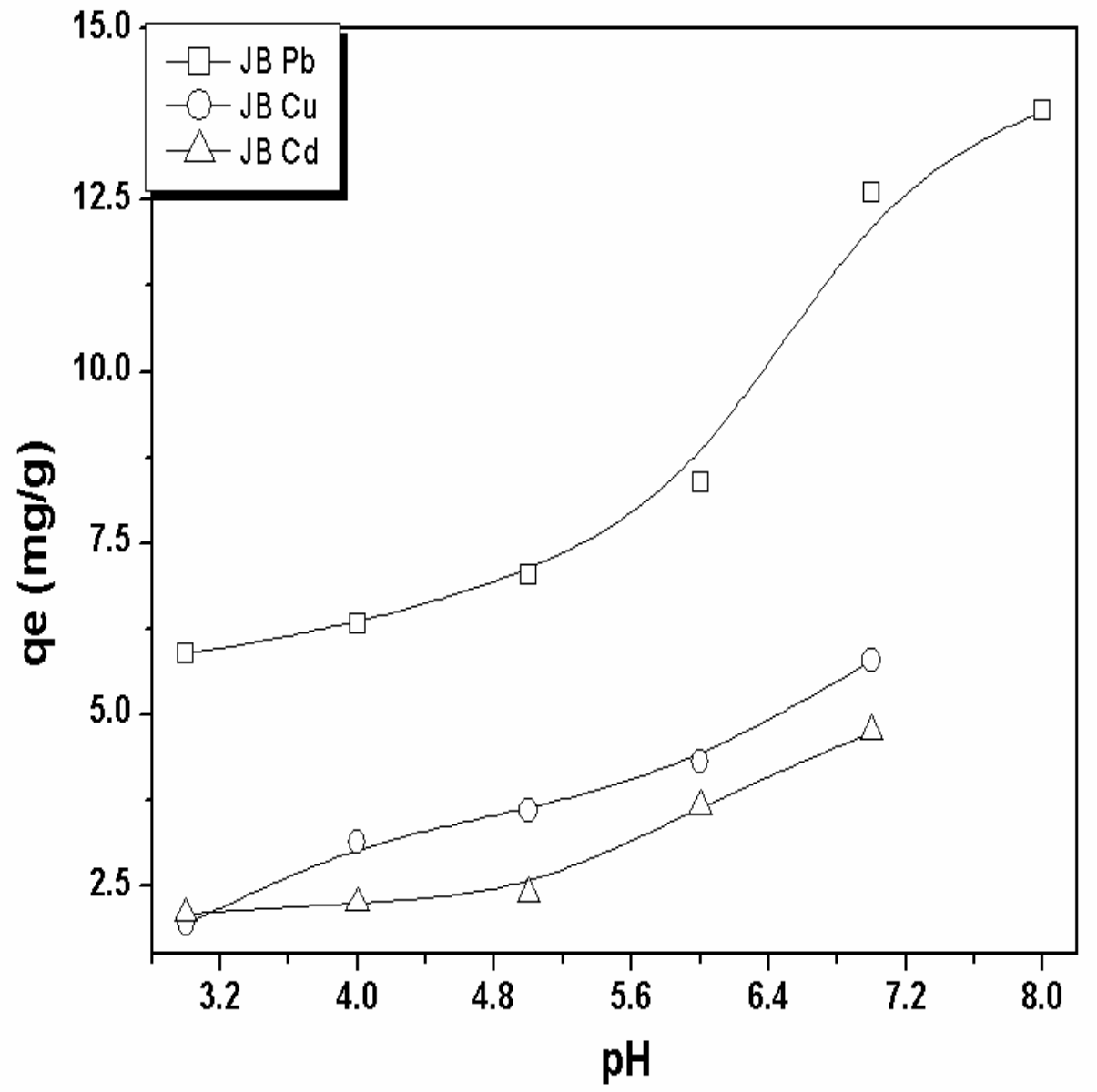

Figure 4.20 *b*. Effect of pH on metals sorptions on JB soil

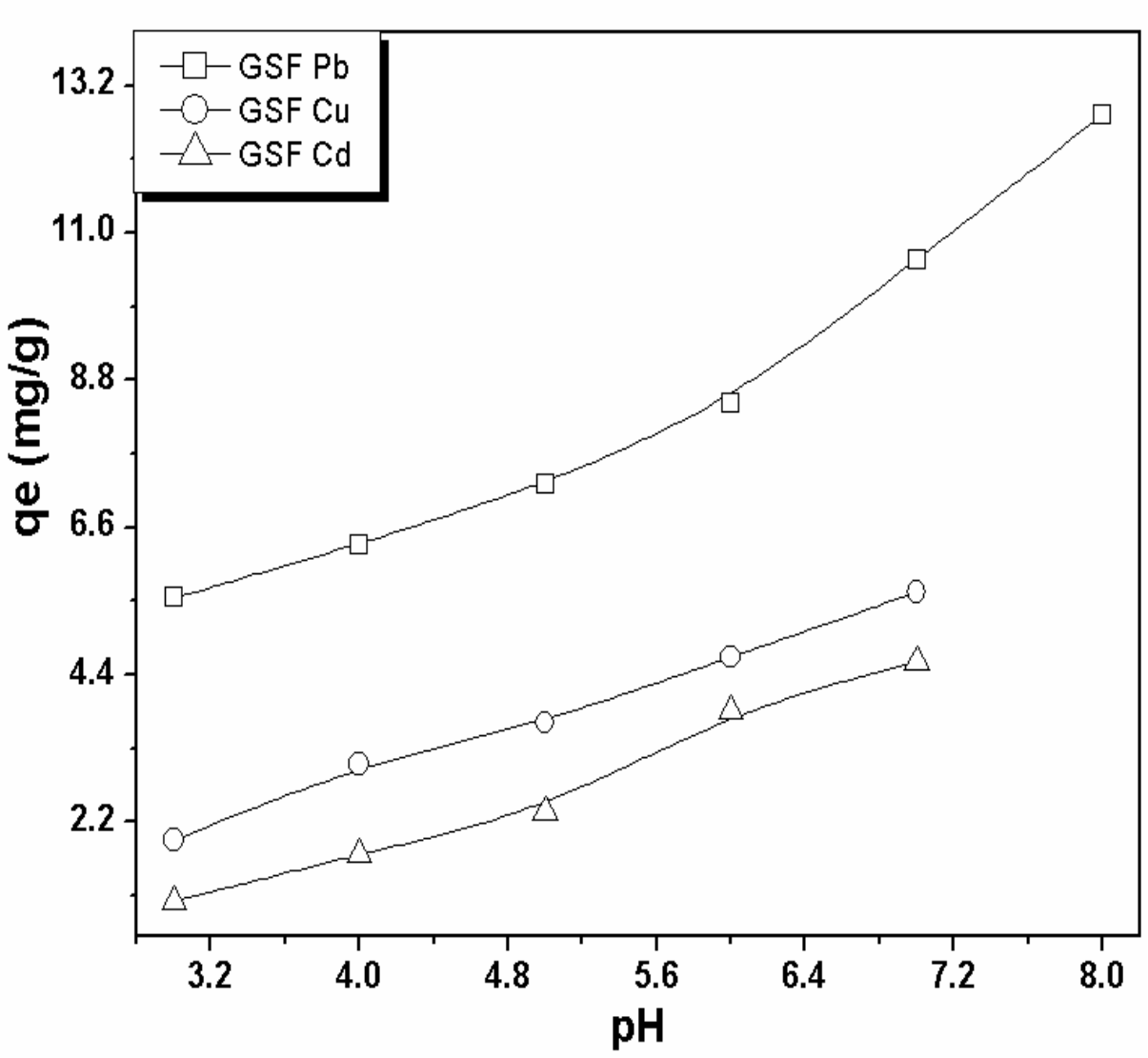

Figure 4.20 *c*. Effect of pH on metals sorptions on GSF soil

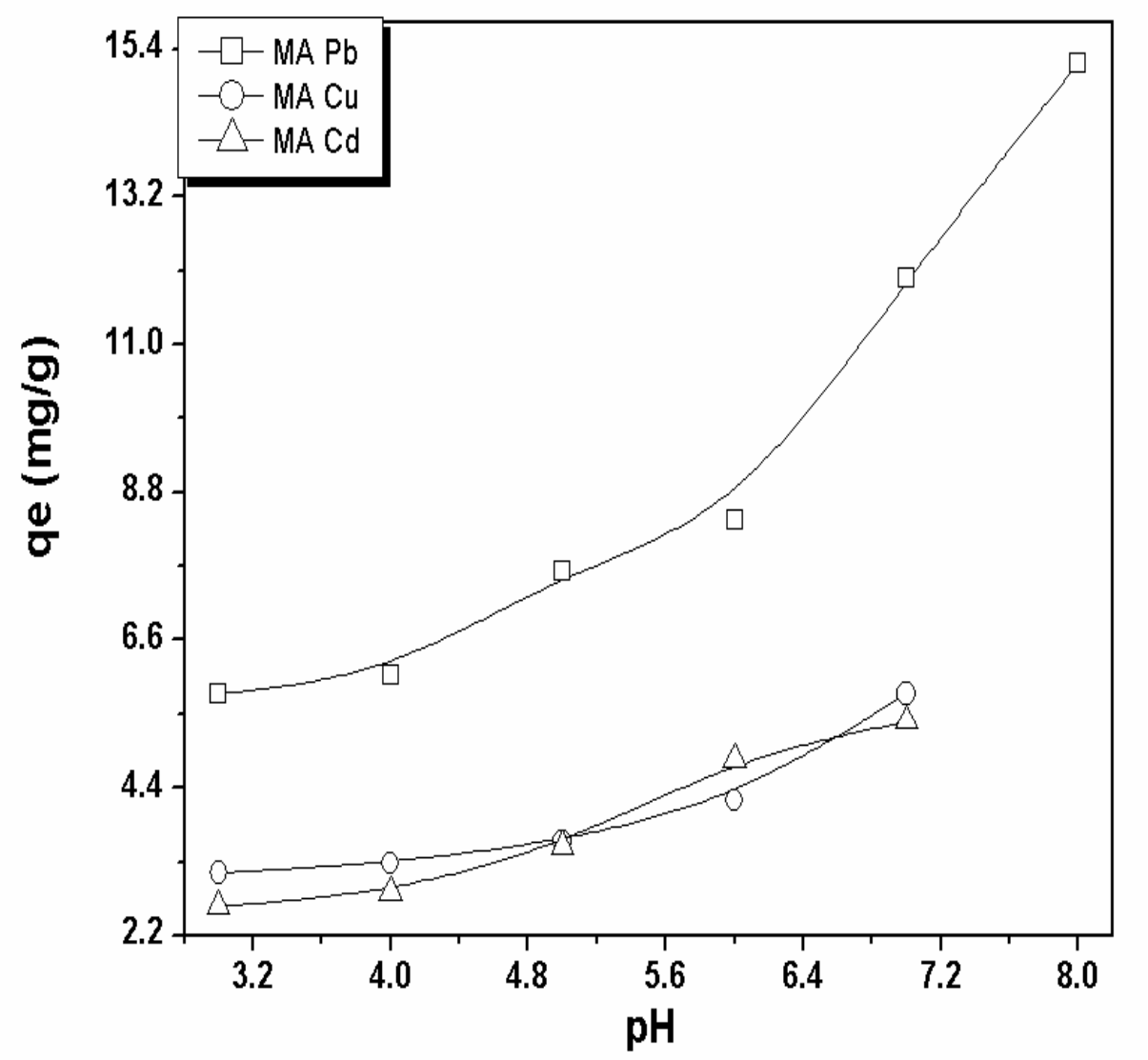

Figure 4.20 *d*. Effect of pH on metals sorptions on MA soil

4.6.4 Equilibrium metals adsorptions

Equilibrium sorptions of these metal ions were investigated at varying heavy metal ions concentrations, two temperatures (25 and 40 °C), ambient soil pH, while incubating for 1440 minutes. The sorption trends with increase in temperature for all metal ions studied are shown in Figures 4.21 (*a–c*) (Figure A21). The Figures showed that until optimum sorption of the specific metal ion were achieved, increase in solution concentration of the metal usually led to increased sorptions at both temperatures (25 and 40 °C). However, comparing the quantities of metal ions adsorbed at both temperatures, it was observed that increase in temperature does not always lead to an increase in metal ions sorptions. The effect of temperature on the sorption was dependent on the metal ion as well as the soil physical and chemical characteristics. For instance, adsorption of Pb(II) ions on the relatively higher organic matter containing soil of LF showed no noticeable improvement with increase in temperature. Similar trend was observed for the relatively lower organic matter containing soil of MA. This was a confirmation of the inference drawn from the intra–particle diffusion kinetics model that the sorptions of metal ions on the LF and MA soils behave more like a surface phenomenon.

Adsorption of Pb(II) ions on the JB and GSF soils behaved quite differently due to the presence of expansive clays in these soils. Increase in temperature was observed to increase adsorptions on both soils because as temperature increases, the soils absorb water, swell or expand increasing soils' internal surface area and leading to adsorptions of more Pb(II) ions from solution.

Sorption of Cu(II) ions on these soils showed no clear effect of increase in temperature. Though at higher solution concentrations apparent higher sorptions were observed and this was attributed to multi–layer adsorptions of Cu(II) ions on these soils' surfaces.

Equilibrium data of the sorptions of Cd(II) ions on the studied soils are shown in Figure 4.21c (Figure A21). The Figure indicates that temperature did not favour the adsorptions of Cd(II) ions on these studied soils. Increase in temperature led to a reduction of the amount of Cd(II) sorbed. This was attributed to the fact that increase in temperature increases the randomness of Cd(II) ions in solution, and this drives the Cd(II) ions to migrate away from the soils' sorption sites leading to the reduced sorptions observed with increase in temperature.

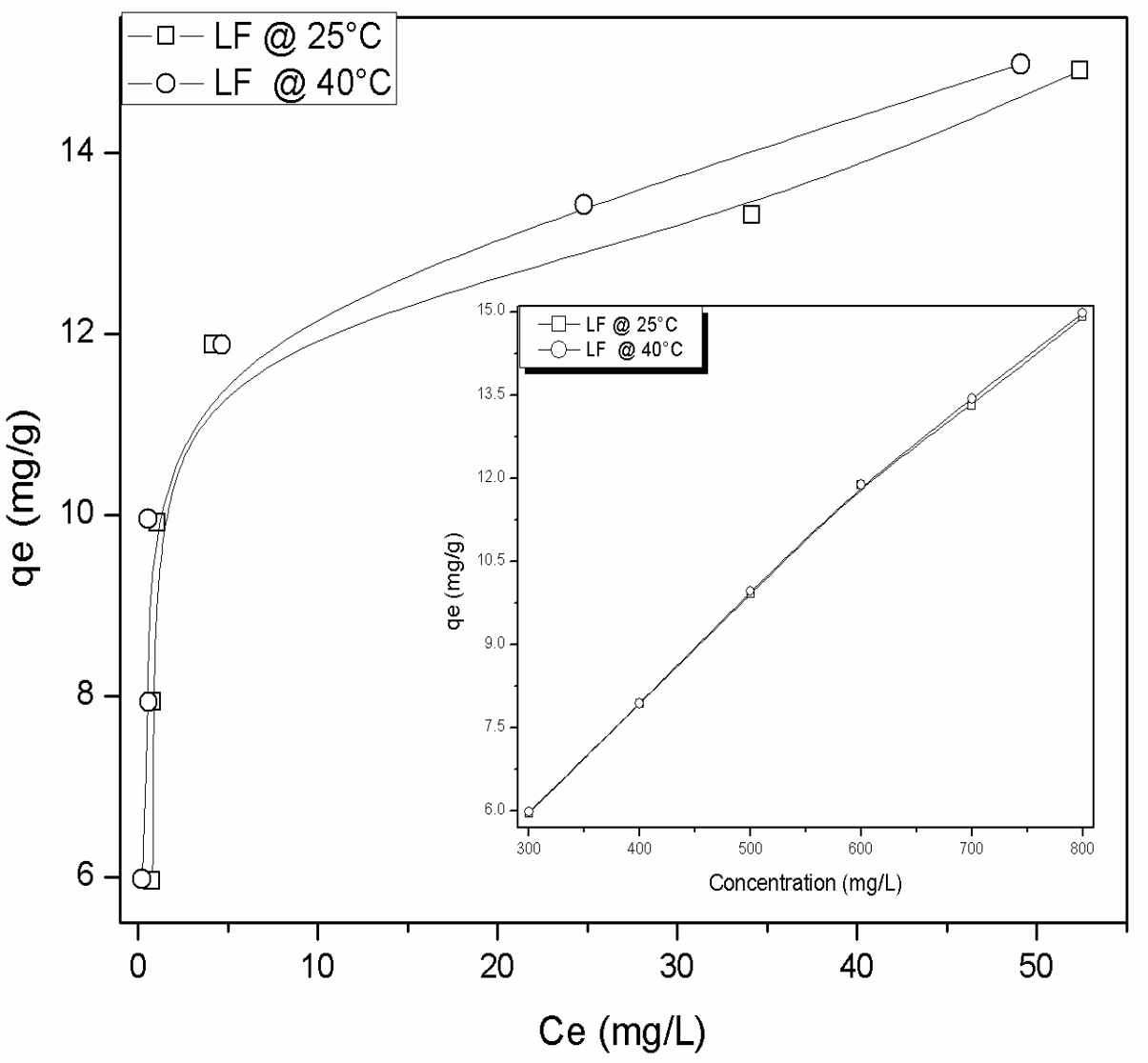

Figure 4.21 *a*. Pb(II) sorption isotherm for LF soil (Insert: Pb(II) sorption trend as concentration varied at 25 and 40 °C)

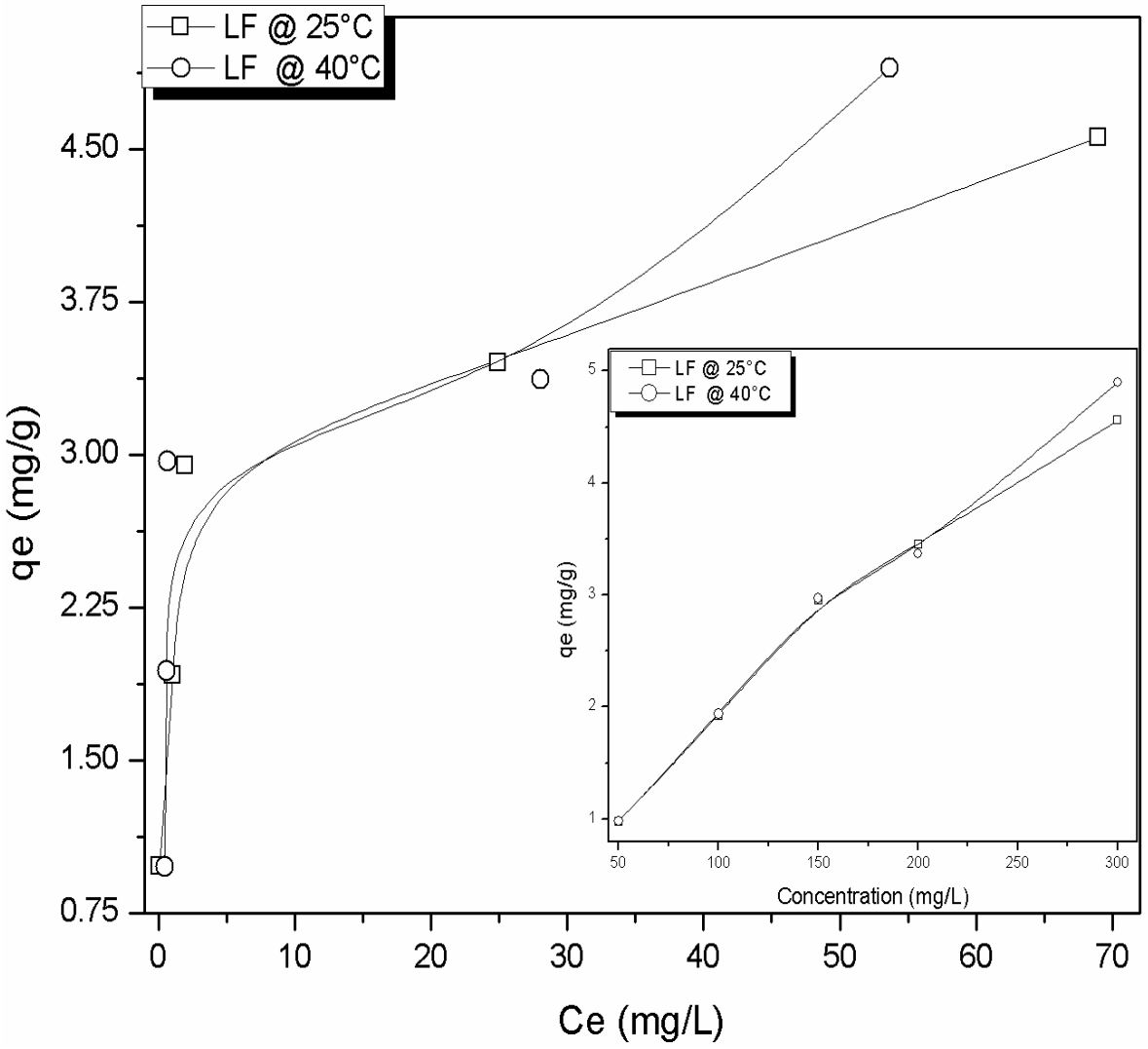

Figure 4.21*b*. Cu(II) sorption isotherm for LF soil (Insert: Cu(II) sorption trend as concentration varied at 25 and 40 °C)

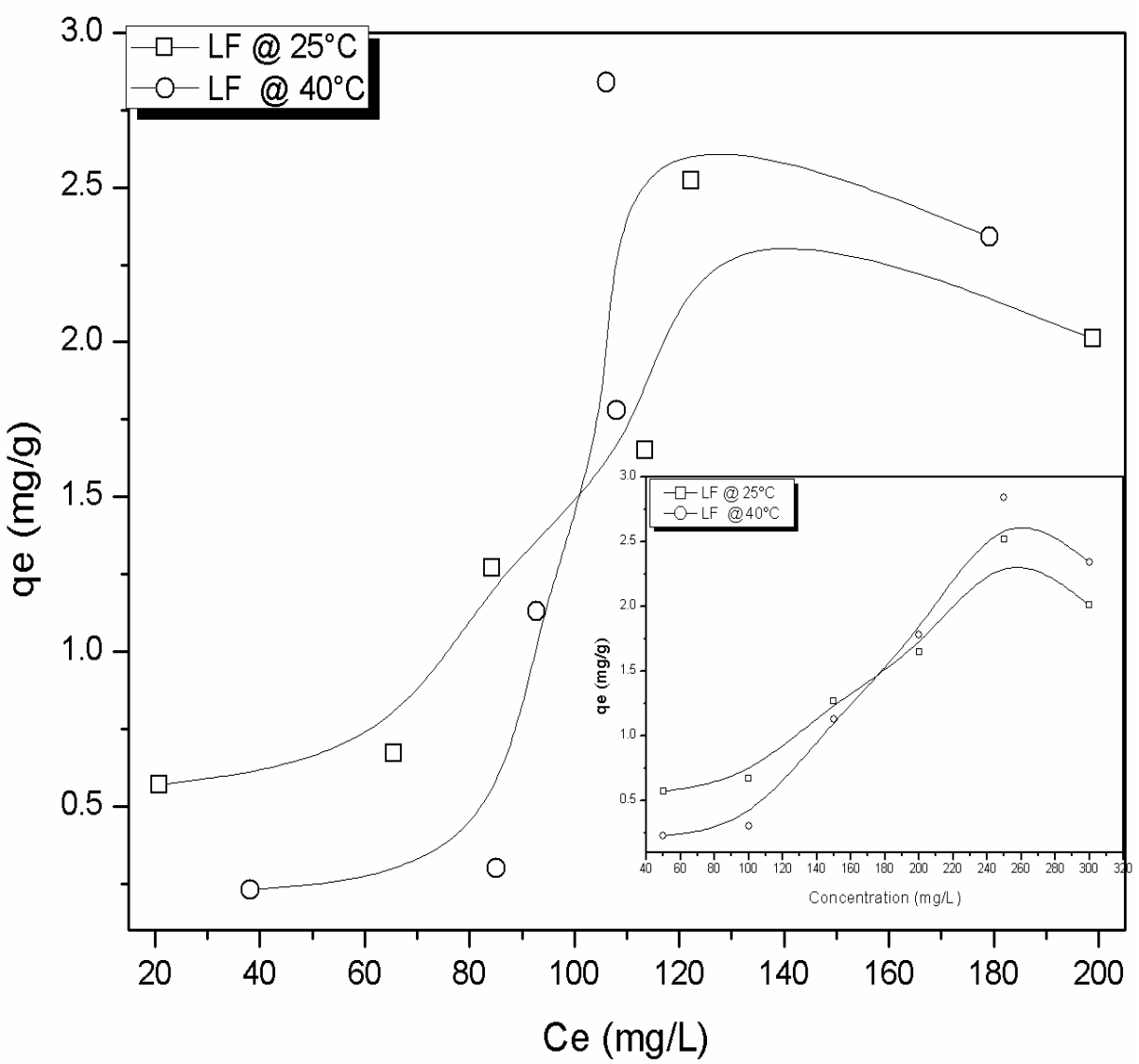

Figure 4.21*c*. Cd(II) sorption isotherm for LF soil (Insert: Cd(II) sorption trend as concentration varied at 25 and 40 °C)

4.6.5 Adsorption isotherm model fitting

These metals equilibrium sorption data for the soils obtained at 25 °C were fitted to the Langmuir and Freundlich adsorption isotherm models. The adsorption isotherm parameters of the Freundlich and Langmuir models were calculated and shown in Table 4.24. It was observed that the adsorptions of Pb(II) and Cu(II) on these soils are better described by the Langmuir adsorption isotherm. The correlation coefficients (r^2) were closer to unity and the model predicted the maximum adsorption capacity (q_e) for each metal better. Since the sorptions data of Pb(II) and Cu(II) fitted the Langmuir isotherm, it thus indicated that the adsorptions occurred on similar adsorption sites of nearly equal adsorption energy and a monolayer adsorption was formed at the adsorption sites at equilibrium. However, it was also observed that the sorptions data could also be described by the Freundlich adsorption isotherm model. This was attributed to the presence of several Langmuir–type isotherm models for the individual soil components. Combination of these Langmuir–type isotherm models gave a good approximation of the Freundlich–type isotherm model (Weber et al., 1992). Hence, the sorptions data could be described by the Langmuir as well as the Freundlich isotherm models.

Adsorptions of Cd(II) on these soils did not fit the Langmuir isotherm model. Table 4.24 showed that the data were better described by the Freundlich isotherm indicating that these soils have heterogeneous adsorptions sites. The sorption trend of the soils for the metal ions was Pb(II) > Cu(II) > Cd(II). The preference exhibited by these soils for Pb(II) over the other metals may be attributed to its lower first hydrolysis constant which makes it a better candidate than other metals ions for electrostatic and inner-sphere surface complexation reactions. Gomez et al. (2001) and Usman (2008) have reported similar preference for Pb(II) sorption relative to other toxic metals ions on soil and soil constituents. The metal ions sorption capacities of the soils followed the trend: LF > GSF ≥ JB > MA. This was in line with decreasing organic matter contents of the studied soils. Table A2 showed the type of isotherm curve for Pb(II), Cu(II), and Cd(II) ions sorptions at 25 and 40 °C. The Table indicated that the sorptions data fitted the same isotherm curve type under different sorption temperature conditions.

Table 4.24. Metal ion adsorption isotherm model parameters for Pb(II), Cu(II), and Cd(II).

Adsorption isotherm	Isotherm parameters	LF			JB			GSF			MA		
		Pb(II)	Cu(II)	Cd(II)	Pb(II)	Cu(II)	Cd(II)	Pb(II)	Cu(II)	Cd(II)	Pb(II)	Cu(II)	Cd(II)
Langmuir	Q_O (mg g^{-1})	14.9	4.59	4.42	7.81	3.23	0.26	8.40	2.86	0.10	11.0	3.17	0.10
	b	0.918	0.445	0.005	0.011	0.095	0.004	0.01	0.074	0.005	0.011	0.033	0.005
	r^2	0.996	0.987	0.289	0.95	0.96	0.462	0.764	0.948	0.604	0.883	0.903	0.438
Freundlich	q_e (mg g^{-1})	15.2	4.77	2.29	6.37	3.07	1.80	6.64	3.04	3.08	9.02	2.48	3.13
	n	0.16	0.22	0.68	0.25	0.24	2.09	0.30	0.31	3.06	0.35	0.27	2.91
	r^2	0.766	0.917	0.753	0.871	0.816	0.808	0.575	0.69	0.845	0.781	0.919	0.858
	K_f	8.11	1.89	0.06	1.41	0.96	0.001	1.12	0.63	0.001	1.14	0.65	0.001
Experimental	q_e (mg g^{-1})	14.9	4.56	2.01	6.88	3.12	1.02	8.82	2.63	1.42	8.85	2.92	1.60

4.6.6 Thermodynamics of Heavy Metals Adsorptions

The data from the effect of temperature on equilibrium metal ions sorption were used to calculate the thermodynamic parameters (standard free energy – ΔG^o, enthalpy change – ΔH^o, and entropy change – ΔS^o) using equations 2.3 to 2.6**,** and the calculated parameters were used in evaluating the feasibility and energetics of the sorption process. The values of the thermodynamic parameters are shown in Table 4.25. The ΔG^o values for all studied soils at both temperatures were negative. This indicated that adsorptions of these metals adsorption are feasible and spontaneous. The magnitudes of the ΔG^o values also indicated that the adsorption energies were of the type associated with the electrostatic interactions.

The ΔS^o values are in the range of −0.09 to 0.34 kJmol^{-1}K^{-1}. The negative values indicated that sorptions were accompanied by a decrease in the entropy of the metal cations in solution at equilibrium. The small positive values obtained may not indicate otherwise but might be attributed to the fact that small errors associated with linear model calculations of the thermodynamic parameters become significant when dealing with low energy adsorption surfaces due to slight shifts of values from the border of one extreme to another, and when this occurs, adsorption processes with thermodynamic parameters having small negative values could shift to small positive values (Olu-Owolabi et al., 2012). The ΔH^o values showed that the adsorptions are endothermic (positive values), i.e. increase in temperature led to increase in sorption. Sorption of Cu(II) ions on LF and GSF soils and Cd(II) on GSF have indicated exothermic processes, and similar tendencies were observed in the experimental data.

Table 4.25. Thermodynamics parameters for Pb(II), Cu(II), and Cd(II) adsorptions.

		LF			JB			GSF			MA		
		Pb(II)	Cu(II)	Cd(II)	Pb(II)	Cu(II)	Cd(II)	Pb(II)	Cu(II)	Cd(II)	Pb(II)	Cu(II)	Cd(II)
ΔH^{o} (kJ mol^{-1})		86.6	-62.0	67.2	42.8	63.4	32.1	4.55	-29.8	-51.0	31.5	31.1	39.9
ΔS^{o} (kJ mol^{-1}K^{-1})		0.34	-0.18	0.26	0.15	0.22	0.16	0.04	-0.09	-0.11	0.12	0.11	0.19
ΔG^{o} (kJ mol^{-1})	300 K	-13.4	-9.11	-10.3	-3.38	-1.46	-16.8	-7.39	-3.71	-17.6	-4.86	-1.80	-17.2
	313 K	-18.4	-6.39	-14.1	-5.69	-4.72	-19.2	-7.93	-2.37	-15.8	-6.65	-3.45	-20.0

4.6.7 Competitive sorptions of Pb(II), Cu(II), and Cd(II) ions on untreated and treated soils

Distribution coefficients (K_d) of the competitive sorptions studies are shown in Figures 4.22 to 4.24, and Tables 4.26 to 4.28 for the various soils and incubation periods. It was observed that K_d values for the LF whole soil (Figure 4.22) were higher than other whole soils; this was attributed to the high OM content and CEC of the LF soil. Competition had the least effect on Pb(II) sorptions while the highest effect was on Cu(II) and Cd(II). The K_d values increased with time; however, depending on the solution concentration ratios there were both reductions and increments after 7 and 90 day periods.

Competitive sorption (at equal cation ratios) showed that K_d values for Pb(II) increased continuously while those of Cu(II) and Cd(II) increased in the first 7 days and then decreased afterwards. This increase was described as superficial because metal ions were easily desorbed resulting in the observed decrease in K_d values. This argument is line with the IPD model parameter *C* described above which showed that sorptions on these whole soils were mainly a surface phenomenon. These high K_d values or preference for Pb(II) ions implied that these soils had higher affinity towards Pb(II) ions.

Higher solution Cu(II) ratio in cocktail ratio *B* did not lead to higher Cu(II) K_d values but to reduction in Pb(II) and Cd(II) K_d values within a 7-day period. This implied that increased competition led to higher disorder in the soil solution system but with no concomitant rise in the sorption of the ion with higher concentration (Cu(II)) or higher sorption for the usually preferred cation (in this case Pb(II)). Hence, K_d for other metals increased with time while the preference for Pb(II) by these soils reduced with time.

Increasing Cd(II) concentration in cocktail ratio *C* led to increase in K_d values of Cu(II) and Cd(II) but a decrease for Pb(II) within the first 7 days. After a 90-day period, there was a 3-fold reduction in K_d values for Pb(II), 6-fold reduction for Cu(II), while no changed was observed for Cd(II). Increasing the ratio of solution Pb(II) in cocktail ratio D increased the Pb(II) K_d value only within the first 7 days while Cd(II) K_d values increased gradually with time. This could mean that the binding of Pb(II) ions has some kind of co-operative binding effect on Cd(II) ions and this is in agreement with the fitting of the non-competitive Cd(II) sorption data to the Freundlich adsorption isotherm implying sorption

on heterogeneous sites of unequal energies. However, the Cu(II) K_d values showed increase (7-folds) and decrease (14-folds) after the 7 and 90 day periods, respectively.

The sorption trends in the GSF whole and treated soils (OMR and IOR) were similar to those of MA and JB whole and treated soils (Figures 4.22 to 4.24, and Tables 4.26 to 4.28); this may not be unrelated to their similar physicochemical characteristics in terms of low clay, CEC, and OM contents of these soils. Hence, the explanation of the GSF whole and treated soils will suffice for these soils too. Comparing the K_d values of these cations for the JB, GSF and MA soils, it was observed that Pb(II) also had higher K_d values than Cu(II) and Cd(II) but in general, there was no significant increase in K_d values of these soils with time. In this study, competition was observed to be greater for Cd(II) than for Cu(II) and Pb(II); the sorption trend of the metal cations in all soils followed the same trend as in the single sorption: Pb(II) >Cu(II) >Cd(II). This trend was attributed to the fact that Cd(II) is basically retained in the soil by exchange reactions, while Cu(II) and Pb(II) form inner-sphere complexes with OM, Fe, Al and Mn oxides. Hence, in competitive adsorption, Cu(II) and Pb(II) maintain their strong affinity on the surface sites, while Cd(II) is displaced from the surface sorption sites. Similar trend has been reported by Lu and Xu (2009) for some Chinese soils.

The preference for Pb(II) over Cu(II) and Cd(II) is not new because it has been recognized that Pb(II) can compete effectively with Cu(II) or other cations for similar adsorption sites (Heidmann et al., 2005; Lu and Xu, 2009); however, the observed reduction in this preference with longer incubation time is interesting. The implication of this is that competition among metal ions in solution for similar adsorption sites tends to suppress the strength and magnitude of some other metals retention.

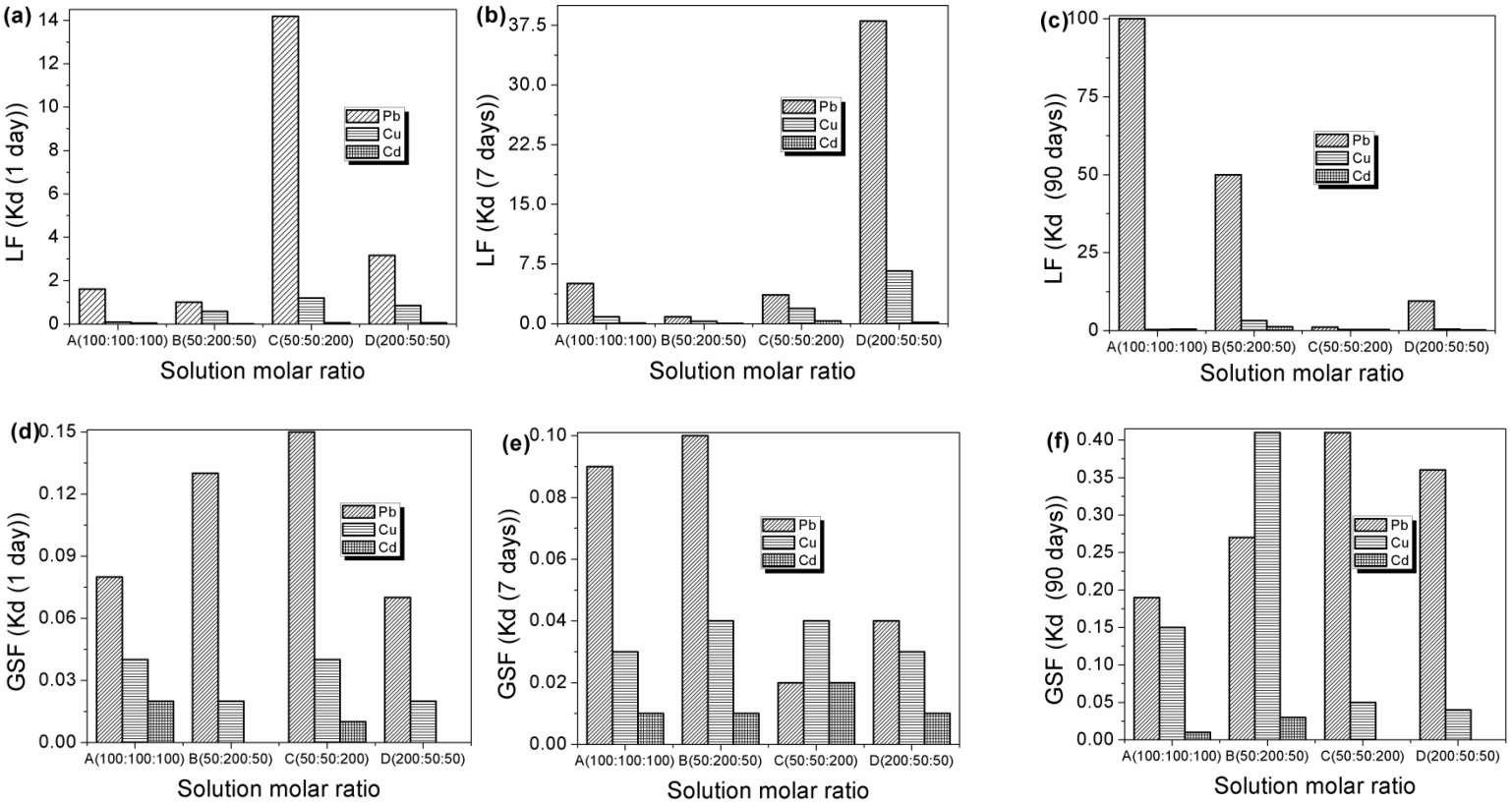

Figure 4.22. Distribution coefficients (K_d) for Pb(II), Cu(II), and Cd(II) ions on LF and GSF whole soils.

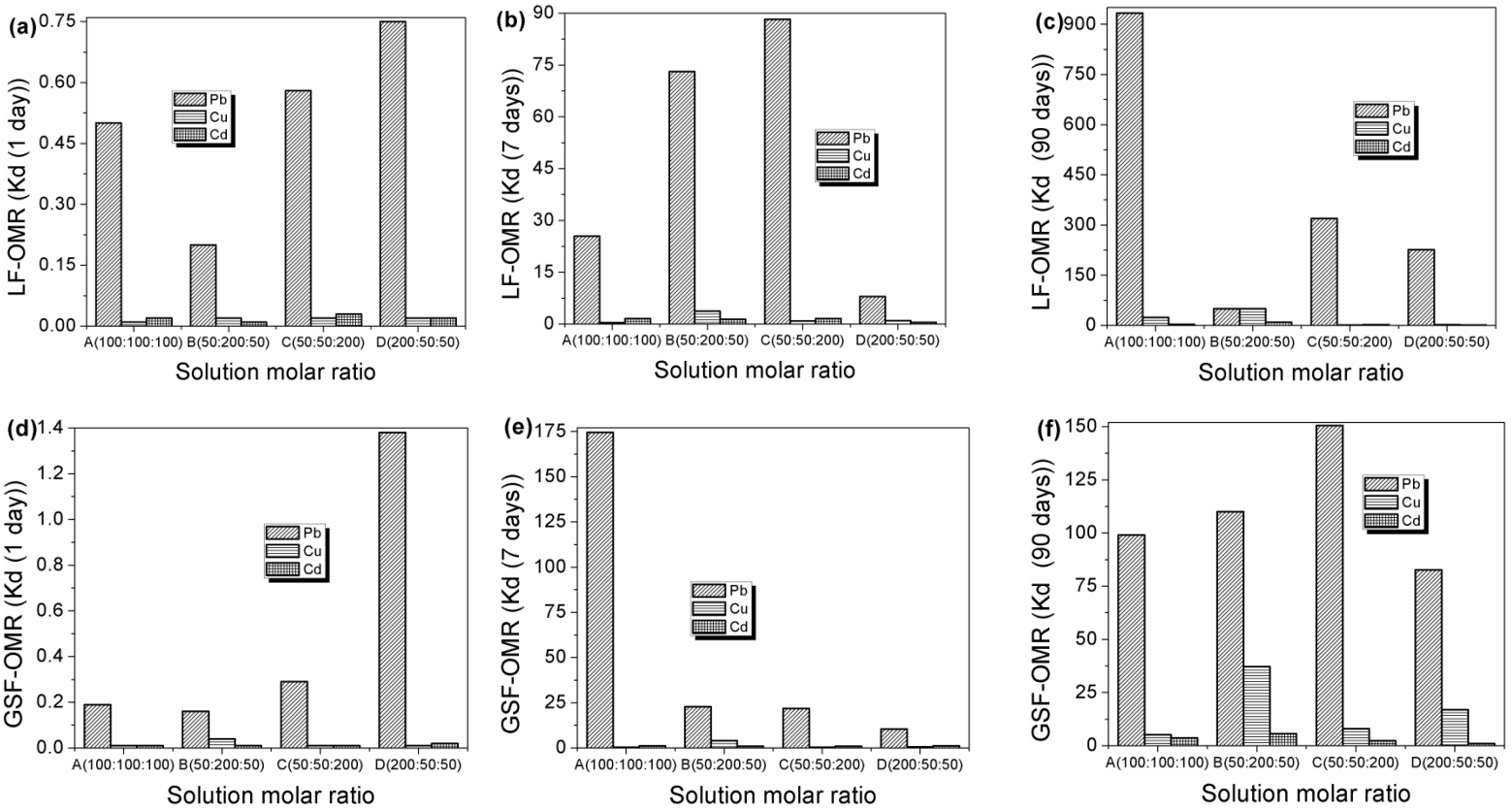

Figure 4.23. Distribution coefficients (K_d) for Pb(II), Cu(II), and Cd(II) ions on LF-OMR and GSF-OMR soils.

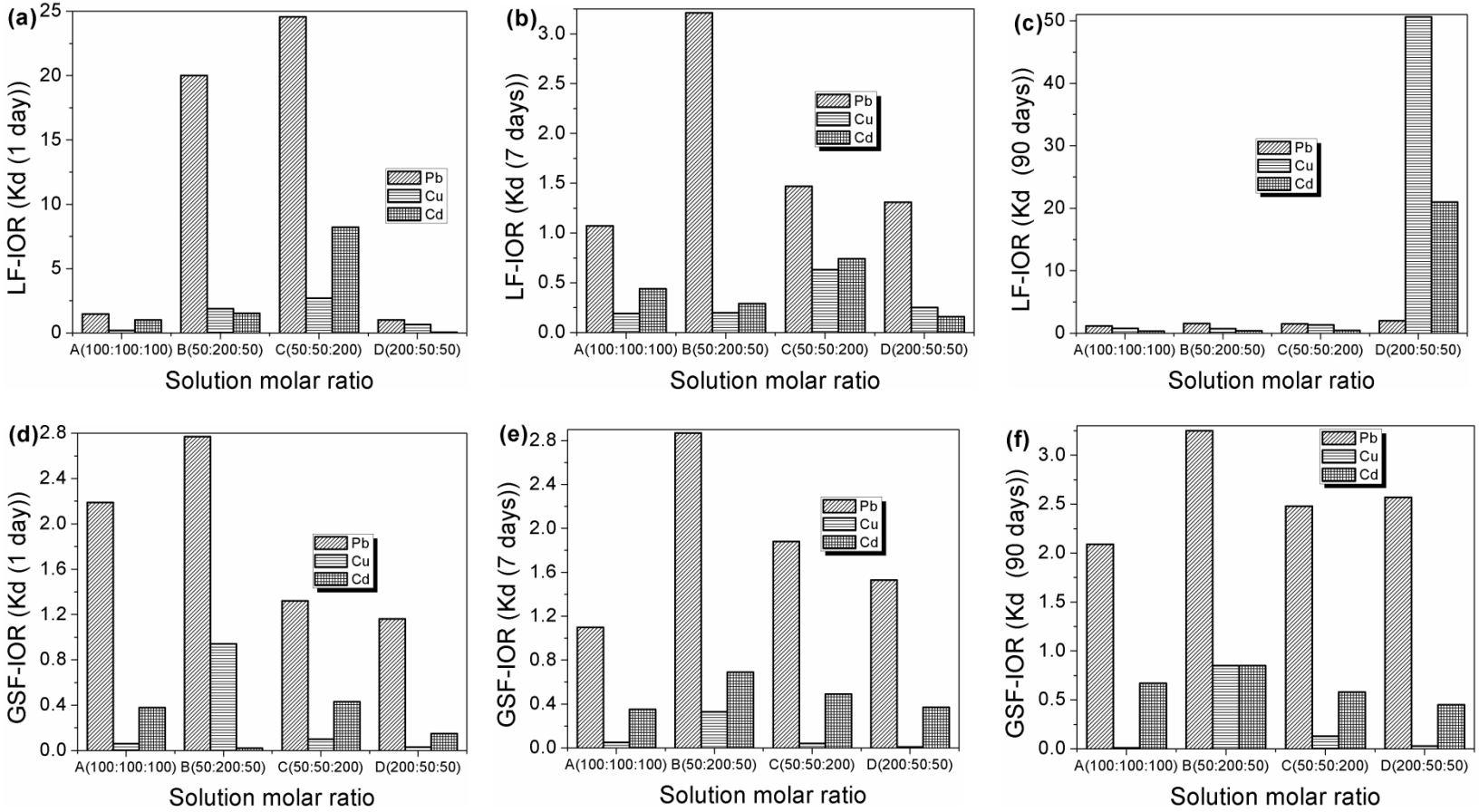

Figure 4.24. Distribution coefficients (K_d) for Pb(II), Cu(II), and Cd(II) ions on LF-IOR and GSF-IOR soils.

The K_d values obtained for competitive sorptions on the treated soils (Figures 4.23 and 4.24, and Tables 4.27 and 4.28) showed similar sorption trend as the whole soils (Pb(II) >Cu(II) >Cd(II)) irrespective of the solution cation ratio and incubation time. Removal of OM in the LF soil (LF-OMR) led to drastic reductions in K_d values (Figure 4.23 and Table 4.27) for all cations when compared to the whole soils (1-day incubation). The K_d values were, however, nearly 100 % higher than after 7 days of incubation, and over 1000 % after a 90-day incubation. The drastic reduction in cations sorption for 1-day incubation of the OMR soils implied that the sorptions on the OM components of the soils were nearly instantaneous, while the enhanced K_d values observed for the same soil samples after a 7 and 90-day incubations indicated that with longer incubation periods sorptions occurred on surfaces which: (i) have been masked by SOM and thus prevented sorption on the whole samples and (ii) become available with longer incubation in aqueous solution such as the expansive clays – montmorillonite and illite (Table 4.1d).

The removal of the iron oxides in the LF sample (LF-IOR) led to higher K_d values (Figure 4.24 and Table 4.28) in the 1 day incubations. These K_d values were higher than those observed in the whole soil after corresponding incubation periods; these high K_d values were regarded as superficial because longer incubation time led to lower K_d values. These superficial adsorptions may be related to the good fit of the adsorption data to the Freundlich adsorption isotherm observed in the non-competitive sorption. This superficial adsorption may easily be desorbed with time; and hence the lower K_d values with longer incubation.

The IOR soil samples with low OM contents (GSF, JB, and MA) showed no significant change in K_d values with time. This confirmed that apart from the OM components of these soils, the iron oxide components played significant roles in metals sorption.

Table 4.26. Competitive adsorption distribution coefficients (K_d) for the untreated JB and MA soils at the various molar concentrations of metals

Solution	K_d (1 day)			K_d (7 days)			K_d (90 days)		
molar ratio	Pb	Cu	Cd	Pb	Cu	Cd	Pb	Cu	Cd
JB A†	0.03	0.01	0.01	0.08	0.04	0.01	0.31	0.04	0.01
JB B‡	0.05	0.02	0.01	0.09	0.03	0.001	0.53	0.17	0.01
JB C§	0.09	0.03	0.01	0.13	0.04	0.02	0.08	0.03	0.001
JB D¶	0.06	0.02	0.01	0.08	0.04	0.01	0.04	0.01	0.001
MA A†	0.05	0.04	0.01	0.06	0.02	0.01	0.13	0.03	0.001
MA B‡	0.04	0.02	0.01	0.05	0.01	0.01	0.07	0.03	0.001
MA C§	0.08	0.02	0.01	0.08	0.07	0.01	0.20	0.13	0.01
MA D¶	0.06	0.07	0.01	0.08	0.04	0.01	0.25	0.08	0.001

†A= (1:1:1); ‡B= (1:4:1); §C= (1:1:4); ¶D= (4:1:1); and the figures in parenthesis represent Pb(II), Cu(II), and Cd(II), respectively.

Table 4.27. Competitive adsorption distribution coefficients (K_d) for the JB-OMR and MA-OMR soils at the various molar concentrations of metals

Conc.	OMR – 1 d			OMR - 7 d			OMR - 90 days		
Ratio	Pb	Cu	Cd	Pb	Cu	Cd	Pb	Cu	Cd
JB A†	0.07	0.01	0.03	5.40	1.38	0.93	27.0	4.61	0.97
JB B‡	0.09	0.02	0.03	3.14	1.62	0.83	75.9	132	3.48
JB C§	0.10	0.01	0.01	9.04	1.64	1.20	51.9	64.2	1.18
JB D¶	0.17	0.01	0.01	53.6	99.8	0.49	11.2	22.3	0.41
MA A†	0.03	0.01	0.01	2.08	0.68	0.72	3.39	1.45	0.28
MA B‡	0.02	0.02	0.01	1.30	0.93	0.22	1.61	1.08	0.09
MA C§	0.05	0.02	0.15	0.28	0.44	0.64	20.8	1.83	0.82
MA D¶	0.04	0.02	0.01	1.90	0.58	0.34	4.87	2.60	0.10

†A= (1:1:1); ‡B= (1:4:1); §C= (1:1:4); ¶D= (4:1:1); and the figures in parenthesis represent Pb(II), Cu(II), and Cd(II), respectively.

Table 4.28. Competitive adsorption distribution coefficients (K_d) for the JB-IOR and MA-IOR soils at the various molar concentrations of metals

Conc.	IOR – 1 d			IOR – 7 d			IOR – 90 d		
Ratio	Pb	Cu	Cd	Pb	Cu	Cd	Pb	Cu	Cd
JB A†	0.81	0.34	1.42	0.21	0.01	0.11	0.39	0.05	0.04
JB B‡	0.87	0.24	0.10	0.05	0.02	0.01	1.70	0.00	0.25
JB C§	0.52	0.10	0.23	0.47	0.02	0.05	0.97	0.07	0.07
JB D¶	0.57	0.24	0.06	0.24	0.01	0.01	0.55	0.03	0.00
MA A†	0.27	0.15	0.13	0.28	0.01	0.08	0.15	0.04	0.01
MA B‡	0.52	0.36	0.02	0.64	8.33	0.01	0.25	0.67	0.01
MA C§	0.67	0.27	1.85	0.63	0.06	0.10	0.33	0.15	0.01
MA D¶	0.34	0.08	0.03	0.53	0.23	0.01	0.14	0.35	0.01

†A= (1:1:1); ‡B= (1:4:1); §C= (1:1:4); ¶D= (4:1:1); and the figures in parenthesis represent Pb(II), Cu(II), and Cd(II), respectively.

CHAPTER FIVE

CONCLUSION

This study investigated the sorptions of two polycyclic aromatic hydrocarbons (pyrene and fluorene), one pesticide (pentachlorophenol) and three heavy metals (Pb(II), Cu(II), and Cd(II)) on soils obtained from different agro–ecological zones of Nigeria.

5.1 The soils

On the basis of the physical, chemical, and mineralogical analysis, the soils were neutral except for GSF and JB which were acidic. The CEC values were mainly low values. The percentages of soil organic matter were higher in soils obtained from the middle and southern parts of Nigeria but lower for soils of the north. Heavy and trace metal levels in the soils were lower than the ranges stipulated for soils by the World Health Organisation. Mineralogical compositions of the soils showed that quartz was the principal soil mineral, followed by the carbonate minerals (aragonite, calcite, and dolomite). The (oxyhydr)oxides minerals (gibbsite, goethite, and hematite) were also common minerals, while the 2:1 clay minerals (illite and montmorillonite) were found to be in LF, JB, MA, and MG.

5.2 Polycyclic aromatic hydrocarbons (Pyrene and fluorene) sorptions

Pyrene and fluorene sorptions on these soils attained equilibrium relatively (compared to literature reports) fast. Sorptions of pyrene and fluorene exhibited better fittings to the pseudo–second order kinetics model than the pseudo–first order kinetics. Intra–particle diffusion model suggested that the sorptions were partly surface adsorption and partly partitioning within soil phases.

It was found that increase in soil pH caused a reduction in the quantity of PAHs sorbed irrespective of the soils' properties.

PAHs sorptions on these soils were exothermic in nature and showed spontaneity usually accompanied by deceased entropy as the sorption proceeded towards equilibrium. Enthalpy values were compatible with energy strength associated with weak hydrophobic forces, such as the van der Waals and π–π interactions.

Soil organic matter contributed ≥50 % of the PAHs sorptions while iron oxides contributed ≤40 %. In general, removal of organic matter was found to lead to reduced PAHs sorptions, but removal of iron oxides had no significant effect on the sorption process. The higher the soil organic matter contents the higher the hysteresis.

Pyrene sorptions were higher than fluorene from both single and PAH mixed (binary) solutions. The amounts of PAHs sorbed and desorbed from mixed PAHs (binary) solutions were lower than those of single solutions. Increase in temperature favoured PAHs sorption from mixed solutions but not from single solutions.

PAHs sorption data from both the single and binary solutions fitted the distributed reactivity model better than the Langmuir and Freundlich adsorption models; implying a combination of several linear and non–linear Freundlich type isotherms.

5.2.1 Implications and environmental significance of PAHs sorption results

- ✓ The exothermic nature of these PAHs sorptions implied higher chances of environmental pollution at higher temperatures.
- ✓ The high desorption from soils with low organic matter content implied a risk of these PAHs being present in the soil water solution, and subsequent contamination of the aquifer.
- ✓ Depletion of soil components, such as the organic matter and iron oxides, may lead to increased risks of the PAHs in the environment.
- ✓ The risk of environmental contamination is higher for fluorene than pyrene.
- ✓ Hence, in the environment, these PAHs especially fluorene, is likely to reach the aquifer faster in the warmer and low organic matter soils of northern Nigeria than the cooler and relatively higher organic matter containing soils of the south.

5.3 Pentachlorophenol (PCP) sorption

PCP sorption equilibria were attained within 24 h. The sorptions data fitted the pseudo–second order kinetics model. The intra–particle diffusion kinetics model suggested that the PCP sorptions were partly surface adsorption and partly partitioning within the voids of the various soil components (clay minerals and organic matters). Removal of organic matter did not significantly affect the sorption equilibrium time but removal of iron oxides reduced sorption equilibrium time.

PCP sorptions were pH and temperature dependent; it reduced with increase in pH as well as temperature. Thermodynamic parameters suggested that the sorptions were all spontaneous and feasible, accompanied by decreased entropy. The sorptive forces associated with the sorption of PCP are weak forces of interactions such as the electrostatic and van der Waal's interactions. PCP sorption isotherms obeyed the Freundlich adsorption isotherm model suggesting sorption on heterogeneous sorption sites. The sorption trend is GSF > JB > LF ≥ AG > IB > MA > MG > PH; i.e. PCP sorptions were better favoured in soils with higher iron oxide contents.

Iron oxides content played significant roles in PCP sorptions than the organic matter content. Removal of iron oxides led to ≥85 % reduction in PCP sorptions. Removal of organic matter nearly had no effect on PCP sorptions on soils with low (< 5%) organic matter content but had significant effect on soils with high (> 5%) organic matter contents (reduced PCP sorptions by ≈50%).

5.3.1 Implications and environmental significance of PCP sorptions results

- ✓ The low sorption of PCP by most northern Nigeria soils with low organic matter contents implied a higher risk of PCP species being present in the soil water solution and subsequent contamination of the aquifer.
- ✓ The exothermic nature of PCP sorptions implied a higher chance of environmental PCP pollution at higher temperatures, especially in the northern parts of the country with warmer ambient temperature.
- ✓ Removal of any soil component, as experienced in soil erosion, will lead to increased risks of PCP pollution of environmental media. This consequence will be more severe on removal of soil iron oxides.

5.4 Pb(II), Cu(II), and Cd(II) sorptions and environmental significance of the results

The metals sorptions were fast and nearly completed in 60 min. The sorption data fitted the pseudo–first order kinetics. The mechanism of sorptions on these soils depended on the soil characteristics.

Metals sorptions are pH dependent and increased with pH. pH of optimum adsorptions for these metals were observed between 5.5 and 6.5.

Equilibrium adsorption data for Pb(II) and Cu(II) could be fitted to both Langmuir and Freundlich adsorption isotherms (suggesting the sorptions generally obeyed the *L*-type isotherm) while adsorption data for Cd(II) fit only the Freundlich isotherm.

The effect of temperature on metals adsorption was found to be dependent on the metal as well as the soil characteristics. Values of thermodynamic parameters of these metals showed that the adsorptions were feasible.

LF soil had higher K_d values (or adsorption capacities) for simultaneous adsorptions. The metals adsorptions sequence of both the single and competitive adsorptions was Pb(II) >Cu(II) >Cd(II). The effect of competition was greater for Cd than for Cu and Pb.

The metals distribution and redistribution patterns for untreated and treated soils showed that soil organic matter played significant role in the short time (less than 7 days) sorption of metals while iron oxides at longer times (within the 90-day period).

The high superficial adsorption capacity of some soils implied a risk of future environmental re-contamination because these metals become desorbed with time.

Irrespective of solution concentration, metals, such as Pb(II) and Cu(II), retained by inner-sphere complexes complexation are preferentially sorbed; however, there was reduction in this preference with time in the presence of high concentrations of metals not retained by this mechanism (such as Cd(II)).

Thus, time and competition among metal ions in solution for similar adsorption sites are vital parameters needed for prediction of the retention, redistribution, and bioavailability of metals in soils undergoing degradation of organic matter and iron oxides.

REFERENCES

Abdel Salam, M. and Burk, R.C. 2010. Thermodynamics and Kinetics Studies of Pentachlorophenol Adsorption from Aqueous Solutions by Multi-Walled Carbon Nanotubes. *Water, Air, and Soil Pollution* 210.1-4: 101–111.

Agbenin, J.O. 2010. Extractability and Transformation of Copper and Zinc Added to Tropical Savanna Soil under Long-Term Pasture. *Communications in Soil Science and Plant Analysis* 41.8: 1016–1027.

Agbenin, J.O. and Olojo, L.A. 2004. Competitive adsorption of copper and zinc by a Bt horizon of a savanna Alfisol as affected by pH and selective removal of hydrous oxides and organic matter. *Geoderma* 119: 85–95

Ali, I., Asim, M. and Khan, T.A. 2012. Low cost adsorbents for the removal of organic pollutants from wastewater. *Journal of Environmental. Management* 113: 170–83.

An, C., Huang, G., Yu, H., Wei, J., Chen, W. and Li, G. 2010. Effect of short-chain organic acids and pH on the behaviors of pyrene in soil-water system. *Chemosphere* 81.11: 1423–1429.

Arias, M., Barral, M.T., and Mejuto, J.C. 2002. Enhancement of copper and cadmium adsorption on kaolin by the presence of humic acids. *Chemosphere* 48: 1081–1088.

Arias-Estévez, M., López-Periago, E., Martínez-Carballo, E., Simal-Gándara, J., Mejuto, J.-C. and García-Río, L. 2008. The mobility and degradation of pesticides in soils and the pollution of groundwater resources. *Agriculture, Ecosystems and Environment* 123.4: 247–260.

ATSDR. 1995. Toxicological Profile for Polycyclic Aromatic Hydrocarbons (PAHs); Agency for Toxic Substances and Disease Registry, U.S. Department of Health and Human Services: Atlanta, GA.

Bailey, G. W., White, J. L. and Rothberg, T. 1968 Adsorption of organic herbicides by montmorillonite: role of pH and chemical character of adsorbate: *Soil Science Society of America Proceeding* 32: 222-234.

Barriuso, E., Houot, S., SerraWittling, C., 1997. Influence of compost addition to soil on the behaviour of herbicides. *Pesticide Science* 49: 65–75.

Benton. J.J. (Jr). 2001. *Laboratory Guide for Conducting Soil Tests and Plant Analysis*. CRC Press, New York.

Boivin, A., Cherrier, R., Perrin-Ganier, C., and Schiavon, M. 2004. Time effect on bentazone sorption and degradation in soil. Pesticide Management Science 60.8: 809–814.

Bouras, O., Bollinger, J–C., and Baudu, M. 2010. Effect of humic acids on pentachlorophenol sorption to cetyltrimethylammonium-modified, Fe- and Al-pillared montmorillonites." *Applied Clay Science* 50.1: 58–63.

Bouyarmane, H., El Asri, S., Rami, A., Roux, C., Mahly, M. A., Saoiabi, A., Coradin, T., and Laghzizil, A. 2010. Pyridine and phenol removal using natural and synthetic apatites as low cost sorbents: influence of porosity and surface interactions. *Journal of Hazardous Material.* 181.1–3: 736–41.

Bradl, H.B. 2004. Adsorption of heavy metal ionson soils and soils constituents. *Journal of Colloid and Interface Science*. 277: 1–18.

Brady, N.C. and Weil, R.R. 2008. *The Nature and Properties of Soils*. 14th Edition. Upper Saddle River, NJ: Prentice-Hall, Inc. 990p.

Breuning-Madsen, H. and Awadzi, T.W. 2005. Harmattan dust deposition and particle size in Ghana. *Catena* 63: 23–38.

Brindley, G.W., Bender, R. and Ray, S. 1963. Sorption of non-ionic aliphatic molecules from aqueous solutions on clay minerals. Clay Oragnic studies – VII. *Geochim. Cosmochim. Acta* 27: 1129–1137.

Brown R.B. 2003. *Soil Texture*. Fact Sheet SL-29. University of Florida, Institute of Food and Agricultural Sciences.

Brunauer S., Deming L.S., Deming W.E., Teller E. 1940. On a theory of the van der Waals adsorption of gases. *Journal of the American Chemical Society* 62: 1723-1732.

Brusseau, M.L., Jessup, R.E., Rao, P.S.C. 1991. Nonequilibrium sorption of organic chemicals: elucidation of rate-limiting processes. *Environmental Science and Technology* 25: 134–142.

Buol, S.W., Hole, F.D. and McCracken, R.J. 1973. *Soil Genesis and Classification*. First, Ames, IA: Iowa State University Press.

Carey P.L., McLaren R.G., and Adams J.A. 1996. Sorption of Cupric, dichromate and Arsenate ions in some New Zealand Soils. *Water, Air and Soil Pollution* 87: 189–203.

Carson, R. 1962. *Silent spring*. Greenwich, Connecticut, Fawcett Publications, Inc.

Celorie, J.A., Woods, S.L., Vinson, T.S., and Istok, J.D. 1989. A comparison of sorption equilibrium distribution coefficients using batch and centrifugation methods. *Journal of Environmental Quality* 18: 307–313.

Chilom, G., Kohl, S.D., and Rice, J.A. 2005. The Influence of Lipids on the Energetics of Uptake of Polycyclic Aromatic Hydrocarbons by Natural Organic Matter. *Journal of Environmental Quality* 34: 1055–1062.

Chiou, C.T., Peters, L.J. and V.H. Freed. 1979. A physical concept of soil-water equilibria for nonionic organic compounds. *Science* 206: 831–832.

Cline, M.G. 1949. Basic Principles of Soil Classification, *Soil Science* 67: 81-91.

Cottin, C.N. and Merlin, G. 2007. Study of pyrene biodegradation capacity in two types of solid media. *Science of the Total Environ*ment 380.1-3: 116-23.

Diagboya, P.N., Olu-Owolabi, B.I. and Adebowale, K.O. 2015. Synthesis of Covalently Bonded Graphene Oxide–Iron Magnetic Nanoparticles and its Kinetics of Mercury Removal. *RSC Advances* 5: 2536-2542.

Diagboya, P.N., Olu-Owolabi, B.I., Zhou, D. and Han, B-H., 2014. Graphene oxide–tripolyphosphate hybrid material: a potent sorbent for cationic dyes. *Carbon* 79: 174–182

Defew, L., Mair, J. and Guzman, H. 2005. An assessment of metal contamination in Mangrove sediments and leaves from Punta Mala Bay, Pacific Panama. *Marine Pollution Bulletin* 50: 547–552

Ding J.Y. and Wu, S.C. 1995. Partition coefficients of organochlorine pesticides on soil and on the dissolved organic matter in water. *Chemosphere* 30:v2259-2266.

Du, C., Linker, R., and Shaviv, A. 2008. Identification of agricultural Mediterranean soils using mid-infrared photoacoustic spectroscopy. *Geoderma* 143:v85–90.

Eisler, R. 1989. Pentachlorophenol hazards to fish, wildlife, and invertebrates: a synoptic review. *Contaminant Hazard Reviews*. Report No. 17.

EPA. 1980. Ambient water quality criteria for pentachlorophenol. U.S. Environ. Protection Agency Rep. 440/5–80–065. 89 pp.

Fagbami, A.A. 1993. Soil as a factor of crop production. In *Fundamentals of Agriculture.* Edited by E.A. Aiyelari, E.O. Lucas, M.O. Abatan, O.A. Akinboade. Afri–link Books (Ibadan).

Fagbami, A.A. and Shogunle, E.A.A. 1995. Nigeria: Reference soil of the moist lowlands near Ife (Oshun state). Soil Brief Nigeria 3. University of Ibadan, and International Soil Reference and Information Centre, Wageningen. Pp 3.

Fairbanks, B.C. and G.A. O'Connor. 1984. Effect of sewage sludge on the adsorption of PCBs by three New Mexico soils. *Journal of Environmental Quality* 13: 297-300.

Fisher, B. 1991. Pentachlorophenol: Toxicology and Environmental Fate. *Journal of pesticide reform* 11.1: 2–5.

Freundlich, H.M.F. 1906. Über die adsorption in lösungen. *Zeitschrift für Physikalische Chemie* 57A: 385-470.

Gauthier, T.D., Seitz, W.R. and Grant, C.L. 1987. Effects of structural and compositional variations of dissolved humic materials on pyrene Koc values. *Environmental Science and Technology* 21: 243-248.

Giessing, A.M.B., Mayer, L.M., and Forbes, T.L. 2003. Synchronous fluorescence spectrometry of 1-hydroxypyrene: a rapid screening method for identification of PAH exposure in tissue from marine polychaetes. *Marine Environmental Research* 56.5: 599-615.

Giles, C.H., MacEwan, T.H., Nakhwa, S.N.; Smith, D. 1960. Studies in Adsorption. Part XI. A system of classification of solution adsorption isotherms and its use in diagnosis of adsorption mechanisms and in measurement of specific surface areas of solids. J. Soc. Dyers Colourists, 74: 3973–3993.

Gomes, P.C., Fontes, M.P.F., Da Silva, A.G., Mendonc¸, E.S., and Netto. A.R. 2001. Selectivity Sequence and Competitive Adsorption of Heavy Metals by Brazilian Soils. *Soil Science Society of America Journal* 65: 1115–1121.

Greaney, K.M. 2005. An Assessment of Heavy Metal Contamination in the Marine Sediments of Las Perlas Archipelago, Gulf Of Panama. M.Sc dissertation submitted to the School of Life Sciences Heriot-Watt University, Edinburgh (unpublished)

Grover, R. and Hance, R.J. 1970. Effect of ratio of soil to water on adsorption of linuron and atrazine. *Soil Science* 109: 136-138.

Guo, X. , Luo, L., Ma, Y., and Zhang, S. 2010. Sorption of polycyclic aromatic hydrocarbons on particulate organic matters. *Journal of Hazardous Materials* 173.1-3: 130-6.

Gupta, S. S., and Bhattacharyya, K. G. 2006. Adsorptions of Ni (II) on Clays. *Journal of Colloid and Interface Science* 295:21.

Guzman, H. and Garcia, E. 2002. Mercury levels in coral reefs along the Caribbean Coast of Central America. *Marine Pollution Bulletin* 44: 1415-1420.

Guzman, H. and Jarvis, K. 1996. Vanadium Century Record from Caribbean Reef Corals: A Tracer of Oil Pollution in Panama. *AMBIO, A Journal of the Human Environment* 25.8: 523-526.

Guzman, H. and Jimemez, C. 1992. Contamination of coral reefs by heavy metals along the Caribbean coast of Central America. *Marine Pollution Bulletin* 24.11: 554-561.

Haftka, J. J. H., Govers, H. A. J., Parsons, J. R. 2010. Influence of temperature and origin of dissolved organic matter on the partitioning behavior of polycyclic aromatic hydrocarbons. *Environ Sci Pollut Res* 17:1070 – 1079.

Hamdi, H., Benzarti, S., Manusadzianas, L., Aoyama, I., and Jedidi, N. 2007. Bioaugmentation and biostimulation effects on PAH dissipation and soil ecotoxicity under controlled conditions. *Soil Biology and Biochemistry* 39:1926–1935.

Hance, R.J. 1967. The speed of attainment of sorption equilibria in some systems involving herbicides. *Weed Research* 7:29-36.

Hance, R.J. 1969. Influence of pH, exchangeable cation and the presence of organic matter on the adsorption of some herbicides by montmorillonite *Canadian Journal of Soil Science* 49.3: 357 -364.

He Y., Yediler A., Sun T., Kettrup A. 1995. Adsorption of fluoranthene on soil and lava: effects of the organic carbon contents and temperature. *Chemosphere* 30.1: 141-150.

He, Y., Xu, J., Wang, H., Zhang, Q. and Muhammad, A. 2006. Potential contributions of clay minerals and organic matter to pentachlorophenol retention in soils. *Chemosphere* 65.3: 497-505.

Hecht, S.S. 2003. Tobacco carcinogens, their biomarkers and tobacco-induced cancer. *Nature Reviews Cancer* 3: 733–744.

Heidmann, I., Christl, I., Leu, C., and Kretzschmar, R. 2005. Competitive sorption of protons and metal cations onto kaolinite: experiments and modeling. *Journal of Colloid Interface Science* 282: 270–282.

Hejazi, S.R., Yadolahi, J., Shahverdi, M., and Malakootikhah, J. 2011. Identifying Nanotechnology-Based Entrepreneurial Opportunities in Line with water-related Problems. *Middle–East Journal of Scientific Research* 8:337–348.

Hong, Y.S., Kim, Y.M., and Lee, K.E. 2012. Methylmercury exposure and health effects. *Journal of Preventive Medicine and Public Health* 45.6: 353-63.

Huang, J., Deng, R., and Huang, K. 2011. Equilibria and kinetics of phenol adsorption on a toluene-modified hyper-cross-linked poly(styrene-co-divinylbenzene) resin. *Chemical Engineering Journal* 171.3: 951-957.

Huang, W., Peng, P., Yu, Z., and Fu, J. 2003. Effects of organic matter heterogeneity on sorption and desorption of organic contaminants by soils and sediments. *Applied Geochemistry* 18.7: 955-972.

Iglesias, A., Lopez, R., Gondar, D., Antelo, J., Fiol, S., and Arce, F. 2010. Adsorption of paraquat on goethite and humic acid-coated goethite. *Journal of Hazardous Materials* 183.1-3: 664-668.

Javier Rivas, F., Garcia de la Calle, R., Alvarez, P., and Acedo, B. 2008. Polycyclic aromatic hydrocarbons sorption on soils: some anomalous isotherms. *Journal of Hazardous Materials* 158.2-3: 375-383.

Kang, R.H., Wang, Y.S., Yang, H.M., Li, G.R., Tan, X., Xue, J.H., Zhang, J.Q., Yuan, Y.K., Shi, L.F. and Xiao, X.L. 2010. Rapid simultaneous analysis of 1-hydroxypyrene, 2-hydroxyfluorene, 9-hydroxyphenanthrene, 1- and 2-naphthol in

urine by first derivative synchronous fluorescence spectrometry using Tween-20 as a sensitizer. *Anal Chim Acta* 658.2: 180-186.

Karickhoff, S.W. 1980. in Contaminants and Sediments: Analysis, Chemistry, and Biology, edited by R. A. Baker. Ann Arbor Science, Ann Arbor, MI, 2:193–205.

Karickhoff, S.W., Brown, D.S. and Scott, T.A. 1979. Sorption of hydrophobic pollutants on natural sediments. *Water Research* 13: 241-248.

Khadhar, S., Higashi, T., Hamdi, H., Matsuyama, S., and Charef, A. 2010. Distribution of 16 EPA-priority polycyclic aromatic hydrocarbons (PAHs) in sludges collected from nine Tunisian wastewater treatment plants. *Journal of Hazardous Materials* 183:98–102.

Kipling, J.J. 1965. Adsorption from Solution of Non-Electrolytes~Academic, London.

Kohl, S.D. and Rice, J.A. 1999. Contribution of lipids to the nonlinear sorption of polycyclic aromatic hydrocarbons to soil organic matter. *Organic Geochemistry* 30: 929–936.

Koskinen, W.C., Anhalt, J.A., Sakaliene, O., Rice, P.J., Moorman, T.B., and Arthur, E.L. 2003. Sorption–desorption of two ‘‘aged’’ sulfonylami-nocarbonyltriazolinone herbicide metabolites in soil. *Journal of Agricultiral and Food Chemistry* 51: 3604–3608.

Kristensen, G.B., Johannesen, H., Aamand, J. 2001. Mineralization of aged atrazine and mecoprop in soil and aquifer chalk. *Chemosphere* 45: 927–934.

Lagergren S. 1898. Zur theorie der sogenannten adsorption gelöster stoffe. Kungliga Svenska Vetenskapsakademiens. *Handlingar* 24.4:1–39.

Lamoureux, E.M., and Brownawell, B.J. 1999. Chemical and bio-logical availability of sediment-sorbed hydrophobic organic contaminants. *Environmental Toxicology Chemistry* 18: 1733–1741.

Langmuir, I., 1916. The constitution and fundamental properties of solids and liquids. *Journal of the American Chemical Society* 38.11: 2221–2295.

Li, R., Wen, B., Zhang, S., Pei, Z., and Shan, X. 2009. Influence of organic amendments on the sorption of pentachlorophenol on soils. *Journal of Environmental Sciences* 21.4:474–480.

Liu, L.C.; Cibes-Viadé, H.; and Koo, F.K.S. 1970. Adsorption of ametryne and diuron by soils. *Weed Science* 18.4: 470–474.

Liu, Y., Chen, L., Huang, Q., Lib, W., Tang, Y., and Zhao, J. 2009. Source apportionment of polycyclic aromatic hydrocarbons (PAHs) in surface sediments of the Huangpu River, Shanghai, China. *Science of the Total Environment* 407: 2931–2938.

Low, M.J.D. 1960. Kinetics of chemisorption of gases on solids. *Chemical Reviews* 60:267–312

Lu, A., Zhang, S., and Shan, X–Q. 2005. Time effect on the fractionation of heavy metals in soils. *Geoderma* 125.3-4:225–234.

Lu, S. G. and Xu Q. F. 2009. Competitive adsorption of Cd, Cu, Pb and Zn by different soils of Eastern China. *Environmetal Geology* 57:685–693.

Lueking, A.D., Huang, W., Soderstrom-Schwarz, S., Kim, M., and Weber Jr., W.J. 2000. The chemical structure of soil/sedi-ment organic matter and its role in the sequestration and bioavailability of sorbed organic contaminants. *Journal of Environmental Quality* 29: 317–323.

McBride, M. B. and Bouldin, D. R. 1984. Long-term reactions of Copper (II) in a contaminated calcareous soil. *Soil Science Society of America Journal* 43: 56-59

McCarthy, J.F. and Jimenez, B.D. 1985. Interactions between polycyclic aromatic hydrocarbons and dissolved humic material: Binding and dissociation. *Environmental Science and Technology* 19: 1072-1076.

McCarty D.F. 2002. Essentials of Soil Mechanics and Foundations. 6th ed. Prentice Hall, NJ.

McKeague, J.A. ed. 1978. Manual on Soil Sampling and Methods of Analysis 2nd Edition. Can. Sot. of Soil Sci. Suite 907, 151 Slater St., Ottawa, Ont.

Mclaren, R.G. and Crawford, D.V. 1973. Studies on Soil Copper. *Soil Science* 24:443-452.

McLean, J.E., and Bledsoe B.E. 1992. Behaviour of Metals in Soils in ground water issue: EPA/540/S-92/018. U. S. EPA Robert S. Kerr Environ. Res. Laboratory, Ada, OK. pp. 1-20.

Meeker, G.P., Lowers, H.A., Swayze, G.A., Van Gosen, B.S., Sutley, S.J., and Brownfield, I.K. 2006. Mineralogy and morphology of amphiboles observed in

soils and rocks in El Dorado Hills, California: December 2006, U.S. Geological Survey Open-File Report 2006–1362, 47p.

Miles, J.R.W., Bowman, B.T. and Harris, E.R. 1981. Adsorption, Desorption, Soil Mobility and Aqueous Persistence of Fensulfothion and Its Sulfide and Sulfone Metabolites. *Journal of Environmental Science and Health* B16.3: 309-324.

Mittal, A., Gajbe, V. and Mittal, J. 2008. Removal and recovery of hazardous triphenylmethane dye, Methyl Violet through adsorption over granulated waste materials. *Journal of Hazardous Materials* 150.2:364–375.

Mockovciakova, A., Orolinova, Z., and Skvarla, J. 2010. Enhancement of the bentonite sorption properties. *Journal of Hazardous Materials* 180.1-3:274-81.

Nam, K., Alexander, M., 1998. Role of nanoporosity and hydrophobicity in sequestration and bioavailability: tests with model solids. *Environmental Science Technology* 32: 71–74

Olu-Owolabi, B.I., Adebowale, K.O., and Oseni, O.T. 2010. Physicochemical and thermodynamic adsorption studies of a ferric luvisol soil in Western Nigeria. *Soil and Sediment Contamination. An International Journal* 19.1:119-131.

Olu-Owolabi, B.I., Diagboya, P.N., and Ebaddan, W.C. 2012. Mechanism of Pb^{2+} removal from aqueous solution using a nonliving moss biomass. *Chemical Engineering Journal* 195–196: 270–275.

Oren, A., Aizenshtat, Z., and Chefetz, B. 2006. Persistent organic pollutants and sedimentary organic matter properties: A case study in the Kishon River, Israel. *Environmental Pollution* 141: 265–274.

Podoll, R.T., Irwin, K.C., and Parish, H.J. 1989. Dynamic studies of naphthalene sorption on soil from aqueous solution. *Chemosphere* 18: 2399-2412.

Pu, X. and Cutright, T.J. 2006. Sorption-desorption behavior of PCP on soil organic matter and clay minerals. *Chemosphere* 64.6: 972–83.

Puls, R.W., Powel, R. M., Clark, D. and Eldred, C.J. 1991. Effect of pH, solid/solution ratio, Ionic strength and organic acids on Pb and Cd adsorption on Kaolinite. *Water, air and soil pollution*. 57-58:423-430

Ramirez, N., Cutright, T., Ju, L-K. 2001. Pyrene biodegradation in aqueous solutions and soil slurries by Mycobacterium PYR-1 and enriched consortium. *Chemosphere* 44: 1079–1086.

Rao, B., Anderson, T.A., Orris, G.J., Rainwater, K.A., Rajagopalan, S., Sandvig, R.M., Scanlon, B.R., Stonestrom, D.A., Walvoord, M.A., and Jackson, W.A. 2007. Widespread Natural Perchlorate in Unsaturated Zones of the Southwest United States. *Environmental Science Technology* 41: 4522–4528.

Schellenberg, K., Leuenberger, C., Schwarzenbach, R.P. 1984 Sorption of chlorinated phenols by natural sediments and aquifer materials. *Environmetal Science Technology* 18.18:652–657.

Serrano, S., Garrido, F., Campbell, C.G., and Garcia-Gonzalez, M.T. 2005. Competitive sorption of cadmium and lead in acid soils of Central Spain. *Geoderma* 124:91–104

Sha'ato, H.R. 1996. Physico-chemical and thermodynamic studies of some soils of the lower Benue valley of Nigeria. Ph.D Thesis, University of Ibadan, Ibadan (Unpublished).

Sharer, M., Park, J.H., Voice, T.C., and Boyd, S.A. 2003. Aging effects on the sorption–desorption characteristics of anthropogenic organic com-pounds in soil. *Journal of Environmental Quality* 32: 1385–1392.

Shin, S.R. and Han, A.L. 2012. Improved chronic fatigue symptoms after removal of mercury in patient with increased mercury concentration in hair toxic mineral assay: a case. *Korean Journal of Family Medicine* 33.5: 320–325.

Shu, Y., Li, L., Zhang, Q., and Wu, H. 2010. Equilibrium, kinetics and thermodynamic studies for sorption of chlorobenzenes on CTMAB modified bentonite and kaolinite. *Journal of Hazardous Materials* 173.1-3:47–53.

Shuman, L.M. 1991. Chemical forms of micro-nutrient in soils. *Soil Soc. Amer.* Bookseries#4. Inc. Madison, WI

Site, A.D. 2001. Factors Affecting Sorption of Organic Compounds in Natural Sorbent/Water Systems and Sorption Coefficients for Selected Pollutants. A Review. *Journal of Physical and Chemical Reference Data* 30.1:187–439.

Smyth, A.J. and Montgomery, R.F. 1962. Soils and Land Use in Central Western Nigeria. The Government of Western Nigeria Printers, Ibadan, pp 265.

Soil Survey Staff. 2006. *Keys to Soil Taxonomy*. United States Department of Agriculture, Natural Resources Conservation Service. 10th Edition.

Sparks, D. L. 2003. *Environmental Soil Chemistry*, 2nd ed. San Deigo, CA: Academic Press. Pp 45–46.

Sposito, G. *The Chemistry of Soils,* 2nd ed. New York, NY: Oxford University Press, 2008.

Sposito, G. *The Surface Chemistry of Natural Particles*. New York, NY: Oxford University Press, 2004.

Stevenson, F.J. 1991. Organic matter micronutrient reaction in soil. Soil Sci. Amer. Book Series #4. Inc, Madison, WI Processes, Soil Science Society of America, Madison, WI, pp. 1–18.

Stucki, J.W. 2012. Soil mineralogy. In Handbook of soil sciences properties and processes. Second edition. Edited by Pan Ming Huang, Yuncong Li, Malcolm E. Summer. CRC Press Taylor and Francis group, Boca Raton, Fl, USA.

Sun, X., Huang, X. Liao, X.P. and Shi, B. 2011. Adsorptive removal of Cu(II) from aqueous solutions using collagen-tannin resin. *Journal of Hazardous Materials* 186.2-3:1058–1063.

Swauger, J.E, Steichen, T.J, Murphy P.A, Kinsler, S. 2002. An analysis of the mainstream smoke chemistry of samples of the U.S. cigarette market acquired between 1995 and 2000. *Regulatory Toxicology Pharmacology* 35:142–156.

Taylor, S.A. and Ashcroft, G.L. 1972. *Physical edaphology: the physics of irrigated and non-irrigated soils.* W.H. Freeman, San Francisco.

Teixeira, S.C.G., Marques, M.R.D.C., Canela, M.C., Ziolli, R.L., and Perez, D.V. 2009. Study of Pyrene Adsorption on Brazilian Soils. *Revista de Chimie (Bucuresti)* 60.6:583–587.

Teixeira, S.C.G., Ziolli, R.L., Marques, M.R.D.C., and Perez, D.V. 2011. Study of Pyrene Adsorption on Two Brazilian Soils. *Water, Air, Soil Pollution* 219:297–301.

ten Hulscher, Th.E.M. and Cornelissen, G. 1996. Effect of temperature on sorption equilibrium and sorption kinetics of organic of organic micropollutants – A Review. *Chemosphere* 32.4:609-626

Thapa, G.B. and Weber, K.E. 1991. Soil erosion in developing countries: a politicoeconomic explanation. *Environmental Management* 15: 461-473.

Thompson, A., and Goyne, K. W. 2012. Introduction to the Sorption of Chemical Constituents in Soils. *Nature Education Knowledge* 4.4: 7.

UNESCO (United Nations Educational, Scientific and Cultural Organization). 1974. FAO/UNESCO Soil map of the world, 1:5,000,000 Vol. 1 Paris: UNESCO.

Unuabonah, E.I., Adebowale, K.O., Olu-Owolabi, B.I., Yang L.Z., and Kong, L.X. 2008. Adsorption of Pb(II) and Cd(II) from aqueous solutions onto sodium tetraborate-modified Kaolinite clay: Equilibrium and thermodynamic studies. *Hydrometallurgy* 93.1-2: 1-9.

USDA. 1978. Soil Taxonomy. Agriculture Handbook no. 436. Washington D.C.: USDA, Soil Conservation Service.

Usman, A. R. 2008. The relative adsorption selectivities of Pb, Cu, Zn, Cd and Ni by soils developed on shale in New Valley, Egypt. *Geoderma* 144:334–343.

Viraraghavan, T. and Slough, K. 1999. Sorption of Pentachlorophenol on Peat-Bentonite mixtures. *Chemosphere* 39.9:1487–1496.

Walkley, A. and Black, I.A. 1934. An examination of the Degtjareff method for soil organic matter and a proposed modification of the chromic acid titration method. *Soil Science* 37:29–38.

Wang, X., Li, Y., and Dong, D. 2008. Sorption of pentachlorophenol on surficial sediments: the roles of metal oxides and organic materials with co-existed copper present. *Chemosphere* 73.1: 1-6.

Weber Jr., W.J., McGinley, P.M., and Katz, L.E. 1992. A distributed reactivity model for sorption by soils and sediments: 1. Conceptual basis and equilibrium assessments. *Environmental Science and Technology* 26: 1955–1962.

Weber, J. B. 1970. Adsorption of s-triazines by montmorillonite as a function of pH and molecular structure. *Soil Science Society of America Proceeding* 34: 401–404.

Weber, W.J., and Morris, J.C. 1963. Kinetics of adsorption on carbon from solutions. *Journal of Sanitary Engineering Division. American Society of Civil Engineers* 89: 31–60.

Westin, F.C., and Brito De, J.G. 1969. Phosphorus fraction of some Venezuelan soils as related to their stage of weathering. *Soil Science* 107: 194–202.

Wijayaratne R.D. and Means J.C. 1984. Adsorption of polycyclic aromatic hydrocarbons by natural estuarine colloids. *Marine Environmental Research* 11: 77-89.

Yim, M.W. and Tam, N.F.Y. 1999. Effects of Wastewater-borne Heavy Metals on Mangrove Plants and Soil Microbial Activities. *Marine Pollution Bulletin* 39.1-12: 179-186.

Yuen, Q.H. and Hilton, H.W. 1962. Soil Adsorption of Herbicides, the Adsorption of Monuron and Diuron by Hawaiian Sugarcane Soils. *Journal of Agriculture and Food Chemistry* 10: 386–392.

Zeledon-Toruno, Z.C., Lao-Luque, C., de Las Heras, F.X., and Sole-Sardans, M. 2007. Removal of PAHs from water using an immature coal (leonardite). *Chemosphere* 67.3: 505–512.

APPENDICES

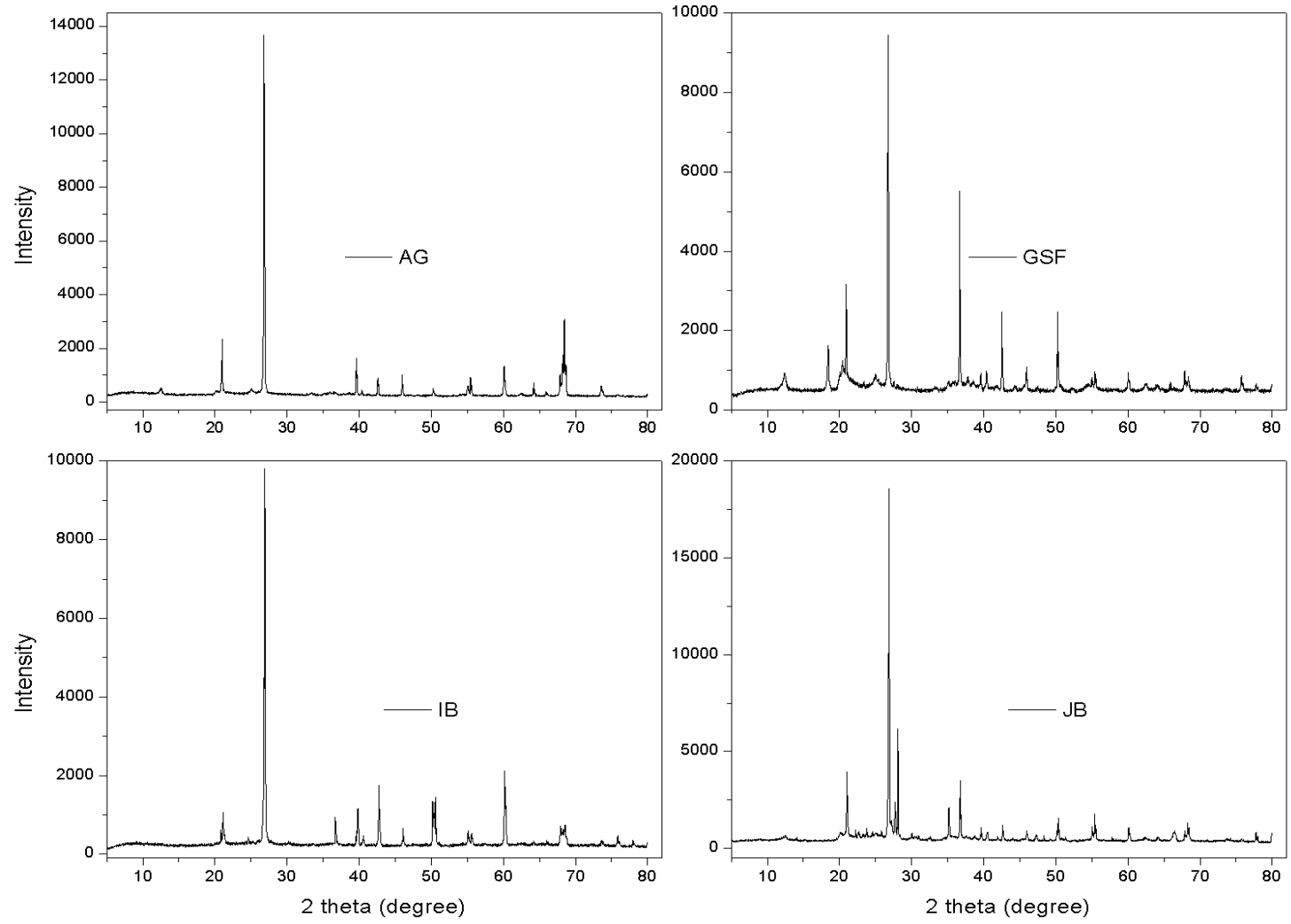

Figure A1. XRD spectra of AG, GSF, IB, and JB soils

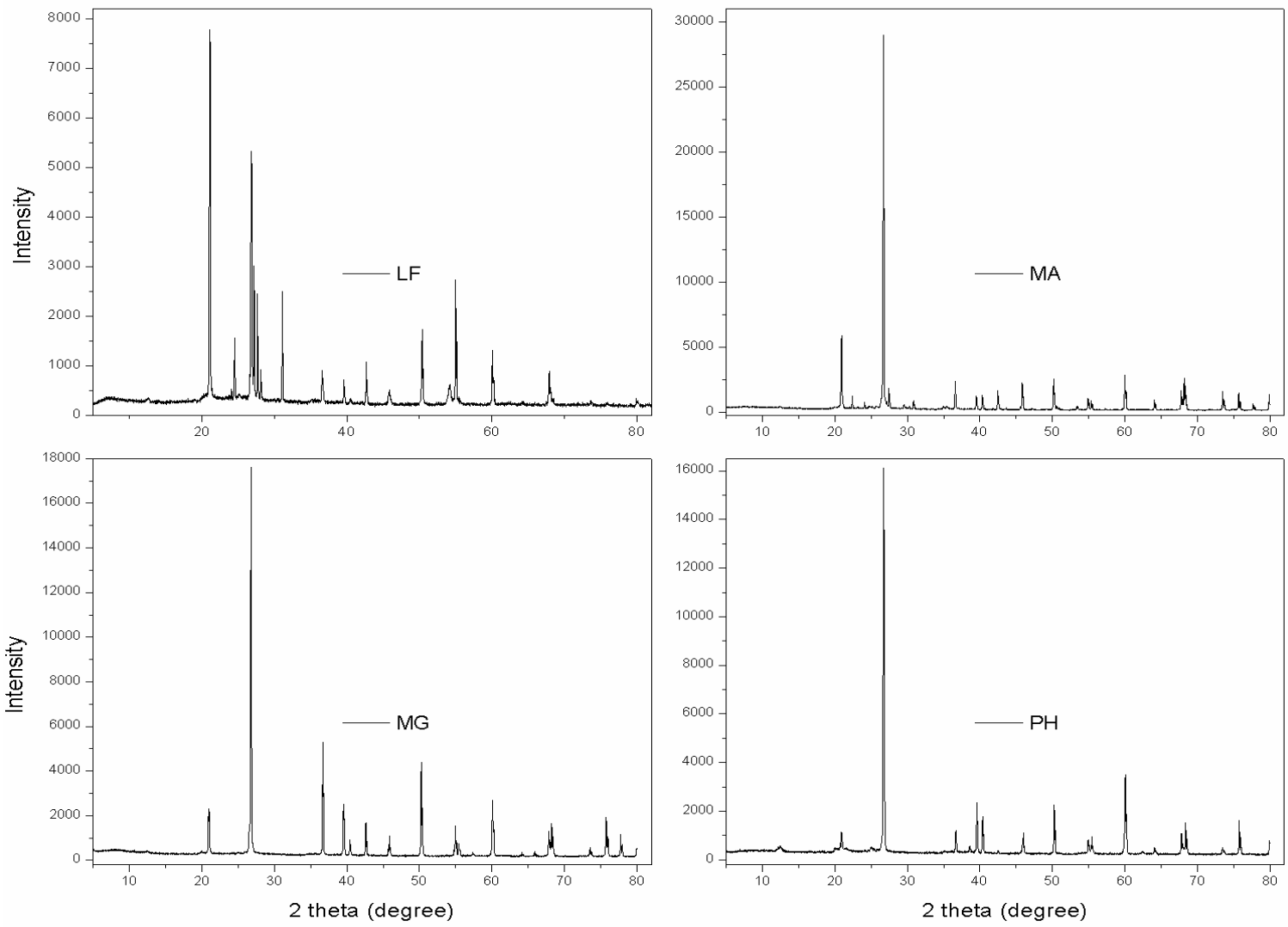

Figure A2. XRD spectra of LF, MA, MG, and PH soils

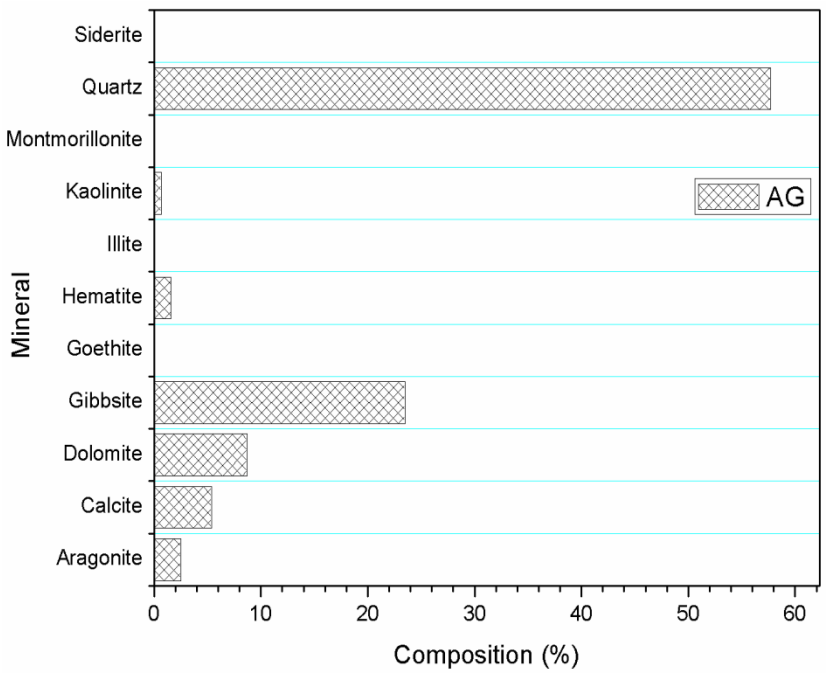

Figure A3. Percentage composition of minerals in AG soil

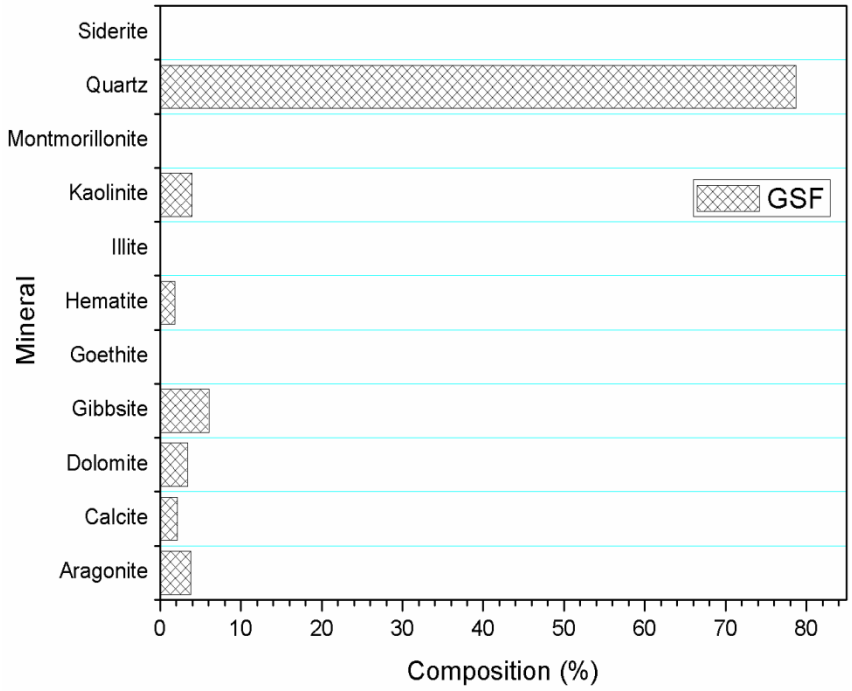

Figure A4. Percentage composition of minerals in GSF soil

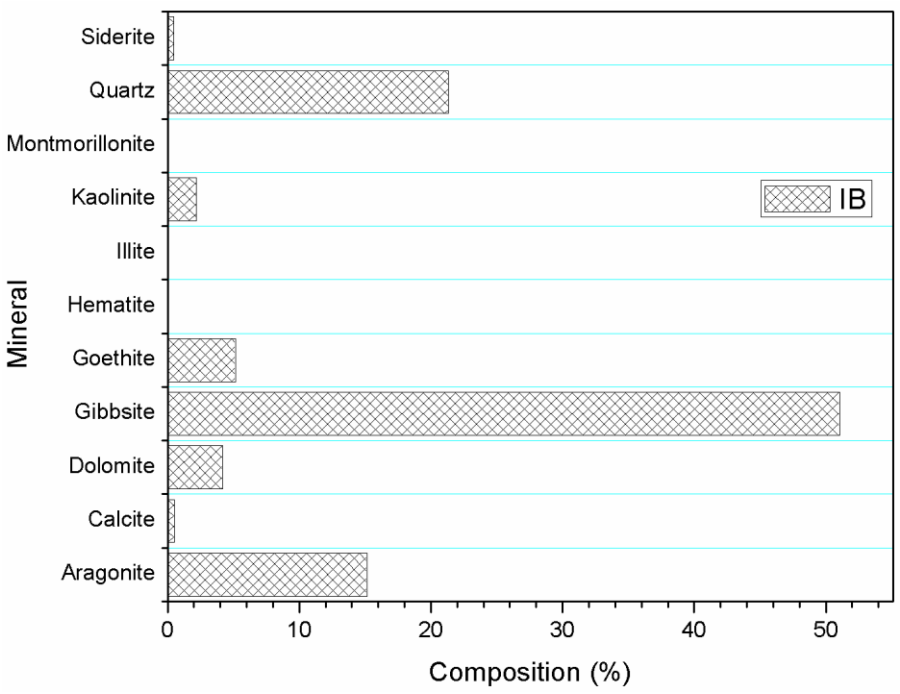

Figure A5. Percentage composition of minerals in IB soil

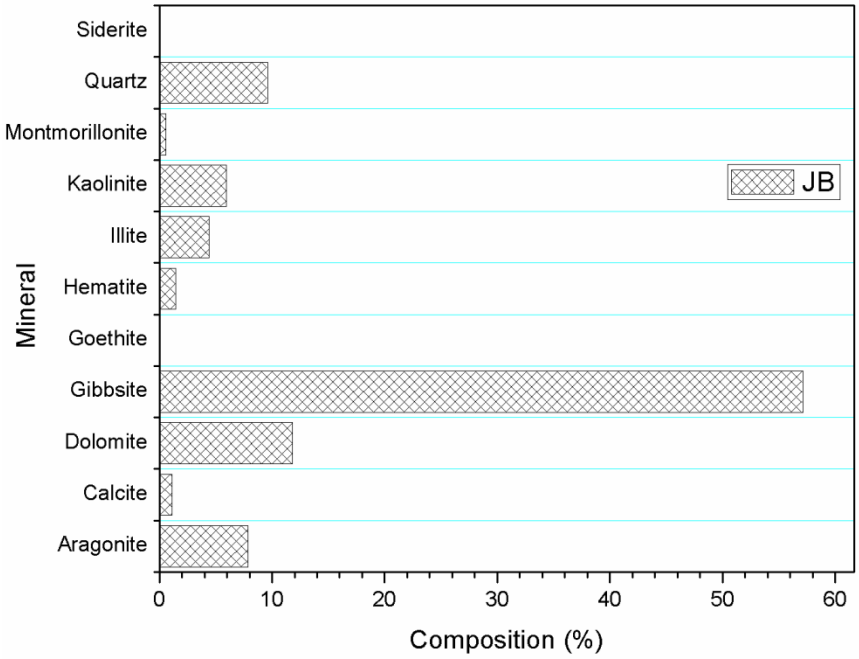

Figure A6. Percentage composition of minerals in JB soil

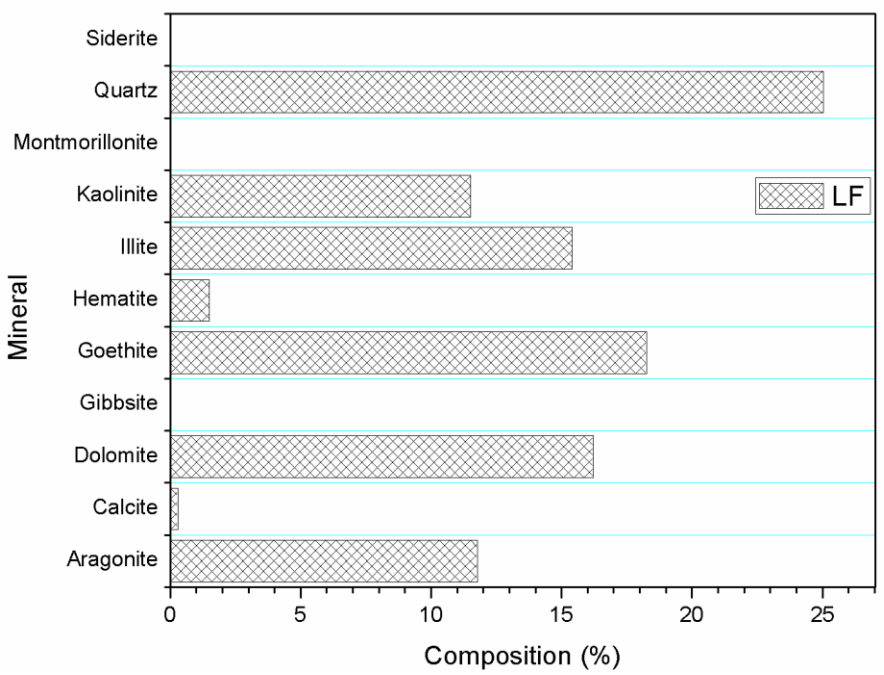

Figure A7. Percentage composition of minerals in LF soil

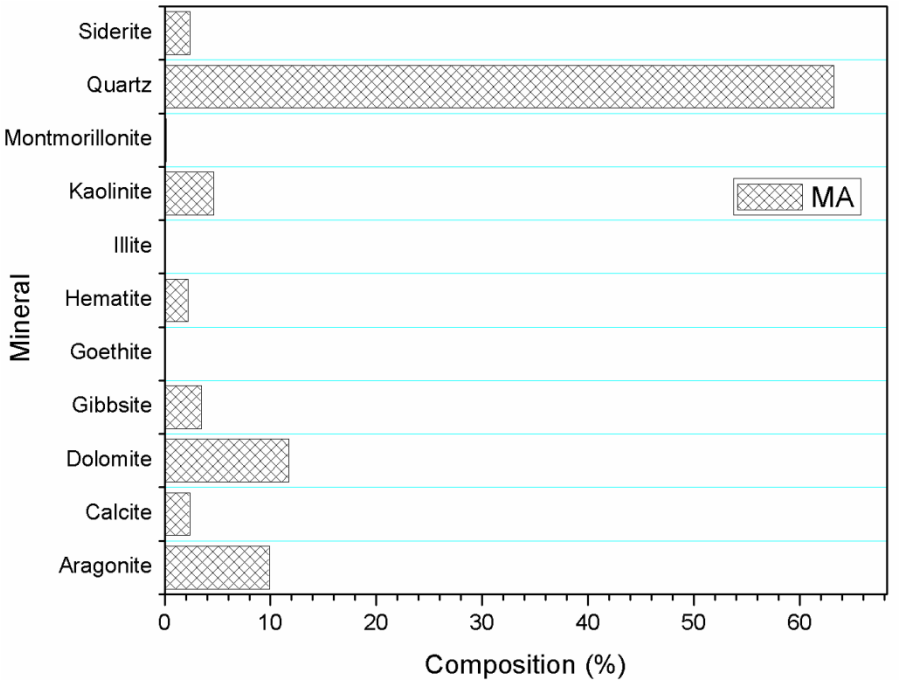

Figure A8. Percentage composition of minerals in MA soil

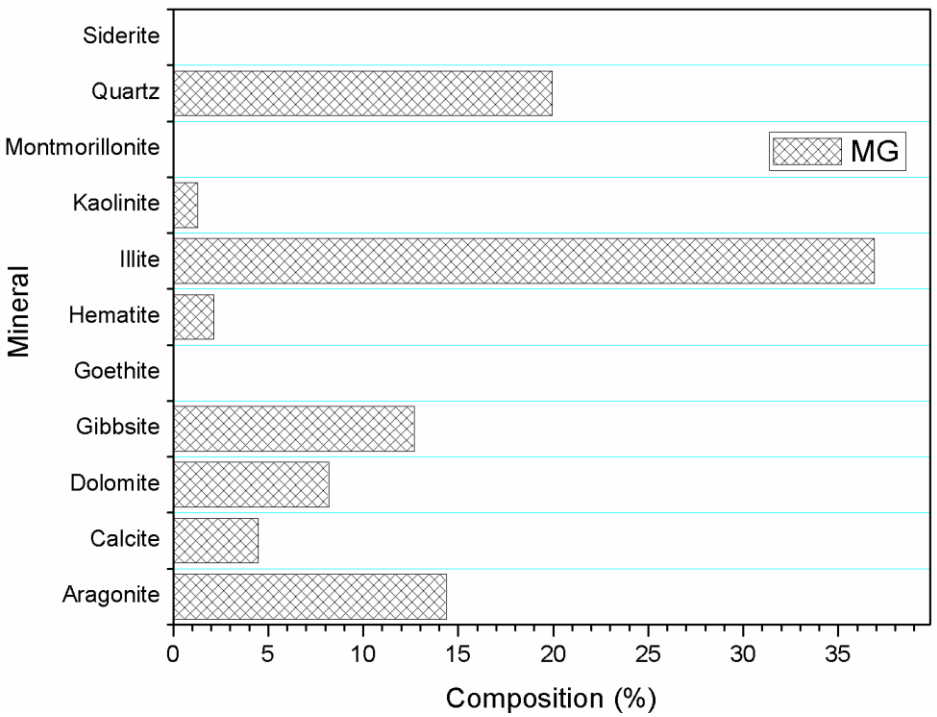

Figure A9. Percentage composition of minerals in MG soil

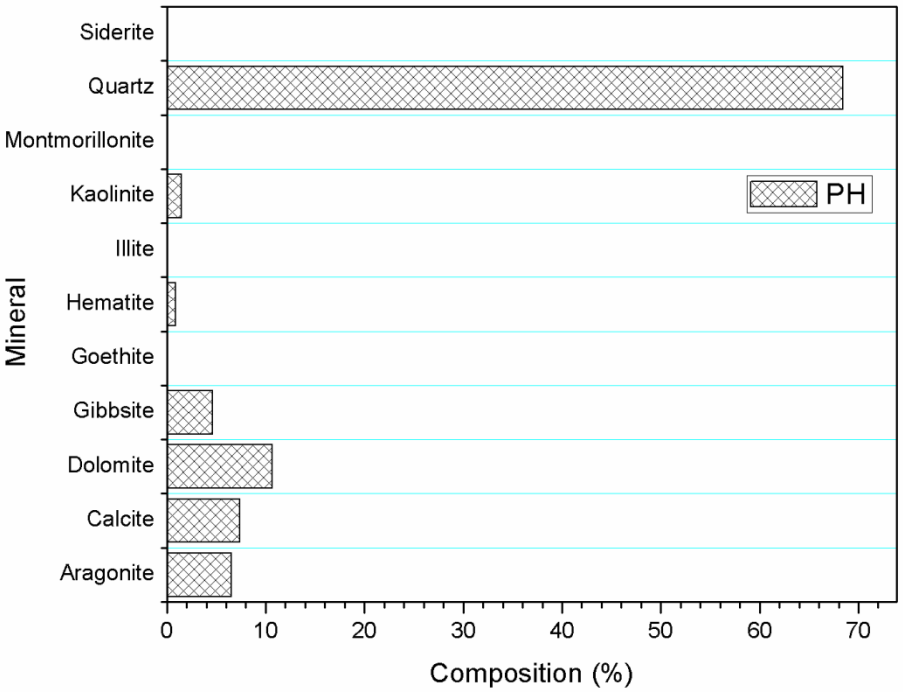

Figure A10. Percentage composition of minerals in PH soil

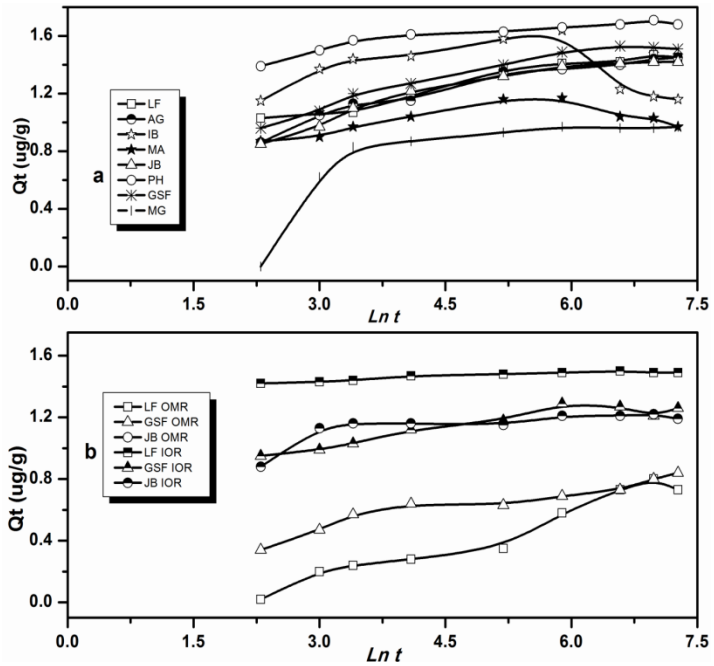

Figure A11. Pyrene sorption Elovich kinetics model for the (a) whole, (b) OMR and IOR samples

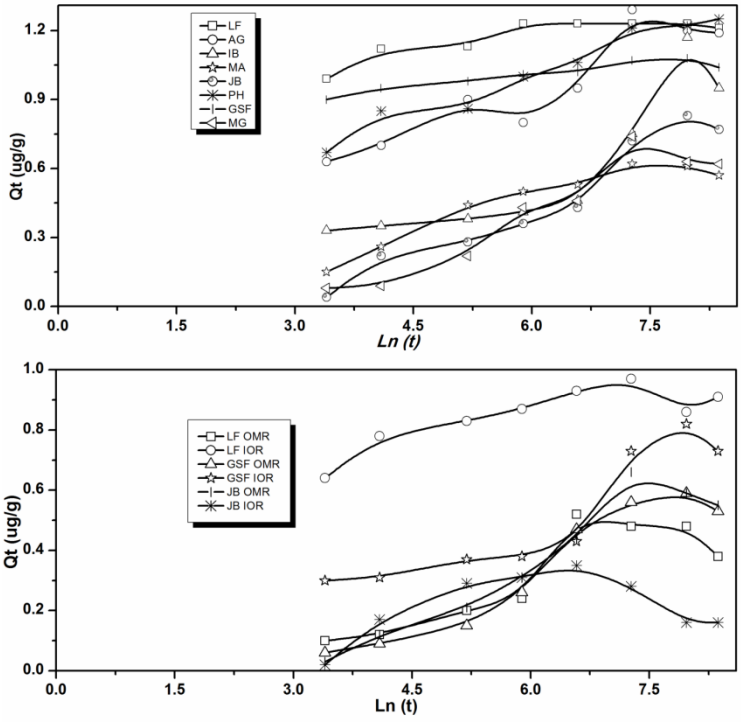

Figure A12. Fluorene sorption Elovich kinetics model for the whole (above), and OMR and IOR (below) samples.

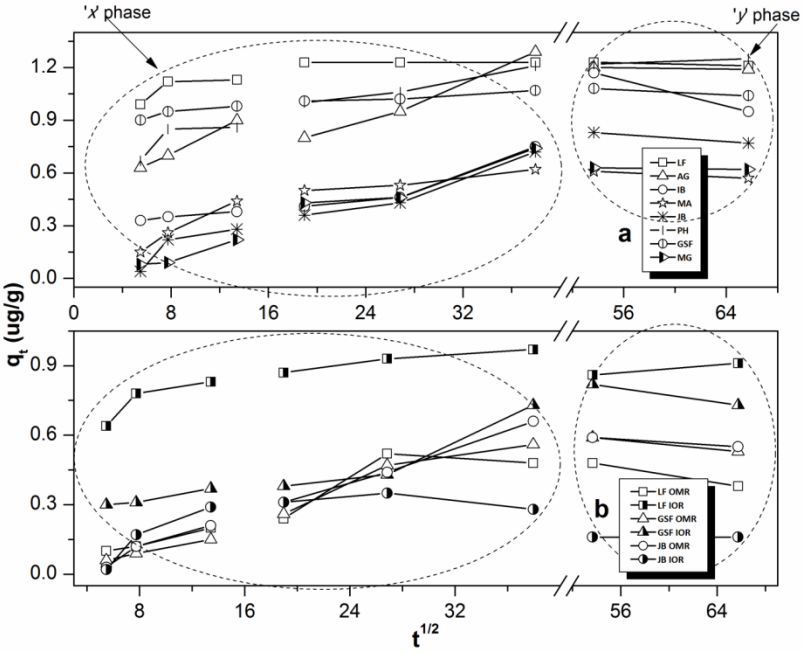

Figure A13. Intraparticle diffusion model plots for fluorene sorption (a) whole soils (b) treated soils

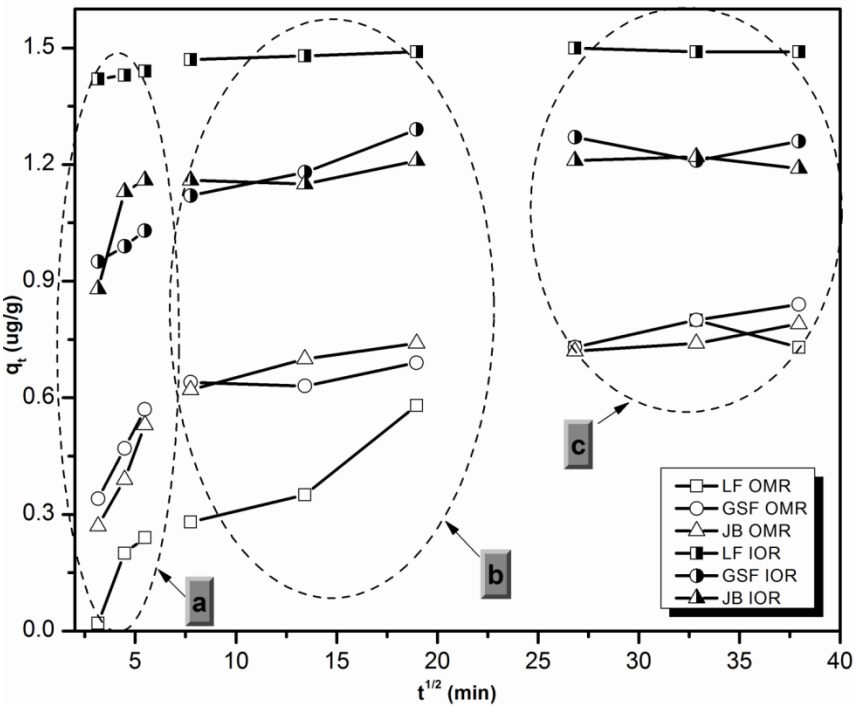

Figure A14. Intraparticle diffusion model plots for pyrene sorption on treated soils

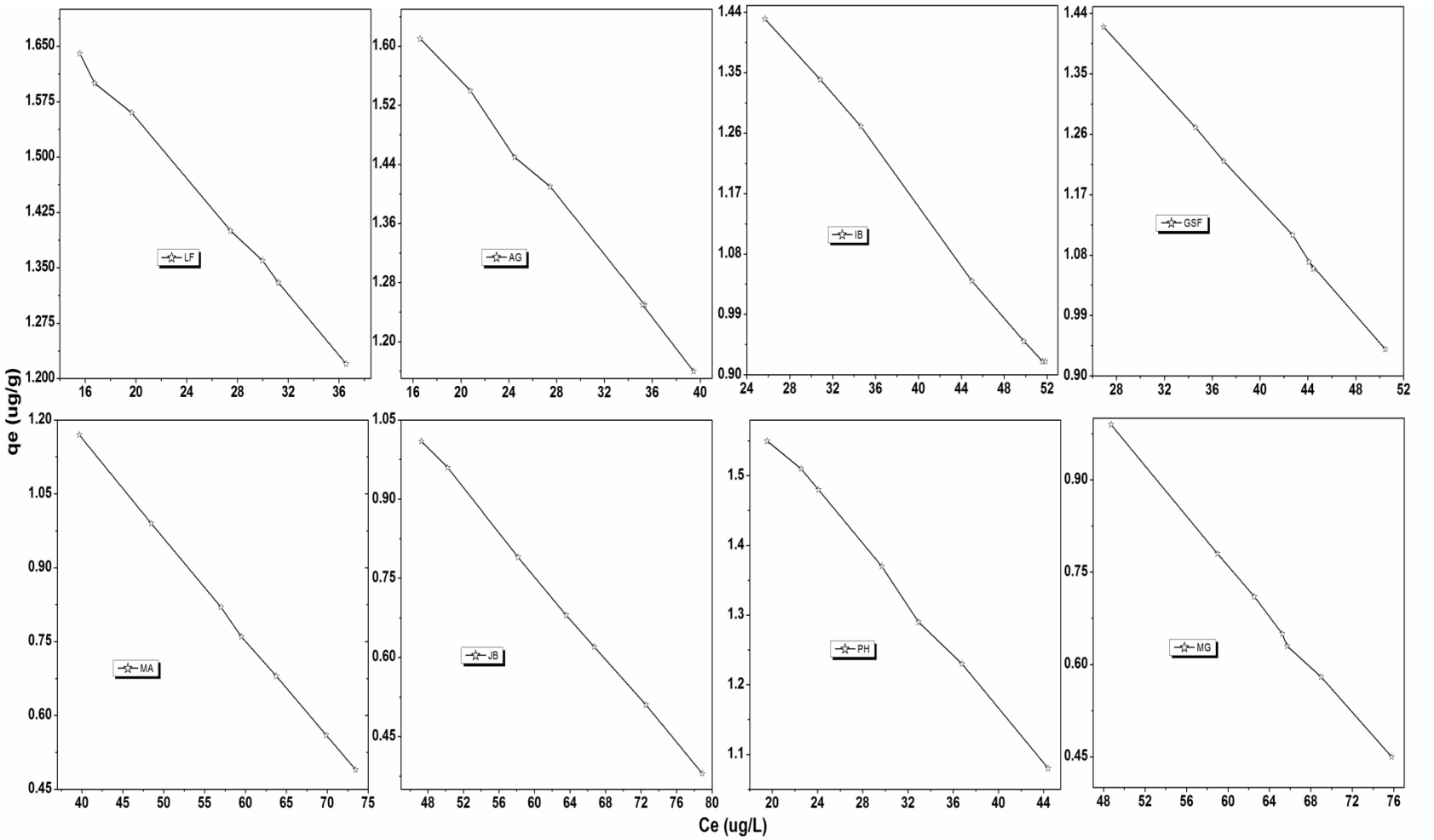

Figure A15. Sorption isotherm of the effect of pH on fluorene sorption on whole soils

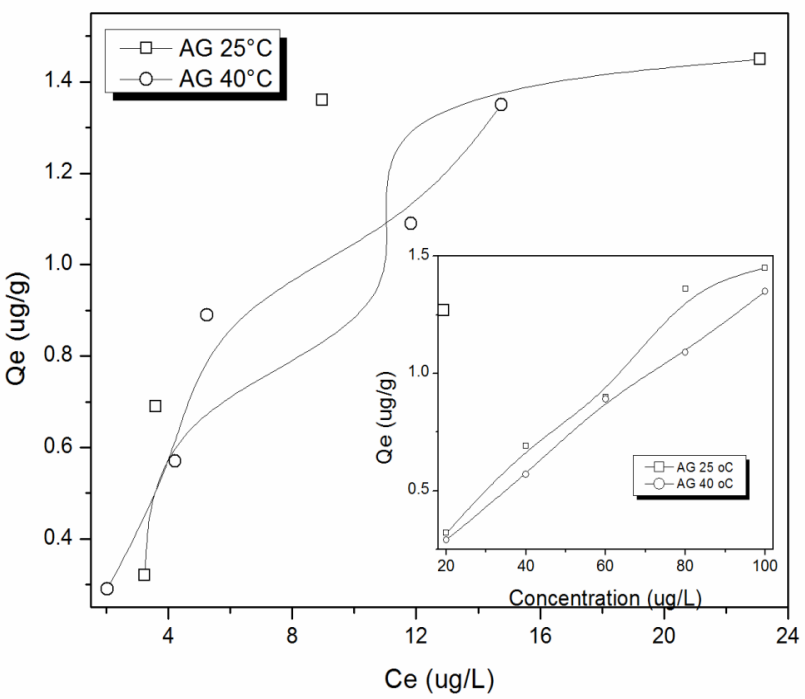

Figure A16*i*. Pyrene sorption isotherm for AG soil (Insert: pyrene sorption trend as concentration varied at 25 and 40 °C)

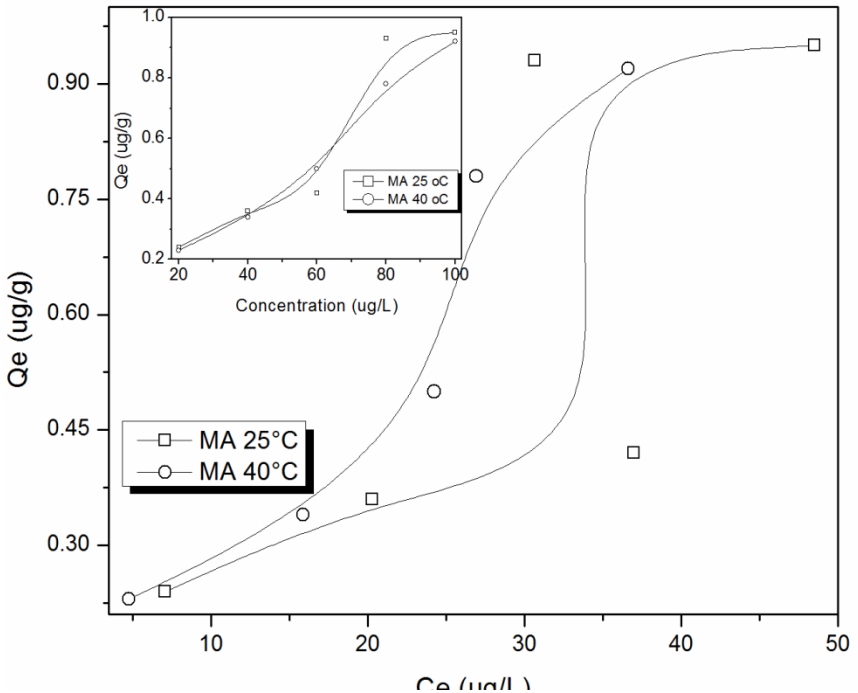

Figure A16 *ii*. Pyrene sorption isotherm for MA soil (Insert: pyrene sorption trend as concentration varied at 25 and 40 °C)

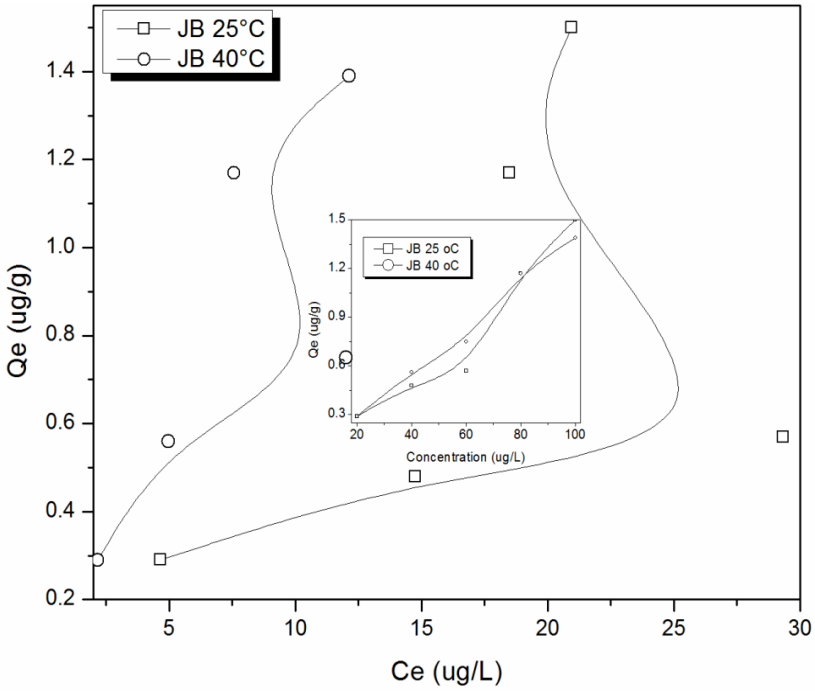

Figure A16 *iii*. Pyrene sorption isotherm for JB soil (Insert: pyrene sorption trend as concentration varied at 25 and 40 °C)

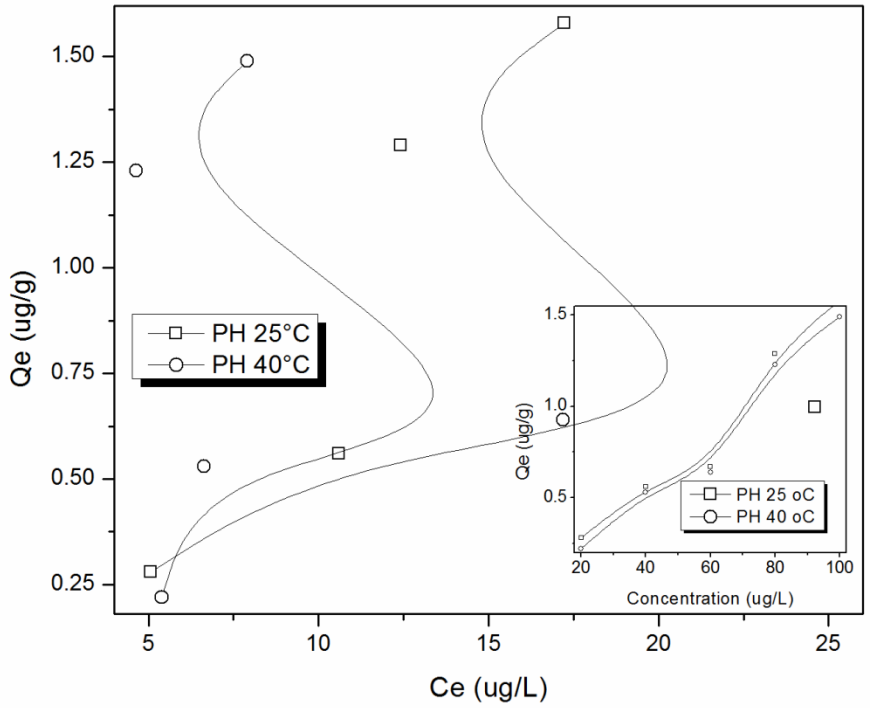

Figure A16 *iv*. Pyrene sorption isotherm for PH soil (Insert: pyrene sorption trend as concentration varied at 25 and 40 °C)

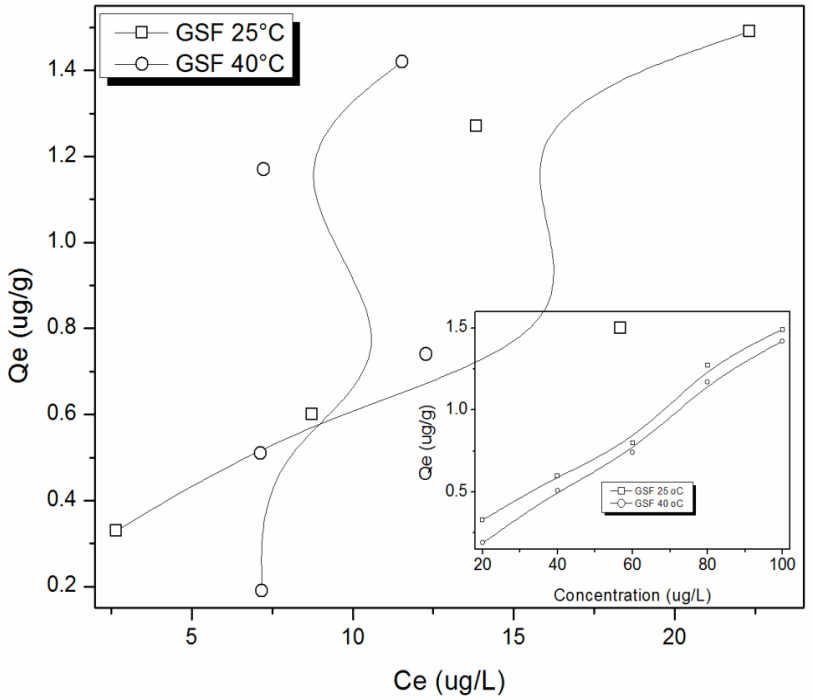

Figure A16 *v*. Pyrene sorption isotherm for GSF soil (Insert: pyrene sorption trend as concentration varied at 25 and 40 °C)

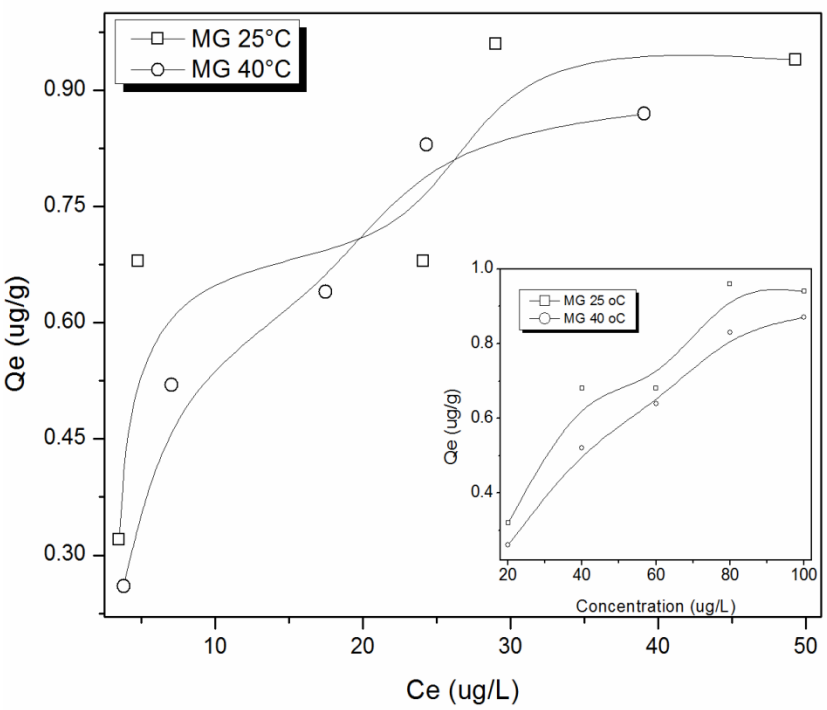

Figure A16 *vi*. Pyrene sorption isotherm for MG soil (Insert: pyrene sorption trend as concentration varied at 25 and 40 °C)

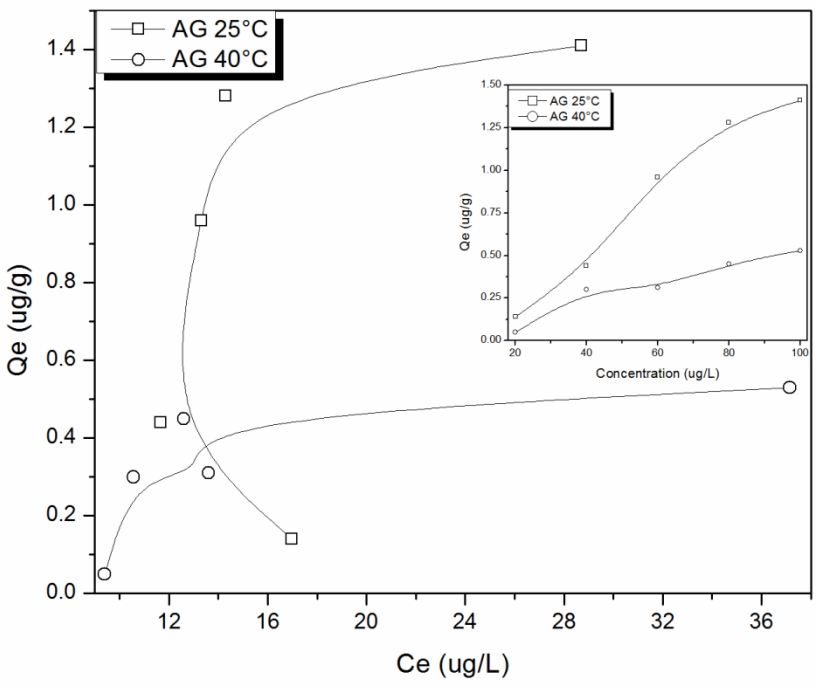

Figure A16 *vii*. Fluorene sorption isotherm for AG soil (Insert: fluorene sorption trend as concentration varied at 25 and 40 °C)

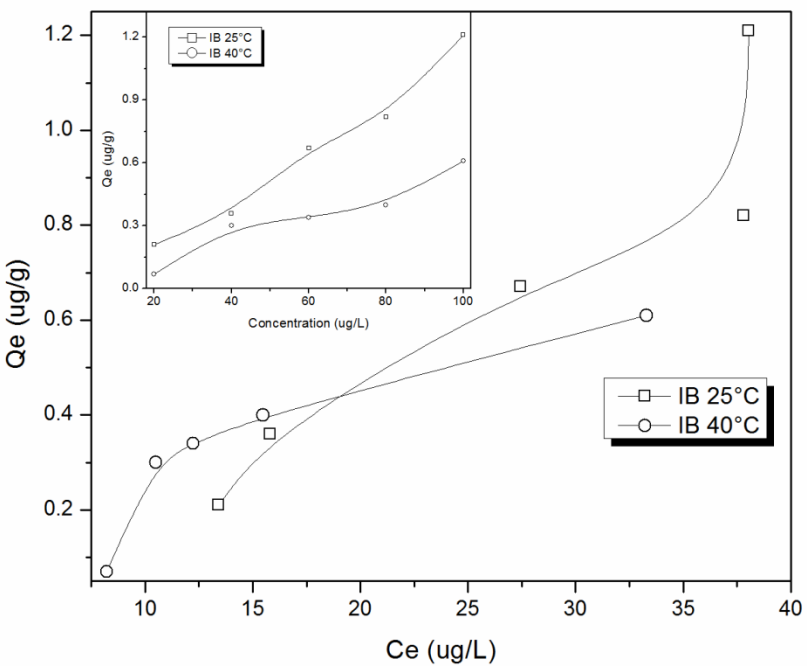

Figure A16 *viii*. Fluorene sorption isotherm for IB soil (Insert: fluorene sorption trend as concentration varied at 25 and 40 °C)

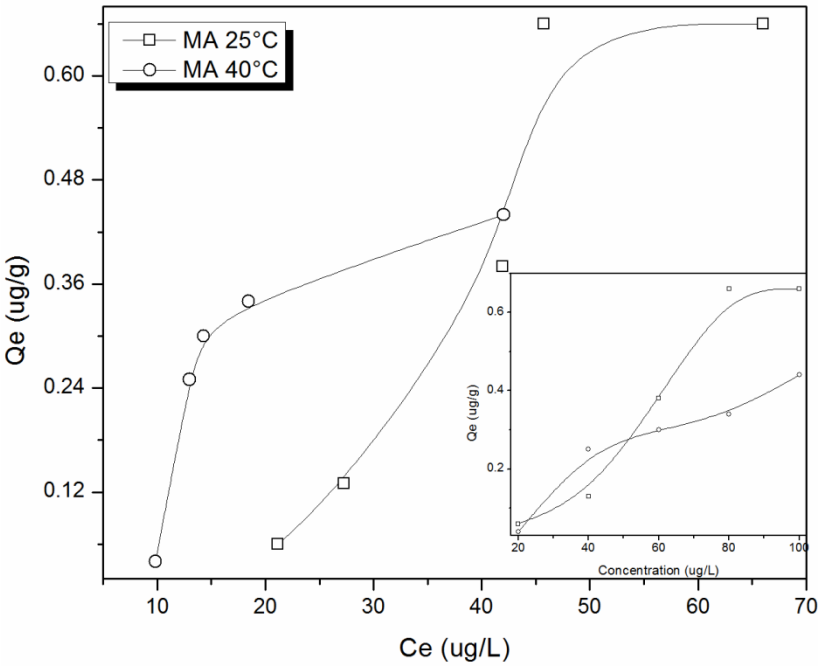

Figure A16 *ix*. Fluorene sorption isotherm for MA soil (Insert: fluorene sorption trend as concentration varied at 25 and 40 °C)

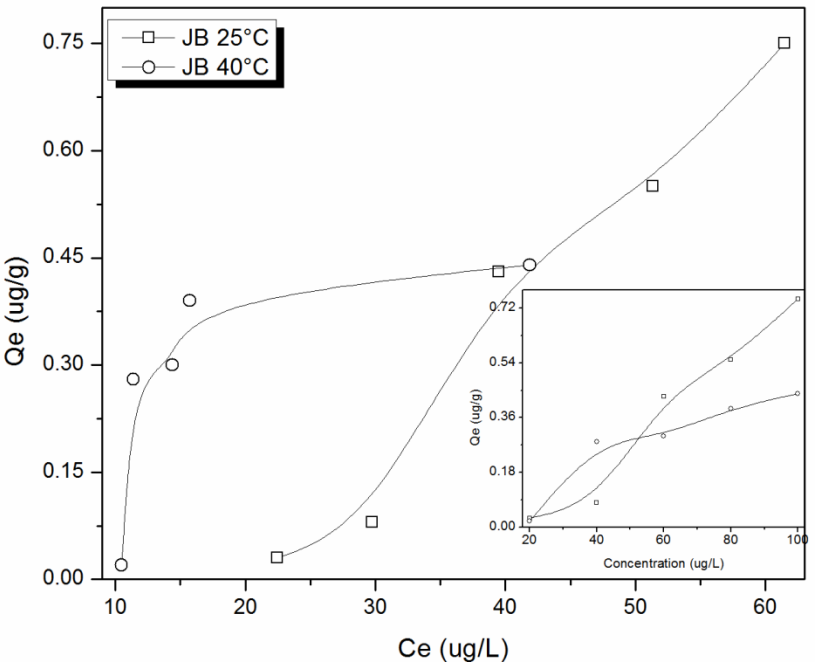

Figure A16 *x*. Fluorene sorption isotherm for JB soil (Insert: fluorene sorption trend as concentration varied at 25 and 40 °C)

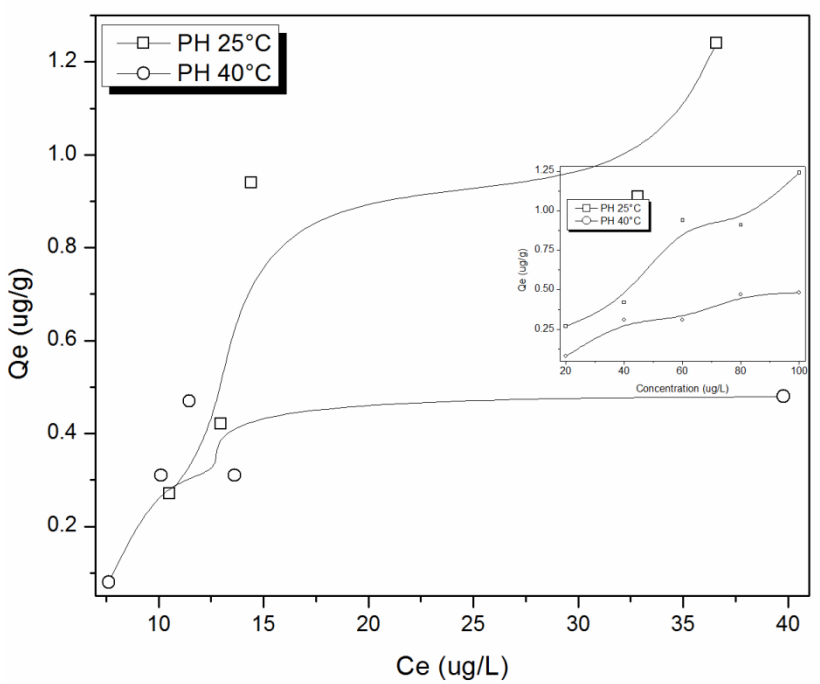

Figure A16 *xi*. Fluorene sorption isotherm for PH soil (Insert: fluorene sorption trend as concentration varied at 25 and 40 °C)

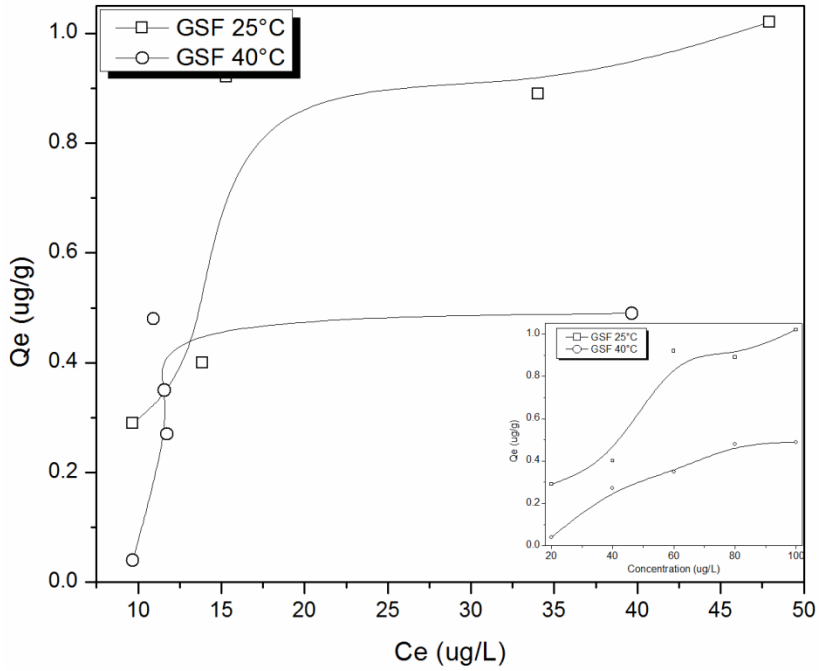

Figure A16 *xii*. Fluorene sorption isotherm for GSF soil (Insert: fluorene sorption trend as concentration varied at 25 and 40 °C)

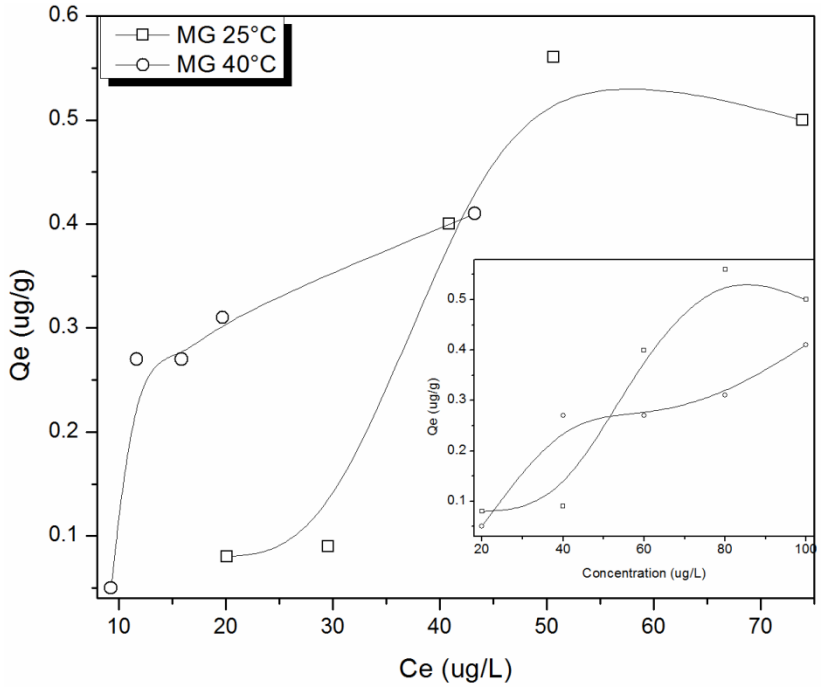

Figure A16 *xiii*. Fluorene sorption isotherm for MG soil (Insert: fluorene sorption trend as concentration varied at 25 and 40 °C)

Table A1. Isotherm curve types for pyrene and fluorene sorptions at 25 and 40 °C

	Pyrene 25 °C	Fluorene 25 °C	Pyrene 40 °C	Fluorene 40 °C
LF	VI	III	I	III
AG	VI	I	III	III
IB	I	II	I	I
MA	IV	V	V	I
JB	VI	V	VI	I
PH	VI	VI	VI	VI
GSF	VI	III	VI	I
MG	IV	V	IV	I

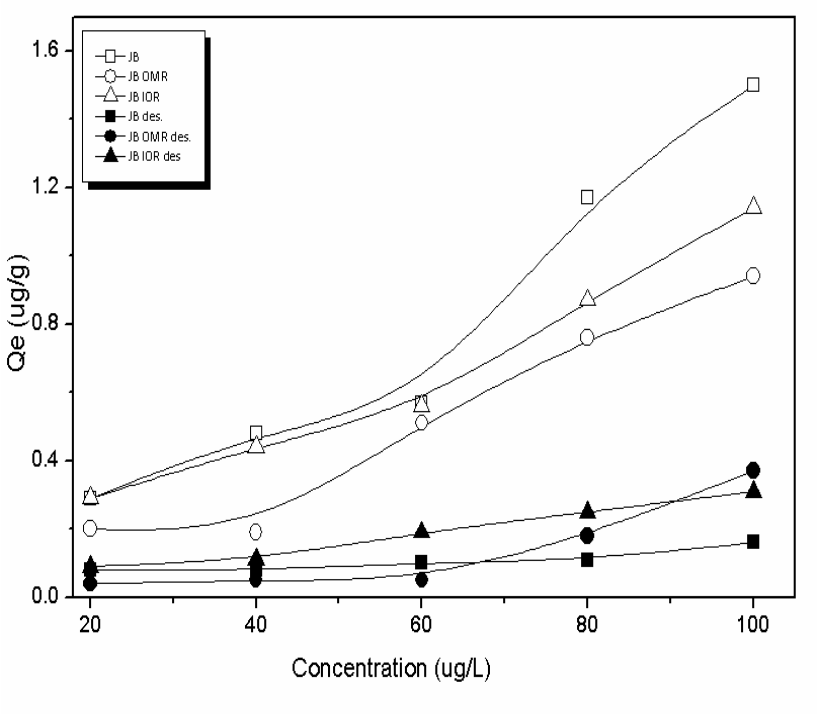

Figure A16 *xiv*. Sorption and desorption of pyrene on JB whole and treated soil

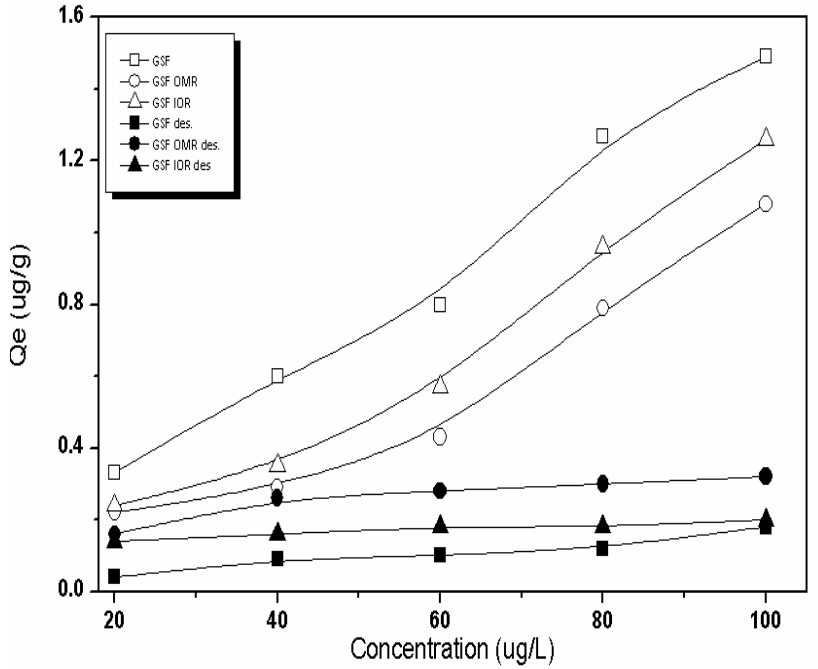

Figure A16 *xv*. Sorption and desorption of pyrene on GSF whole and treated soil

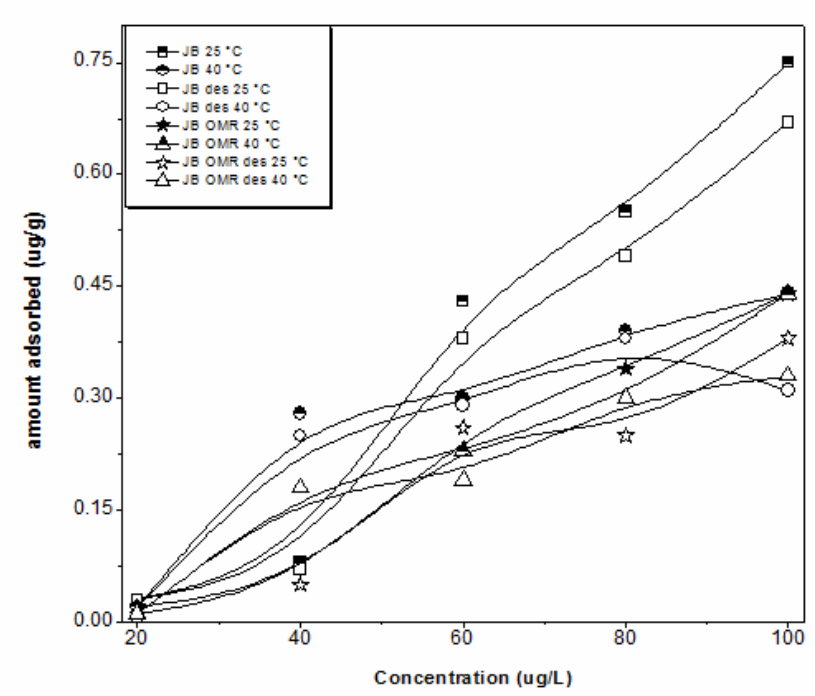

Figure A16 *xvi*. Sorption (half–filled symbols) and desorption (empty symbols) of fluorene on JB whole and treated soil (OMR) at 25 and 40 °C

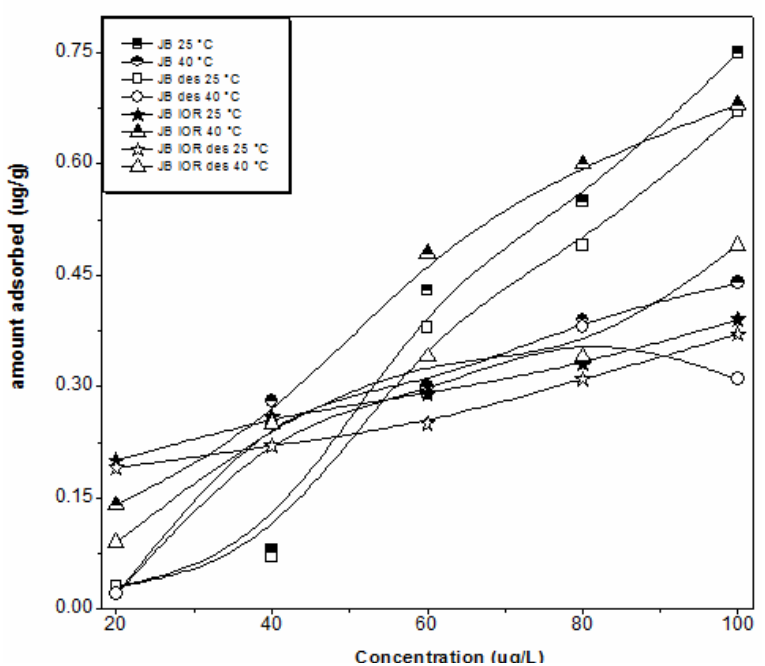

Figure A16 *xvii*. Sorption (half–filled symbols) and desorption (empty symbols) of fluorene on JB whole and treated soil (IOR) at 25 and 40 °C

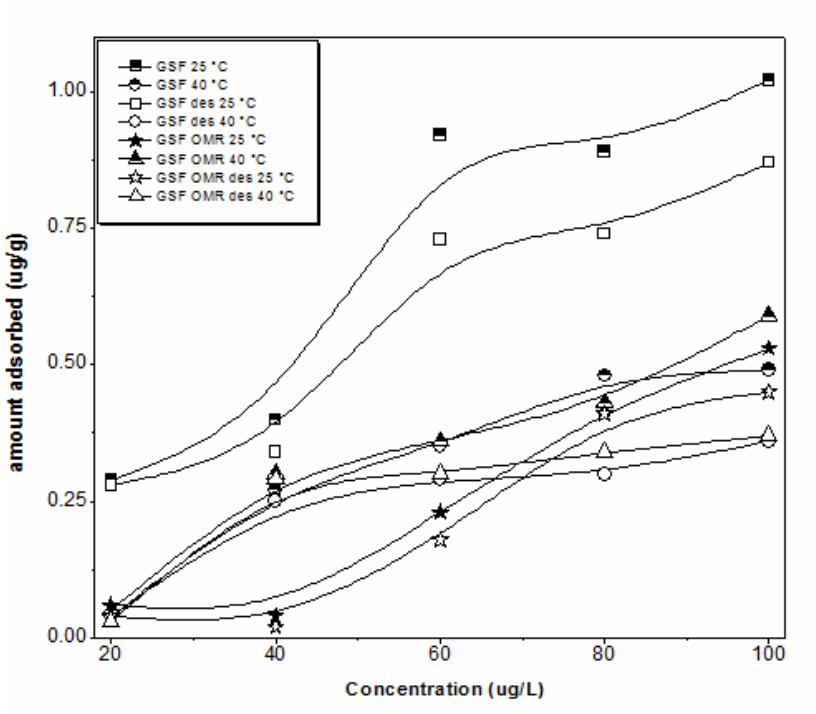

Figure A16 *xviii*. Sorption (half–filled symbols) and desorption (empty symbols) of fluorene on GSF whole and treated soil (OMR) at 25 and 40 °C

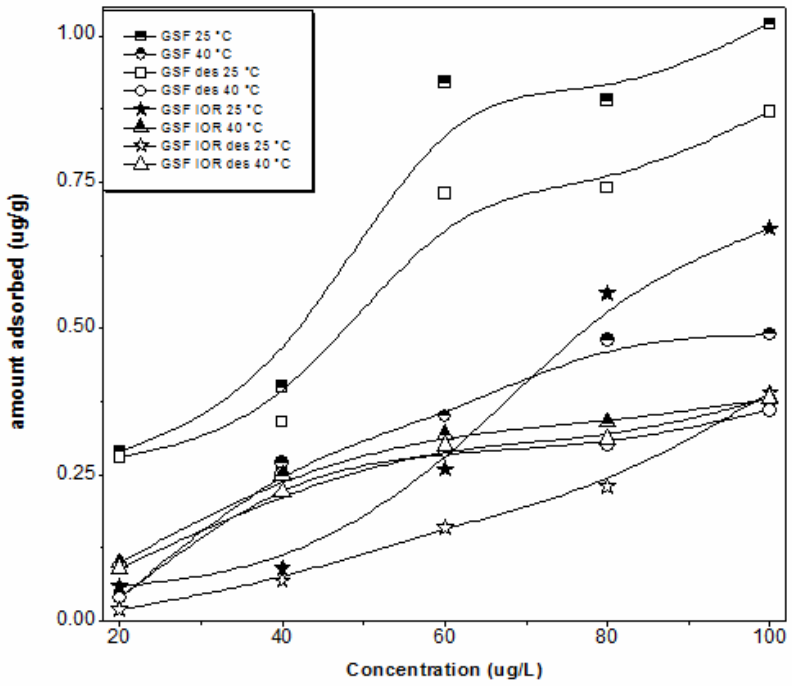

Figure A16 *xix*. Sorption (half–filled symbols) and desorption (empty symbols) of fluorene on GSF whole and treated soil (IOR) at 25 and 40 °C

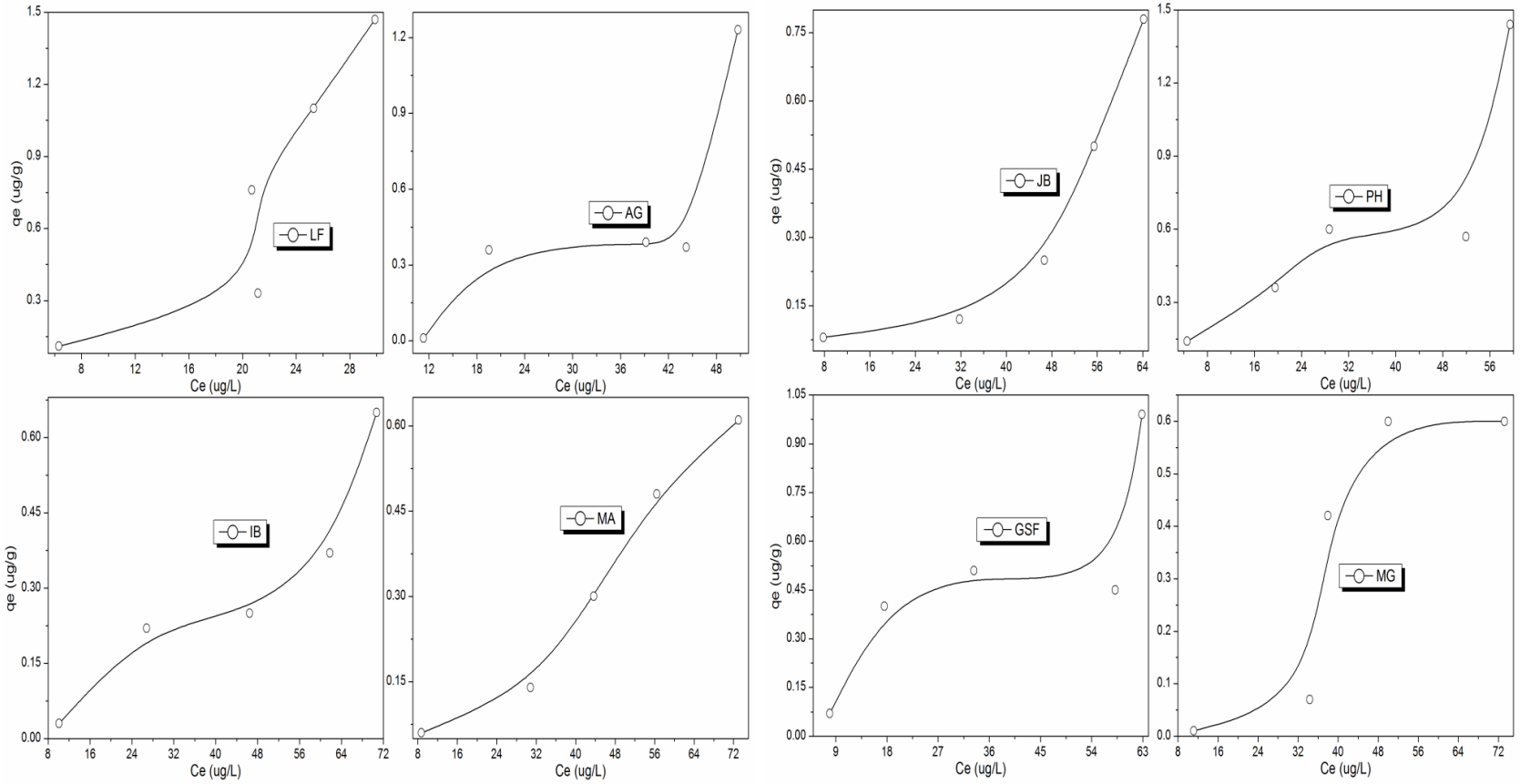

Figure A17 *i*. Competitive fluorene sorptions isotherm

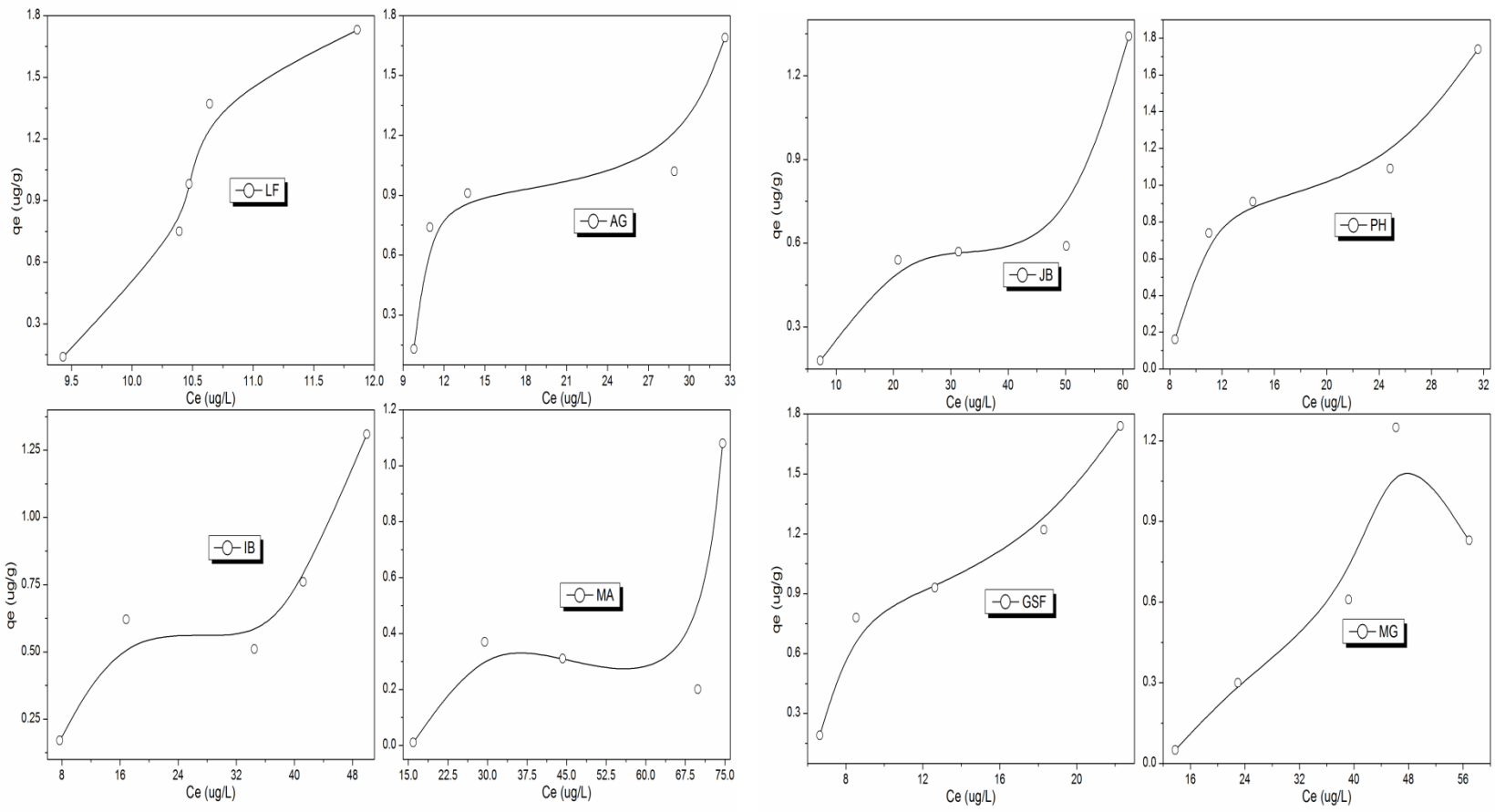

Figure A17 *ii*. Competitive pyrene sorptions isotherms

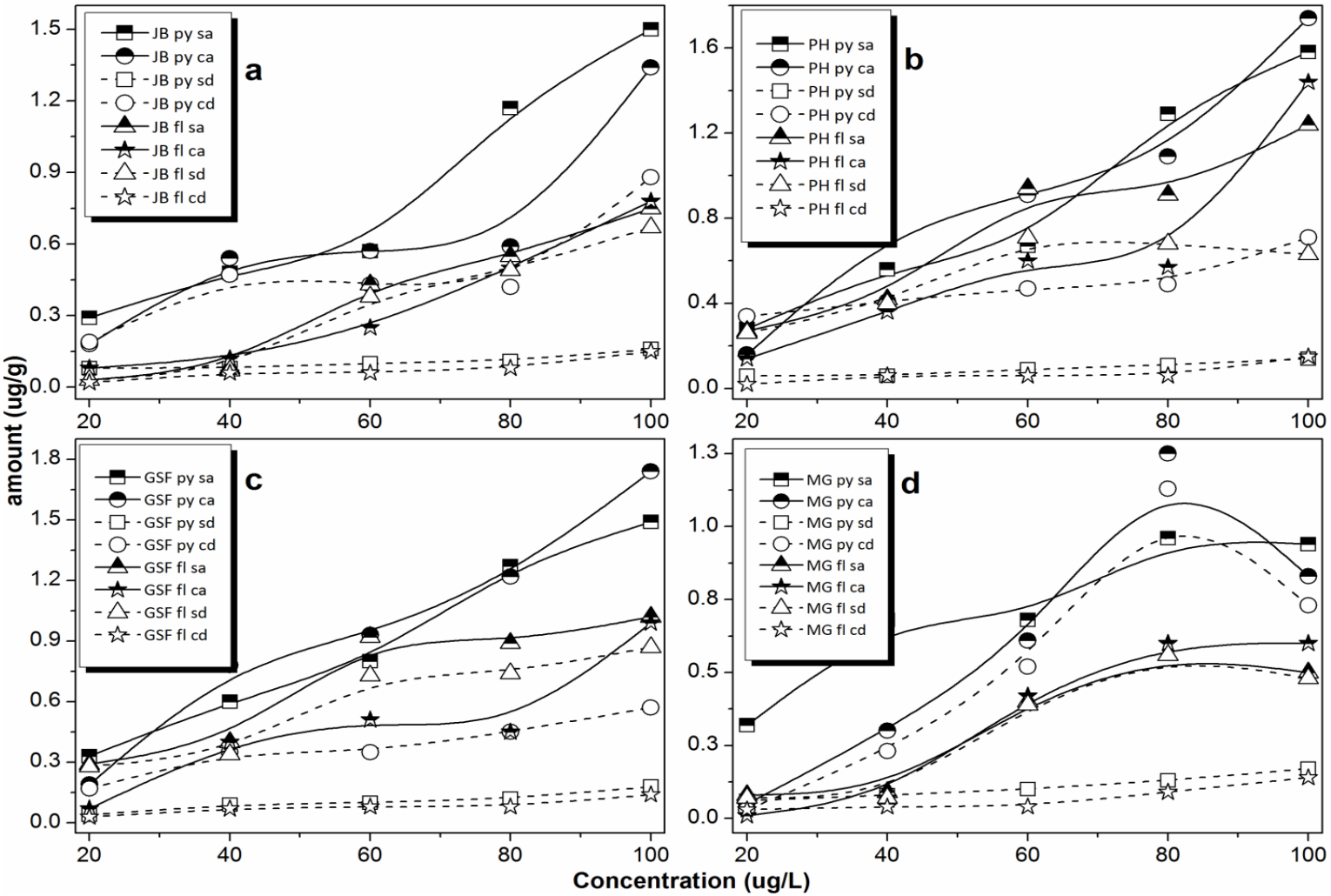

Figure A17 *iii*. Single and competitive sorptions (solid lines and half filled symbols) and desorptions (broken lines and empty symbols) of pyrene and fluorene on (a) JB, (b) PH, (c) GSF, and (d) MG whole soils at varying initial concentrations. Codes in figure: sa = single adsorption, ca competitive adsorption, sd = single desorption, cd = competitive desorption.

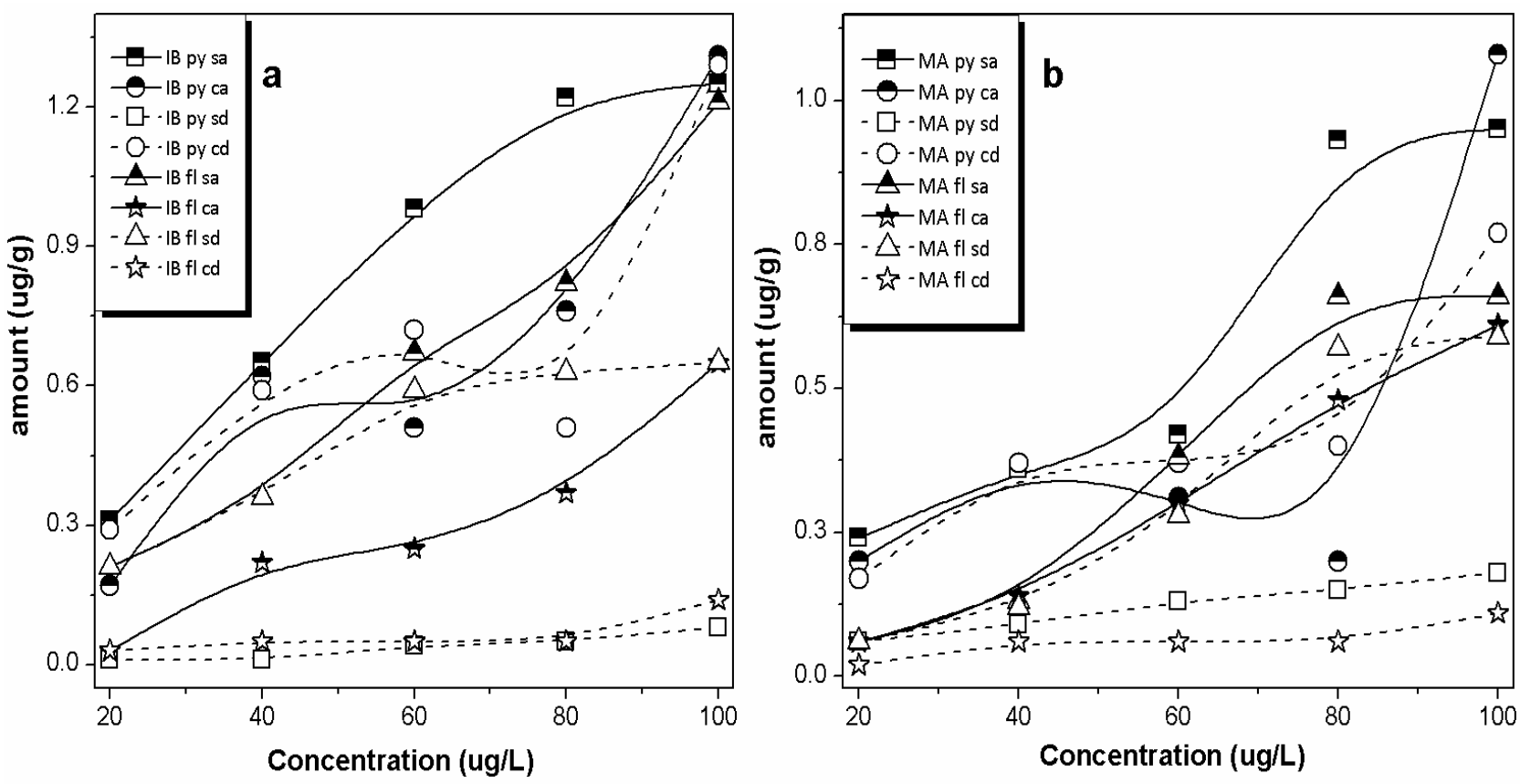

Figure A17 *iv*. Single and competitive sorptions (solid lines and half filled symbols) and desorptions (broken lines and empty symbols) of pyrene and fluorene on (a) IB and (b) MA whole soils at varying initial concentrations. Codes in figure: sa = single adsorption, ca competitive adsorption, sd = single desorption, cd = competitive desorption.

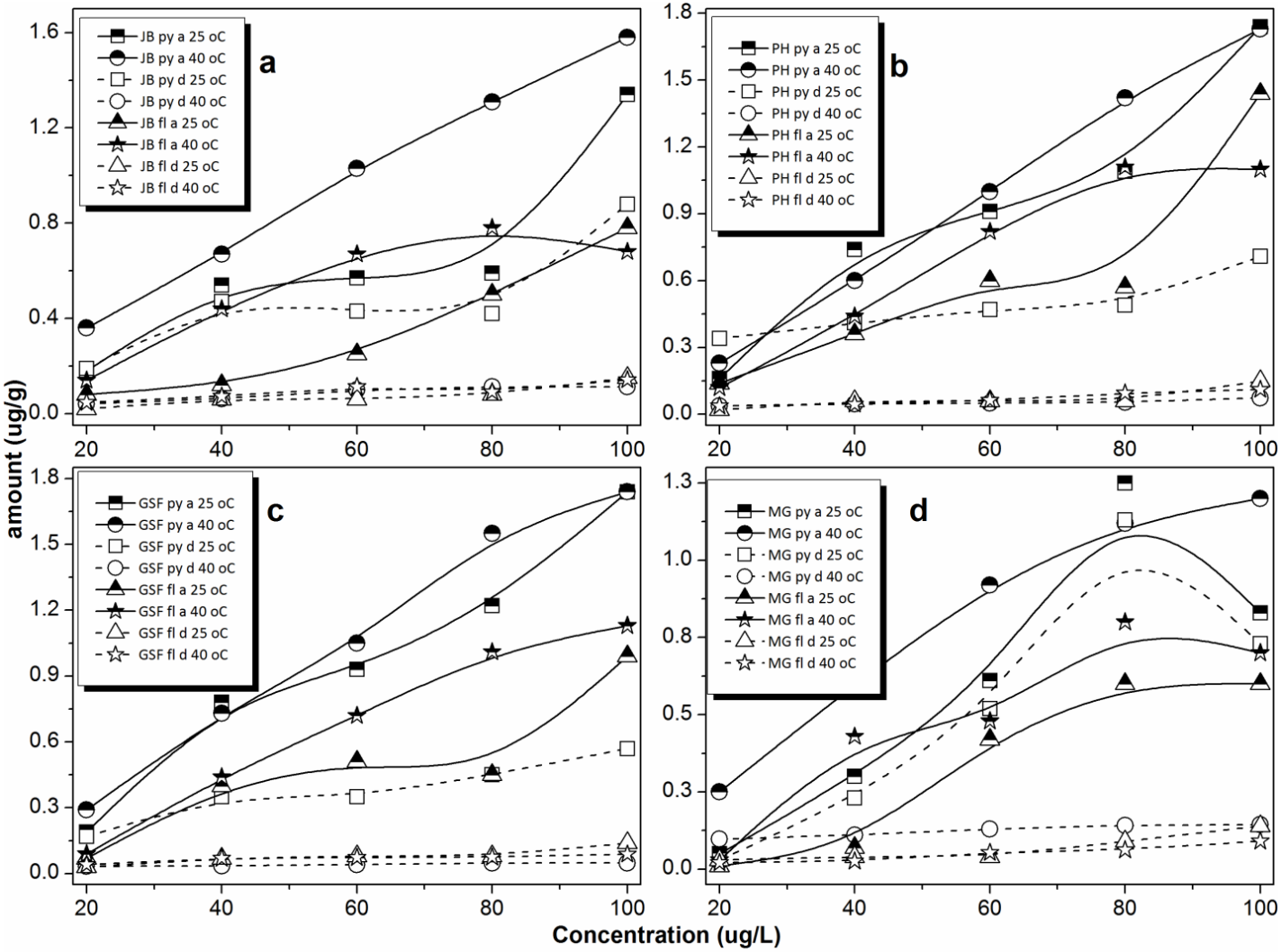

Figure A17 *v*. Competitive sorptions (solid lines) and desorptions (broken lines) of pyrene and fluorene on the (a) JB, (b) PH, (c) GSF, and (d) MG whole soils at varying initial concentrations and at 25 and 40 °C. Codes in figure: a = adsorption, d = desorption

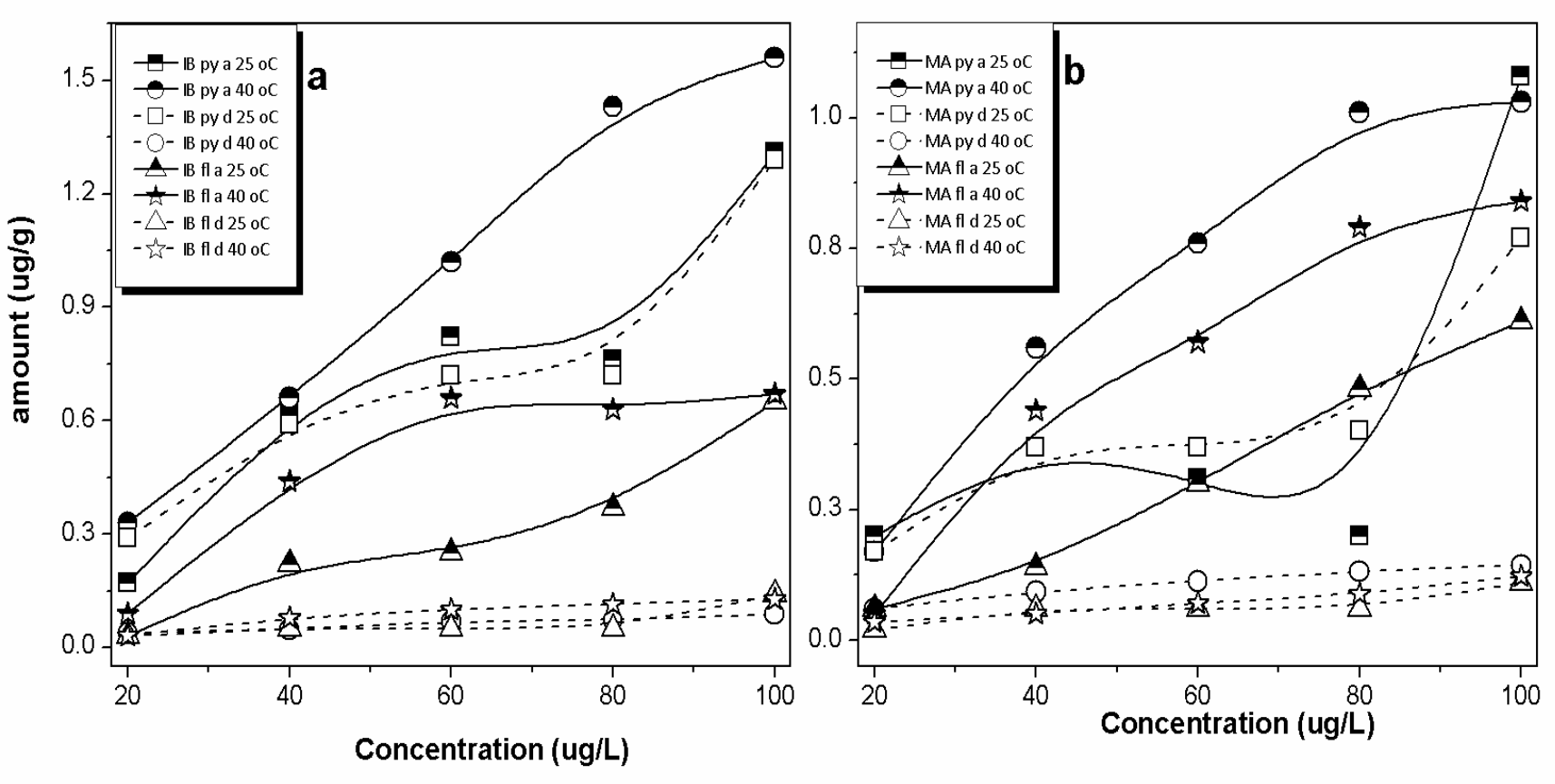

Figure A17 *vi*. Competitive sorptions (solid lines) and desorptions (broken lines) of pyrene and fluorene on the (a) IB and (b) MA whole soils at varying initial concentrations and at 25 and 40 °C. Codes in figure: a = adsorption, d = desorption

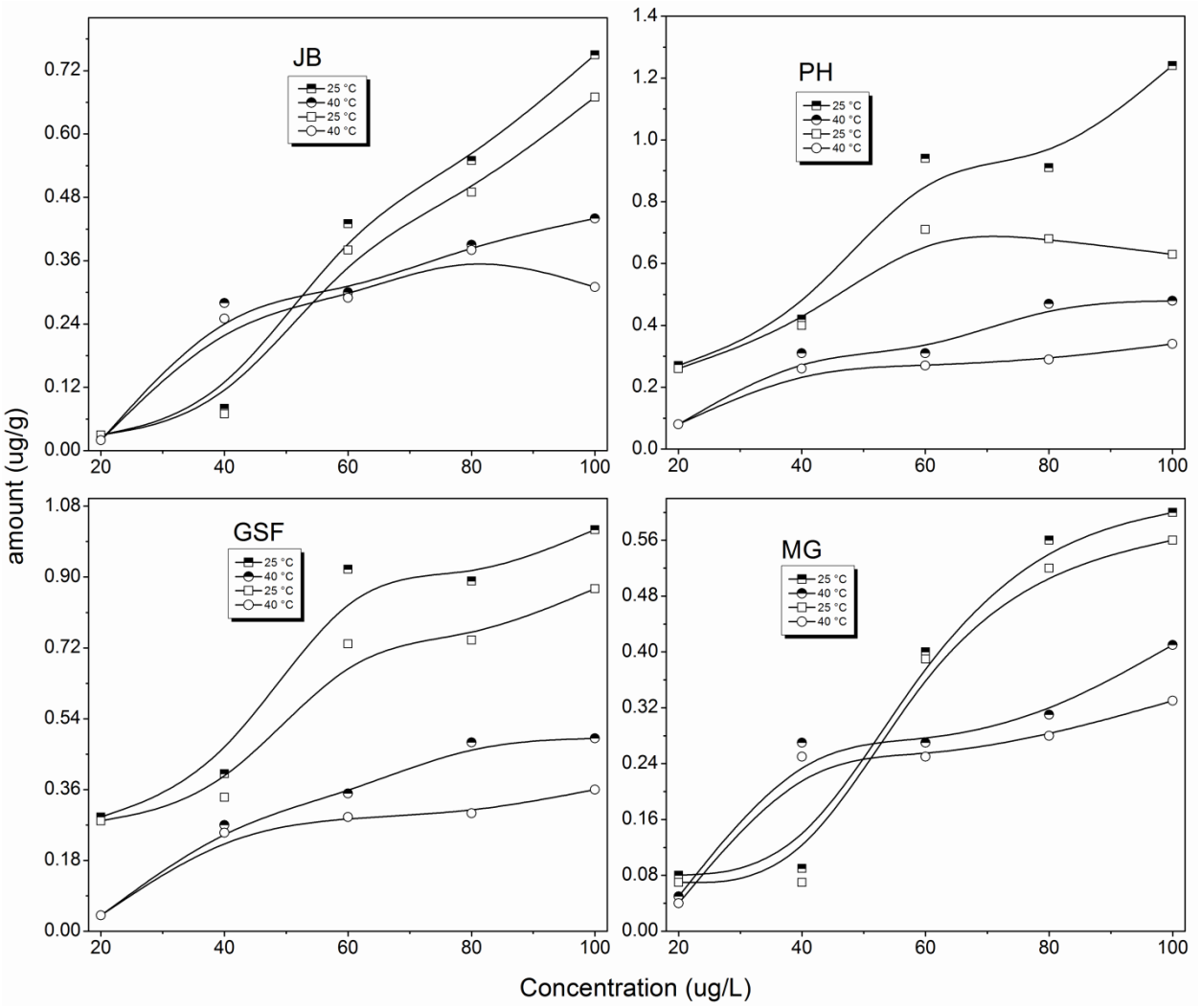

Figure A17. Fluorene sorption (half–filled symbols) and desorption (empty symbols) for JB, PH, GSF, and MG at 25 °C and at 40 °C.

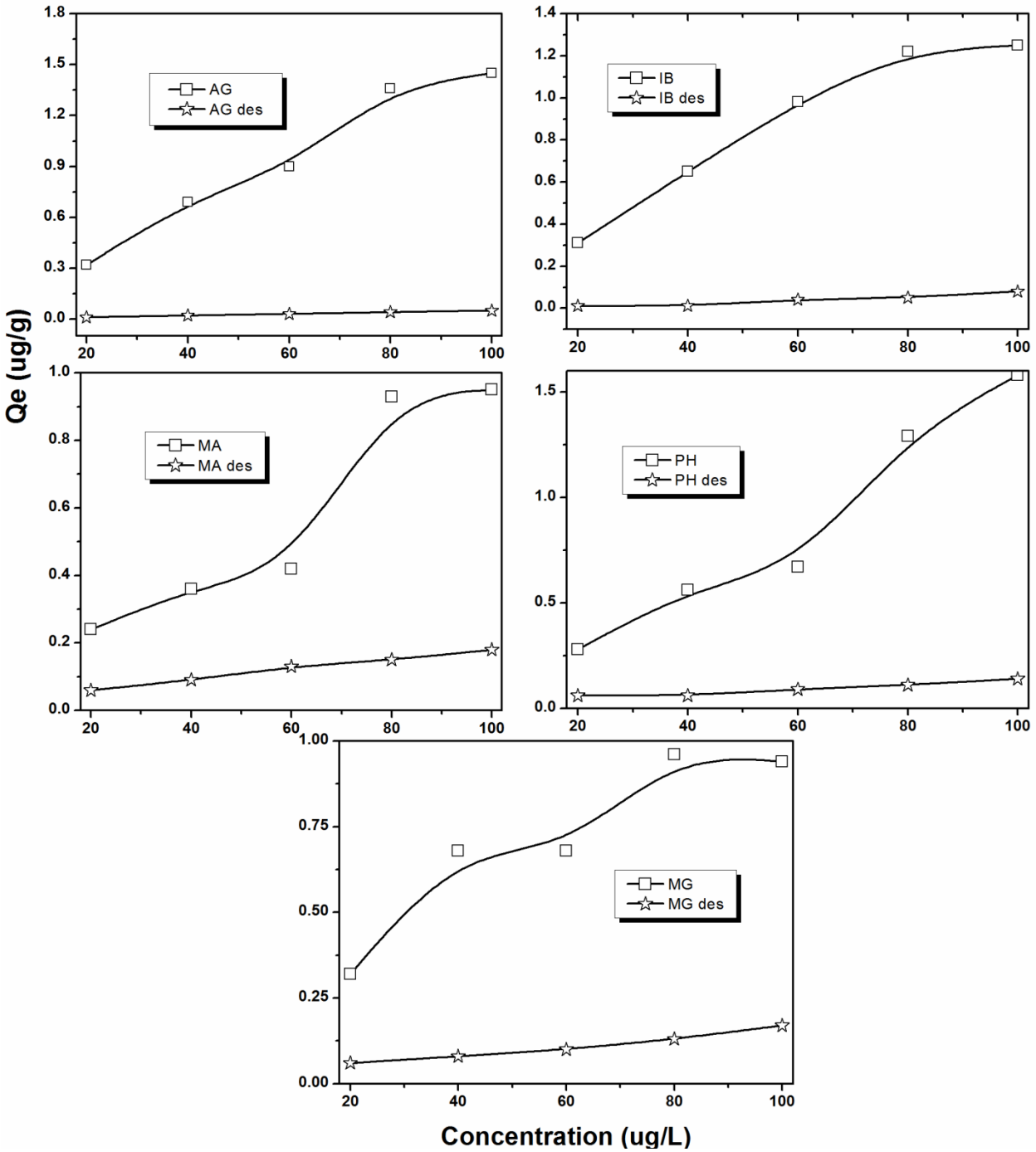

Figure A18. Pyrene sorption and desorption curves for whole soil samples

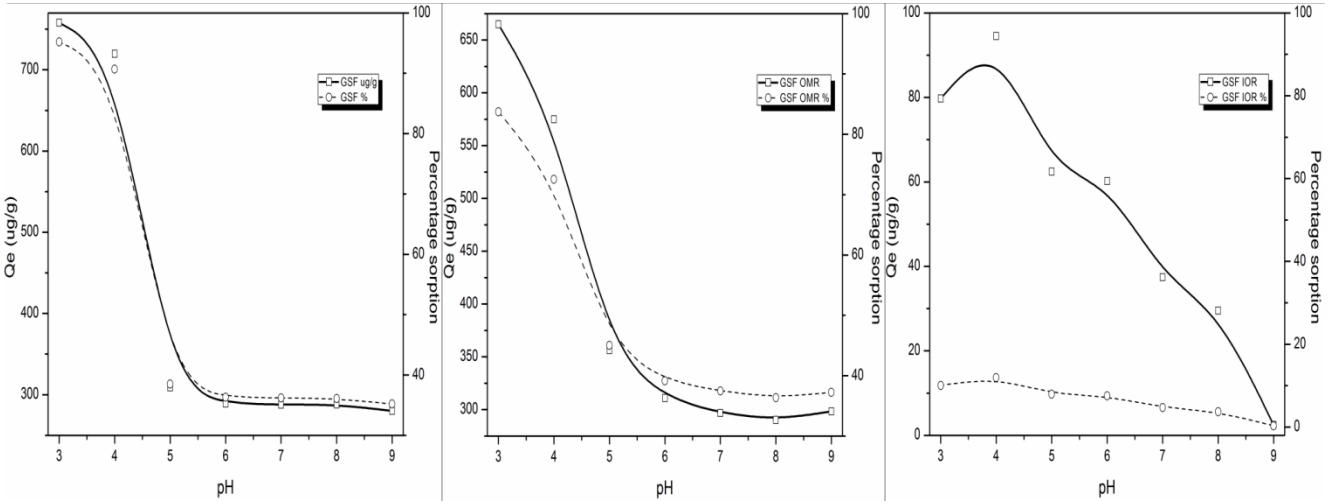

Figure A19 *i*. Effect of pH on the amount of PCP sorbed (full lines) and percentage sorbed (broken lines) on GSF whole soils (left row), OMR soils (middle row), and IOR soils (right row)

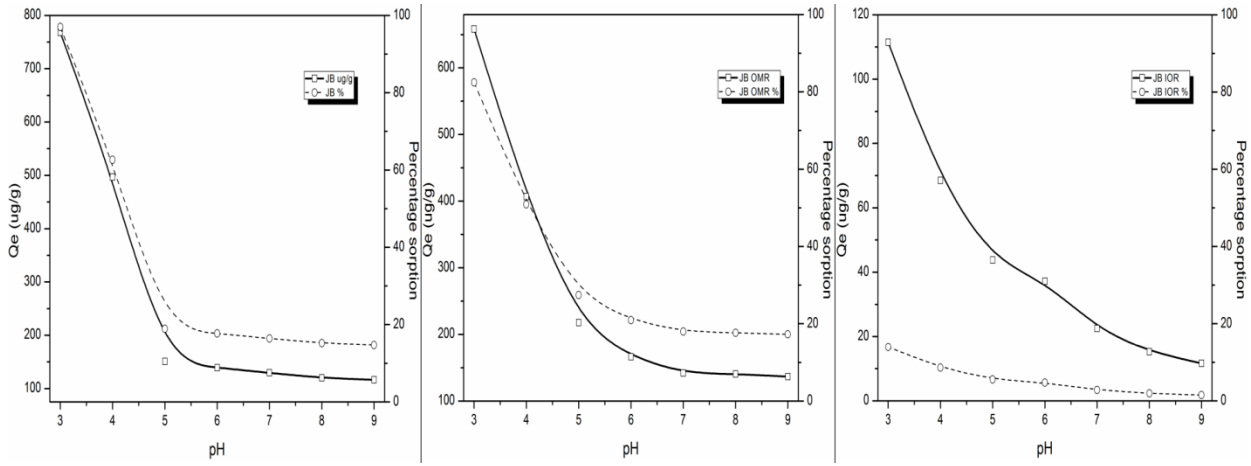

Figure A19 *ii*. Effect of pH on the amount of PCP sorbed (full lines) and percentage sorbed (broken lines) on JB whole soils (left row), OMR soils (middle row), and IOR soils (right row).

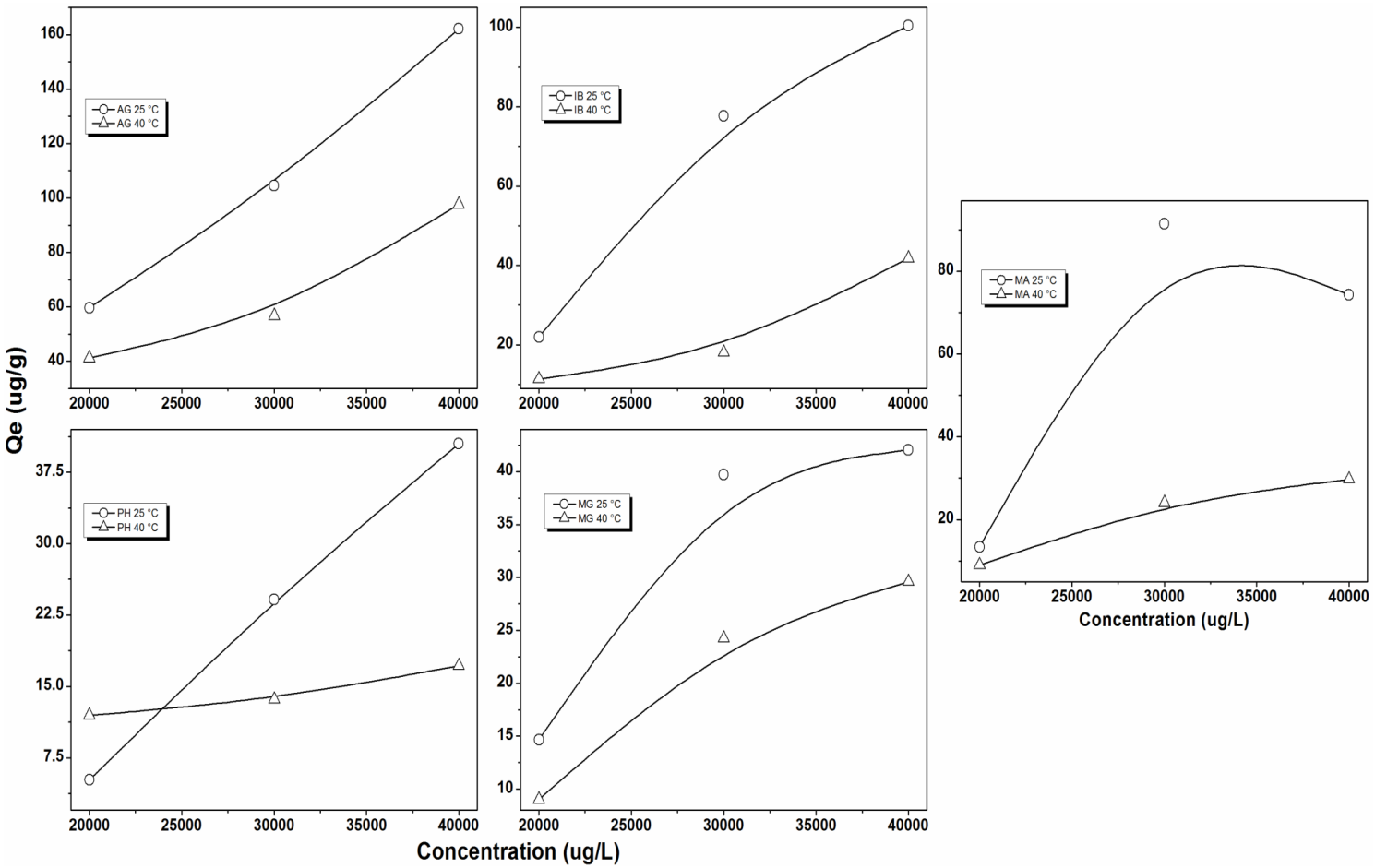

Figure A20. Sorption of PCP on the whole soils at varying PCP concentrations at 25 °C (circular symbols) and 40 °C (triangular symbols)

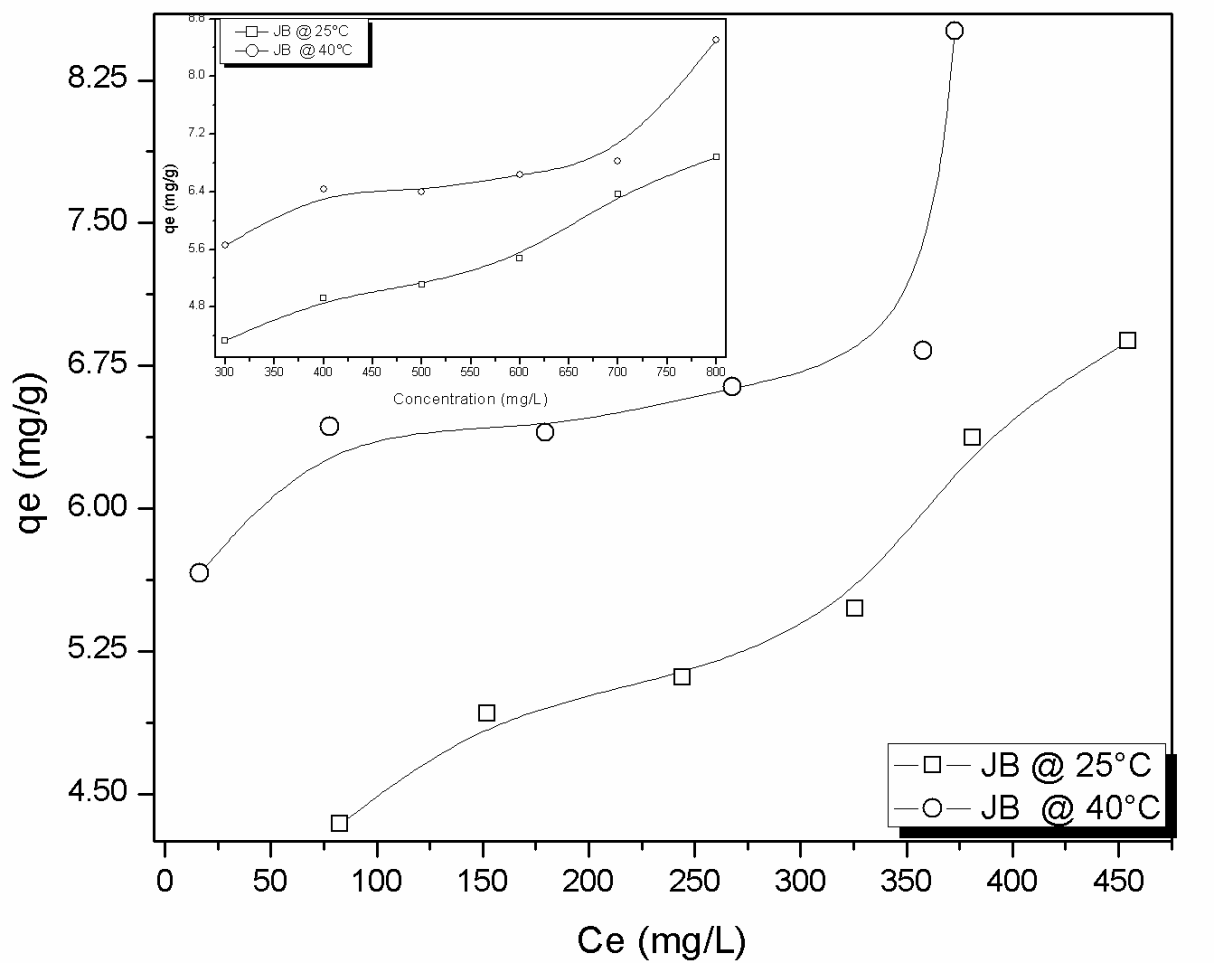

Figure A21 *a*. Pb(II) sorption isotherm for JB soil (Insert: Pb(II) sorption trend as concentration varied at 25 and 40 °C)

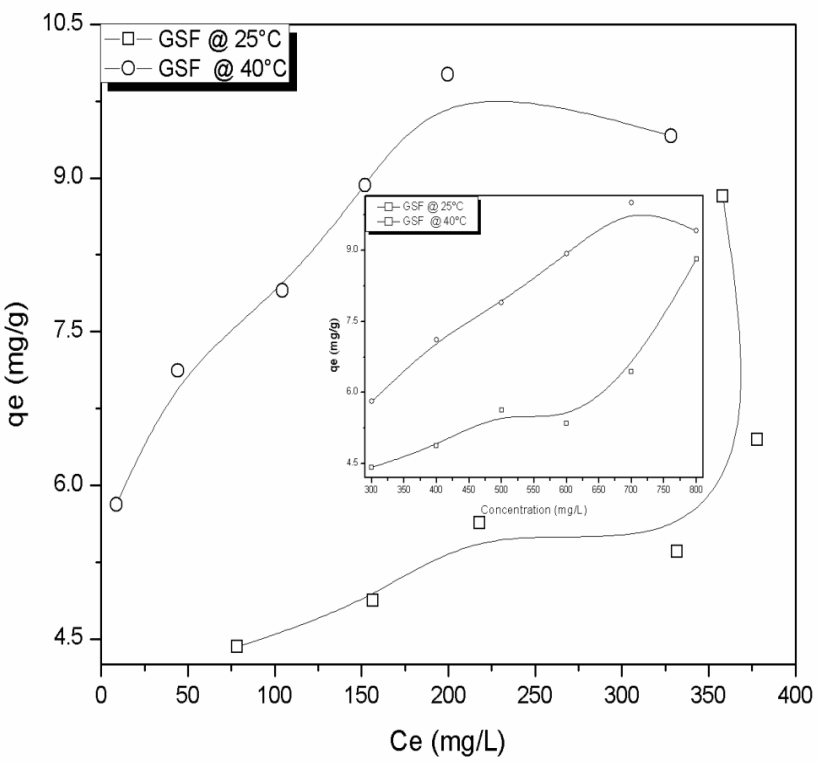

Figure A21 *b*. Pb(II) sorption isotherm for GSF soil (Insert: Pb(II) sorption trend as concentration varied at 25 and 40 °C)

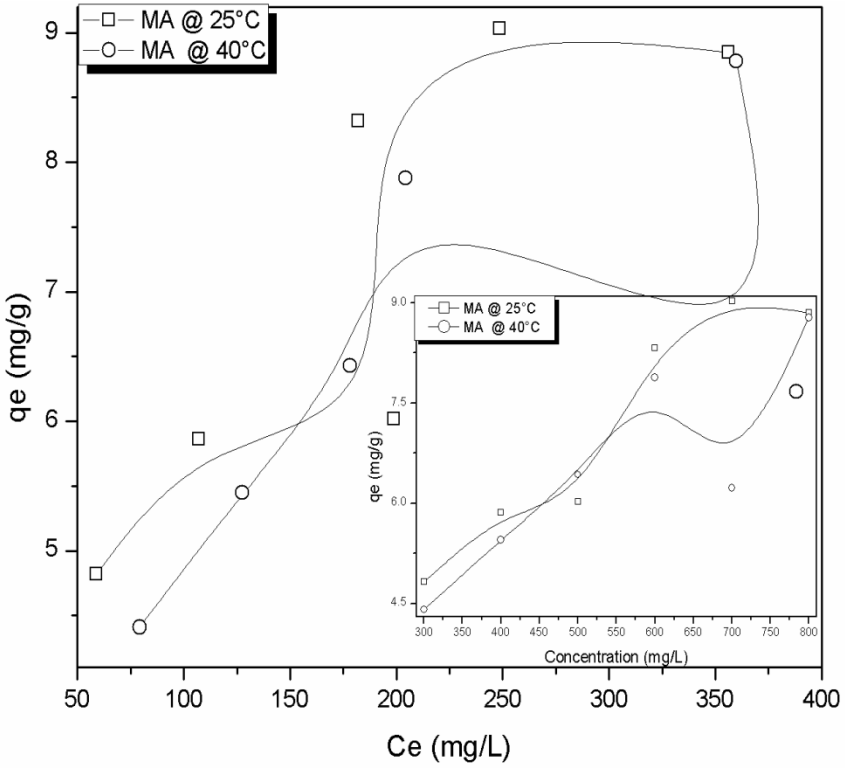

Figure A21 *c*. Pb(II) sorption isotherm for MA soil (Insert: Pb(II) sorption trend as concentration varied at 25 and 40 °C)

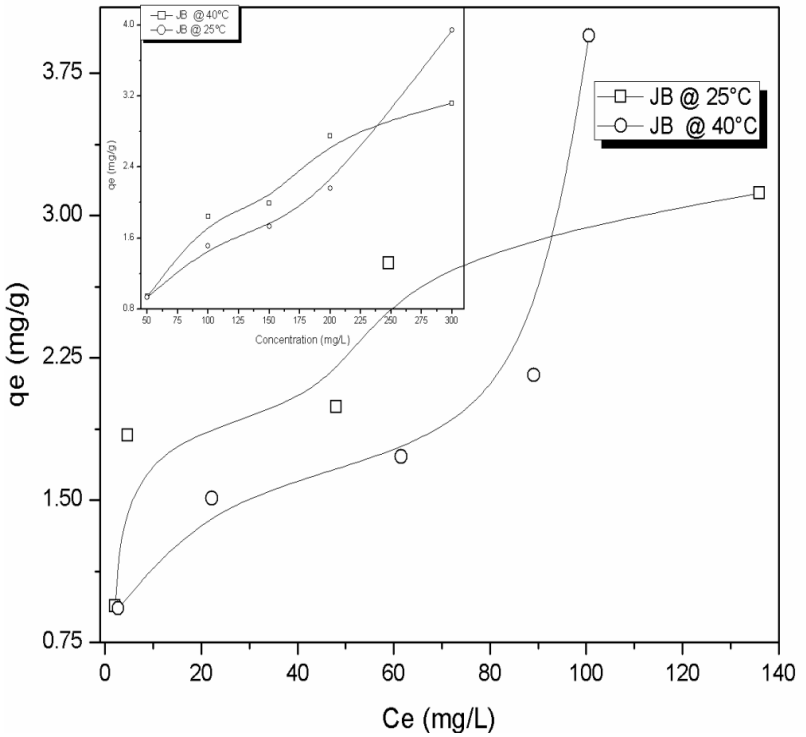

Figure A21 *d*. Cu(II) sorption isotherm for JB soil (Insert: Pb(II) sorption trend as concentration varied at 25 and 40 °C)

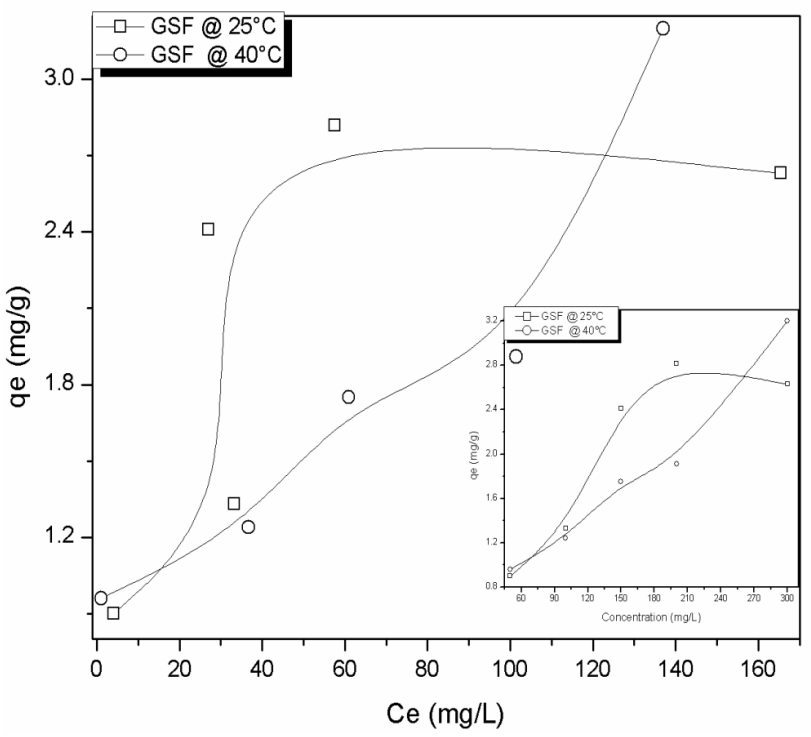

Figure A21 *e*. Cu(II) sorption isotherm for GSF soil (Insert: Pb(II) sorption trend as concentration varied at 25 and 40 °C)

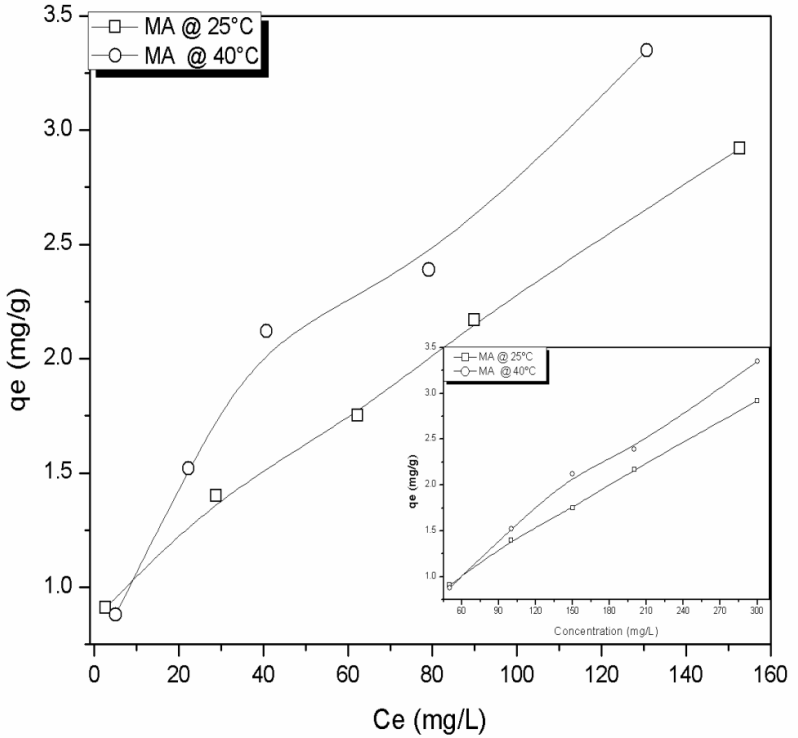

Figure A21 *f*. Cu(II) sorption isotherm for MA soil (Insert: Pb(II) sorption trend as concentration varied at 25 and 40 °C)

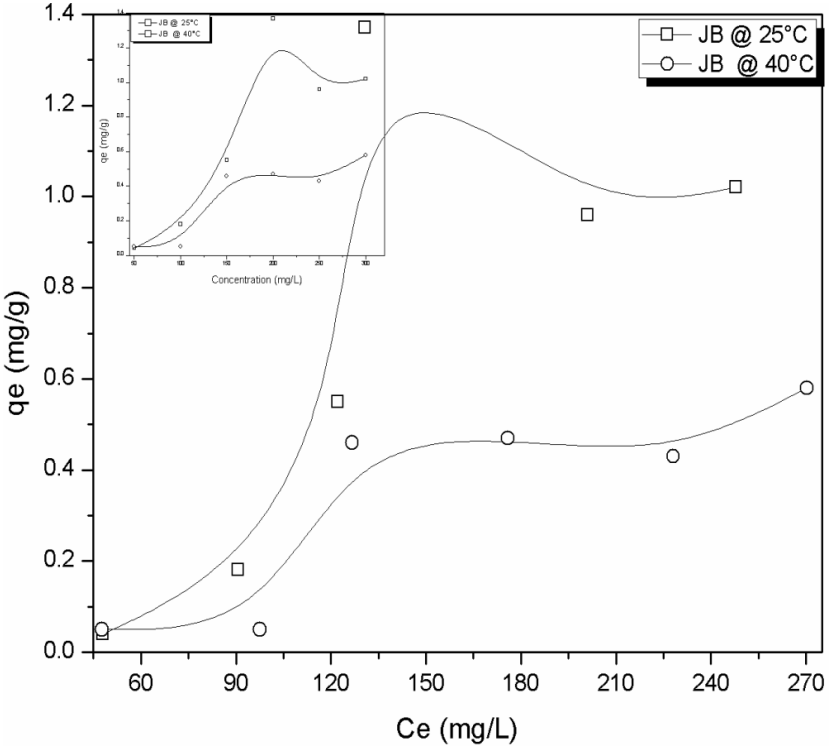

Figure A21 *g*. Cd(II) sorption isotherm for JB soil (Insert: Pb(II) sorption trend as concentration varied at 25 and 40 °C)

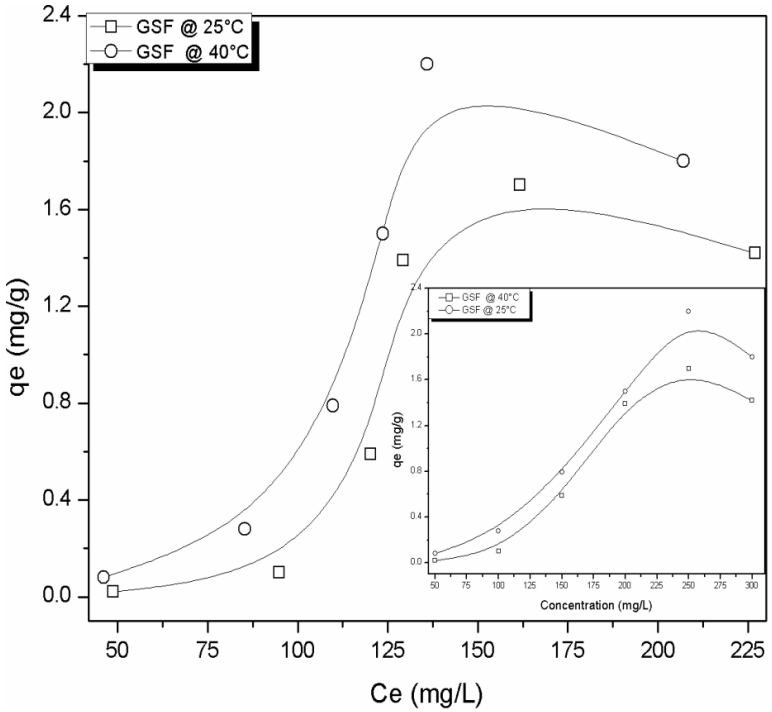

Figure A21 *h*. Cd(II) sorption isotherm for GSF soil (Insert: Pb(II) sorption trend as concentration varied at 25 and 40 °C)

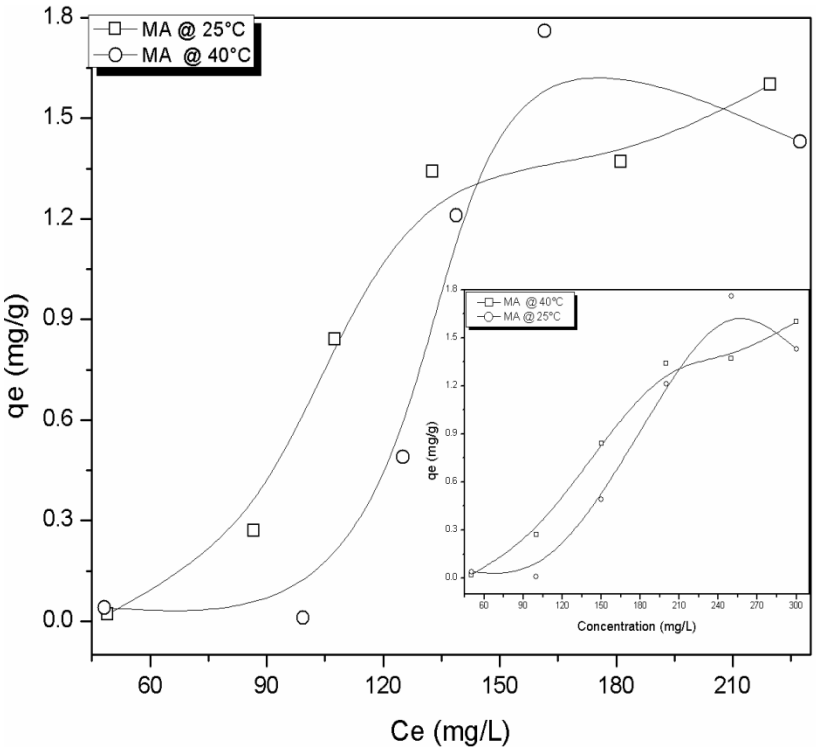

Figure A21 *i*. Cd(II) sorption isotherm for MA soil (Insert: Pb(II) sorption trend as concentration varied at 25 and 40 °C)

Table A2. Isotherm curve types for Pb(II), Cu(II), and Cd(II) sorptions at 25 and 40 °C

	Pb(II) 25 °C	Pb(II) 40 °C	Cu(II) 25 °C	Cu(II) 40 °C	Cd(II) 25 °C	Cd(II) 40 °C
LF	I	I	III	III	V	V
JB	IV	III	III	III	IV	IV
GSF	VI	VI	I	V	V	V
MA	VI	VI	I	III	V	V

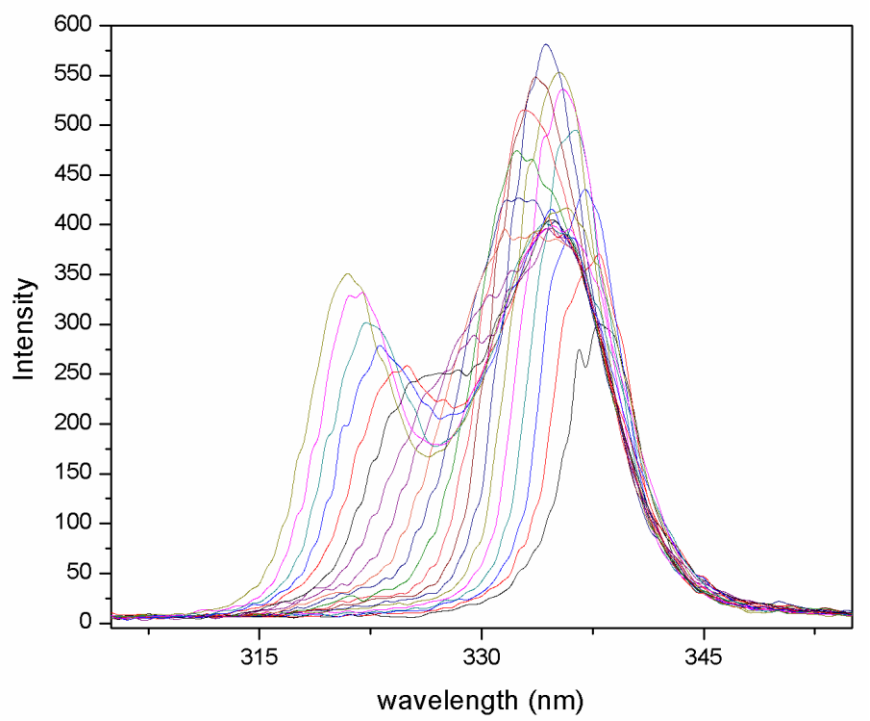

Figure A22 *i*. Optimization of wavelength offset (Δλ) for determination of pyrene. Scanning was done from Δλ of 30 nm through 49 nm. The best spectra for the Δλ was obtained at 36 nm. This was then followed by scan speed optimization

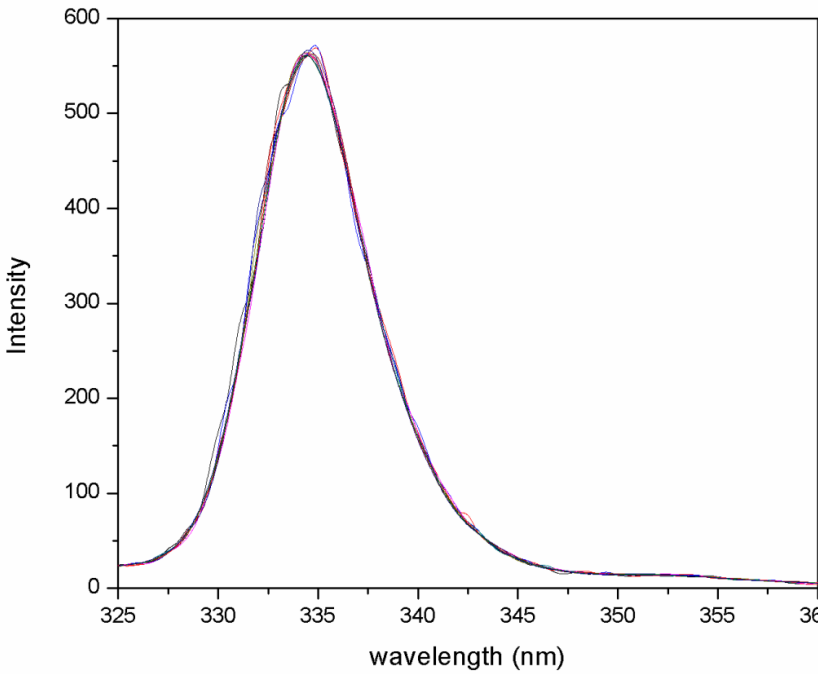

Figure A22 *ii*. Optimization of scan speed for determination of pyrene. The scanning was done from 100nm/min through 1000nm/min. The optimum scan speed was obtained at 500nm/min. This was then followed by slit length optimization

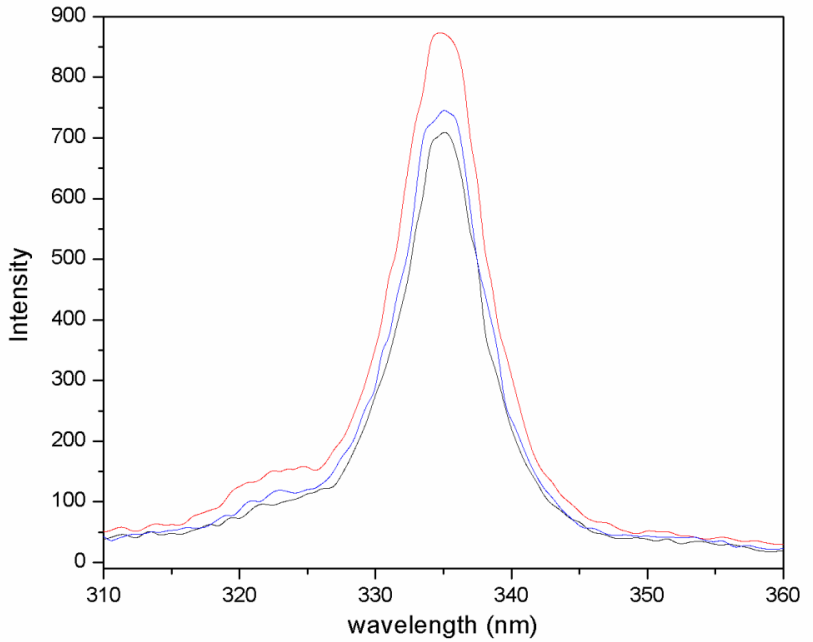

Figure A22 *iii*. Slit optimization for determination of pyrene. The slit optimization was done by scanning the excitation and emission slit widths from 2.5 to 20 nm. The best peak for pyrene was obtained at smaller excitation slit and wider emission slit – 2.5 nm and 20 nm, respectively

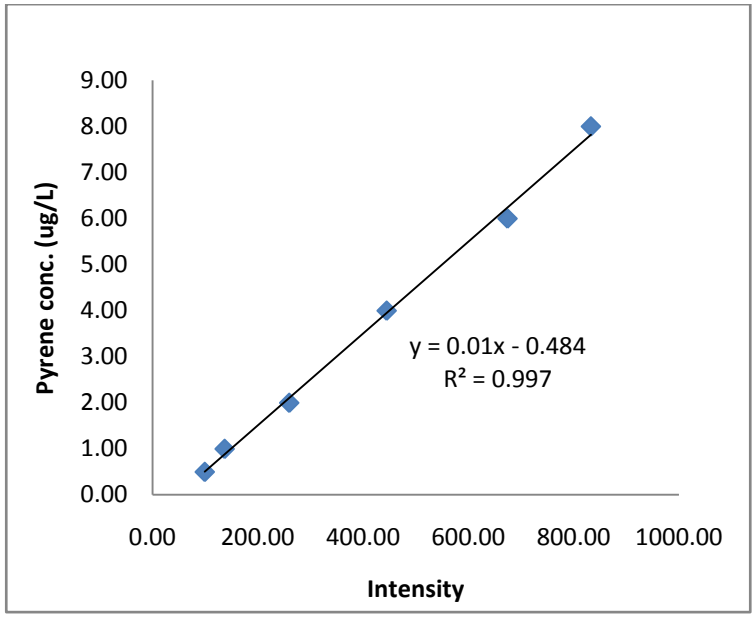

Figure A22 *iv*. Typical pyrene calibration curve

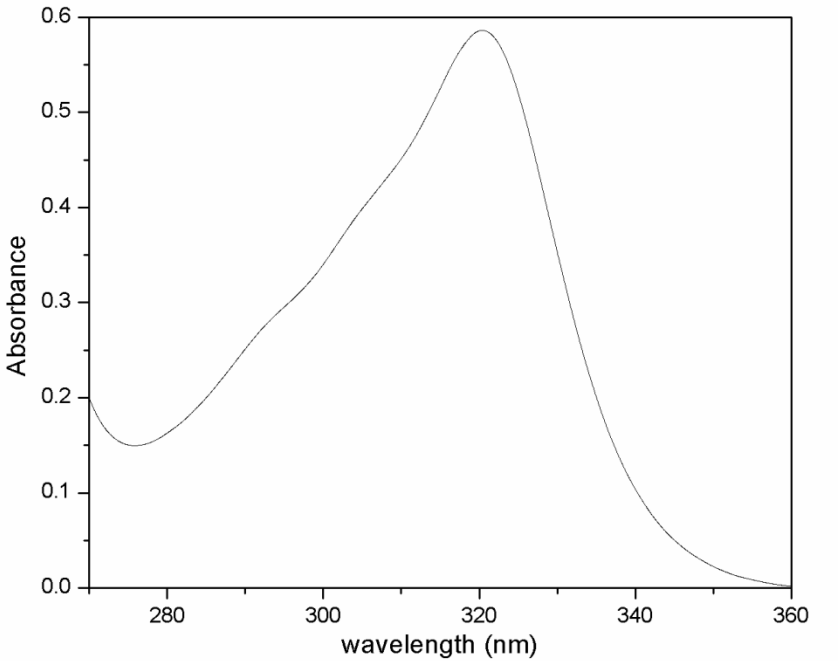

Figure A23 *i*. Curve showing a typical pentachlorophenol UV peak

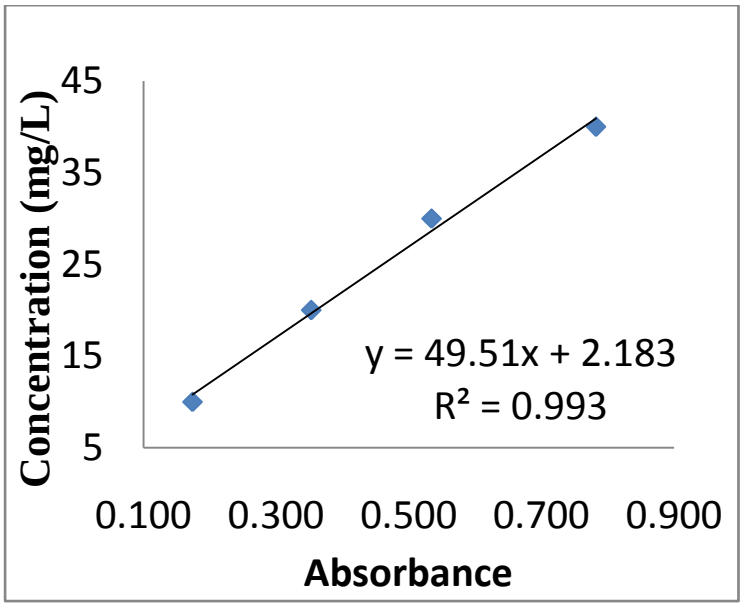

Figure A23 *ii*. Typical pentachlorophenol calibration curve

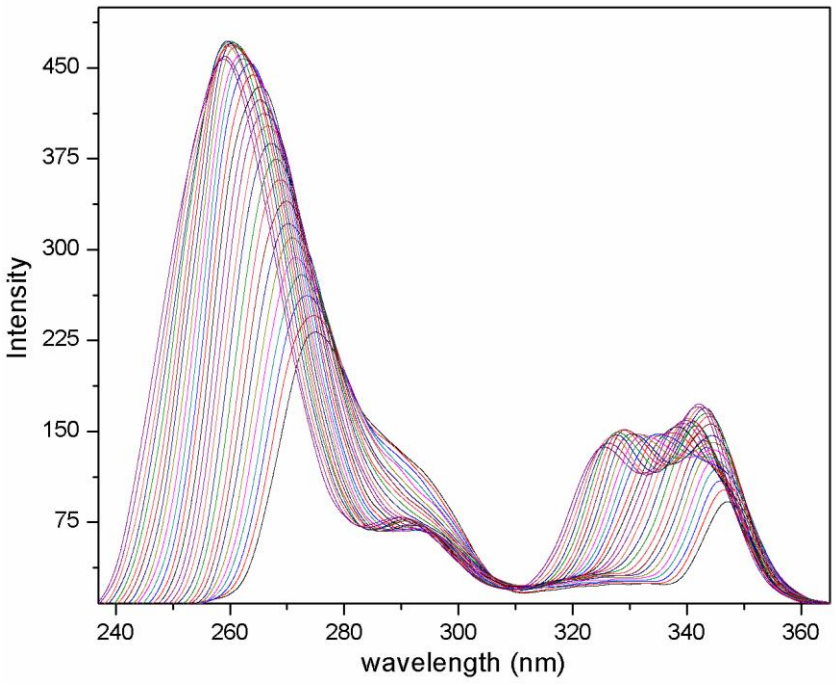

Figure A24 *i*. Optimization of wavelength offset (Δλ) for fluorene determination. Scanning was done from Δλ of 25 nm through 52 nm. The best spectra for the Δλ was obtained at 45 nm. This was then followed by scan speed optimization

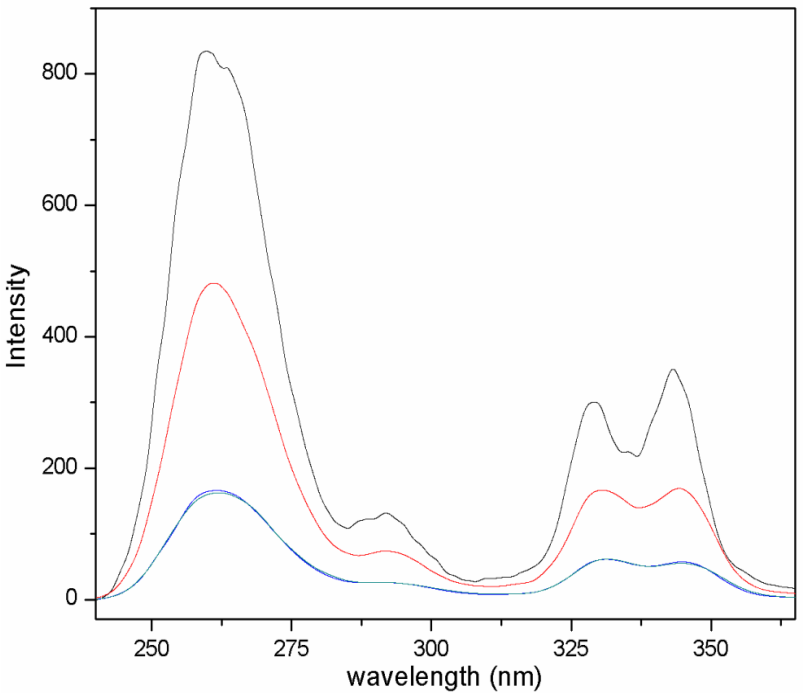

Figure A24 *ii*. Optimization of scan speed for fluorene determination. The scanning was done from 100nm/min through 1000nm/min. The optimum scan speed was obtained at 1000nm/min. This was then followed by slit length optimization

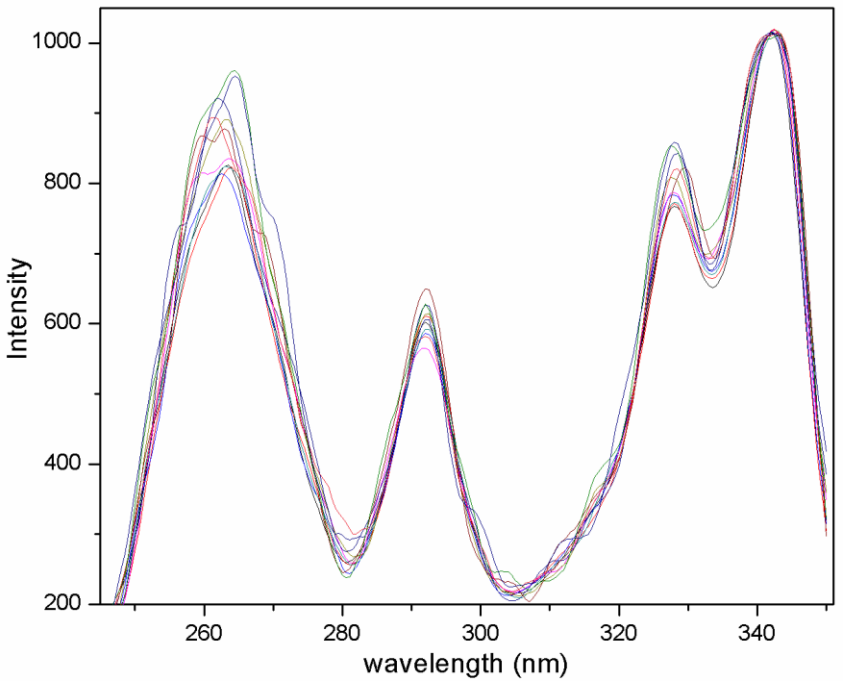

Figure A24 *iii*. Slit optimization for fluorene determination. The slit optimization was done by scanning the excitation and emission slit widths from 2.5 to 20 nm. The best peak for fluorene was obtained at smaller excitation slit and wider emission slit – 2.5 nm and 20 nm, respectively